

Electronic Thesis and Dissertation Repository

6-11-2013 12:00 AM

Regulation of Lipid Homeostasis, Inflammatory Signalling and Atherosclerosis by the Peroxisome Proliferator-Activated Receptor Delta

Lazar A. Bojic
The University of Western Ontario

Supervisor
Dr. Murray Huff
The University of Western Ontario

Graduate Program in Biochemistry
A thesis submitted in partial fulfillment of the requirements for the degree in Doctor of Philosophy
© Lazar A. Bojic 2013

Follow this and additional works at: <https://ir.lib.uwo.ca/etd>



Part of the [Biochemistry Commons](#), [Cardiovascular Diseases Commons](#), and the [Molecular Biology Commons](#)

Recommended Citation

Bojic, Lazar A., "Regulation of Lipid Homeostasis, Inflammatory Signalling and Atherosclerosis by the Peroxisome Proliferator-Activated Receptor Delta" (2013). *Electronic Thesis and Dissertation Repository*. 1307.

<https://ir.lib.uwo.ca/etd/1307>

This Dissertation/Thesis is brought to you for free and open access by Scholarship@Western. It has been accepted for inclusion in Electronic Thesis and Dissertation Repository by an authorized administrator of Scholarship@Western. For more information, please contact wlsadmin@uwo.ca.

Regulation of Lipid Homeostasis, Inflammatory Signalling and Atherosclerosis
by the Peroxisome Proliferator-Activated Receptor Delta

(Thesis format: Integrated-Article)

by

Lazar A. Bojic

Graduate Program in Department of Biochemistry

Submitted in partial fulfillment of
the requirements for the degree of
Doctor of Philosophy

The School of Graduate and Postdoctoral Studies
The University of Western Ontario
London, Ontario, Canada

© Lazar A. Bojic 2013

ABSTRACT

The peroxisome proliferator-activated receptor (PPAR) δ is a ligand-dependent transcription factor that has been implicated in metabolic and inflammatory regulation. The molecular and physiological mechanisms by which PPAR δ activation regulates lipid metabolism, inflammatory signaling and protection from atherosclerosis in states of metabolic disturbance such as insulin resistance and dyslipidemia, were investigated in a series of *in vitro* and *in vivo* studies. *In vitro* experiments were performed in THP-1 human macrophages. These studies demonstrated that PPAR δ activation inhibits atherogenic lipoprotein-induced lipid accumulation and the associated proinflammatory responses. Specifically, treatment of macrophages with the synthetic PPAR δ agonists GW0742 or GW1516 attenuated triglyceride (TG) accumulation and cytokine expression induced by very low-density lipoprotein (VLDL). The primary mechanisms for these effects were increased fatty acid β -oxidation, decreased lipoprotein lipase (LPL) activity, reduced MAPK signaling and improved insulin signaling. With regard to cholesteryl ester (CE)-rich low-density lipoprotein (LDL), the PPAR δ activators stimulated cholesterol efflux via ABCA1 to apoAI, resulting in the inhibition of native and modified LDL-induced CE accumulation. *In vivo* studies were conducted in high fat, high cholesterol (HFHC)-fed low-density lipoprotein receptor null (*Ldlr*^{-/-}) mice. Following a 4-week induction phase of HFHC-feeding to stimulate early atherosclerotic lesion development, dietary supplementation with GW1516 for a subsequent 8-weeks prevented further plaque progression. This prevention was linked to inhibition of dyslipidemia, hyperinsulinemia, and glucose and insulin intolerance. Furthermore, GW1516 strongly attenuated aortic inflammation, insulin resistance and endoplasmic reticulum (ER)-stress, which likely contributed to inhibition of lesion progression.

Additional studies in the liver showed that PPAR δ activation inhibits hepatic TG accumulation induced by HFHC-feeding. To further probe the mechanism for this effect, experiments were conducted in primary mouse hepatocytes isolated from wild-type (WT) or adenosine monophosphate-activated protein kinase (AMPK) $\beta 1^{-/-}$ mice. These studies revealed that PPAR δ activation in the liver stimulates fat oxidation due to upregulation of the PPAR δ -target gene carnitine palmitoyl transferase (*Cpt*) 1a, which occurred independent of AMPK activation. Furthermore, GW1516 inhibited *de novo* lipogenesis, which was partially dependent on AMPK activation. The residual inhibitory effect on fatty acid synthesis was associated with correction of selective hepatic insulin resistance.

In summary, these studies provide significant insight and support for PPAR δ activation as a therapeutic strategy to treat the dysregulation of lipid homeostasis, inflammatory signaling, metabolic disease, and their cardiovascular complications.

Keywords: PPAR δ , macrophage foam cells, intervention, inflammation, atherosclerosis, insulin resistance, mouse model

*To my late great-grandfather Lazar Pantelic.
If there is a heaven, I know you are still teaching there.*

CO-AUTHORSHIP

The contribution of co-authors to chapters 2-5 of this thesis are acknowledged and outlined below.

Dr. Murray Huff, Ph.D, provided intellectual input and scientific expertise into the hypothesis, design and experimental details of the studies outlined in Chapters 2, 3, 4 and 5. Dr. Huff also reviewed and edited the manuscripts for Chapters 2-5. Dr. Robert Hegele, M.D. F.R.C.P, provided blood samples from patients in his clinic for isolation of very low-density lipoproteins and low-density lipoproteins used in Chapters 2 and 3. Dr. Hegele also provided intellectual input into the studies conducted in Chapters 2-5, and edited the manuscripts for Chapters 2 and 3. Dr. Robert Gros, Ph.D., provided intellectual input into the studies for Chapters 2-5. Dr. Gros also provided access to the Comprehensive Lab Animal Monitoring System and edited the manuscript for the studies described in Chapter 5. Cynthia Sawyez, B.Sc. (Hons), research technician, assisted with lipid mass experiments and oleate incorporation for Chapters 2-3, and performed tissue and plasma analyses for Chapters 4 and 5. Dawn Telford, B.Sc. (Hons), research technician, assisted with PCR analyses for Chapters 2 and 3, and assisted with animal studies, oleate incorporation assays, beta oxidation studies and fatty acid synthesis experiments for Chapters 4 and 5. Jane Edwards, B.Sc. (Hons), research technician, assisted with PCR and immunoblotting analyses for Chapters 2-5. Brian Sutherland, A.R.T., research technician, assisted with animal studies and tissue lipid analyses described in Chapters 4-5. Dr. Morgan Fullerton, Ph.D., post-doctoral fellow, provided intellectual input into the planning and execution of the studies and edited the manuscript for Chapter 5. Dr. Rebecca Ford, Ph.D., post-doctoral fellow, provided intellectual input into the planning and execution of the studies, and edited the manuscript for Chapter 5. Dr. Gregory Steinberg, Ph.D., provided intellectual input and

scientific expertise into the planning of the studies and edited the manuscript for Chapter 5. Dr. Steinberg also provided access to AMPK β 1^{-/-} mice for the primary mouse hepatocyte experiments described in Chapter 5.

ACKNOWLEDGEMENTS

I would like to start by expressing my gratitude to my supervisor Dr. Murray Huff. Thank you for providing your expertise, support, and encouragement throughout the completion of my doctoral research. I truly appreciate the time and effort invested into the guidance and mentorship you have provided me during my time in the lab; science-related or otherwise. I thoroughly enjoyed my time here and I have taken away invaluable scientific and life lessons.

To my advisory committee members, Dr. Robert Gros and Dr. Robert Hegele, thank you for your many helpful discussions regarding my research, and for your encouragement and support throughout my training. Your doors were always open to me to discuss any problems or ideas, and I am sincerely grateful for everything you have done for me.

The work in this thesis was supported by grants from the Canadian Institutes of Health Research (FRN-8014) and Heart and Stroke Foundation of Canada (PRG-5967), as well as OGS and OGSST scholarships from the Ontario Graduate Scholarship Program.

To the Huff lab family, past and present, in alphabetical order: Amy, Brian, Cindy, Dawn, Erin, Jane, Josh, Julia, Nica, Sanjiv, Scott and several talented summer and undergraduate students. Thank you for everything. From technical expertise and assistance, to scientific planning and strategizing. From morning coffees to afternoon coffees; political debates to religious debates; smiles to frowns and a tear here and there. Thank you for making our lab such a great place to work and for your continuous encouragement and support during the mania and the pits. I could go on-and-on, and as you all know, I usually would. But for the sake of space, I'll stop there!

Mom, Dad, Mila, Grandpa, Pedja, Sandra, Simona, Stefanie and Sasha: to say that I couldn't have done this without you guys is a vastly unbelievable understatement.

I am extremely blessed to have a wonderful family that provides endless love and support. Thank you.

To the loves of my life, Kathryn and Marley. Without you, none of this would have been at all possible. Thank you for your encouragement, support and unconditional love. I appreciate you more than I could ever put into words.

And last but certainly not least, I would like to thank my friends that made this experience one for the ages: Jake, Brad, Joe, Chris, Piya, Elnaz and Anthony. I still think that Federer is the greatest tennis player of all time, that cryopreservation will be on the cover of Science one day, that Jagerbombs never end well, that the Leafs will win the cup before we die, that if you get a good deal you should 'take it 'n go', that Tebow's game-winning pass in OT was a spectacle and that Usher is a better dancer than Michael Jackson. But we should probably get together for a beer or two on Friday afternoon to discuss these matters some more!

TABLE OF CONTENTS

	Page
Abstract and Key Words	ii
Dedication	iv
Co-Authorship	v
Acknowledgments	vii
Table of Contents	ix
List of Figures	xv
List of Tables	xix
List of Appendices	xx
List of Abbreviations	xxi
Chapter 1 – Thesis topics review	
1.1 General Introduction	1
1.2 Dyslipidemia and Cardiovascular DiseaseGeneral Introduction	2
1.2.1 Atherosclerosis	5
1.2.2 Cholesterol-Rich Macrophage Foam Cells	9
1.2.3 Inflammation and Apoptosis in Cholesterol-Rich Foam Cells	13
1.2.4 Triglyceride-Rich Macrophage Foam Cells	15
1.2.5 Inflammation in Triglyceride-Rich Foam Cells	18
1.2.6 Atherosclerotic Lesion Progression	19
1.3 Lipoprotein Metabolism	25
1.3.1 Lipoproteins	25
1.3.2 Exogenous Lipoprotein Metabolism	27
1.3.3 Endogenous Lipoprotein Metabolism	28
1.4 Regulation of Fatty Acid and Cholesterol Metabolism	32

1.4.1 Sterol Regulatory Element Binding Proteins	32
1.4.2 De Novo Lipogenesis	37
1.4.3 Cholesterol Esterification	39
1.4.4 Fatty Acid Oxidation	40
1.4.4.1 Fatty Acid Oxidation – PPAR Regulation	43
1.4.5 AMPK – The Pivotal Regulator of Fat Oxidation and Lipogenesis	44
1.5 Insulin Signaling	48
1.5.1 Insulin-Regulated Hepatic Glucose Metabolism	48
1.5.2 Insulin-Regulated Hepatic Lipid Metabolism	51
1.5.3 Insulin Resistance	51
1.5.3.1 Insulin Resistance in the Liver	52
1.5.3.2 Insulin Resistance in the Vasculature	56
1.6 Type 2 Diabetes	57
1.7 Peroxisome Proliferator-Activated Receptors	58
1.7.1 PPAR Overview	58
1.7.2 PPAR δ in Macrophages	61
1.7.3 PPAR δ Activation and the Protection from Diet-Induced Atherosclerosis	65
1.7.4 PPAR δ Activation in Hepatocytes	66
1.7.5 PPAR δ Agonists in Humans	67
1.8 Models to be Used	69
1.8.1 Cell Culture	69
1.8.2 <i>Ldlr</i> ^{-/-} mice	70
1.8.3 Animal Diets	70
1.8.3.1 Chow diet	70

1.8.3.2 Western diet with added cholesterol (HFHC diet)	72
1.9 Scope of Thesis and Hypotheses	72
1.10 References	75
Chapter 2 - Activation of PPARδ inhibits human macrophage foam cell formation and the inflammatory response induced by very low-density lipoprotein.	
2.1 Introduction	94
2.2 Materials and Methods	96
2.2.1 Lipoproteins	96
2.2.2 Cell Culture	96
2.2.3 Luciferase Reporter Assays	97
2.2.4 Cellular Lipid Mass	98
2.2.5 Enzyme-linked Immunosorbent Assay	98
2.2.6 Quantitative Real-Time PCR Gene Abundance Analysis	98
2.2.7 LPL Activity, TG Synthesis, FA β -oxidation and FA Uptake	99
2.2.8 Immunoblot Analysis and Densitometry	100
2.2.9 Statistical Analyses	101
2.3 Results	101
2.4 Discussion	135
2.5 References	142
Chapter 3 - Activation of PPARδ inhibits human macrophage foam cell formation induced by native and modified low-density lipoprotein	
3.1 Introduction	148
3.2 Materials and Methods	152
3.2.1 Lipoproteins	152
3.2.2 Cell Culture	152
3.2.3 Cellular Lipid Mass	152

3.2.4 Cholesterol Esterification	153
3.2.5 Cholesterol Efflux	153
3.2.6 Quantitative Real-Time PCR Gene Abundance Analysis	154
3.2.7 Immunoblot Analysis and Densitometry	154
3.2.8 Statistical Analyses	155
3.3 Results	156
3.4 Discussion	170
3.5 References	174
Chapter 4 - PPARδ agonist GW1516 attenuates diet-induced atherosclerosis and associated aortic inflammation in <i>Ldlr</i>^{-/-} mice	
4.1 Introduction	179
4.2 Materials and Methods	183
4.2.1 Animals and Diets	183
4.2.2 Plasma Lipid, Blood Glucose and Plasma Insulin Determinations	183
4.2.3 Glucose Tolerance and Insulin Tolerance	184
4.2.4 Tissue Histology and Immunohistochemistry	184
4.2.5 Immunoblotting and Densitometry	185
4.2.6 Quantitative Real-Time PCR Gene Abundance Analysis	185
4.2.7 Statistical Analyses	186
4.3 Results	187
4.4 Discussion	208
4.5 References	213

Chapter 5 - PPAR δ -specific activation in liver attenuates triglyceride accumulation via enhanced fatty acid oxidation, reduced fatty acid synthesis and improved insulin sensitivity

5.1 Introduction	221
5.2 Materials and Methods	225
5.2.1 Animals and Diets	225
5.2.2 Activation of AMPK <i>in vivo</i>	225
5.2.3 Energy Expenditure	226
5.2.4 Primary Mouse Hepatocyte Isolation, Lipogenesis and Fatty Acid Oxidation	226
5.2.5 Plasma, Blood and Tissue Analyses	227
5.2.6 Immunoblotting and Densitometry	227
5.2.7 Quantitative Real-Time PCR Gene Abundance Analysis	228
5.2.8 Statistical Analyses	228
5.3 Results	229
5.4 Discussion	248
5.5 References	252

Chapter 6 - Discussion

6.1 Summary of Findings	257
6.2 Conclusions and Future Directions	265
6.2.1 Chapter 2 Conclusions	265
6.2.2 Chapter 2 Future Directions	267
6.2.3 Chapter 3 Conclusions	269
6.2.4 Chapter 3 Future Directions	271
6.2.5 Chapter 4 Conclusions	273
6.2.6 Chapter 4 Future Directions	274

6.2.7 Chapter 5 Conclusions	277
6.2.8 Chapter 5 Future Directions	279
6.3 Overall Thesis Conclusion	281
6.4 References	284
Curriculum Vitae	294

LIST OF FIGURES

Figure	Description	Page
1.1	Composition of the arterial wall	7
1.2	Cholesterol homeostasis in macrophages	11
1.3	VLDL-induced foam cell formation	17
1.4	VLDL-induced MAPK signaling in macrophage foam cells	21
1.5	Atherosclerotic lesion progression	23
1.6	Endogenous and exogenous lipoprotein metabolism	30
1.7	Regulation of the sterol regulatory element binding proteins	35
1.8	The carnitine palmitoyl-transferase system	42
1.9	Regulation of fatty acid synthesis and oxidation by AMPK	46
1.10	Insulin signaling	50
1.11	Selective versus pure insulin resistance	55
1.12	Consequences of PPAR δ activation and PPAR δ deletion	64
2.1	PPAR δ -specific activation attenuates VLDL-induced triacylglycerol mass accumulation	103
2.2	GW0742 and GW501516 are PPAR δ -specific agonists	106
2.3	PPAR δ activation regulates triglyceride metabolism	108
2.4	Effect of PPAR δ activation on FFA re-esterification mechanisms	111
2.5	PPAR δ agonists attenuate VLDL-stimulated expression of AP-1 associated inflammatory cytokines	113
2.6	PPAR δ activation does not affect basal cytokine expression in THP-1 human macrophages	115

2.7	The effect of PPAR δ agonists on media IL-1 β protein; the effect of VLDL on TNF α or IL-6 expression and the VLDL-induced inflammatory response in the presence of an inhibitor of NF κ B	117
2.8	Prevention of VLDL-induced TG accumulation and cytokine expression are independent effects of PPAR δ activation	120
2.9	Free fatty acids are the primary effectors of the VLDL-induced inflammatory response in human macrophages	122
2.10	MAPK signaling in THP-1 human macrophages in response to VLDL	125
2.11	Effects of inhibitors on cell signalling cascades	127
2.12	VLDL induces human macrophage inflammation via AKT/FoxO1 signaling	129
2.13	PPAR δ activation normalizes VLDL-stimulated inflammatory signaling	132
2.14	Inhibition of β -oxidation had no effect on the ability of PPAR δ activation to correct VLDL-induced inflammatory signaling	134
2.15	Effects of PPAR δ agonists on expression of <i>ILK</i> and <i>PDK1</i>	141
3.1	PPAR δ activation attenuates LDL-induced cholesteryl ester mass accumulation	158
3.2	Effect of PPAR δ activation on uptake and FFA re-esterification into cholesteryl ester	160

3.3	PPAR δ activation enhances ABCA1 and ABCG1 mRNA and protein, leading to increased cholesterol efflux	163
3.4	PPAR δ agonists and ACAT inhibitors do not further affect the oxLDL-mediated reduction in proinflammatory cytokine expression	165
3.5	oxLDL dose-dependently reduces proinflammatory cytokine expression which is associated with a dose-dependent increase in LXR, PPAR γ and PPAR δ target genes	169
4.1	GW1516 regresses diet-induced dyslipidemia	189
4.2	GW1516-treatment attenuates rate of body weight gain and epididymal fat mass	191
4.3	GW1516 improves diet-induced dysregulation of metabolic indices	193
4.4	GW1516 attenuates HFHC-induced atherosclerosis	196
4.5	GW1516 attenuates lipid accumulation, M1 macrophage markers and induces a shift towards M2 macrophage markers in full length aortae	198
4.6	GW1516 corrects aberrant MAPK and NF- κ B signaling in full-length aortae of HFHC-fed mice	201
4.7	GW1516 corrects aberrant insulin signaling, the UPR and ER-stress in aortae of HFHC-fed mice	204
4.8	GW1516 activates aortic PPAR δ but not PPAR α or PPAR γ	207
4.9	GW1516 stimulates aortic expression of regulators of G-protein coupled receptor signaling Rgs4 and Rgs5	212

5.1	GW1516 attenuates diet-induced hepatic steatosis, in part, via increased fatty acid oxidation	231
5.2	GW1516 increases AMPK and ACC phosphorylation, which is not required for fatty acid oxidation	234
5.3	GW1516 activates hepatic AMPK in vivo, yet stimulates carbohydrate utilization	237
5.4	GW1516 inhibits hepatic fatty acid synthesis as a consequence of AMPK activation and correction of selective hepatic insulin resistance	240
5.5	GW1516 corrects the gluconeogenic branch of insulin signalling during selective hepatic insulin resistance which improves fasting hyperglycemia	244
5.6	GW1516 attenuates hepatic inflammation and ER-stress	246
6.1	PPAR δ activation inhibits macrophage foam cell formation and the inflammatory response	260
6.2	Thesis Summary	283

LIST OF TABLES

Table	Description	Page
1.1	Lipoprotein Classification	26
1.2	Animal Diets	71

LIST OF APPENDICES

Appendix	Description	Page
7.1	Copyright permission (Chapter 1)	291
7.2	Copyright permission (Chapter 2)	292
7.3	Ethics Approval – Animal Research	293

LIST OF ABBREVIATIONS

ABCA1	ATP binding cassette transporter A1
ABCG1	ATP binding cassette transporter G1
ACAT	acyl CoA:cholesterol acyltransferase
ACC	acetyl-coenzyme A carboxylase
ACOX	acyl-coenzyme A oxidase
ADFP	adipocytes differentiation related protein
AMPK	adenosine monophosphate-activated protein kinase
ANGPTL4	angiopoietin-like 4
ANOVA	analysis of variance
AP-1	activated protein-1
apoB	apolipoprotein B
apoC	apolipoprotein C
apoE	apolipoprotein E
Arg	arginase
ASO	antisense oligonucleotides
AUC	area under the curve
BCL-6	B-cell lymphoma 6
CCL	chemokine ligand
CD	cluster of differentiation
CD36	scavenger receptor class B, member 3
CE	cholesteryl ester
CETP	cholesteryl ester transfer protein
CPT1 α	carnitine palmitoyltransferase-1 alpha
CVD	cardiovascular disease
DGAT	diacylglycerol acyltransferase

DHCR24	24-dehydrocholesterol reductase
DMSO	dimethylsulfoxide
DNA	deoxyribonucleic acid
dpm	disintegrations per minute
ELISA	enzyme linked immunosorbent assay
ERK	extracellular signal-regulated kinase
FA	fatty acid
FABP	fatty acid binding protein
FAF-BSA	fatty acid free- bovine serum albumin
FAS	fatty acid synthase
FC	free cholesterol
FFA	free fatty acid
FH	familial hypercholesterolemia
FoxO	forkhead box O
FPLC	fast performance liquid chromatography
G-6-Pase	glucose-6-phosphatase
GAPDH	glyceraldehyde-3-phosphate dehydrogenase
GK	glucokinase
GLUT	glucose transporter
GRB2	growth factor receptor binding protein
GTT	glucose tolerance test
HDL	high density lipoprotein
HFHC	high-fat high cholesterol
HL	hepatic lipase
HMG-CoA	3-hydroxy-3-methylglutaryl coenzyme A
HOMA-IR	homeostasis model assessment of insulin resistance

ICAM	intracellular adhesion molecule
IDL	intermediate density lipoprotein
IL	interleukin
INSIG	insulin signaling protein
iNos	inducible nitric oxide synthase
<i>i.p.</i>	intraperitoneal
IR	insulin receptor
IRS	insulin receptor substrate
ITT	insulin tolerance test
JNK	c-Jun N-terminal kinase
LCAT	lecithin-cholesterol acyltransferase
LCM	laser capture microdissection
LDL	low density lipoprotein
LDLR	low-density lipoprotein receptor
LPDS	lipoprotein deficient serum
LPL	lipoprotein lipase
LPS	lipopolysaccharide
LXR	liver X receptor
MAPK	mitogen activated protein kinase
MCP	macrophage chemoattractant protein
MEK	mitogen activated protein kinase kinase
MGAT	monoacylglycerol acyltransferase
MIP	macrophage inflammatory protein
mTORC	mammalian target of rapamycin complex
MTP	microsomal triglyceride transfer protein
NEFA	non-esterified fatty acid

Nfkb	nuclear factor kappa B
NS	not significant
OA	oleic acid
oxLDL	oxidized low-density lipoprotein
PCSK9	proprotein convertase subtilisin/kexin type 9
PDK	pyruvate dehydrogenase kinase
PEPCK	phosphoenolpyruvate carboxykinase
PGC1 α	peroxisome proliferator activated receptor gamma coactivator1 α
PI3-K	phosphatidylinositol 3-kinase
PL	phospholipid
PPAR	peroxisome proliferator activated receptor
PPRE	peroxisome proliferator response element
RGS	regulators of G-protein coupled receptor signaling
qRT-PCR	quantitative real-time reverse transcriptase polymerase chain
reaction	
SCAP	SREBP cleavage activating protein
SEM	standard error of the mean
SMC	smooth muscle cell
SOCS	suppressor of cytokine signaling
SREBP	sterol response element binding protein
TC	total cholesterol
TG	triacylglycerol
TLC	thin layer chromatography
TLR	toll like receptor
TNF	tumour necrosis factor
UPR	unfolded protein response

VLDL	very low density lipoprotein
VSMC	vascular smooth muscle cell

Chapter 1*

Thesis topics review

1.1 GENERAL INTRODUCTION

Cardiovascular disease (CVD) represents the leading cause of death in the industrialized world, and will likely soon achieve this status worldwide (Lloyd-Jones et al., 2010). The underlying cause of most cardiovascular events is atherosclerosis, a decades-long chronic inflammatory disease of large and medium sized arteries, ultimately resulting in the formation of complex lesions known as plaques (Glass and Witztum, 2001, Moore and Tabas, 2011). Unstable plaques are prone to rupture, resulting in the formation of thrombi that can subsequently induce the acute clinical manifestations of myocardial infarction or stroke (Libby et al., 2011). Major risk factors for the development of atherosclerosis include age, hypertension, smoking, obesity, diabetes and increased plasma concentrations of cholesterol and triglycerides (TG) (Libby et al., 2011). Despite the success of pharmacological treatment of many of these risk factors, the prevalence of CVD in all groups of Canadians has continued to rise (Lee et al., 2009). The class of drugs known as statins effectively lower plasma cholesterol levels and CVD (Cannon et al., 2004). However, significant residual risk remains, possibly due to the fact that statins do not improve other cardiometabolic risk factors such as high plasma TG, obesity and diabetes. Consequently, novel therapeutic strategies to alleviate these unmet medical needs are highly sought-after.

This thesis focuses on defining the mechanism of action and therapeutic potential of peroxisome proliferator-activated receptor (PPAR) δ activation in the regulation of lipid metabolism, inflammatory signaling and protection from

*a version of the PPAR δ section of this chapter is published:
Bojic and Huff (2013) *Curr Opin Lipidol* **24(2)**, 171-177.

atherosclerosis in states of metabolic disturbance such as insulin resistance and dyslipidemia.

1.2 DYSLIPIDEMIA AND CARDIOVASCULAR DISEASE

Cholesterol is an essential precursor in the synthesis of all steroid hormones, bile acids and the myelin sheath that surrounds axons (Goldstein and Brown, 2009). Furthermore, cholesterol is a major component of all cellular membranes, providing barrier functions between microenvironments and modulating membrane fluidity (Goldstein and Brown, 2009). Cells acquire cholesterol from a number of sources including *de novo* cholesterol synthesis, as well as uptake of cholesteryl ester (CE)-rich apoB100 containing lipoproteins, namely low-density lipoprotein (LDL) in the periphery, and CE-rich high-density lipoprotein (HDL) in the liver.

Since 1913 when Anitschkow and Chaladow first experimentally demonstrated the link between plasma cholesterol and atherosclerosis (Chaladow, 1983), clinical studies have clearly shown that a 2-fold increase in plasma cholesterol is associated with a 6-fold increase in CVD risk (Neaton and Wentworth, 1992). The fact that the cholesterol biosynthetic pathway was a regulated process that could be manipulated to modulate plasma cholesterol was well established in the 1950s and 1960s, which launched the search for cholesterol synthesis inhibitors (Vance and Van den Bosch, 2000). Three-hydroxy-3-methyl-glutaryl-CoA (HMG-CoA) reductase converts 3-hydroxy-3-methylglutaryl-coenzyme A to mevalonate, the rate-limiting step in the production of cholesterol, which subsequently became the major target for the treatment of hypercholesterolemia using the class of drugs called statins (Tobert, 2003). Although compactin (mevastatin), isolated from *Penicillium citrinum*, was the first potent inhibitor of HMG-CoA reductase reported by Akiro Endo in 1976 (Endo et al., 1976), the first statin to be approved for use in the clinical arena was lovastatin, discovered by Alberts and colleagues at Merck Research Laboratories (Alberts et al., 1980). Since these early

studies, statins have become the standard of care in reducing plasma LDL-cholesterol (LDL-C) in a variety of patient populations, yielding primary and secondary prevention against CVD (Mills et al., 2008). Despite the overwhelming evidence from large randomized controlled trials demonstrating the success of statins in reducing morbidity and mortality in high risk CVD patients, about 50-75% of cardiovascular events are not prevented with these drugs (Mazzone et al., 2008). In addition to high plasma LDL-C, atherogenic dyslipidemia is now characterized by increased plasma TG-rich very low-density lipoprotein (VLDL) and low plasma HDL, neither of which are appreciably affected by statin treatment (Musunuru, 2010). Therefore, additional therapeutic strategies are required to complement existing medical therapies in CVD risk management.

Fasting hypertriglyceridemia is strongly associated with elevated rates of atherosclerotic CVD, particularly in patients with type 2 diabetes (Talayero and Sacks, 2011). The extent of atherosclerosis in this patient population is positively correlated with plasma concentrations of TG-rich lipoproteins, namely VLDL as well as intermediate density lipoprotein (IDL), also known as VLDL-remnants (Reyes-Soffer et al., 2013). Importantly, individuals with type 2 diabetes are at significantly higher risk for developing CVD, even if LDL-C has been reduced to the therapeutic goal (Talayero and Sacks, 2011). Since each of VLDL, IDL and LDL harbors one apoB100 molecule, measuring total apoB reflects the total number of potentially atherogenic particles in plasma and is therefore a stronger predictor of CVD risk than simply measuring LDL-C (Walldius and Jungner, 2006). As such, targeting apoB100 specifically represents an attractive therapeutic target in the treatment of dyslipidemia. Antisense oligonucleotides (ASO) against apoB100 successfully reverse diet-induced dyslipidemia in mice without affecting intestinal lipid absorption or accumulation, and without causing hepatic steatosis (Crooke et al., 2005, Mullick et al., 2011). Furthermore, apoB100 ASOs profoundly inhibit the

development of murine atherosclerosis (Mullick et al., 2011). Preliminary trials in humans have shown that apoB100 ASOs are generally well-tolerated, and effectively lower all plasma apoB100-containing lipoproteins (Lippi and Favaloro, 2011). Future trials are required to determine whether apoB ASOs will reach the clinical arena. Nevertheless, reducing plasma apoB100 may confer protection from development of CVD.

Raising plasma HDL-cholesterol (HDL-C) has been given considerable attention as a potential therapeutic strategy based on a substantial body of evidence suggesting the cardioprotective capacity of these lipoproteins. HDL is responsible for reverse cholesterol transport, the process by which cholesterol is drawn from peripheral tissues, and is transported to the liver for biliary excretion (Rader et al., 2009). Furthermore, epidemiological evidence reproducibly shows an inverse correlation between plasma HDL-C levels and CVD (Nicholls et al., 2012). As a result, this has led to the development of the HDL hypothesis: interventions to raise HDL-C will confer reduced CVD risk (Rader and Tall, 2012). However, recent human trials have suggested that simply raising total HDL-C levels may not be the appropriate goal. Torcetrapib, the first generation cholesteryl ester transfer protein (CETP) inhibitor, successfully raised plasma HDL-C levels yet cardiovascular events and all cause mortality were significantly higher in the treatment arm of the phase III clinical trial (Barter and Rye, 2012). The increased mortality in torcetrapib-treated individuals was attributed to off-target effects of the drug (Barter and Rye, 2012), prompting further evaluation of CETP inhibition as therapeutic approach to treating CVD. The next major phase III clinical trial involving a CETP inhibitor (dalcetrapib-OUTCOMES) was conducted by Roche and was halted early due to interim analyses demonstrating that the drug was not providing reduced CVD risk, despite significantly raising HDL-C (Schwartz et al., 2012). These results suggest that the HDL-C hypothesis may require replacement by the 'HDL flux hypothesis', in which interventions to raise HDL reverse cholesterol transport capacity and HDL turnover may

confer protection from CVD (Rader and Tall, 2012). Although the application of this hypothesis is in its infancy, interventions that increase reverse cholesterol transport and not simply bulk HDL-C are in development (Nicholls et al., 2012).

In summary, therapeutic interventions that lower LDL-C beyond statin monotherapy, decrease plasma apoB100 concentrations, decrease plasma triglycerides or increase the capacity of HDL to promote reverse cholesterol transport may prove to be effective in reducing CVD.

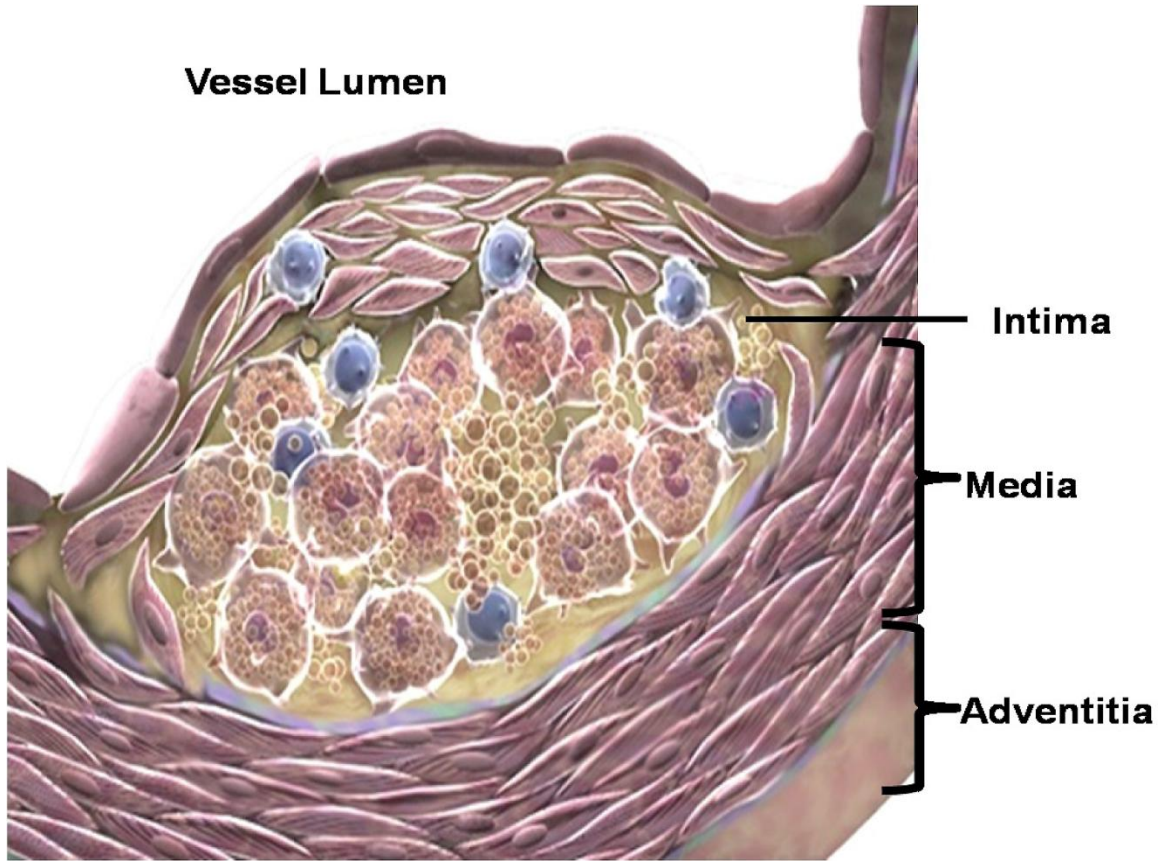
1.2.1 ATHEROSCLEROSIS

Atherogenesis begins with the entry and retention of apoB-containing lipoproteins within the arterial intima of susceptible regions of large and medium sized arteries (Tabas et al., 2007). Subsequent to lipoprotein retention, a series of biological and maladaptive immune responses ensue (Tabas et al., 2010). Complex interactions between the endothelium, vascular smooth muscle cells and immune cells such as macrophages, drive plaque progression through a non-resolving expansion of the arterial intima which protrudes into the arterial lumen (Moore and Tabas, 2011). Although this protrusion can eventually lead to tissue ischemia, the predominant acute clinical events are myocardial infarction or stroke caused by rupture of unstable plaques generating thrombi that can occlude local or distal arteries (Libby et al., 2011).

An artery consists of three morphologically distinct layers: the intima, media and adventitia (Figure 1.1). The intima is the innermost layer, which is defined by an endothelial cell monolayer on the luminal side, the internal elastic lamina on peripheral side and extracellular matrix collagen and proteoglycans in between (Lusis, 2000). Endothelial cells of the intima regulate vascular tone via the production of vasoactive mediators (Sudano et al., 2006). The medial layer consists of vascular smooth muscle cells that participate in the regulation of vascular tone as well as the synthesis and secretion of elastin, collagen and sulfated glycosaminoglycans. The intimal side of the

Figure 1.1: Composition of the arterial wall.

Arteries contain three distinct layers: **(1) the intima** which is defined by an endothelial cell monolayer on the luminal side that protects the subendothelial intima from entry of atherogenic lipoproteins, **(2) the media** which consists of vascular smooth muscle cells that participate in the regulation of vascular tone as well as the synthesis and secretion of elastin, collagen and sulfated glycosaminoglycans and **(3) the adventitia** which is comprised of connective tissue with sporadic fibroblasts, smooth muscle cells and progenitor cells.



Adapted from illustrations by Christine Rudewich for the Robarts Research Institute

arterial media is defined by the internal elastic lamina, while the adventitial side is defined by the external elastic lamina (Lusis, 2000). Finally, the adventitia, the outermost arterial layer, is comprised of connective tissue with sporadic fibroblasts, smooth muscle cells and progenitor cells.

Normally the endothelial monolayer provides a protective barrier between the arterial lumen and the subendothelial intima (Libby et al., 2011). However, in curvatures and bifurcations of the arterial tree, blood flow is disturbed, characterized by retrograde and oscillatory shear stress which promotes a proinflammatory endothelial cell phenotype (Cybulsky and Jongstra-Bilen, 2010). In turn, these regions of the endothelial monolayer exhibit increased adhesiveness and permeability to atherogenic lipoproteins. Upon entry into the intima, apoB100 interacts with extracellular matrix glycosaminoglycans resulting in lipoprotein trapping which in turn leads to oxidative and hydrolytic modification of apoB by secretory phospholipase A2 and secretory sphingomyelinase, both of which are produced by macrophages (Moore and Tabas, 2011). In response to retention and modification of apoB, the proinflammatory phenotype of endothelial cells is extended to the upregulation of adhesion molecules such as P-selectin, intracellular adhesion molecule (ICAM) and vascular cell adhesion molecule (VCAM), which collectively promote the endocytosis of monocytes into the subendothelial space (Moore and Tabas, 2011).

Once resident in the intima, monocytes give rise to a heterogeneous population of cells that regulate immune responses (Becker et al., 2012). Monocyte-derived dendritic cells internalize, process and present antigens (such as lipid or modified apoB fragments) to T-cells, potentiating immune cell recruitment (Becker et al., 2012). Monocyte-derived macrophages engulf lipoprotein-derived lipids in attempt to clear the atherogenic substrate, and are hence considered atheroprotective in early lesions (Moore and Tabas, 2011). However, overwhelming accumulation of apoB100-containing

lipoproteins in the intima renders macrophage lipid uptake and efflux mechanisms dysregulated, which generates lipid-laden macrophage foam cells (Libby et al., 2011). The accumulation of foam cells coupled with the inflammatory response contributed by both dendritic cells and macrophages defines the unresolving nature of a growing atheroma (Libby et al., 2011).

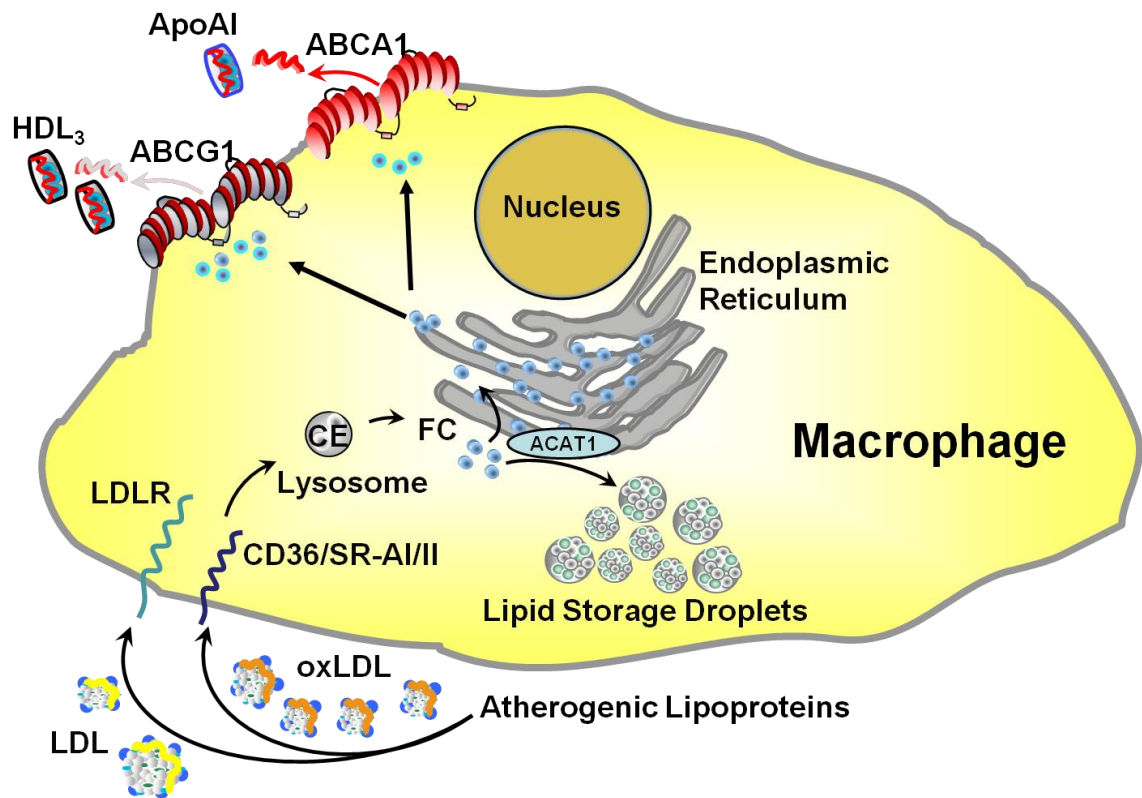
1.2.2 CHOLESTEROL-RICH MACROPHAGE FOAM CELLS

Macrophage cholesterol homeostasis is regulated by uptake, storage and efflux (Figure 1.2). The development of CE-rich lipoprotein-induced “macrophage foam cells” - a histological term that reflects the microscopic appearance of lipid-laden macrophages - is initiated by the ingestion and processing of LDL in both its native and modified forms (Libby et al., 2011). Native LDL uptake occurs via the LDL receptor (LDLR), which undergoes negative feedback regulation under high intracellular sterol concentrations (Goldstein and Brown, 2009). Although this pathway certainly contributes to foam cell development (Goldstein and Brown, 2009), the predominant LDL uptake pathway by macrophages in lesions is that of modified LDL via the scavenger receptors cluster of differentiation (CD) 36 and scavenger receptor A I/II (SRAI/II). Upon entry into the intima, LDL particles undergo oxidative modification rendering them high-affinity scavenger receptor ligands (Moore and Freeman, 2006). Unlike the native LDLR, scavenger receptors do not undergo negative feedback regulation in response to intracellular sterol accumulation (Moore and Freeman, 2006). Consequently, macrophage uptake of modified LDL particles in lesions can persist indefinitely, and is only limited by substrate availability and cell viability.

Once internalized, lipoprotein derived cholesteryl esters are hydrolyzed in the late endosomes to free cholesterol and fatty acids (Maxfield and Tabas, 2005). Through mechanisms that are poorly understood, the late endosomal protein Niemann Pick C1 (NPC1) traffics late endosomal free cholesterol to the endoplasmic reticulum (ER),

Figure 1.2: Cholesterol homeostasis in macrophages.

The LDL receptor (LDLR) mediates the uptake of native LDL particles through receptor-mediated endocytosis. Modified LDL, namely oxLDL is also taken up via receptor mediated endocytosis by the scavenger receptors CD36 and SRAI/II. Upon internalization, CE is hydrolyzed in the late endosomes/early lysosomes into free cholesterol and transferred to the endoplasmic reticulum for processing. The two major pathways for this free cholesterol are: (1) efflux via the cholesterol efflux transporters ABCA1 (to apoA1) and ABCG1 (to HDL₃), and (2) re-esterification by ACAT into cholesteryl ester for storage in cytoplasmic lipid droplets.



where acyl-CoA:cholesterol acyltransferase (ACAT) re-esterifies free cholesterol to cholesteryl fatty acid esters for storage in cytoplasmic lipid droplets (Brown et al., 1980, Ikonen, 2008). Lipid droplet CE is a defining feature of LDL-induced macrophage foam cells in atherosclerotic plaques. However, it has been suggested that as lesions progress, ACAT activity diminishes (Rong et al., 2013). As proof-of-concept, the ablation of macrophage ACAT1 in hypercholesterolemic mouse models of atherosclerosis results in increased atherosclerotic lesion area (Accad et al., 2000, Fazio et al., 2001). Subsequent studies demonstrated that the increase in atherosclerosis in ACAT-deficient settings is due to enrichment of free cholesterol in ER membranes, which initiates the ER-stress response and promotes a proinflammatory, apoptosis-susceptible macrophage (Li et al., 2005, Seimon et al., 2009). As a result, hyperlipidemia coupled to diminishing ACAT activity in advanced plaques contributes to the potentiation of plaque progression. Under these circumstances, it is critical that the rate of cholesterol efflux maintains intracellular free cholesterol content below inflammatory and cytotoxic levels.

Normally free cholesterol released from the late endosomal pathway, as well as free cholesterol mobilized from cytoplasmic lipid droplets, can traffic to the plasma membrane via the Golgi-to-membrane vesicular pathway to become accessible for cholesterol efflux out of the cell (Tall et al., 2008). The removal of plasma membrane cholesterol from macrophages is the predominant pathway for cholesterol mobilization from plaques during atherosclerosis regression (Fisher et al., 2012), and occurs via ATP-binding cassette (ABC) A1- and ABCG1-mediated free cholesterol transport to apolipoprotein A1 (apoA1) and HDL respectively (Tall et al., 2008). HDL particles are also recognized by the scavenger receptor, class B type I (SR-BI) in the periphery as well as the liver (Trigatti et al., 2003). Increasing the cholesterol efflux pathway has very clear cardioprotective effects (Fisher et al., 2012). Intravenous injection of apoA1 into hypercholesterolemic rabbits successfully delayed lesion progression, and intravenous

infusion of a recombinant form of apoAI induced significant regression of atherosclerosis in apoE deficient mice (Miyazaki et al., 1995, Shah et al., 2001). Conversely, as predicted, combined deletion of ABCA1 and ABCG1 in macrophages significantly increases lesion development in mice (Yvan-Charvet et al., 2007). Interestingly, ABCG1 deletion alone is atheroprotective due to compensatory upregulation of ABCA1 (Tarling et al., 2010).

In summary, dynamic regulation of cholesterol uptake, storage and efflux requires a fine balance in plaque macrophages, and ultimately dictates the fate of atherosclerotic lesions.

1.2.3 INFLAMMATION AND APOPTOSIS IN CHOLESTEROL-RICH FOAM CELLS

As alluded to in sections 1.1 and 1.2.1, a major characteristic of atherosclerosis is chronic low-grade inflammation. Although it has recently been challenged (Spann et al., 2012), the generally accepted paradigm is that cholesterol-treated macrophages exhibit a proinflammatory phenotype (Moore and Tabas, 2011). Specifically, oxidized LDL (oxLDL) has been reported to stimulate proinflammatory cytokine expression through CD36 in concert with the pattern recognition toll-like receptors (TLR) (Moore and Tabas, 2011). The assembly of CD36-TLR complexes leads to the activation of nuclear factor kappa B (Nfkb) signal transduction to simulate expression of inflammatory mediators (Stewart et al., 2010). In macrophages isolated from CD36 deficient patients, oxLDL fails to stimulate cytokine expression (Janabi et al., 2000), and loss of this scavenger receptor protects mice against diet-induced atherosclerosis and aortic inflammation (Febbraio et al., 2000, Manning-Tobin et al., 2009). Furthermore, specific deletion of TLR4 or TLR6 abrogates oxLDL-induced inflammatory responses *in vitro* (Stewart et al., 2010), while TLR1, TLR2 and TLR6 deletion attenuates atherogenesis in a variety of atherosclerosis mouse models (Curtiss et al., 2012, Mullick et al., 2005).

In addition to lipoprotein-mediated cell-surface stimulation of inflammatory signal transduction, intracellular cholesterol accumulation can also lead to macrophage inflammation. In particular, free cholesterol loading stimulates an ER-stress pathway known as the unfolded protein response (UPR), which serves as a repair pathway during times of ER perturbation (Martinet et al., 2012, Tabas and Ron, 2011). However, prolonged ER-stress leads to the induction of a specific branch of the UPR involving C/EBP homologous protein (CHOP), which in turn stimulates Nfkb signaling, and eventually apoptosis and secondary necrosis. These latter consequences of free cholesterol-induced ER-stress are central features of advanced atherosclerotic lesions that are vulnerable to rupture (Li et al., 2005, Thorp et al., 2009). Increased ER-stress markers have been visualized in plaques isolated from hypercholesterolemic mice (Zhou et al., 2005). Furthermore, *Chop/apoE* double knockout mice background exhibit substantially smaller atherosclerotic lesions than *Chop+/+;apoE-/-* mice (Thorp et al., 2009). Moreover, the global deletion of *Chop* reduced plaque macrophage apoptosis and necrosis, thus resulting in more stable atherosclerotic lesions (Thorp et al., 2009). Subsequently it was shown that macrophage-specific deletion of *Chop* also reduced plaque vulnerability (Tsukano et al., 2010). Importantly, free cholesterol loaded macrophages with ER-stress-induced inflammation and apoptosis are significant contributors to the accelerated atherosclerosis progression observed in the insulin resistant state (Tabas et al., 2010).

Despite the overwhelming evidence that cholesterol-treated and cholesterol-loaded macrophages are proinflammatory the data are not consistent across all experimental settings. THP-1 human monocytes that are differentiated into macrophages and treated with LDL that has been mildly or extensively oxidized displayed reduced expression of a panel of proinflammatory cytokines (Qiu et al., 2007). In a subsequent study, addition of the TLR2/TLR4 ligand lipopolysaccharide (LPS)

stimulated an Nfkb-mediated inflammatory response in primary human monocytes, which was completely inhibited by the addition of oxLDL (Kannan et al., 2012). Recently, Spann et al. demonstrated that cholesterol loading of mouse peritoneal macrophages results in downregulation of cholesterol biosynthesis, which consequently increases intracellular concentrations of a very specific oxysterol, desmosterol. Importantly, desmosterol is a potent activator of the liver X receptor (LXR), a nuclear hormone receptor that is known to mediate anti-inflammatory processes (Spann et al., 2012). Collectively, these studies suggest that understanding macrophage inflammatory responses in the context of hypercholesterolemia requires further study. This controversy will be further elaborated on in Chapter 3 of this thesis.

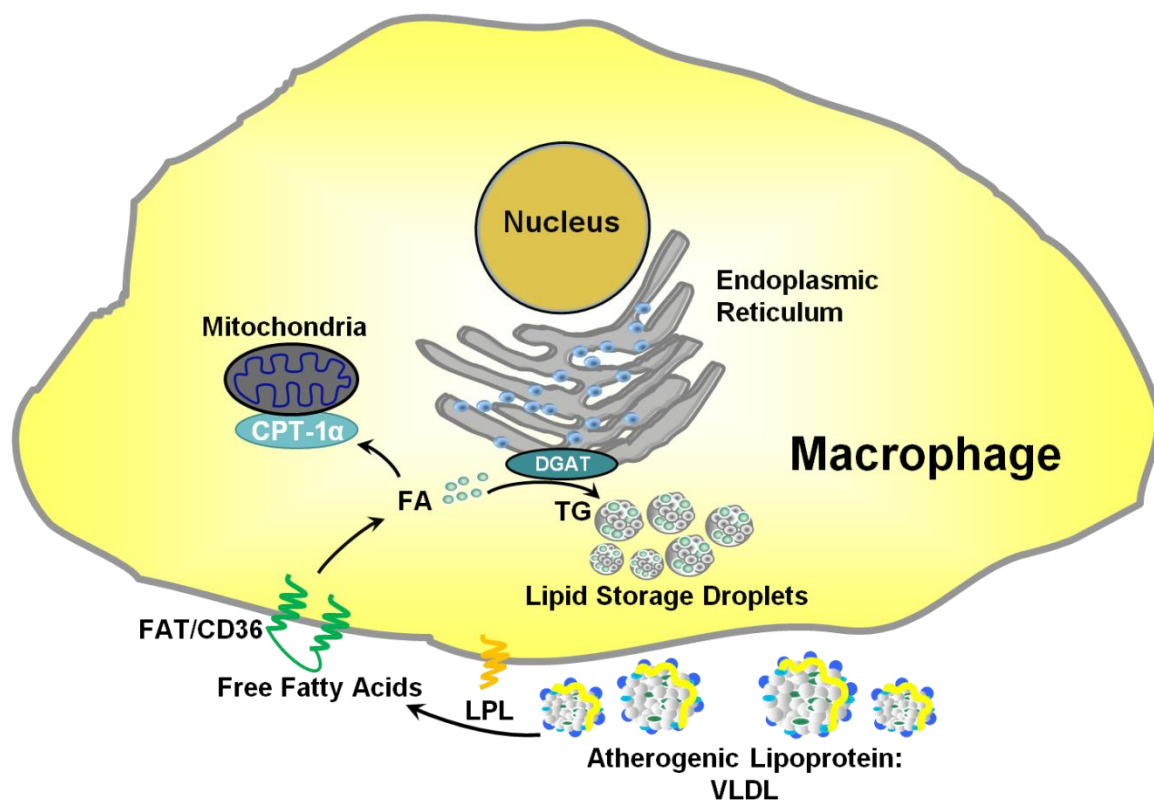
1.2.4 TRIGLYCERIDE-RICH MACROPHAGE FOAM CELLS

The canonical atherogenic lipoprotein is CE-rich LDL. However, elevated plasma TG-rich VLDL is now regarded as a significant contributor to the development of cardiovascular disease, particularly in the context of insulin resistance and type 2 diabetes (Talayero and Sacks, 2011). Although a causal relationship between TGs and atherosclerosis has been difficult to establish (Goldberg et al., 2011), TG-rich apoB-containing lipoproteins have been localized in plaques isolated from humans as well as animal models of disease (Proctor and Mamo, 1998, Rapp et al., 1994), justifying further investigation of the impact of these lipoproteins on macrophage foam cell formation.

It is well established that VLDL readily stimulates TG accumulation in macrophages (Figure 1.3), which is initiated by cell-surface bound lipoprotein lipase (LPL) hydrolyzing the TG-rich core of VLDL particles (Bates et al., 1984, Huff et al., 1991). The liberated fatty acids (FAs) are subsequently taken up by cells either via passive diffusion or via protein-mediated uptake by the FA translocase (FAT)/CD36. Upon internalization, FA binding proteins transport FAs to the outer mitochondrial membrane for activation to fatty acyl-CoAs by acyl-CoA synthetases (Yen et al., 2008).

Figure 1.3: VLDL-induced foam cell formation.

The interaction between VLDL and cell-surface bound lipoprotein lipase (LPL) results in the hydrolysis of the VLDL TG-rich core to free fatty acids (FFAs). These FFAs are internalized either via passive diffusion or protein-mediated uptake by the fatty acid translocase (FAT) CD36. Upon internalization, FFAs are either re-esterified into TG by the DGAT enzymes for storage in cytoplasmic lipid droplets, or transported into the mitochondria by CPT1 α for fatty acid β -oxidation. Excessive fatty acid uptake without sufficient β -oxidation results in the development of TG-rich macrophage foam cells.



This activation step is a requirement for further FA trafficking within the cell. For example, the acyl-CoA:diacylglycerol acyltransferase (DGAT) enzymes catalyze the re-esterification of FAs into triacylglycerol for storage in cytoplasmic lipid droplets, and use activated fatty acyl-CoAs as the acyl donors (Yen et al., 2008). Although the exact process by which TG is deposited into lipid droplets is not fully understood, it is believed that the DGAT enzymes synthesize TGs mainly at the lipid bilayer of the ER (Walther and Farese, 2012). Nevertheless, macrophage exposure to VLDL stimulates foam cell formation due to substantial accumulation of cytoplasmic TG. It is therefore important that the process of FA β -oxidation maintains TG homeostasis to prevent excessive accumulation of lipid-laden macrophages in the arterial intima. Fatty acid oxidation will be discussed in detail in section 1.4.4.

1.2.5 INFLAMMATION IN TRIGLYCERIDE-RICH FOAM CELLS

Although TG-rich macrophages are by definition foam cells, the induction of inflammatory responses does not occur in response to TG accumulation *per se*. Rather, the stimulation of macrophage inflammation and cytotoxicity is thought to occur as a consequence of VLDL-derived free fatty acid (FFA) exposure to cells. Inhibition of LPL resulted in complete abrogation of the VLDL-stimulated inflammatory response in mouse peritoneal macrophages (Saraswathi and Hasty, 2006). Additionally, peritoneal macrophages and bone marrow-derived macrophages isolated from *Dgat1* transgenic mice fed a high fat diet accumulate a significant amount of TG, but were protected from an inflammatory response (Koliwad et al., 2010), which further demonstrates that FFAs are responsible for an inflamed macrophage phenotype rather than TGs themselves. A number of groups independently suggested that FFAs activate TLR-dependent signaling to generate macrophage inflammation and lipotoxicity (Lee et al., 2004a, Shi et al., 2006). However, this claim has more recently been cast in doubt by other studies (Anderson et al., 2012, Erridge and Samani, 2009).

VLDL-derived FAs elicit macrophage inflammatory responses, at least in part due to stimulation of MAPK signaling. The MAP kinases extracellular signal-related kinase (ERK)1/2 and p38 cooperatively regulate the activated protein (AP)-1 transcription factor (Figure 1.4), which is known to participate in the induction of a host of proinflammatory cytokines (Eferl and Wagner, 2003). VLDL not only stimulates ERK1/2 activation (Saraswathi and Hasty, 2006), but it also potentiates LPS-induced cytokine expression (Stollenwerk et al., 2005), attributable to the simultaneous activation of parallel pathways by each stimulus. In addition to inducing MAPK signaling, VLDL-derived FAs can also promote an insulin-resistant macrophage phenotype, which can potentiate the inflammatory response (Su et al., 2009). The impact of macrophage insulin resistance on inflammation, apoptosis and atherosclerosis will be further discussed in section 1.5.3.2 of this thesis. Interestingly, in contrast to free cholesterol-induced macrophage inflammation, FFA-induced cytokine expression does not require Nfkb activation (Erridge and Samani, 2009).

The induction of macrophage foam cell formation and the inflammatory response by VLDL, as well as the ability of peroxisome proliferator-activated receptor (PPAR)- δ activation to attenuate these effects is the topic of Chapter 2 of this thesis (Bojic et al., 2012).

1.2.6 ATHEROSCLEROTIC LESION PROGRESSION

The stages of atherosclerosis are numerically classified based on histological features at each stage of the disease (Stary, 2000). Initial lesions, classified as Type I (Stary et al., 1994), are characterized by thickening of the arterial intima due to the accumulation of lipoproteins and increased cellularity (Figure 1.5), with development of isolated groups of macrophage foam cells. In many cases, Type I lesions can be detected during infancy (Stary et al., 1994). As foam cell accumulation persists to the point of gross microscopic detection, the lesion becomes classified as Type II, also

Figure 1.4: VLDL-induced MAPK signaling in macrophage foam cells.

VLDL-derived FAs stimulate the phosphorylation of the MAP kinases extracellular signal-related kinase (ERK)1/2 and p38 via mechanisms that remain to be elucidated. Phosphorylated ERK1/2 and p38 cooperatively stimulate the activation of the activated protein (AP)-1 transcription factor. Activated AP-1 translocates into the nucleus where it binds to AP-1 response elements (AP-1RE) within promoter regions of proinflammatory cytokine genes.

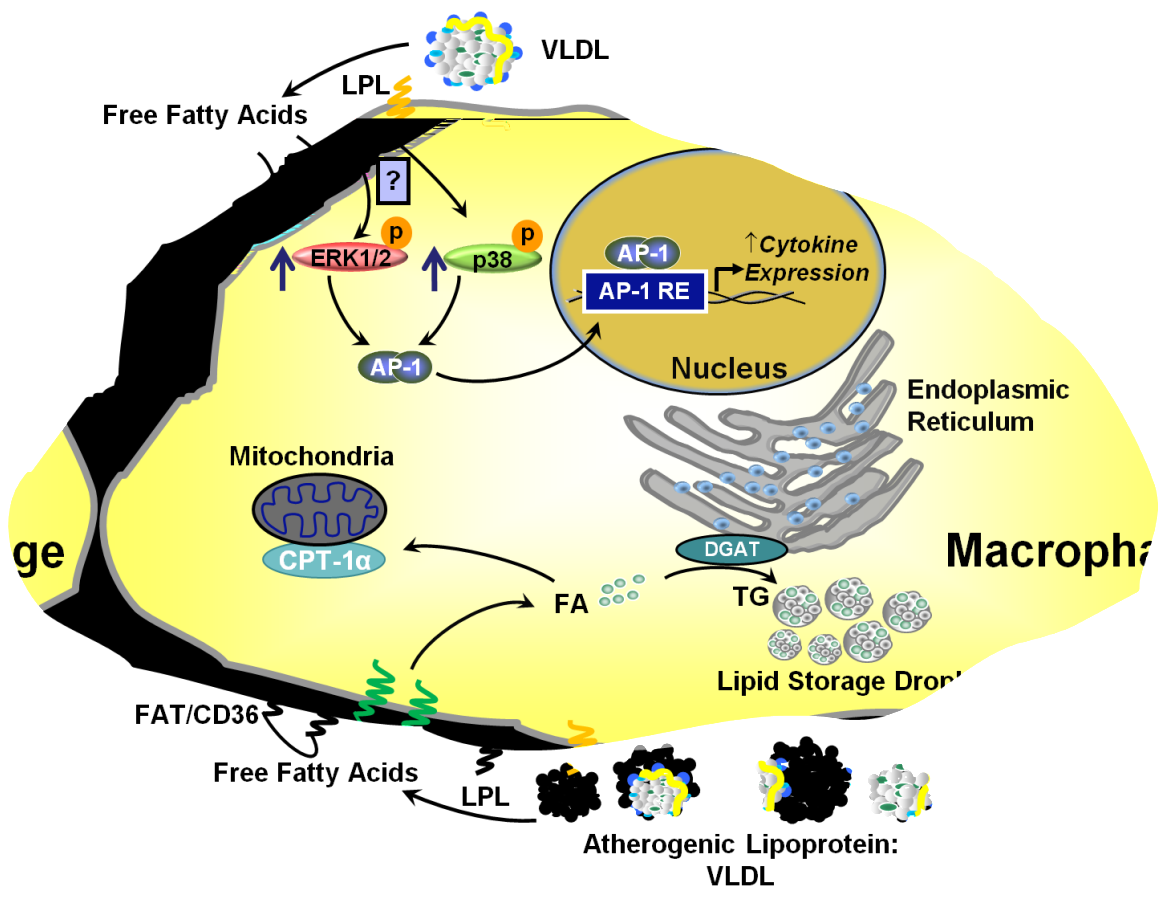
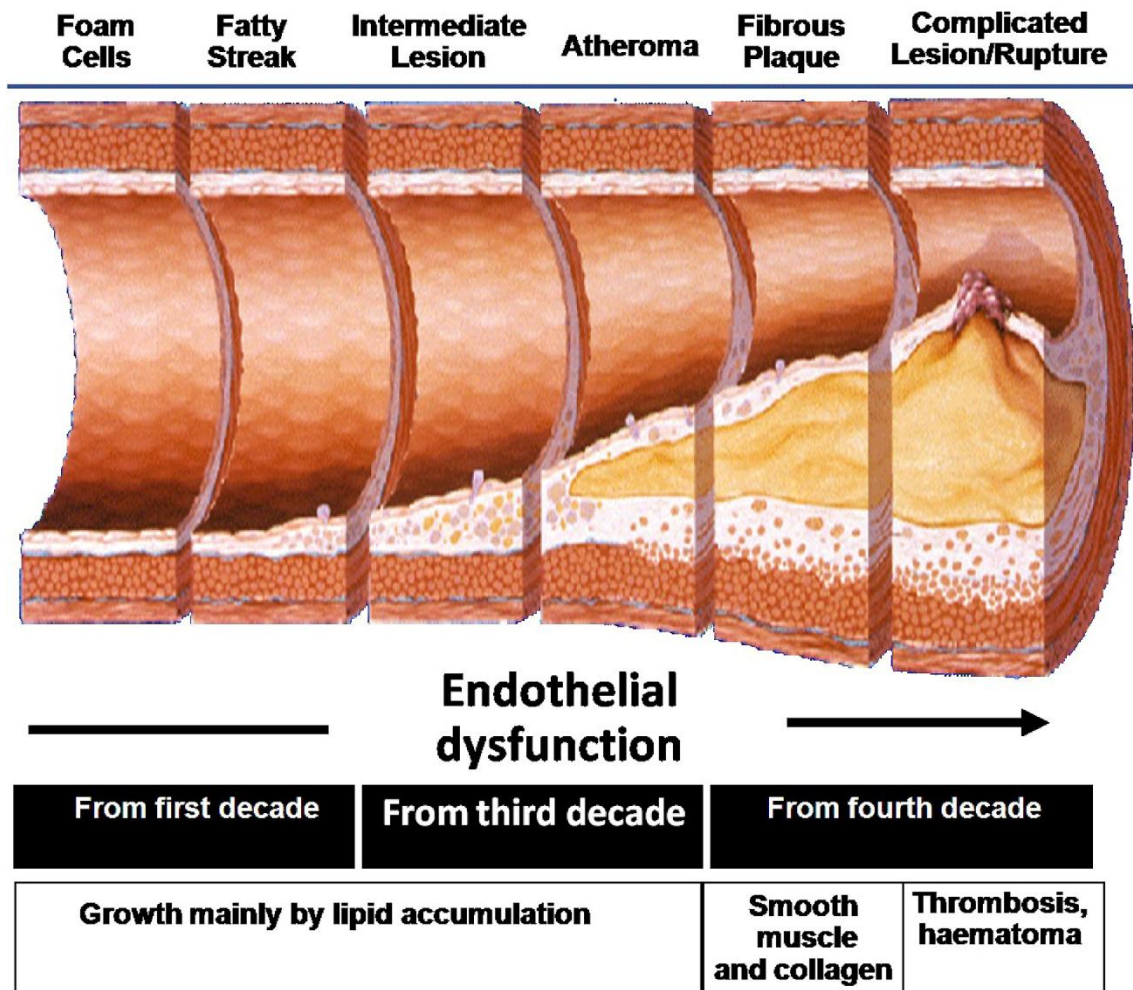


Figure 1.5: Atherosclerotic Lesion Progression.

Endothelial dysfunction and build up of arterial lipids and lipoproteins stimulate the recruitment of macrophages to the site of vascular insult. Macrophages of the arterial intima scavenge lipoprotein-derived lipids, resulting in foam cell formation. Excessive macrophage foam cell accumulation results in the development of a lipid core associated with proinflammatory immune responses. To stabilize the expanding lipid core, smooth muscle cells are stimulated by inflammatory effectors from the lesion to proliferate into the plaque and deposit extracellular matrix proteins such as collagen. This results in the formation of a fibrous plaque. Consequences of unresolved atherogenesis include vessel occlusion, rupture and thrombosis, all of which can induce an acute cardiovascular event such as myocardial infarction or stroke.



Adapted from illustration an illustration by Grahams Child

referred to as a fatty streak. At this stage, smooth muscle cells indigenous to the lesion location can also take up lipid resulting in a smooth muscle cell-foam cell phenotype (Stary et al., 1994). The bridge between Type II lesions and advanced plaques are Type III intermediate lesions, for which the major histological feature is microscopically visible extracellular pools of lipid, namely cholesterol crystals (Stary et al., 1994). This is most likely due to the onset of ER-stress-induced apoptosis of macrophage foam cells as a consequence of unresolved inflammation in the plaque, coupled to defective clearance of dead cells and debris by phagocytic immune cells (Moore and Tabas, 2011). Despite monocyte recruitment persisting at all stages of lesion development in efforts to clear the atherogenic substrates and debris (Swirski et al., 2006), the presence of extracellular cholesterol crystals and debris disrupts and displaces extracellular matrix within the lesion. Consequently, the classification extends to Type IV lesions, or atheromas, which are characterized by the presence of a defined lipid core causing severe intimal disorganization (Stary et al., 1995). Secondary necrosis is also a major feature of Type IV lesions as a result of continued ER-stress-induced apoptosis as discussed in section 1.2.3. It is important to note that Type I to III lesions are clinically silent, and it is at the Type IV lesion stage that blood flow may begin to be significantly disrupted and lead to compromised arterial function (Stary, 2000). Intimal and newly recruited medial smooth muscle cells increase the presence of fibrotic tissue in the plaque, which consists of elastin, collagen, proteoglycans and glycoproteins that forms a fibrous cap as an effort to stabilize the necrotic lipid core. The presence of this cap is the prominent new feature that defines the progression to Type V lesions (Stary et al., 1995). Despite increased fibrous cap formation, local immune cells produce matrix-metalloproteinases that degrade the deposited extracellular matrix, which eventually leads to fibrous cap thinning (Weber et al., 2008). The resultant lesions are prone to neovascularization, which increases leakage, hemorrhage, and rupture (Weber et al., 2008). All of these processes

contribute to the contact of plaque debris with the circulation, triggering coagulation and thrombus formation, thereby increasing likelihood of arterial occlusion leading to myocardial infarction or stroke. Therefore, whether lesion progression, stabilization or regression occurs is determined by the complex interactions between the physical and environmental factors within the lesion.

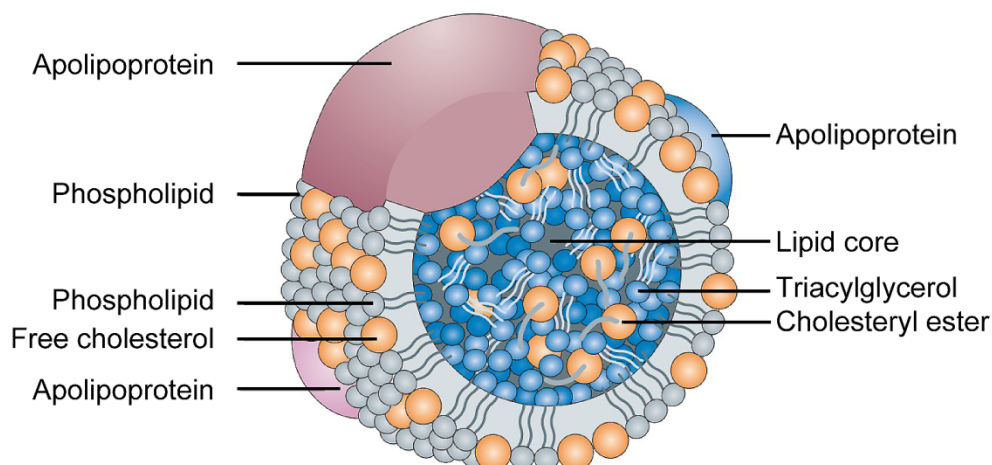
1.3 LIPOPROTEIN METABOLISM

Whole body lipid homeostasis is maintained through a balance between exogenous uptake and endogenous synthesis of fatty acids and cholesterol, as well as the trafficking of these lipids in macromolecular complexes called lipoproteins.

1.3.1 LIPOPROTEINS

All lipoproteins are spherical, soluble lipid carriers comprised of a hydrophobic TG and CE rich core encased by a hydrophilic monolayer of phospholipids, free cholesterol and apolipoproteins (Hegele, 2009). The classification of lipoproteins is based on their density, lipid composition and apolipoprotein association (Table 1.1). In addition to providing structural support to lipoprotein complexes, apolipoproteins also determine the interaction of lipoproteins with cell surface receptors as well as their rate of catabolism.

The largest lipoproteins are chylomicrons which are formed in the intestine and transport dietary TGs on an apoB48 backbone, with trace amounts of dietary cholesterol. Very low-density lipoproteins (VLDL), secreted by hepatocytes, carry endogenous TG with modest amounts of endogenous as well as exogenous CE on an apoB100-backbone, and are associated with apoEs and apoCs. The catabolism of VLDL results in VLDL-remnant lipoproteins called intermediate density lipoproteins (IDL), which transport roughly equal partitions of TG and CE. Further catabolism of IDL followed by a series of

TABLE 1-1 Lipoprotein Classification

Lipoprotein Class	Percent Composition	Site of Origin	Associated Apolipoproteins	Primary Function
Chylomicrons	84% TG 8% PL 6% CE 2% protein	Intestine	A1, AII, AIV, B48, CII, CIII, E	Delivery of dietary TG
Very Low Density Lipoproteins (VLDL)	56% TG 20% PL 15% CE 9% protein	Liver	B100, C1, CII, CIII, E	Delivery of endogenous TG
Intermediate Density Lipoproteins (IDL)	29% TG 26% PL 34% CE 11% protein	VLDL catabolism	B100, C1, CII, CIII, E	Delivery of endogenous TG and CE
Low Density Lipoproteins (LDL)	8% TG 22% PL 50% CE 20% protein	VLDL catabolism	B100	Delivery of cholesterol
High Density Lipoproteins (HDL)	8% TG 30% PL 29% CE 33% protein	Peripheral lipidation of liver and intestine secreted apoA1	A1, AII	Reverse cholesterol transport from periphery to liver

Adapted from (Wasan et al., 2008). *Nat Rev Drug Discov*, 1, 84-99.

modifications and lipid exchanges with various lipoproteins, results in the formation of CE-rich LDL particles (Hegele, 2009).

Cholesteryl Ester is also transported by HDL, the smallest lipoprotein type. The protein backbone of HDL particles is apoA1, which is predominantly secreted from the liver and initially lipidated by hepatic ABCA1 (Timmins et al., 2005). This lipidation results in the formation of nascent HDL which enters the plasma and undergoes a series of enzymatic lipid transfer modifications to form mature HDL (Sorci-Thomas and Thomas, 2012). Cholesterol is effluxed to HDL as free cholesterol and is re-esterified into the hydrophobic core of the particles by HDL-associated lecithin-cholesterol acyltransferase (LCAT). Once HDL becomes CE-enriched, it can be remodeled by cholesteryl ester transfer protein (CETP) in plasma which facilitates the movement of CE from HDL to VLDL in exchange for TG. In turn, HDL particles become better substrates for hepatic lipase (HL). Mature HDL particles serve as carriers of cholesterol from the periphery to the liver, where cholesterol is converted to bile acids for subsequent excretion (Repa and Mangelsdorf, 2000).

1.3.2 EXOGENOUS LIPOPROTEIN METABOLISM

Absorption of dietary lipids occurs in the jejunal portion of the small intestine. Cholesterol is absorbed via protein-mediated uptake by the transporter Niemann-Pick C1-like1 (NPC1L1) on the brush-boarder membrane of the intestinal lumen (Huff et al., 2006), whereas dietary TG requires hydrolysis by pancreatic lipase before it can be taken up by soluble passive diffusion. Upon internalization into intestinal enterocytes, fatty acids are sequentially re-esterified into TG by the MGAT and DGAT enzymes. It is dietary TG, rather than cholesterol, which determines the rate of formation of the exogenously derived TG-rich chylomicron particles (Karpe, 2002). The apoB48 backbone of chylomicrons is derived from editing of full-length *APOB* mRNA by the apoB mRNA editing enzyme (APOBEC1), which deaminates cytidine 6666 of the *APOB*

transcript to a uridine (Rosenberg et al., 2011). This results in a change at position 2153 of the apoB protein from glutamine to a stop codon, yielding a translated protein that is the N-terminal 48% of the 550kDa polypeptide apoB100 chain (Chen et al., 1987). In humans, APOBEC1 is expressed exclusively in the intestine, whereas mice express this enzyme in both intestine and liver. ApoB48 is cotranslationally lipidated with TG, CE and phospholipids by microsomal triglyceride transfer protein (MTP) within the ER of intestinal enterocytes prior to secretion into the lymphatic system as a chylomicron (Figure 1.6).

Chylomicrons, upon entry into the lymphatics and into plasma, become associated with apoEs and apoCs, both of which are required for the metabolism of chylomicron particles. Specifically, apoCII is required for the activation of TG hydrolysis by LPL, an enzyme which is secreted by parenchymal cells of muscle and adipose tissue, and is anchored to capillary endothelial cells by heparin sulfate proteoglycans. Chylomicron-derived FFAs and glycerols are taken up predominantly by adipose tissue and re-esterified into TGs for storage. The resultant chylomicron remnant particles are efficiently taken up by the liver through LDLR- and LDL receptor related protein (LRP)-mediated uptake by recognition of apoE (Blasiolo et al., 2007), concluding the exogenous lipid metabolism pathway.

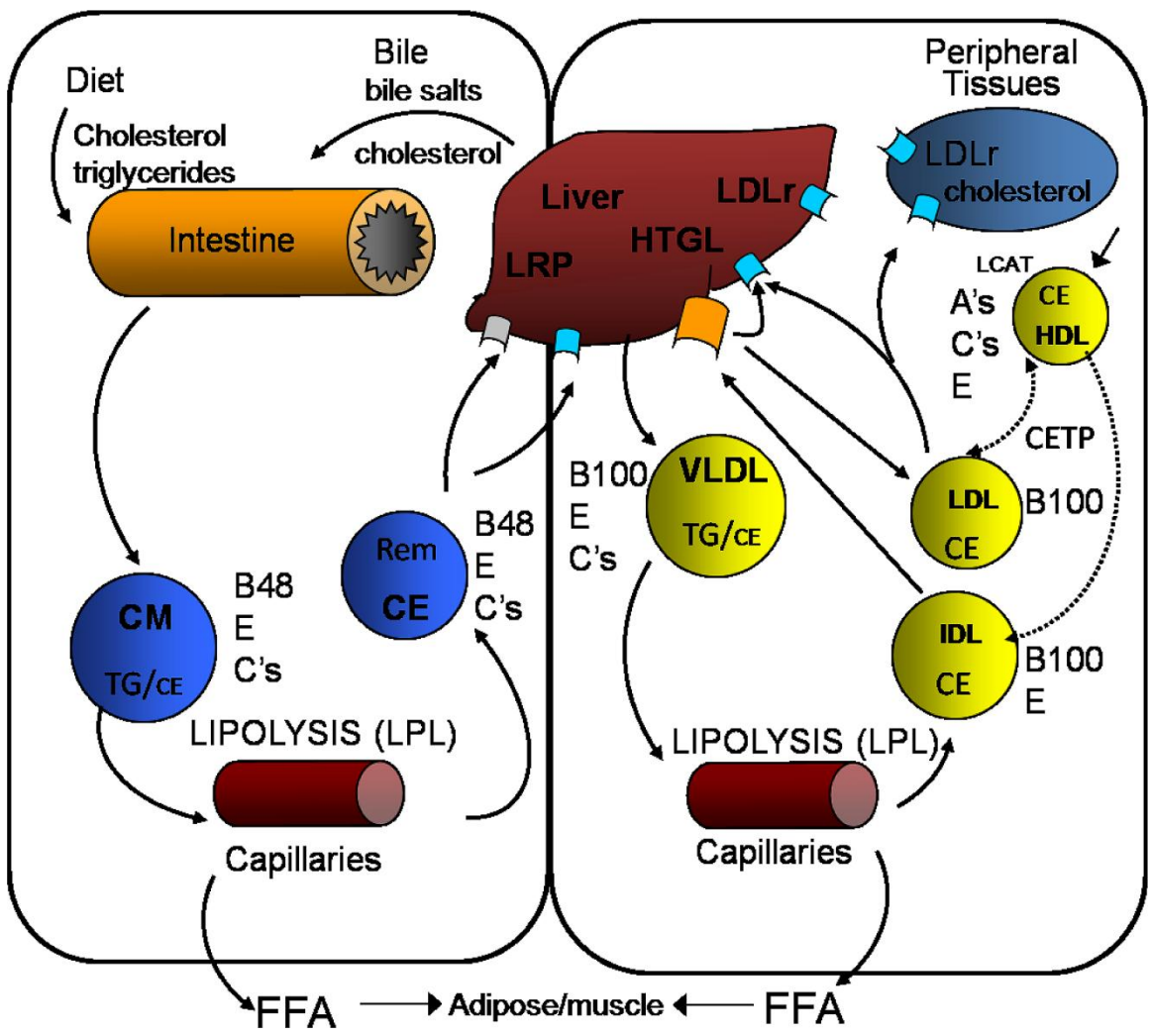
1.3.3 ENDOGENOUS LIPOPROTEIN METABOLISM

The endogenous lipoprotein pathway begins with the recycling of TG and cholesterol from chylomicron remnants in the liver, intersecting with the hepatic *de novo* synthesis of these lipids. Approximately 80% of circulating cholesterol is produced by the body, mostly in hepatocytes, making the liver the primary regulator of whole body cholesterol and lipid homeostasis (Hegele, 2009).

Synthesis of both cholesterol and TG begins with the formation of acetyl-CoA derived from the metabolism of glucose or fatty acids. The 32-step cholesterol

Figure 1.6: Endogenous and Exogenous Lipoprotein Metabolism.

Dietary triglycerides and cholesterol are packaged onto apoB48 within the intestinal enterocytes. The resultant chylomicron particles are secreted into the lymphatics, which subsequently enter the blood stream. Lipoprotein lipase (LPL) hydrolyzes triglycerides (TGs) which allows uptake of free fatty acids (FFAs) into peripheral tissues. The remnant cholesteryl ester (CE)-rich particle is taken up by the liver through LDL receptor (LDLR)- and LDLR related protein (LRP)-mediated endocytosis. Dietary and newly synthesized lipids are packaged onto apoB100, which is secreted by the liver as VLDL. These particles also undergo hydrolysis by LPL. The CE-rich VLDL-remnant particles (IDL), and IDL modified to LDL particles, can be taken up by the liver or peripheral tissues through the LDLR. The reverse cholesterol transport pathway involves the removal of cholesterol from peripheral tissues via efflux to HDL. This lipoprotein particle is efficiently cleared by SR-BI in the liver, where cholesterol is converted to bile acids for excretion in bile.



biosynthetic pathway is initiated by the condensation of two acetyl-CoA molecules to produce acetoacetyl-CoA, which is the substrate for HMG-CoA-synthase in the formation of HMG-CoA. Subsequently, HMG-CoA-reductase, the rate-limiting enzyme in the cascade and target of statins, catalyzes the generation of mevalonate, which through a series of condensation reactions yields squalene. The cyclization of squalene produces lanosterol, which is converted to cholesterol through a further 19-step process with the final reaction being the conversion of desmosterol to cholesterol by dehydrocholesterol reductase (DHCR) 24.

Fatty acid synthesis is initiated by the carboxylation of acetyl-CoA by acetyl-CoA carboxylase (ACC) to malonyl-CoA, which is subsequently elongated to palmitic acid by fatty acid synthase (FAS). Fatty acids can then be further elongated and/or monounsaturated prior to subsequent esterification into TG by the MGAT and DGAT enzymes in the ER.

The availability of both cholesterol and TG is required for the formation of VLDL particles. The apoB100 backbone of VLDL is cotranslationally lipidated by MTP exclusively in the liver prior to its secretion into the bloodstream. Within capillary beds of target tissues such as adipose and muscle, endothelial cell LPL hydrolyzes the TG-rich VLDL core liberating FFAs and glycerol which are taken up via soluble passive diffusion or CD36-mediated uptake. Re-esterification into TGs in adipose or fatty acid oxidation in muscle ensues. Following LPL-mediated hydrolysis of VLDL particles, VLDL-remnants or IDLs are formed, which can be taken up by recognition of apoE by the LDLR or the LRP following HL modification (Hu et al., 2008). Alternatively, IDL can become further enriched in CE from HDL via CETP, and can be further modified by HL, consequently resulting in the formation small dense CE-rich LDL particles. In humans, IDL modification leading to LDL formation is the predominant pathway.

The final lipoprotein in the endogenous pathway is CE-rich LDL, which is mainly taken up receptor-mediated endocytosis. The LDLR is expressed ubiquitously, recognizes apoB100 and mediates the principal mechanism of LDL uptake. It accounts for approximately one third of LDL uptake by extrahepatic tissues. However, the liver is the primary site of LDLR expression and therefore regulates most of the clearance of circulating LDL particles.

1.4 REGULATION OF FATTY ACID AND CHOLESTEROL METABOLISM

1.4.1 STEROL REGULATORY ELEMENT BINDING PROTEINS

The sterol regulatory element binding proteins (SREBPs) are the master transcriptional regulators of lipid homeostasis (Horton et al., 2002). The three isoforms of the SREBP family are encoded by two genes; *SREBP1*, which generates the SREBP-1a and SREBP-1c isoforms through the use of different promoters to produce alternate forms of exon 1, and *SREBP2* (Horton et al., 2002). The three members of the SREBP family have distinct but overlapping transcriptional programs. SREBP-1c is expressed predominantly in hepatocytes, where it directly activates the expression of genes involved in fatty acid synthesis and elongation in response to increases in plasma insulin levels. SREBP-1a and SREBP-2 are expressed ubiquitously where they regulate genes involved in cholesterol homeostasis in response to intracellular sterol concentrations (Shao and Espenshade, 2012).

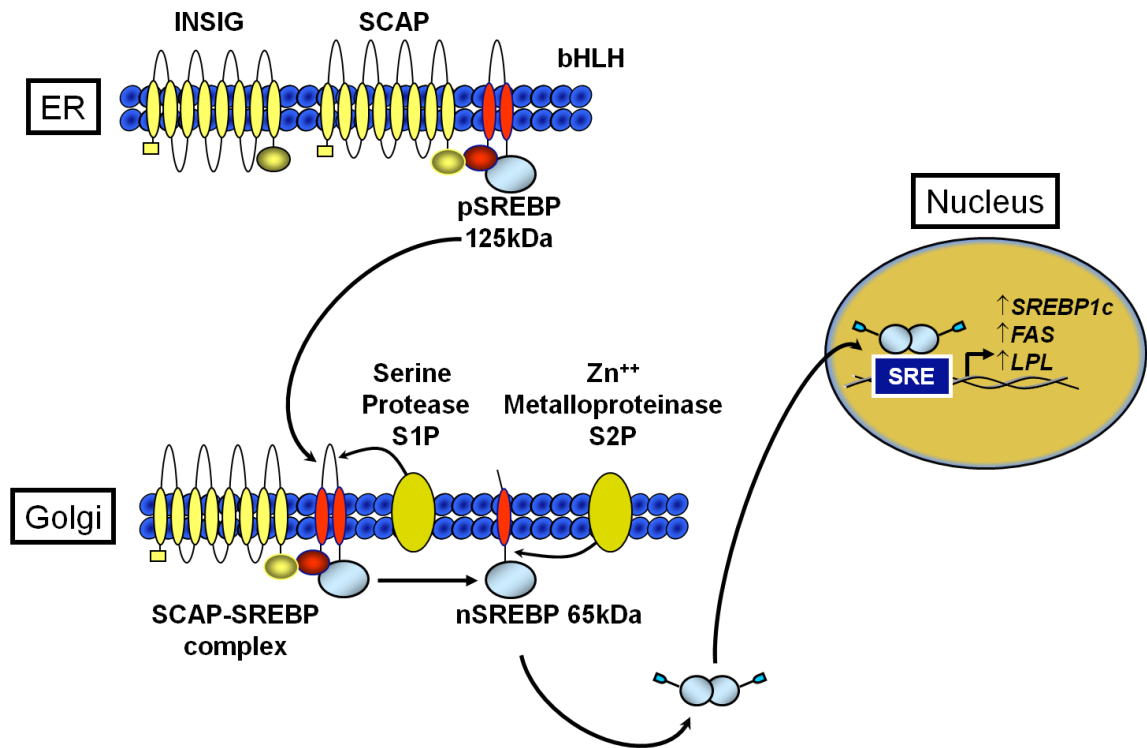
All three SREBPs contain three basic domains: (i) an N-terminal basic helix-loop-helix (bHLH) leucine zipper DNA binding motif for binding to sterol response elements (SREs) within promoter regions of their target genes, (ii) two hydrophobic transmembrane domains separated by a short loop that projects into the lumen of the ER and (iii) a regulatory C-terminal domain that interacts with the SREBP cleavage activating protein (SCAP) (Horton et al., 2002). The SREBPs are synthesized as inactive precursors, retained in the ER due to their interaction with SCAP through the MELADL

peptide sequence (Sun et al., 2005). Under conditions of high intracellular sterols, SCAP also interacts with the insulin induced genes (INSIG) 1/2; ER-anchor proteins that retain the SCAP/SREBP complex in the ER. When sterols are depleted, SCAP undergoes a conformational change resulting in the dissociation from INSIG, which allows access of COPII vesicles containing a Sar-1/Sec23/Sec24 complex to SCAP/SREBP. In turn, the SCAP/SREBP complex is trafficked to the Golgi for processing to active transcription factors (Sun et al., 2005). Depletion of hepatic SCAP results in the complete absence of processing of all three SREBPs, concomitant with normalization of lipogenesis and hypertriglyceridemia (Moon et al., 2012), demonstrating a lack of redundancy for SCAP-mediated SREBP transport to the Golgi. Once the SCAP/SREBP complex reaches the Golgi, SREBPs undergo sequential cleavage by the Site 1 and Site 2 proteases (Shao and Espenshade, 2012). The Site 1 protease is a serine protease that cleaves the ER-luminal loop separating the SREBP transmembrane domains. Subsequently, the Site 2 zinc metalloproteinase releases the N-terminal bHLH leucine zipper fragment, allowing for its translocation into the nucleus where it binds to SREs within target gene promoters (Figure 1.7) (Shao and Espenshade, 2012). SREBP-1a and SREBP-2 activate transcription of genes involved in cholesterol uptake and cholesterol synthesis such as LDLR and HMG-CoA reductase, to restore sterol balance (Shao and Espenshade, 2012). SREBP-1c on the other hand, stimulates the expression of genes involved in fatty acid synthesis and elongation, including ACC, FAS and stearoyl-CoA desaturase (SCD) (Moon et al., 2012).

In addition to SCAP, the INSIGs provide another layer of trafficking regulation to the SREBPs, owing to a convergent feedback loop (Goldstein et al., 2006). The two INSIG isoforms (INSIG-1 and INSIG-2) are protein products of separate genes and are differentially regulated. INSIG-1 transcription is activated by SREBP-1c in a feed forward mechanism to regulate the amount of cholesterol being restored. INSIG-2 produces two

Figure 1.7: Regulation of the Sterol Regulatory Element Binding Proteins.

The sterol regulatory element binding proteins (SREBP) reside in the endoplasmic reticulum (ER) membrane as inactive precursors. During periods of high intracellular sterol, SREBPs interact with SREBP cleavage activating protein (SCAP), which in turn interacts with Insig to retain SREBPs within the ER membrane. Upon depletion of intracellular sterol, or insulin-mediated degradation of Insig, the dissociation of SCAP from Insig results in the trafficking of the SCAP-SREBP complex to the Golgi where sequential processing by Site 1 (S1P) and Site 2 proteases (S2P) releases the active nuclear SREBP transcription factor. SREBP transcription factors translocate into the nucleus and bind to sterol regulatory elements (SREs) within promoter regions of genes required for lipogenesis.



Adapted from (Shao and Espenshade, 2012). *Cell Metab*, 16, 414-9.

transcripts that encode the same protein, but are differentially regulated. INSIG-2a is a liver-specific isoform whereas INSIG-2b is ubiquitously expressed, yet has very low liver expression (Goldstein et al., 2006). Evidence that the INSIGs are required for the regulation of lipid homeostasis in liver was provided by Engelking and colleagues, when they simultaneously disrupted hepatic INSIG-1 and -2 (Engelking et al., 2005). The resultant phenotype was profound hepatic steatosis on a chow diet as a result of hyperactive SREBP-mediated lipogenesis, demonstrating that the INSIG proteins are essential for SREBP feedback regulation (Engelking et al., 2005).

The INSIGs are also regulated by plasma insulin, which sets the stage for reciprocal regulation during fasting and feeding cycles (Goldstein et al., 2006). As mentioned above, SREBP-1c is activated in response to increases in circulating insulin. During the fasted state, plasma insulin is low. In turn, SREBP-1c is inactive meaning that INSIG-1 expression is low. However, INSIG-2a levels are high, which contributes to SREBP-1c retention in the ER during the fasted state. As plasma insulin rises during feeding, INSIG-2a is rapidly degraded by Akt-dependent mechanisms allowing for SREBP-1c processing and translocation into the nucleus (Yecies et al., 2011). As a result, INSIG-1 levels increase owing to convergent feedback regulation, resulting in the prevention of SREBP-1c hyperactivity. In mice overexpressing hepatic *Insig1*, normal fasting/re-feeding regulation of INSIG-2 ensues, yet the livers of these animals are resistant to acute lipogenesis in the fed state (Engelking et al., 2004). This suggests that insulin-mediated suppression of INSIG-2 is required for insulin-induced SREBP-1c lipogenesis during feeding. In states of insulin resistance, hyperinsulinemia persists during fasting, resulting in the chronic downregulation of INSIG-2, which in part contributes to the hyperactivity of SREBP-1c-mediated lipogenesis (Yecies et al., 2011).

1.4.2 DE NOVO LIPOGENESIS

Lipolysis of adipose tissue TG is the major contributor of FAs to VLDL-TG during periods of fasting (Zechner et al., 2012), while *de novo* lipogenesis is a minor contributor (Barrows and Parks, 2006). However during feeding, adipose tissue lipolysis is suppressed whereas hepatic *de novo* lipogenesis is simultaneously increased by insulin. Consequently, a major contributor to the pool of FAs for VLDL-TG in the fed state is *de novo* lipogenesis.

The synthesis of FAs begins with the carboxylation of acetyl-CoA to malonyl-CoA by ACC. Subsequently, malonyl-CoA provides two carbon units to FAS for the synthesis of 16 and 18 carbon saturated fatty acids. The resultant fatty acids require activation by long chain acyl-CoAs synthetase to fatty acyl-CoA before they can become substrates for subsequent processing or partitioning (Walther and Farese, 2012). Fatty acyl-CoAs are stearoyl CoA-desaturase (SCD) substrates for desaturation and subsequent esterification to cholesterol in the production of cholesteryl esters. Additionally, activated fatty acids are also used by CPT1 α and DGAT for entrance into the mitochondria for fatty acid oxidation and for re-esterification of fatty acids into TGs, respectively (Walther and Farese, 2012).

The generation of TG is the major mechanism for metabolic fuel storage in living organisms (Yen et al., 2008). Two convergent pathways contribute to TG production, both of which utilize fatty acyl-CoAs as acyl donors. The canonical glycerol phosphate pathway occurs in most tissues and begins with the acylation of glycerol-3-phosphate by acyl-CoA:glycerol-3-phosphate acyltransferase to yield lysophosphatidic acid. Subsequently, lysophosphatidic acid is further acylated and dephosphorylated to produce diacylglycerol (DG) (Liu et al., 2012). In the monoacylglycerol pathway, which occurs mainly in the intestine, liver and adipose tissue, fatty acyl-CoAs are esterified to the 2-position of monoacylglycerol by acyl-CoA:monoglycerol acyltransferase (MGAT) to

produce DG (Liu et al., 2012). In the final step of TG synthesis, fatty acyl-CoAs are esterified to the 3-position of the resultant DG from either pathway by the DGAT enzymes (Liu et al., 2012). Newly synthesized TGs from both pathways are then transferred to cytoplasmic lipid droplets for storage via mechanisms that are not completely understood (Walther and Farese, 2012), or become incorporated into apoB-containing lipoproteins via MTP in the liver and intestine for secretion.

The esterification of fatty acyl-CoAs onto DG occurs via sequential reactions in the ER by the resident DGAT enzymes DGAT1 and DGAT2. Despite having similar function, the two DGAT isoforms differ in gene family as well as protein sequence, with *DGAT1* encoding a polypeptide chain approximately 35% longer than *DGAT2* (Liu et al., 2012). Nevertheless, DGAT1 is ubiquitously expressed but is most abundant in the small intestine and adipose tissue and is least abundant in the liver. Gene knockout studies revealed that *Dgat1*^{-/-} mice are resistant to diet-induced dyslipidemia, obesity and insulin resistance (Smith et al., 2000), whereas *Dgat2*^{-/-} mice die soon after birth due to lipopenia (Stone et al., 2004). Together these studies suggest that DGAT2 is responsible for the majority of TG synthesis required for survival.

Interestingly, overexpression of *Dgat1* specifically in white adipose tissue results in protection from diet-induced insulin resistance despite increased adiposity (Chen et al., 2002). Furthermore, overexpression of either form of DGAT in the liver results in a similar phenomenon. *Dgat1* or *Dgat2* liver-transgenic mice develop profound hepatic steatosis in the complete absence of insulin resistance. In addition, these mice do not accumulate any appreciable fat in skeletal muscle or adipose tissue and surprisingly display substantially reduced plasma triglycerides (Monetti et al., 2007). As discussed in section 1.2.5, macrophages isolated from *Dgat1* transgenic mice display significant TG accumulation without an overt inflammatory phenotype (Koliwad et al., 2010). Collectively these studies suggest that the efficient synthesis of TG by DGAT1 results in

the partitioning of fat into cytoplasmic lipid droplets which protects cells from FA overload, lipotoxicity and lipoprotein overproduction thus conferring protection from metabolic disturbance (Monetti et al., 2007).

1.4.3 CHOLESTEROL ESTERIFICATION

The ACAT enzymes are another group within the superfamily of membrane bound acyltransferases. ACAT1 and ACAT2 utilize fatty acyl-CoA donors and cholesterol as substrates in the esterification of cholesterol to generate CE for storage in cytoplasmic lipid droplets and lipoprotein secretion. The two isoforms are encoded by different genes and also differ in their tissue distribution. ACAT1 is ubiquitously expressed, whereas ACAT2 is found exclusively in the small intestine and liver. Knockout of *Acat1* results in normal cholesterol absorption as well as normal intestinal, hepatic and plasma lipids due to the compensation of cholesterol esterification by ACAT2. The most significant change in *Acat1*^{-/-} mice compared to their wild-type counterparts was virtually undetectable CE in the adrenal cortex and in isolated peritoneal macrophages (Meiner et al., 1996). In contrast, *Acat2*^{-/-} mice cannot synthesize CE within the intestine and as a result, have reduced capacity to absorb cholesterol from the diet. Additionally, these mice cannot synthesize CE in the liver and therefore do not become hypercholesterolemic when fed a high-fat high-cholesterol diet (Buhman et al., 2000).

The different physiological roles of the ACAT isoforms become more readily apparent when examining atherosclerosis. Breeding *Acat1*^{-/-} mice to either atherosclerosis susceptible *apoE*^{-/-} or *Ldlr*^{-/-} background does not protect from atherosclerosis (Accad et al., 2000). In fact, lesion complexity is exacerbated compared to *Acat1* WT on either background. In addition, bone marrow transplantation from *Acat1*^{-/-} mice to these atherogenesis models also worsens atherosclerosis lesion pathology (Fazio et al., 2001). As discussed in section 1.2.2, this is likely due to FC-induced ER-

stress, apoptosis and secondary necrosis as a result of the inability of macrophages to sequester cholesterol as metabolically inert CE. Subsequently, *Acat2*^{-/-} mice were bred to both *Ldlr*^{-/-} and *apoE*^{-/-} mice. In contrast to the *Acat1*^{-/-} crosses, *Acat2* deficiency protects against atherosclerosis (Lee et al., 2004b, Willner et al., 2003), probably owing to the lack of hypercholesterolemia in these animals as outlined above (Buhman et al., 2000). Finally, tissue-specific targeting of *Acat2* attenuates atherogenic dyslipidemia (Zhang et al., 2012). Collectively, these studies demonstrate that pharmacological inhibition of ACAT2 would likely be beneficial for treatment of atherosclerosis.

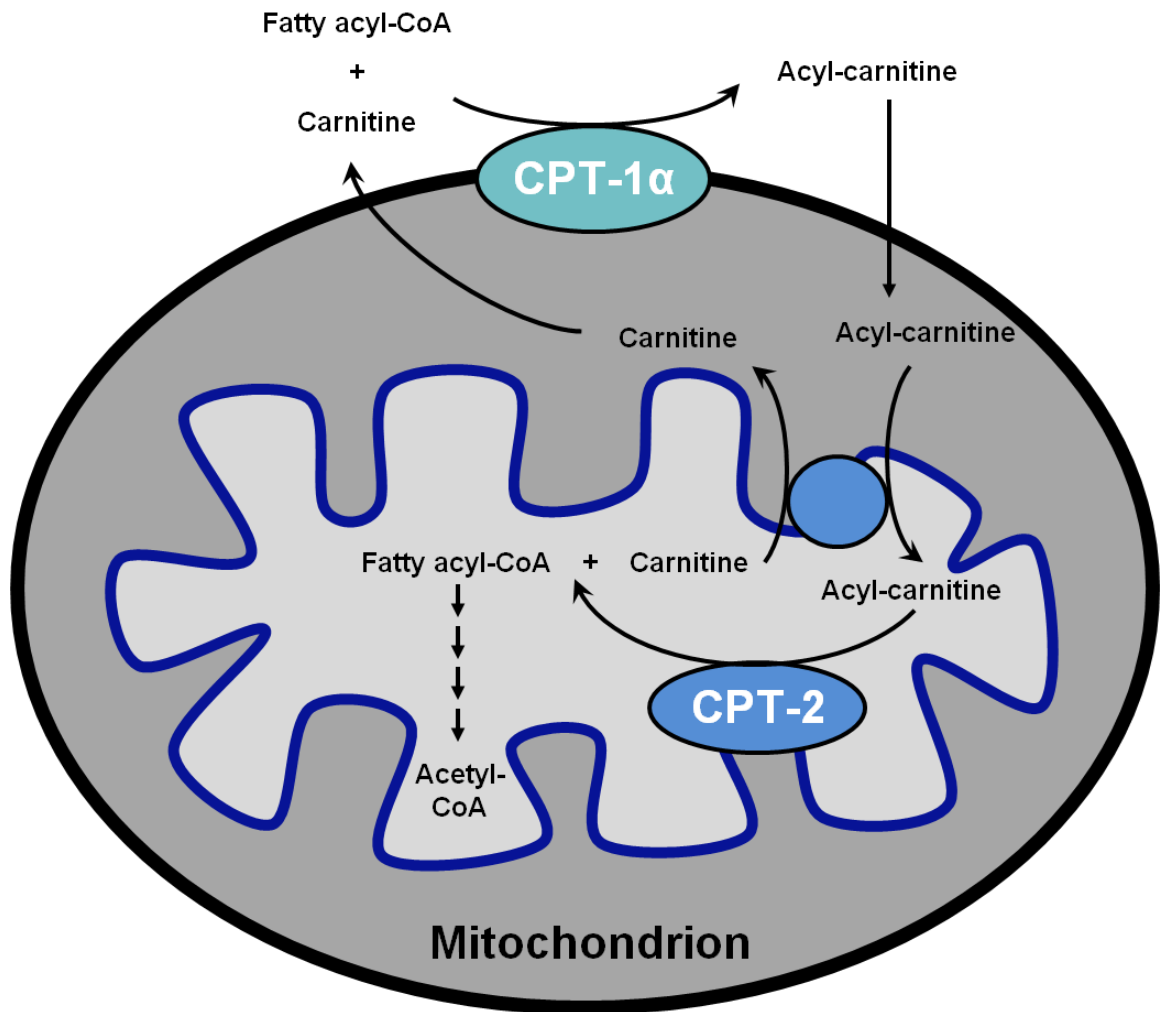
1.4.4 FATTY ACID OXIDATION

A critical process in maintaining lipid homeostasis and generating ATP is the oxidation of fatty acids. In hepatocytes, stimulation of fat oxidation also limits TG availability for VLDL assembly and secretion, in turn contributing to reduced plasma TG levels. In the muscle and heart, fatty acid oxidation is vital for the generation of ATP required for contractility. In macrophages, activation of fat oxidation is crucial to maintaining intracellular TG in balance with uptake and storage, which can contribute to reduced foam cell formation.

The rate-limiting step in the oxidation of fatty acids is CPT1-mediated entry into the mitochondria (Figure 1.8) (Bonnetfont et al., 2004). CPT1 is an outer mitochondrial membrane enzyme that uses activated fatty acyl-CoA donors in the production of acylcarnitine. Subsequently, acylcarnitine can freely translocate across the outer and inner mitochondrial membranes. Upon entry into the mitochondrial matrix, CPT2, which is localized on the inner mitochondrial membrane, catalyzes the reformation of fatty acyl-CoA, and liberates carnitine for subsequent CPT1-mediated reactions (Bonnetfont et al., 2004). Fatty acyl-CoA processing via four enzymatic steps ensues in the mitochondrial matrix to generate acetyl-CoA groups that can enter the Krebs's cycle to be oxidized for

Figure 1.8: The carnitine palmitoyl-transferase system.

Carnitine palmitoyl-transferase (CPT) 1 is located on the outer mitochondrial membrane, and uses activated fatty acyl-CoA donors in the production of acylcarnitine. The production of this intermediate allows for fatty acyl-carnitine to freely translocate across the outer and inner mitochondrial membranes. Upon entry into the mitochondrial matrix, CPT2, which is localized on the inner mitochondrial membrane, catalyzes the reformation of fatty acyl-CoA, and liberates carnitine for subsequent CPT1-mediated reactions. Fatty acyl-CoA processing via four enzymatic steps ensues in the mitochondrial matrix to generate acetyl-CoA groups which enter the Krebs's cycle to be oxidized for the production of ATP, CO₂ and water.



the production of ATP, CO₂ and water. In most tissues, CPT1 α is the predominant isoform that regulates fat oxidation. However, a CPT1 β isoform also exists, which is mainly expressed in the skeletal muscle, adipose tissue and heart (Bonnetfont et al., 2004).

Regulation of fat oxidation occurs via multiple mechanisms. CPT1 is regulated at a transcriptional level by a series of complex transcription factors including PPAR γ -coactivator 1 α (PGC1 α), PPAR α and PPAR δ . Additionally, CPT1 is also allosterically regulated by malonyl-CoA (Rasmussen et al., 2002). During periods of feeding, malonyl-CoA levels are high due to increased flux through the ACC *de novo* lipogenesis pathway as outlined above. Conversely, during periods of fasting, malonyl-CoA levels drop due to decreased ACC activity, alleviating the impediment on CPT1-mediated fatty acid oxidation (O'Neill et al., 2013). Animal models in which malonyl-CoA levels are manipulated can vastly alter metabolic phenotypes. Liver-specific deletion of fatty acid synthase results in substantially increased hepatic malonyl-CoA content, reduced CPT1 α -mediated oxidation and as a result, hepatic steatosis (Chakravarthy et al., 2005). On the other hand, hepatic overexpression of malonyl-CoA decarboxylase (which degrades malonyl-CoA to acetyl-CoA) resulted in depletion of hepatic malonyl CoA. Consequently, fat oxidation was increased, and dyslipidemia and insulin resistance were normalized (An et al., 2004). Collectively, these studies highlight the importance of fatty acid β -oxidation in whole body lipid homeostasis, and suggest that therapeutic interventions to increase fat oxidation may confer protection from metabolic disease.

1.4.4.1 FATTY ACID OXIDATION – PPAR REGULATION

The PPARs are a class of ligand-dependant transcription factors that regulate whole body lipid homeostasis (Harmon et al., 2011). Two members of this family, namely PPAR α and PPAR δ , stimulate transcriptional programs that initiate fat oxidative machinery. In the liver, the major PPAR isoform is PPAR α , which binds to PPAR

response elements (PPREs) within promoters of specific genes as an obligate heterodimer with the retinoid X receptor (RXR) (Harmon et al., 2011). This heterodimerization and initiation of transcription occurs in response to activation by endogenous ligands such as FAs and FA metabolites, or by synthetic ligands such as fibrates (Mandard et al., 2004). The canonical PPAR α target is acyl-CoA oxidase (ACO), which stimulates peroxisomal oxidation of long chain FAs (Mandard et al., 2004). This stimulation of hepatic fatty acid oxidation is likely the key component in the ability of fibrates, synthetic ligands for PPAR α , to effectively lower plasma TG levels. Fibrates are the current standard of care in the treatment of hypertriglyceridemia in dyslipidemic patients with insulin resistance (Reyes-Soffer et al., 2013).

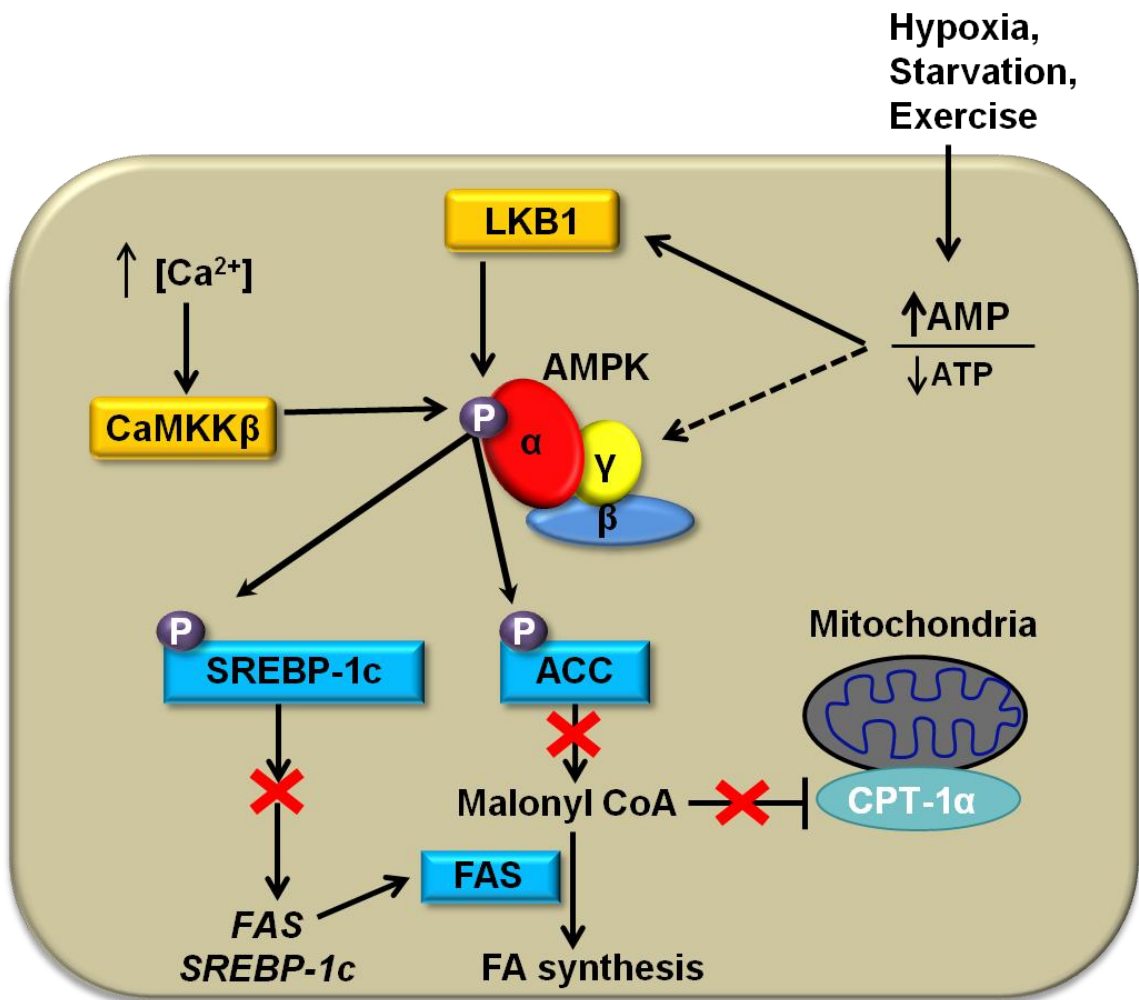
In addition to PPAR α , the other PPAR isoform that can stimulate fat utilization is PPAR δ (Wang et al., 2003). In fact, *CPT1 α* is a known PPAR δ target gene (Lee et al., 2006a). The ability of PPAR δ activation to regulate fatty acid oxidation and consequently prevent macrophage foam cell formation and hepatic steatosis is a significant component of the data in chapters 2 and 5 of this thesis. A more detailed discussion of PPAR δ -regulated processes and functions will be presented in section 1.7.

1.4.5 AMPK – THE PIVOTAL REGULATOR OF FAT OXIDATION AND LIPOGENESIS

The adenosine monophosphate-activated protein kinase (AMPK) is an evolutionarily conserved serine/threonine kinase that controls cellular and whole body energy metabolism (O'Neill et al., 2013). The heterotrimeric protein consists of an α -catalytic subunit, as well as β - and γ -regulatory subunits both of which are required for the catalytic activity of the α -subunit (O'Neill et al., 2013). Hepatocytes isolated from mice lacking the β 1-subunit display significantly reduced AMPK activity (Dzamko et al., 2010). As an energy-sensing protein kinase, AMPK operates as a fulcrum between anabolic and catabolic processes in response to changes in cellular AMP and ATP levels (Figure 1.9). During periods of low energy such as fasting, increases in cellular

Figure 1.9: Regulation of FA synthesis and oxidation by AMPK activation.

AMPK operates as a fulcrum between anabolic and catabolic processes in response to changes in adenylate charge. During periods of low energy, increased cellular AMP binds to the γ -subunit of AMPK, inducing a conformational change in the heterotrimer that unmasks α -catalytic subunit to upstream kinases. The two major AMPK-activating kinases are liver kinase B1 (LKB1) and calcium/calmodulin-dependent protein kinase kinase (CaMKK), both of which phosphorylate AMPK on Thr172 within the α -catalytic subunit. LKB is an AMP-sensitive kinase. Activated AMPK stimulates the phosphorylation of SREBP-1c which inhibits SREBP-1c processing and reduces expression of genes required for fatty acid synthesis. Concomitantly, AMPK phosphorylates ACC, which inhibits ACC function thereby inhibiting the production of malonyl CoA. This limits substrate availability for fatty acid synthesis. Reduced malonyl-CoA also results in the derepression of CPT1 α , thus increasing fatty acid oxidation.



ADP and AMP results in the binding of either of these nucleotides to the γ -subunit of AMPK, inducing a conformational change in the heterotrimer that unmasks the activation loop of the α -catalytic subunit to upstream kinases (O'Neill et al., 2013). The two major AMPK-activating kinases are liver kinase B1 (LKB1) and calcium/calmodulin-dependent protein kinase kinase (CaMKK), both of which phosphorylate AMPK on Thr172 within the α -catalytic subunit. In addition, ADP and AMP suppress AMPK inactivation by preventing the dephosphorylation of phospho-Thr172 by protein phosphatases PP2A and PP2C (Oakhill et al., 2011, Sanders et al., 2007). Activated AMPK inhibits anabolic processes (such as lipogenesis) and stimulates catabolic processes (such as fatty acid oxidation) to simultaneously conserve and produce energy. Once cellular energy has been restored, or feeding has occurred thus providing energy excess due to the stimulation glycolysis and fatty acid oxidation by dietary glucose and TG, respectively, AMP levels are depleted and ATP levels are increased. Accordingly, PP2A and PP2C reduce AMPK activity, catabolic processes cease and anabolic processes ensue (O'Neill et al., 2013).

Amongst the myriad of AMPK targets is ACC, which is thought to be the major contributor to the pivotal regulation of lipogenesis and oxidation (O'Neill et al., 2013). ACC exists in two isoforms, ACC1 and ACC2, which are phosphorylated by AMPK on Ser79 and Ser221, respectively (O'Neill et al., 2013). Phosphorylation of these ACC sites by AMPK results in the inactivation of ACC thus reducing malonyl-CoA production. In turn, substrate availability for FAS is limited, thereby downregulating lipogenesis to conserve energy. Additionally, low malonyl-CoA alleviates allosteric inhibition of CPT1 α and therefore stimulates fat oxidation. Given the ability of activated AMPK to favorably regulate metabolic processes and so collectively reduce cellular fat deposition, pharmacological modulators of AMPK represent a promising therapeutic strategy to regulate of lipid imbalances observed in cardiometabolic disease (Pinkosky et al., 2013).

1.5 INSULIN SIGNALING

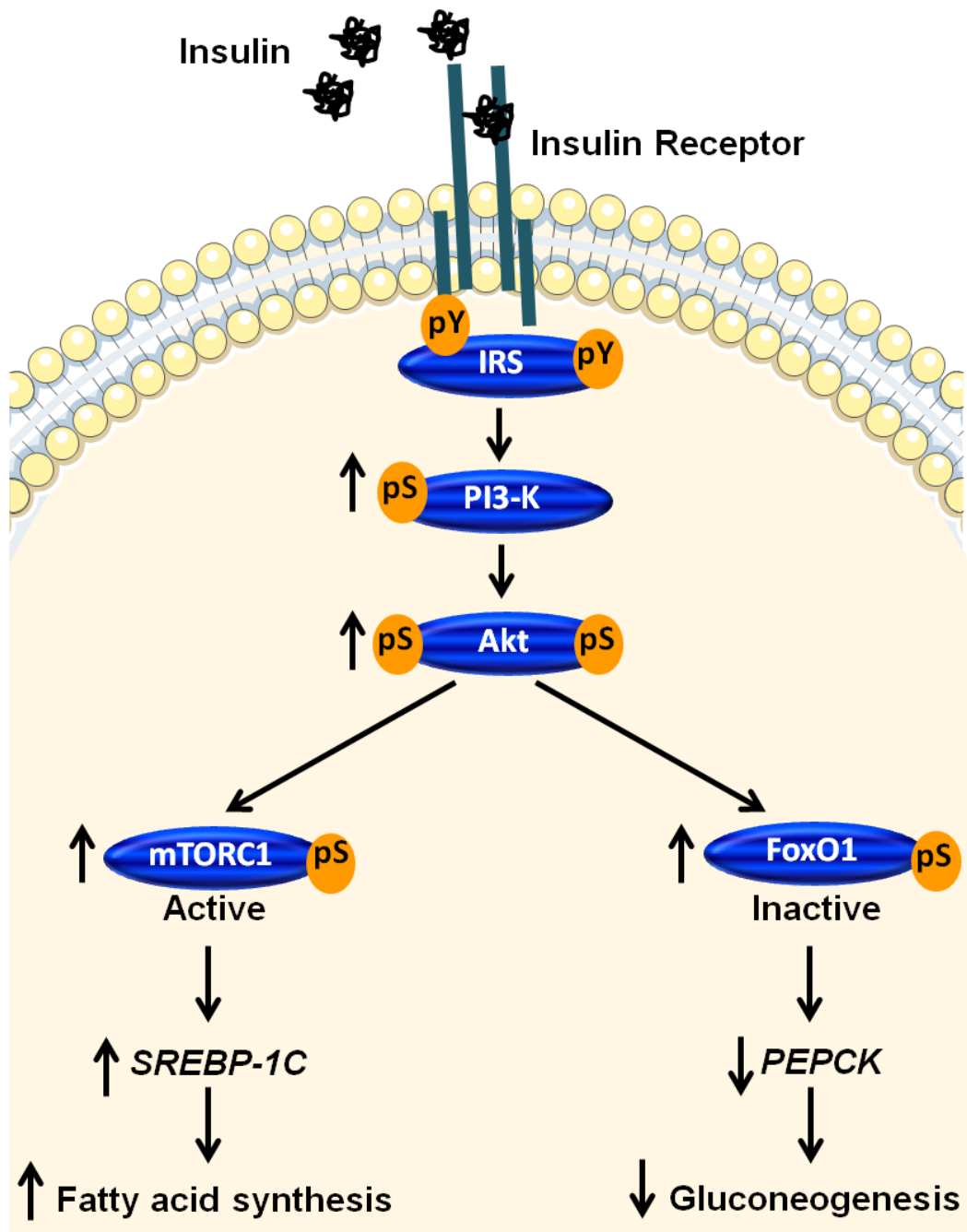
Insulin is a peptide hormone that is produced, processed and secreted by the β -cells of the pancreas in response to feeding, and is central to regulating the metabolism of carbohydrate, protein and lipids. Insulin responsive tissues such as muscle, adipose and liver among others, express plasma membrane bound insulin receptors which transduce the insulin signal. Binding of insulin to the extracellular ligand-binding domain rapidly stimulates the intrinsic activity of the receptor tyrosine kinase, resulting in autophosphorylation of tyrosine residues in the intracellular subunit domains (Kido et al., 2001). This autophosphorylation event causes the recruitment of insulin receptor substrate (IRS) proteins to the cytoplasmic tail of the insulin receptor that serve as docking proteins between the membrane-bound receptor and its intracellular effectors. One major downstream target of the insulin signal is phosphoinositide 3 (PI3)-kinase, which signals the phosphorylation and activation of protein kinase B/Akt (Kido et al., 2001). Under normal physiology, the downstream consequences of acute insulin-stimulated Akt activation include suppression of hepatic glucose production and promotion of *de novo* lipogenesis.

1.5.1 INSULIN-REGULATED HEPATIC GLUCOSE METABOLISM

Dietary glucose stimulates the release of insulin from the pancreas, which induces a feedback loop to suppress hepatic gluconeogenesis to maintain normal (low) blood glucose levels (Brown and Goldstein, 2008). Molecularly, insulin inhibits hepatic glucose production by stimulating the phosphorylation of forkhead box O1 (FoxO1) through the action of Akt (Figure 1.10). Phosphorylated FoxO1 is excluded from the nucleus, which effectively downregulates the transcription of genes involved in gluconeogenesis, most prominently glucose 6-phosphatase (*G6PC*) and phosphoenolpyruvate carboxykinase (*PEPCK*) (Matsumoto et al., 2006). Mice overexpressing constitutively active hepatic FoxO1 exhibit hyperglycemia and

Figure 1.10: Insulin signaling.

Insulin signalling via the insulin receptor results in enhanced IRS/PI3K signalling, leading to Akt phosphorylation. In turn Akt phosphorylates its downstream effector substrates mTORC1 and FoxO1. Akt-induced phosphorylation of mTORC1 renders the protein active, resulting in increased SREBP-1c-mediated fatty acid synthesis. In contrast, Akt-mediated phosphorylation of FoxO1 results in the inhibition of FoxO1 translocation into the nucleus. This suppresses *PEPCK* expression and consequently inhibits gluconeogenesis.



hyperinsulinemia, whereas RNAi knockdown of FoxO1 reverses these metabolic abnormalities (Kamagate et al., 2008).

1.5.2 INSULIN-REGULATED HEPATIC LIPID METABOLISM

Another major effect of insulin signaling in the liver is stimulation of *de novo* lipogenesis by activation of SREBP-1c. Mice lacking hepatic insulin receptors have severely diminished expression of the SREBPs and their targets (Biddinger et al., 2008), suggesting that hepatic insulin signaling is required for the stimulation of lipogenesis in the fed state. The molecular basis for insulin-stimulated SREBP activity occurs through dual actions of Akt in the insulin signaling cascade. As outlined in section 1.4.1, Akt can directly target INSIG2a for degradation via mechanisms that are not completely understood, thereby allowing for SREBP processing and translocation into the nucleus (Yecies et al., 2011). On the other hand, activated Akt stimulates the phosphorylation of the mammalian target of rapamycin complex (mTORC) 1 (Figure 1.10), which is known to enhance the transcription of SREBP-1c and its targets (Li et al., 2010, Yecies et al., 2011). Despite the insulin-mediated increase in hepatic *de novo* lipogenesis, insulin signaling also acutely suppresses hepatic VLDL secretion. The Akt-mediated phosphorylation and nuclear exclusion of FoxO1 reduces *MTP* expression (Kamagate et al., 2008), thus inhibiting cotranslational lipidation of apoB100. Additionally, insulin activates the MAPK^{erk} pathway, which also regulates *MTP* expression and reduces lipid availability for VLDL secretion (Allister et al., 2005).

1.5.3 INSULIN RESISTANCE

The metabolic syndrome is defined as a cluster of abnormalities including increased waist circumference, hypertension, low plasma HDL, high fasting blood glucose and high plasma TG, which collectively puts individuals at risk for the development of premature cardiovascular disease (Eckel et al., 2010). Insulin resistance is considered central to the pathophysiology of the metabolic syndrome and is clinically

defined as the inability of insulin to maintain glucose homeostasis (Haas and Biddinger, 2009). In response to elevated blood glucose levels during fasting in the insulin resistant state, the pancreas responds by increasing insulin secretion to compensate for the lack of sensitivity in peripheral tissues, thus maintaining glycemic control (Eckel et al., 2010). Eventually the pancreas cannot provide sufficient insulin, blood glucose increases, and the diabetic state ensues. Therefore, insulin resistance has been causally linked to the development of type 2 diabetes (Eckel et al., 2010).

Although the clinical definition of insulin resistance is useful, it fails to address other processes that are a result of insulin resistance. Insulin resistance is most prominently manifest in three organs: adipose, muscle and liver (Li et al., 2010). In the adipose tissue, failure of insulin to suppress TG lipolysis increases FA release and contributes to elevated plasma FFAs as well as the hepatic pool of FA available for TG re-synthesis and VLDL assembly and secretion. In muscle, the inability of insulin to stimulate glucose transporter (GLUT) 4 translocation to the plasma membrane, reduces insulin-mediated glucose uptake and contributes to fasting hyperglycemia. In the liver, however, an interesting paradox occurs where the lipogenic SREBP-1c branch of insulin signaling remains sensitive, whereas the gluconeogenic FoxO1 branch becomes resistant.

1.5.3.1 INSULIN RESISTANCE IN THE LIVER

As alluded to above, hepatic insulin resistance cannot simply be defined as the failure of insulin to propagate signal transduction through the insulin receptor. Impaired insulin receptor signaling has been observed in a variety of settings (Nyomba et al., 1990, Nyomba et al., 1991, Ozcan et al., 2004), and likely contributes to insulin resistance at certain stages of disease progression. However, in mice with hepatic insulin receptor ablation (termed pure insulin resistance), hyperinsulinemia and hyperglycemia still develop, yet in the complete absence of hepatic steatosis and

hypertriglyceridemia due to reduced SREBP-1c activity (Biddinger et al., 2008). Hence, the diabetic triad of hyperinsulinemia, hyperglycemia and hypertriglyceridemia breaks down in pure insulin resistance. This resulted in the hypothesis that normal insulin signaling must occur in the liver to at least some particular point (Brown and Goldstein, 2008). After this hypothesized point, the insulin signal should bifurcate to generate insulin resistant and insulin sensitive branches of the pathway (termed selective insulin resistance) (Figure 1.11). This dual action of insulin is a major contributor to the hypertriglyceridemia and hyperglycemia observed in the insulin resistant state.

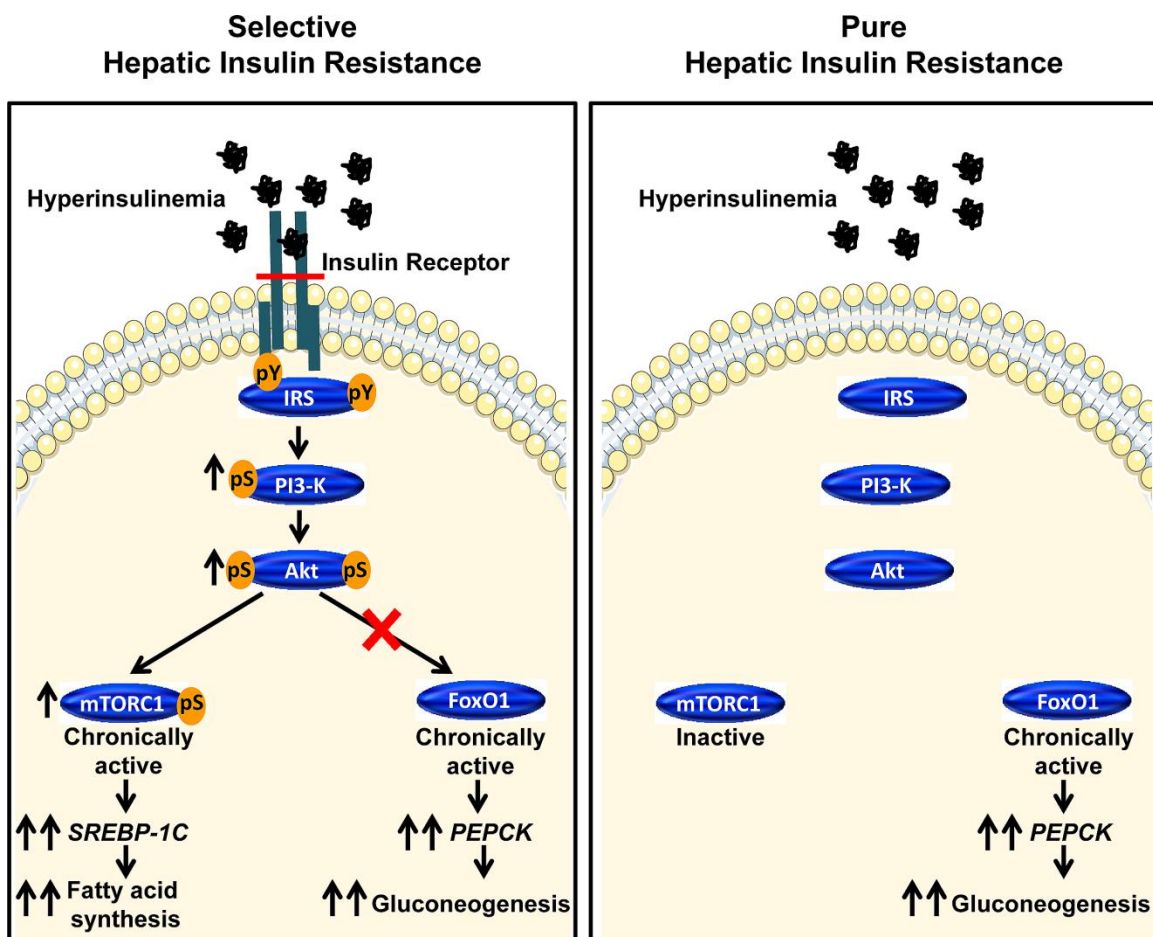
Inhibition of PI-3K and Akt kinase activity in primary rat hepatocytes revealed that these were common mediators of the gluconeogenic and lipogenic branches of the insulin signal (Li et al., 2010). However, mTORC1 inhibition abolished insulin-induced *SREBP-1c* expression, but had no effect on insulin-mediated suppression of *PEPCK* (Li et al., 2010), demonstrating that the bifurcation point of the insulin signal is Akt. Hence, fasting hyperinsulinemia during insulin resistance chronically drives *de novo* lipogenesis, but fails to suppress gluconeogenesis due to the inability of Akt to phosphorylate and inactivate FoxO1. Furthermore, active FoxO1 results in constitutive activation of *MTP* expression, and together with increased lipogenesis contributes to increased apoB100 secretion (Biddinger et al., 2008, Kamagate et al., 2008).

The bifurcation of the insulin signaling cascade begs the questions of how and why Akt phosphorylates and activates mTORC1 but fails to phosphorylate and inactivate FoxO1. Recently, it has been demonstrated that a particular cytosolic calcium sensing kinase, calcium-calmodulin dependent kinase II gamma (CaMKII γ), stimulates the phosphorylation of FoxO1 on non-Akt sites, thereby promoting FoxO1 entry into the nucleus to stimulate hepatic glucose production (Ozcan et al., 2012). Importantly, activity of CaMKII γ was significantly increased in obese *ob/ob* mice as well as wild type mice fed a high-fat diet for 20-weeks. Adenoviral knockdown of CaMKII γ in either of these settings

Figure 1.11: Selective versus pure insulin resistance.

Selective hepatic insulin resistance – Under hyperinsulinemic/insulin resistant conditions, the elevated plasma insulin results in chronic phosphorylation of the cascade to Akt. Paradoxically, the ability of Akt to phosphorylate mTORC1 remains sensitive, whereas Akt-mediated phosphorylation of FoxO1 becomes resistant. In turn, mTORC1-driven SREBP-1c-mediated lipogenesis is significantly increased, whereas FoxO1-processes remain activated rather than inhibited as in normal insulin signalling. Consequently, PEPCK-mediated gluconeogenesis ensues. The combined physiological effects of selective hepatic insulin resistance are: hyperinsulinemia, hypertriglyceridemia and hyperglycemia (the so-called diabetic triad) as well as hepatic TG accumulation.

Pure hepatic insulin resistance – With liver-specific deletion of the insulin receptor, the diabetic triad breaks down. Although these animals develop hyperinsulinemia, the liver cannot respond to the plasma insulin. As a result, mTORC1 remains inactive, whereas the lack of impediment on FoxO1 renders it chronically active. The physiological consequences in this scenario are: hyperinsulinemia and hyperglycemia, with normal plasma and hepatic TG.



Adapted from Brown and Goldstein, 2008. *Cell Metab*, 7, 95-96.

diminished hepatic gluconeogenic gene expression, decreased fasting glycemia and improved insulin sensitivity (Ozcan et al., 2012). Given that ER-stress is known to accompany insulin resistance in the liver (Ozcan et al., 2004), and that ER-stress can dramatically increase cytosolic calcium levels (Fu et al., 2012), it is plausible that the CaMKII γ -specific phosphorylation of FoxO1 is significantly induced during hepatic insulin resistance and prevents insulin-mediated phosphorylation and suppression of FoxO1 activity. However, this hypothesis has yet to be explored.

1.5.3.2 INSULIN RESISTANCE IN THE VASCULATURE

In addition to promoting atherogenic risk factors, namely dyslipidemia, insulin resistance may also drive atherosclerosis directly at the level of the artery wall (Tabas et al., 2010). Bone marrow transplantation from *insulin receptor* knockout mice (*Insr*^{-/-}) into *Ldlr*^{-/-} recipients substantially increased atherosclerotic lesion formation, specifically due to ER-stress induced apoptosis and necrotic core formation (Han et al., 2006). Furthermore, crossing *Akt1*^{-/-} mice onto the *apoE*^{-/-} background yields profound coronary atherosclerosis, attributable to increased inflammation in the vessel wall (Fernandez-Hernando et al., 2007). In macrophages deficient for the insulin receptor, FC-induced ER-stress and apoptosis involves increased nuclear FoxO1 translocation and activity (Senokuchi et al., 2008). Consistent with this, FoxO1 is known to stimulate the transcription of at least one proatherogenic inflammatory cytokine in macrophages (Su et al., 2009), and FoxO1 ablation in vascular endothelial cells attenuates atherosclerosis development (Tsuchiya et al., 2012). All of these studies use proof-of-concept genetic ablation of insulin signaling strategies and consequently fail to address whether a selective insulin resistant phenotype may be occurring in the vessel wall during diet-induced atherogenesis.

A recent study demonstrated that macrophages isolated from *Insr*^{-/-} or *ob/ob* mice displayed a significant reduction in expression and activity of the sarcoplasmic

endoplasmic reticulum calcium ATPase, which led to reduced flux of cytosolic calcium back into the ER and as a result, increased ER-stress-induced apoptosis (Liang et al., 2012). This study suggests that a similar mechanism of insulin resistance may occur in the liver as well as in the vasculature. Thus, therapeutic agents that correct selective hepatic insulin resistance may also alleviate vascular insulin resistance, and reduce atherosclerosis through either of these mechanisms.

1.6 TYPE 2 DIABETES

As insulin resistance persists, the pancreas responds by continuously increasing insulin secretion in an attempt to maintain glycemic control. However, maintenance of blood glucose homeostasis does not occur indefinitely, as pancreatic β -cells cannot undergo hyperplasia *ad infinitum* to keep up with the insulin resistant state of the periphery (Prudente et al., 2009). Consequently, the full type 2 diabetic state ensues, putting patients at up to four-fold higher risk of developing CVD than non-diabetic subjects (Fox et al., 2007, Fox et al., 2004). The proatherogenicity of type 2 diabetes has been thought to be multi-factorial, as hyperlipidemia, hyperglycemia, hyperinsulinemia and increased oxidative stress and inflammation combine to accelerate atherogenesis (Ginsberg, 2000).

Despite considerable data demonstrating a positive correlation between diabetes and development of cardiovascular disease, delineating the relative contribution of each process outlined above to cardiovascular risk has proven difficult. Elevated plasma TG remains an independent risk factor for CVD development (Musunuru, 2010), and residual CVD risk left behind by statin monotherapy is at least 50% (Mazzone et al., 2008). The ACCORD Lipid trial tested whether LDL-C lowering statin therapy in combination with TG-lowering fibrate therapy further reduced CVD risk. There was no significant reduction observed in patients receiving combination therapy compared to those receiving statin alone (Ginsberg et al., 2010). With respect to hyperglycemia,

intensive long-term glucose lowering has not proven successful in reducing cardiovascular events (Gerstein et al., 2011). Finally, the conjecture that hyperinsulinemia is atherogenic is also controversial, as this would imply that insulin is a proatherogenic molecule. If this were the case, then insulin therapy would be a poor choice for patients with insulin resistance or type 2 diabetes (Ginsberg, 2000). However, results from the United Kingdom Prospective Diabetes Study (UKPDS) demonstrated a nearly statistically significant ($P=0.052$) effect of insulin and sulfonylurea treatment in reducing cardiovascular events (Group, 1998), and insulin glargine treatment for 6 years had a neutral effect on cardiovascular outcomes (Gerstein et al., 2012). Although assessment of long-term CVD prevention with insulin secretagogues such as GLP-1 analogues and DPP4 inhibitors has not been completed, the data accumulated thus far suggests that CVD risk is not worsened and might be reduced, due at least in part to TG-lowering (Anagnostis et al., 2011, DeFronzo et al., 2008). Interestingly, the GLP-1 analogue exenatide reverses FC-induced ER-stress and apoptosis in macrophages (Liang et al., 2012). Collectively, these studies suggest that patients with type 2 diabetes should be treated to the current standard of care for hyperglycemia and hyperlipidemia, until new clinical trials further our understanding of how to manage CVD risk in patients with type 2 diabetes.

1.7 PEROXISOME PROLIFERATOR-ACTIVATED RECEPTORS

The peroxisome proliferator-activated receptor (PPAR) δ has emerged as an important regulator of lipid homeostasis and inflammatory signaling. Recent *in vitro*, *in vivo* and human clinical studies have highlighted a role for PPAR δ activation in prevention and treatment of insulin resistance and atherosclerosis.

1.7.1 PPAR OVERVIEW

The PPARs are a class of ligand-dependant transcription factors within the nuclear receptor superfamily. The three isoforms (PPAR α , PPAR γ and PPAR δ) are

encoded by three separate genes, which exhibit overlapping but largely distinct patterns of tissue distribution and function (Chawla et al., 1994, Kliewer et al., 1994). PPARs follow the basic modular structure common to most nuclear receptors (Harmon et al., 2011). Six exons encode four distinct domains which regulate PPAR function (Fournier et al., 2007). Exon 1 encodes the N-terminal activating function (AF)-1 domain which is a ligand-independent modulation domain amenable to post-translational modifications (Fournier et al., 2007). Exons 2 and 3 encode the zinc-finger DNA binding domain of PPARs, which bind to the PPAR response element (PPRE) direct repeat sequence AGGTCAnAGGTCA within promoter regions of PPAR-target genes (Fournier et al., 2007). The hinge region, which is thought to participate in the nuclear translocation signal, is encoded by exon 4 (Fournier et al., 2007). The carboxy-terminal AF-2 domain, encoded by exons 5 and 6, contains the ligand binding domain and co-factor dimerization domains (Fournier et al., 2007). Additionally, the AF-2 domain includes the RXR-heterodimerization interface (Fournier et al., 2007).

In an unliganded state, the PPAR-RXR heterodimer is bound to the PPRE by co-repressors such as the nuclear co-repressor (NCoR) or the silencing mediator of retinoid and thyroid hormone receptor (SMRT), which are part of the histone deacetylase (HDAC) complex. Deacetylated histones keep chromatin tightly wound, thereby repressing gene expression. Consequently, in the absence of ligand, PPARs exert active repression of their target genes (Harmon et al., 2011). However, the binding of ligand induces a PPAR conformational change that results in the dissociation of co-repressor complexes from the PPAR-RXR heterodimer. This conformational change in PPARs results in a so-called “PPAR LxxLL charge clamp” in the AF-2 domain, which stimulates the recruitment of LxxLL-containing co-activator complexes, such as the nuclear co-activator (NCoA) and the steroid receptor co-activator (SRC). NCoA and SRC are part of the histone acetyl transferase (HAT) complex (Harmon et al., 2011), which modifies

chromatin structure thereby allowing for gene transcription to ensue (Fournier et al., 2007). Hence, ligand-dependent activation of PPARs results in active gene transcription.

In addition to active repression and ligand-dependent activation, regulation of PPAR target genes can occur as a result of post-translational modification of the AF-1 domain. One such example is the phosphorylation of the AF-1 domain of PPAR γ by cyclin-dependent kinase (CDK) 5 (Choi et al., 2010). Consequently, PPAR γ target genes are further actively repressed as a result of stronger association of the receptor with co-repressor complexes which exert greater HDAC activity (Choi et al., 2010). Ligand-binding in the AF-2 domain of PPAR γ inhibits CDK5-mediated phosphorylation of PPAR γ , which is one mechanism by which thiazolidinediones exert their anti-diabetic action (Choi et al., 2010). Additionally, inhibition of CDK5 results in the de-repression of PPAR γ target genes as a result of this ligand-independent modification of the AF-1 domain (Choi et al., 2011). Although this discovery has led to the search for novel approaches of modulating PPAR activity by manipulating the co-regulator complexes associated with PPARs, this field is still in its infancy and requires further study.

PPARs most prominently differ in their ligand binding pockets as well as the tissues in which they are expressed. However, these receptors have a large complement of target genes, which can create difficulties in establishing PPAR-specific effects (Harmon et al., 2011). Nevertheless, PPAR α is predominantly expressed in hepatocytes, where activation of this isoform stimulates the catabolism of fatty acids while suppressing inflammatory responses (Mandard et al., 2004). Fibrates are synthetic ligands for PPAR α which are currently used as therapeutic agents in the treatment of hypertriglyceridemia. PPAR γ is expressed primarily in adipocytes where it functions as an essential regulator of adipose tissue inflammation, fat storage and differentiation (Barak et al., 1999, Rosen et al., 1999, Tontonoz et al., 1994). In addition, PPAR γ activation increases expression of adiponectin, an adipokine that enhances insulin

sensitivity (Yamauchi et al., 2001). PPAR γ is the target of thiazolidinediones, used clinically in the treatment of type 2 diabetes. In contrast to the more restricted tissue distribution of PPAR α and PPAR γ , PPAR δ is ubiquitously expressed with particularly high abundance in muscle tissue and macrophages (Vosper et al., 2001, Wang et al., 2004). Although PPAR δ activation has yet to achieve clinical application, recent advancements have reduced the gap between preclinical studies and clinical use.

1.7.2 PPAR δ IN MACROPHAGES

Macrophage exposure to VLDL or VLDL-derived fatty acids readily stimulates foam cell formation (Whitman et al., 1999), the inflammatory response and ER-stress induced apoptosis, independent of lipopolysaccharide (Anderson et al., 2012, Saraswathi and Hasty, 2006). Induction of the inflammatory response was independent of toll-like receptors 4 or 2 (Anderson et al., 2012). Paradoxically, VLDL-derived fatty acids also activate macrophage PPAR δ resulting in up-regulation of genes involved in fatty acid catabolism, including *CPT1 α* (Chawla et al., 2003, Lee et al., 2006a). Thus, from an evolutionary standpoint, PPAR δ serves as a fatty acid sensor in cells of the vasculature to prevent arterial lipid accumulation under normolipidemic conditions. However, in the context of hypertriglyceridemia, if PPAR δ -regulated lipid homeostasis induced by fatty acids were sufficient to clear the incoming atherogenic substrate, atherosclerosis would not ensue. The requirement for potent synthetic agonists of PPAR δ to reduce VLDL-induced macrophage lipid deposition has not been examined.

PPAR δ also regulates the macrophage inflammatory response, in part, through the repressor protein B-cell lymphoma 6 (BCL-6) (Lee et al., 2003). In the absence of ligand, PPAR δ is bound to BCL-6, thereby repressing its function. Consequently, proinflammatory cytokine expression is elevated. Ligand activation induces a conformational change in PPAR δ resulting in dissociation of BCL-6 from the PPAR δ corepressor complex and subsequent transrepression of proinflammatory mediators

(Figure 1.12). This phenomenon has also been documented in PPAR δ knockout cells and cells expressing dominant negative PPAR δ , suggesting that defective PPAR δ , the absence of PPAR δ , or ligand-activation of PPAR δ render similar anti-inflammatory effects, due to the lack of BCL-6 sequestration (Figure 1.12) (Barish et al., 2008, Lee et al., 2003, Takata et al., 2008). Thus, in addition to protection from lipid overload, activation of PPAR δ by fatty acids also serves to protect macrophages from lipotoxic proinflammatory responses under normolipidemic conditions. However, as discussed in sections 1.2.5 and 1.5.3.2, VLDL and VLDL-derived fatty acids mediate proinflammatory cytokine expression through MAPK activation (Anderson et al., 2012, Saraswathi and Hasty, 2006), and insulin resistant macrophages display enhanced proinflammatory cytokine expression due to dysregulated Akt/forkhead box protein O1 (FoxO1) signaling (Su et al., 2009). The impact of PPAR δ activation on VLDL-induced macrophage inflammatory responses remains to be established.

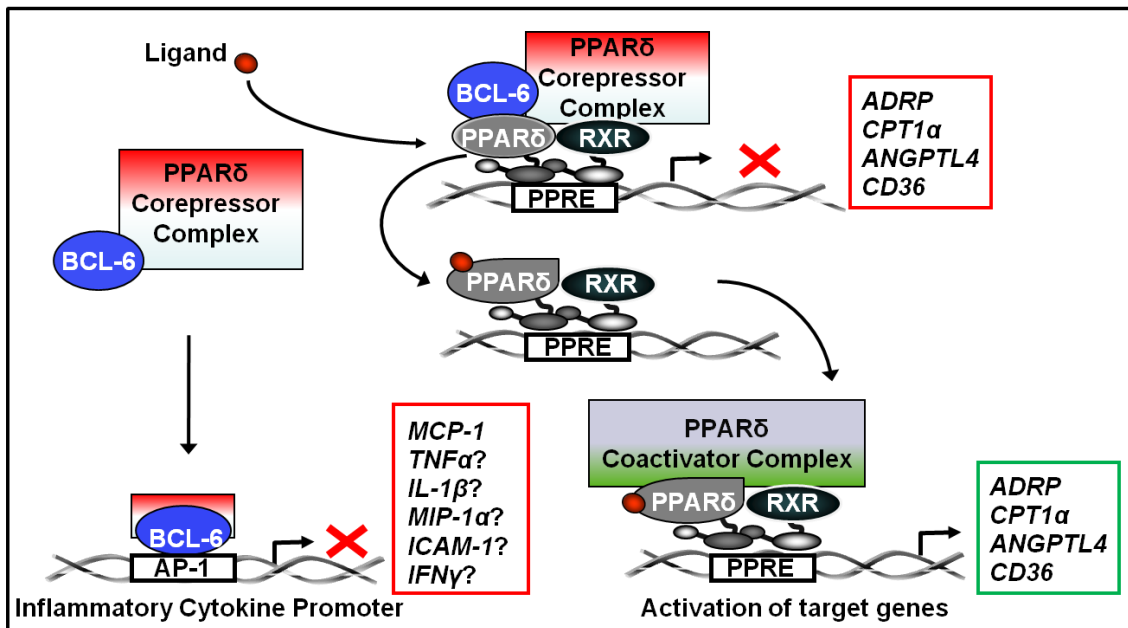
Clinically relevant plaques are prone to rupture and exhibit lipid rich necrotic cores as a result of inflammation and ER-stress-induced apoptosis (Moore and Tabas, 2011). Defective macrophage apoptosis is central to necrotic core formation and is therefore a major component of the progression of complex lesions to clinically relevant lesions (Tabas, 2010). Phagocytosis of apoptotic cells results in the engulfment of large amounts of lipids, including FAs, into the macrophage (Erwig and Henson, 2008), which in turn activates PPAR δ expression (Mukundan et al., 2009). Bone marrow derived macrophages (BMDMs) from *Ppar δ ^{-/-}* mice displayed significantly reduced phagocytosis of apoptotic cells (Mukundan et al., 2009), concomitant with a significant reduction in the expression of opsonins, molecules that regulate enhanced recognition and phagocytosis of apoptotic cells (Erwig and Henson, 2008, Lauber et al., 2004). In wild-type BMDMs, the PPAR δ agonist GW0742 stimulated the expression of opsonins and enhanced clearance of apoptotic cells which was entirely PPAR δ -dependent

Figure 1.12: Consequences of PPAR δ activation and PPAR δ deletion:

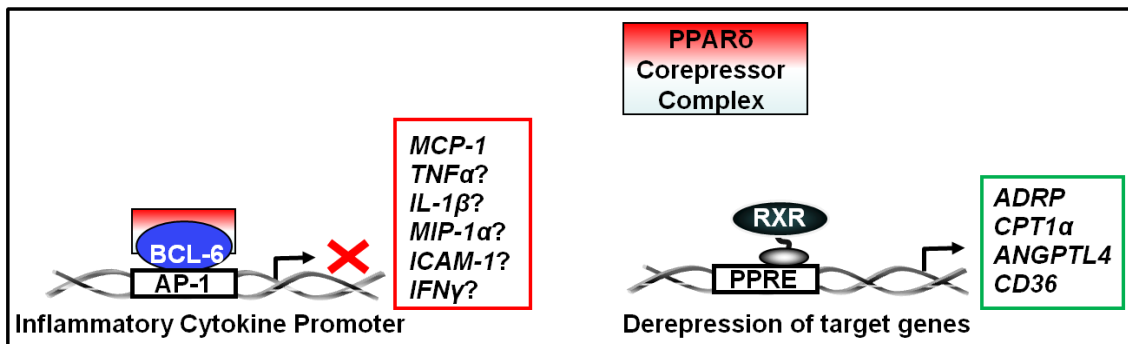
PPAR δ Activation - PPAR δ binding sites within promoter regions of its target genes are known as PPAR response elements (PPREs). In an unliganded state, the PPAR δ -retinoid X receptor (RXR) obligate heterodimer is bound to corepressor complexes, which inhibits basal transcription of PPAR δ target genes. Ligand activation results in a conformational change in the receptor leading to dissociation of the corepressor complexes and subsequent recruitment of coactivator complexes to the PPAR δ -RXR heterodimer. As a result, PPAR δ -responsive genes are transcriptionally activated. Part of the PPAR δ corepressor complex is the BCL-6 protein, which acts as an inflammatory repressor protein in response to ligand activation of PPAR δ . The ligand-induced conformational change in PPAR δ results in the dissociation of BCL-6 from the PPAR δ corepressor complex. Subsequently, BCL-6 corepressor complexes are recruited to promoter regions of inflammatory cytokine genes, leading to the inhibition of proinflammatory mediator expression.

PPAR δ Deletion – Genetic ablation of PPAR δ mimics the liganded state of the receptor, as the presence PPAR δ is required for the corepressor complex to maintain basal target gene expression suppressed. Moreover, PPAR δ is required for BCL-6 sequestration. Hence, when PPAR δ is eliminated, cytokine expression is suppressed by BCL-6, and PPAR δ -target genes are derepressed.

PPAR δ Activation



PPAR δ Deletion



Adapted from Lee et al., 2003. *Science*, 302, 453-457.

(Mukundan et al., 2009). These studies uniquely demonstrate that PPAR δ activation in macrophages orchestrates efficient clearance of dying cells by induction of opsonin expression and represents a therapeutically relevant mechanism. Collectively, studies in cultured macrophages suggest that PPAR δ activation may serve as a guardian of the vascular insult, and thus impact atherogenesis.

1.7.3 PPAR δ ACTIVATION AND THE PROTECTION FROM DIET-INDUCED ATHEROSCLEROSIS

The *in vivo* role of PPAR δ on atherosclerosis has proven elusive, due, in part, to the unique transcriptional regulation of proinflammatory processes (when associated) and anti-inflammatory processes (when dissociated) by the PPAR δ :BCL-6 complex. Lee *et al.* demonstrated that transplantation of *Ppar δ ^{-/-}* bone marrow into *Ldlr^{-/-}* recipient mice resulted in significant atheroprotection (Lee et al., 2003). As discussed above, these studies revealed that deletion of *Ppar δ* mimicked the liganded state of the receptor, and suggested that ligand-activation may be atheroprotective. However, in subsequent studies involving prevention protocols, administration of synthetic PPAR δ agonists produced conflicting reports. The first two reports PPAR δ activation *in vivo* utilized the GW0742 compound, and only showed an effect at megadoses at which this ligand is no longer PPAR δ -specific (Li et al., 2004) (Graham et al., 2005). A subsequent study showed that lower PPAR δ -specific doses of GW0742 reduced lesions and aortic expression of inflammatory cytokines in the angiotensin II-induced mouse model of atherosclerosis (Takata et al., 2008). It is important to note that angiotensin II significantly increases PPAR δ expression, resulting in increased BCL-6 sequestration and enhanced inflammation (Takata et al., 2008). The next generation PPAR δ agonist, GW1516, at PPAR δ -specific doses, prevented atherosclerosis in *apoE^{-/-}* mice fed a high-fat diet, concomitant with reduced aortic inflammatory cytokine expression (Barish et al.,

2008). However, lesion complexity and morphometry were not examined. Nevertheless, the prevention protocols used to date have not examined the ability of PPAR δ activation to attenuate or to induce regression pre-established lesions. Furthermore, insulin resistance within arterial macrophages is known to enhance lesion development. The impact of PPAR δ activation on arterial wall insulin sensitivity remains to be determined.

1.7.4 PPAR δ ACTIVATION IN HEPATOCYTES

Hyperinsulinemia results in amplified stimulation of mTORC1, which consequently drives the master transcriptional regulator of lipogenesis, sterol regulatory element binding protein (SREBP)-1c (Haas et al., 2012, Horton et al., 2002, Yecies et al., 2011). In turn, SREBP-1c activates the lipogenic transcriptional program, which includes genes such as fatty acid synthase (*Fasn*), acetyl-CoA carboxylase (*Acc*) and stearoyl-CoA desaturase (*Scd*) (Horton et al., 2002). In *db/db* mice GW1516 treatment increased hepatic expression of *Fasn*, *Acc* and *Scd2* leading to a modest increase in hepatic triglyceride (Lee et al., 2006b). In *Ldlr*^{-/-} mice, adenoviral PPAR δ (adPPAR δ) gene delivery stimulated the expression of *Fasn*, *Acc1*, *Acc2*, *Srebf1c* and *Pgc1b*, and increased liver triglyceride content (Liu et al., 2011). In contrast, HepG2 cells treated with GW0742 displayed a marked reduction in TG accumulation, due to reduced processing of nuclear SREBP-1, which resulted in attenuated expression of *Fasn* and *Scd1* (Qin et al., 2008). GW0742 increased expression of insulin-induced gene (*Insig*)-1, an SREBP-1 endoplasmic reticulum (ER) retention protein which contains a PPAR response element within its promoter. These results were reproduced in livers of *db/db* mice injected with adPPAR δ (Qin et al., 2008). The spectrum of results observed in these studies can be explained by different mouse models, diets, selection of drugs used, or gene delivery versus drug strategies of increasing PPAR δ activity. However, that PPAR δ activation increases hepatic steatosis is counterintuitive, given the overwhelming data demonstrating that PPAR δ activation improves whole-body insulin

sensitivity and lipid homeostasis, and stimulates fatty acid oxidation in a variety of cell types and tissues (Lee et al., 2006b, Tanaka et al., 2003, Wang et al., 2003). Therefore, additional studies are required to reconcile the ability of PPAR δ activation to regulate resistant hepatic steatosis linked to insulin resistance.

Liver inflammation has been implicated as a major contributor to hepatic insulin resistance (Gregor and Hotamisligil, 2011, Hummasti and Hotamisligil, 2010). PPAR δ activation in HepG2 cells attenuates interleukin (IL)-6-induced inflammation and insulin resistance. These effects were mediated via PPAR δ inhibition of IL-6-induced signal transducer and activator of transcription (STAT)-3, resulting in restoration of normal insulin signaling (Serrano-Marco et al., 2011). Importantly, livers of *Ppar δ* ^{-/-} mice displayed significantly elevated phospho-STAT-3, suggesting that PPAR δ regulates STAT-3 *in vivo*, contributing to improved insulin resistance (Serrano-Marco et al., 2011). Kupffer cell-specific deletion of *Ppar δ* in mice resulted in impaired hepatic Akt phosphorylation coupled with increased hepatic inflammation (Odegaard et al., 2008). Together, these studies demonstrate that activation of hepatic PPAR δ attenuates inflammation and contributes to improved hepatic insulin sensitivity. Further experimentation is required to determine whether selective PPAR δ agonists reduce hepatic inflammation *in vivo*.

1.7.5 PPAR δ AGONISTS IN HUMANS

The available *in vitro* and *in vivo* data prompted the examination of selective PPAR δ agonists in human clinical trials for the treatment of metabolic dysregulation, including dyslipidemia. In healthy volunteers, GW1516 (2.5 mg or 10 mg/day for 2 weeks) reduced plasma TG concentrations, enhanced post-prandial TG clearance and increased plasma HDL-cholesterol (Sprecher et al., 2007). In moderately obese men, GW1516 (10 mg/day for 2 weeks) stimulated moderate weight loss, reduced plasma TG, NEFA, total cholesterol and LDL cholesterol. Hepatic fat content was reduced in the

GW1516-treated cohort. Fasting plasma insulin and fasting blood glucose levels were decreased and insulin sensitivity improved as calculated by the homeostasis model assessment of insulin resistance (HOMA-IR). No adverse effects were observed (Riserus et al., 2008). Recently, a large multi-dose study of GW1516 (2.5, 5.0 and 10 mg/day for 12 weeks) in subjects with low HDL-C revealed significant increases in HDL-C and apo A-I with concomitant reductions in plasma FFA, apoB, VLDL, IDL and large LDL particles, all of which demonstrate a transition toward a less atherogenic lipoprotein profile (Olson et al., 2012). In dyslipidemic men with central obesity, a recent randomized double-blind, crossover trial of 6-week intervention periods with placebo or GW1516 (2.5mg/day), lipoprotein kinetic studies provided mechanistic insight into the anti-dyslipidemic properties of GW1516 (Ooi et al., 2011). Decreased plasma TG, NEFA, apoB-100 and apoB-48 concentrations were observed. GW1516 decreased VLDL apoB concentrations due to an enhanced fractional catabolic rate, which was related to a significantly lower production rate of apo C-III. GW1516 increased plasma HDL-cholesterol, concomitant with increased apo A-II production and reduced CETP activity (Ooi et al., 2011).

Recent back-to-back randomized, double-blind, placebo-controlled, parallel group studies involving a novel PPAR δ agonist (MBX-8025) administered as monotherapy or in combination with atorvastatin, examined the ability of PPAR δ agonists to improve dyslipidemia in overweight patients (Bays et al., 2011, Choi et al., 2012). In the first study, MBX-8025 alone or in combination with atorvastatin significantly reduced plasma concentrations of apoB100 and LDL-cholesterol. However, the combination did not significantly reduce either of these parameters beyond that of atorvastatin alone. In contrast to atorvastatin monotherapy, MBX-8025 alone or in combination with atorvastatin significantly reduced plasma TGs and NEFAs, and increased HDL-C (Bays et al., 2011). In addition, MBX-8025 reduced HOMA-IR, the

number of patients meeting diagnostic criteria for the metabolic syndrome, VLDL particle number, the preponderance of small and very small LDL particles and increased LDL peak diameter (Bays et al., 2011, Choi et al., 2012). MBX-8025 was well tolerated, with no major adverse effects (Bays et al., 2011, Choi et al., 2012). Collectively, these human trials demonstrate that PPAR δ agonists exert favourable effects on CVD risk factors that are not improved by statin monotherapy. Whether PPAR δ agonists reduce the residual CVD risk beyond statin treatment requires longer-term outcome and safety studies.

1.8 MODELS TO BE USED

1.8.1 CELL CULTURE

THP-1 cells are a monocytic cell line initially derived from the blood of a one-year-old boy with acute monocytic leukemia (Tsuchiya et al., 1980). Treatment of THP-1 monocytes with phorbol esters such as phorbol 12,13-dibutyrate, results in their differentiation into macrophage-like cells, which exhibit many characteristics of native, mature macrophages (Auwerx, 1991). Although the extent to which differentiated THP-1 cells mimic vascular wall macrophages is not fully understood, these cells have been used extensively as a model to gain insight into macrophage foam cell formation and function (Qin, 2012). Treatment of THP-1 cells with a phorbol ester results in the upregulation of scavenger receptors (Johnson et al., 2003), which makes THP-1 macrophages a reasonable model to recapitulate macrophage behavior during atherogenesis. One caveat to these cells is that phorbol ester treatment results in the downregulation of LDLR expression (Johnson et al., 2003), which results in reduced uptake of native LDL compared to modified LDL. However, high doses of LDL (100-200 μ g/mL) will stimulate CE uptake and foam cell formation (Banka et al., 1991), which still makes THP-1 macrophages a fundamentally good model to study foam cell formation in response to native LDL in the context of hypercholesterolemia. In the context of hypertriglyceridemia, THP-1 macrophages synthesize and secrete LPL (Qin,

2012), and can therefore readily take up VLDL-derived fatty acids resulting in foam cell formation. These cells were used extensively for the studies described in Chapters 2 and 3.

1.8.2 *Ldlr*^{-/-} MICE

Deletion of the *Ldlr* in C57Bl/6J disrupts normal murine lipoprotein metabolism, resulting in elevated plasma cholesterol, particularly in the LDL fraction as a result of defective LDL clearance (Ishibashi et al., 1993). Furthermore, these animals develop increased cholesterol in both VLDL and IDL when fed a high-fat diet (Getz and Reardon, 2006). *Ldlr*^{-/-} mice fed a high-fat, cholesterol containing (HFHC) diet for 12 weeks recapitulate many features of the metabolic syndrome such as dyslipidemia, hyperinsulinemia, insulin resistance and hepatic steatosis (Assini et al., 2013). Furthermore, these animals develop atherosclerotic lesions that are relatively advanced, exhibiting significant lipid accumulation, increased macrophage and smooth muscle cell infiltration and enhanced collagen deposition (Assini et al., 2013). *Ldlr*^{-/-} mice were extensively used for the studies described in Chapters 4 and 5.

1.8.3 ANIMAL DIETS

1.8.3.1 CHOW DIET

Laboratory chow was used as a control diet which provided a reference for metabolic indices altered by feeding the HFHC diet. The chow diet contains complex carbohydrates and 14% calories as fat (4% by weight). The caloric value of the chow diet is 3.0 kcal/g (Table 1-2). The chow diet was fed *ad libitum* to mice in studies described in Chapters 4 and 5.

TABLE 1-2 Animal Diets

Formula	Traditional Chow Diet	High-fat, high cholesterol (HFHC) diet
	TD 8604	TD09268
		g/kg
Casein	*See represented	195
DL-Methionine	ingredients, exact amounts	3
Sucrose	not specified	341.46
Corn starch		150.75
Corn Oil		
Anhydrous Milkfat		160
Lard, (Pork)		50
Cellulose		35.13
Mineral Mix		50
Zinc Carbonate		0.04
Vitamin Mix		10
Choline Bitartrate		3
Ethoxyquin		0.02
Macronutrients		
% by weight (% of calories)		
Protein	24.3 (32)	17.3 (15.2)
Carbohydrate	40.2 (54)	48.7 (42.8)
Fat	4.7(14)	21.2 (42)
Kcal/g	3.0	4.5
Cholesterol (wt%)	0.005%	0.2%

*Represented Ingredients: Dehulled soybean meal, wheat middlings, flaked corn, ground corn, fish meal, soybean oil, brewers dried yeast, cane molasses, dried whey, dicalcium phosphate, calcium carbonate, iodized salt, choline, chloride, magnesium oxide, Vitamin A acetate, Vitamin D3, Vitamin E, niacin, pyridoxine hydrochloride, menadione, sodium, bisulfite, Vitamin B 12, manganous oxide, ferrous sulfate copper sulfate, zinc oxide, calcium, iodate, cobalt carbonate, chromium, potassium sulfate, kaolin

1.8.3.2 WESTERN DIET WITH ADDED CHOLESTEROL (HFHC DIET)

The western diet commonly used to induce metabolic abnormalities and atherosclerosis is composed of 42% calories as fat (21.2% by weight). Of the total fat, saturated fatty acids comprise 58% by weight, monounsaturated fatty acids 36% and polyunsaturated fatty acids 5%. This diet contains 0.05% cholesterol (by weight), derived from milkfat and lard (Harlan Teklad, TD96125). The addition of 0.15% cholesterol (for a total of 0.2%) modifies the western diet to the HFHC diet (Harlan Teklad, TD09268). Diets with the same or similar amounts of dietary cholesterol are known to increase macrophage inflammation and exacerbate the development of dyslipidemia, insulin resistance, hepatic steatosis and atherosclerosis (Subramanian et al., 2011, Subramanian et al., 2008). The carbohydrate component is 42.8% of calories (48.7% by weight) and is derived from sucrose, while the protein source is casein (15.2% of calories, 17.3% by weight). This diet does not contain any cholate. The caloric value of the HFHC diet is 4.5 kcal/g (Table 1-2). The HFHC diet was fed *ad libitum* to mice in studies described in Chapters 4 and 5.

1.9 SCOPE OF THESIS AND HYPOTHESES

Dyslipidemia and insulin resistance are major risk factors for the development of premature atherosclerosis. Specifically, elevated plasma TG-rich VLDL can readily induce macrophage foam cell formation, and insulin resistance is becoming increasingly accepted to accelerate foam cell formation. Therapeutic strategies that improve insulin sensitivity, the atherogenic lipid profile of the insulin resistant state and have direct effects on cells of the vessel wall to reduce macrophage foam cell formation and atherosclerosis, remain sparse. Therefore, identification and characterization of the novel therapeutic strategies that correct the metabolic consequences of insulin resistance are becoming increasingly important.

The studies in this thesis were undertaken to understand the physiological and molecular mechanisms involved in the attenuation of macrophage foam cell formation, the inflammatory response, atherosclerosis and metabolic dysregulation by activation of PPAR δ . We first examine the ability of synthetic PPAR δ ligands (GW0742 and GW501516) to specifically activate PPAR δ and attenuate VLDL-induced macrophage foam cell formation. We investigated both the lipid lowering and anti-inflammatory capabilities of PPAR δ -specific activation in this setting, and determined the mechanism by which the GW compounds lower macrophage TG accumulation and prevent VLDL-induced proinflammatory cytokine expression. We next examined the ability of these compounds to attenuate CE-rich lipoprotein-induced foam cell formation. To determine if our *in vitro* results translated *in vivo*, we subsequently determined whether intervention to a high-fat high-cholesterol diet with GW501516 was able to either prevent progression, or induce regression of pre-established atherosclerotic lesions. Additionally, we studied whether GW501516 was capable of correcting pre-established metabolic dysregulation, including hepatic steatosis, and sought to define the mechanisms involved. Therefore, Chapters 2 to 5 of this thesis address the following hypotheses:

1. PPAR δ -specific activation in macrophages attenuates TG accumulation and the inflammatory response, induced by VLDL (Chapter 2).
2. PPAR δ -specific activation in macrophages attenuates CE accumulation and the inflammatory response, induced by native and modified forms of LDL (Chapter 3).
3. PPAR δ -specific activation *in vivo* attenuates progression of diet-induced atherosclerosis, aortic inflammation and aortic insulin resistance in *Ldlr*^{-/-} mice (Chapter 4).

4. Hepatic PPAR δ -specific activation attenuates steatosis via increased fatty acid oxidation, reduced *de novo* lipogenesis and improves insulin sensitivity in *Ldlr*^{-/-} mice (Chapter 5).

1.10 REFERENCES

Accad, M., Smith, S.J., Newland, D.L., Sanan, D.A., King, L.E., Jr., Linton, M.F., Fazio, S., and Farese, R.V., Jr. (2000). Massive Xanthomatosis and Altered Composition of Atherosclerotic Lesions in Hyperlipidemic Mice Lacking Acyl Coa:Cholesterol Acyltransferase 1. *J Clin Invest* 105, 711-719.

Alberts, A.W., Chen, J., Kuron, G., Hunt, V., Huff, J., Hoffman, C., Rothrock, J., Lopez, M., Joshua, H., Harris, E., *et al.* (1980). Mevinolin: A Highly Potent Competitive Inhibitor of Hydroxymethylglutaryl-Coenzyme a Reductase and a Cholesterol-Lowering Agent. *Proc Natl Acad Sci U S A* 77, 3957-3961.

Allister, E.M., Borradaile, N.M., Edwards, J.Y., and Huff, M.W. (2005). Inhibition of Microsomal Triglyceride Transfer Protein Expression and Apolipoprotein B100 Secretion by the Citrus Flavonoid Naringenin and by Insulin Involves Activation of the Mitogen-Activated Protein Kinase Pathway in Hepatocytes. *Diabetes* 54, 1676-1683.

An, J., Muoio, D.M., Shiota, M., Fujimoto, Y., Cline, G.W., Shulman, G.I., Koves, T.R., Stevens, R., Millington, D., and Newgard, C.B. (2004). Hepatic Expression of Malonyl-Coa Decarboxylase Reverses Muscle, Liver and Whole-Animal Insulin Resistance. *Nat Med* 10, 268-274.

Anagnostis, P., Athyros, V.G., Adamidou, F., Panagiotou, A., Kita, M., Karagiannis, A., and Mikhailidis, D.P. (2011). Glucagon-Like Peptide-1-Based Therapies and Cardiovascular Disease: Looking Beyond Glycaemic Control. *Diabetes Obes Metab* 13, 302-312.

Anderson, E.K., Hill, A.A., and Hasty, A.H. (2012). Stearic Acid Accumulation in Macrophages Induces Toll-Like Receptor 4/2-Independent Inflammation Leading to Endoplasmic Reticulum Stress-Mediated Apoptosis. *Arterioscler Thromb Vasc Biol* 32, 1687-1695.

Assini, J.M., Mulvihill, E.E., Sutherland, B.G., Telford, D.E., Sawyez, C.G., Felder, S.L., Chhoker, S., Edwards, J.Y., Gros, R., and Huff, M.W. (2013). Naringenin Prevents Cholesterol-Induced Systemic Inflammation, Metabolic Dysregulation, and Atherosclerosis in Ldlr(-)/(-) Mice. *J Lipid Res* 54, 711-724.

Auwerx, J. (1991). The Human Leukemia Cell Line, Thp-1: A Multifaceted Model for the Study of Monocyte-Macrophage Differentiation. *Experientia* 47, 22-31.

Banka, C.L., Black, A.S., Dyer, C.A., and Curtiss, L.K. (1991). Thp-1 Cells Form Foam Cells in Response to Coculture with Lipoproteins but Not Platelets. *J Lipid Res* 32, 35-43.

Barak, Y., Nelson, M.C., Ong, E.S., Jones, Y.Z., Ruiz-Lozano, P., Chien, K.R., Koder, A., and Evans, R.M. (1999). Ppar Gamma Is Required for Placental, Cardiac, and Adipose Tissue Development. *Mol Cell* 4, 585-595.

Barish, G.D., Atkins, A.R., Downes, M., Olson, P., Chong, L.W., Nelson, M., Zou, Y., Hwang, H., Kang, H., Curtiss, L., *et al.* (2008). Ppardelta Regulates Multiple Proinflammatory Pathways to Suppress Atherosclerosis. *Proc Natl Acad Sci U S A* 105, 4271-4276.

Barrows, B.R., and Parks, E.J. (2006). Contributions of Different Fatty Acid Sources to Very Low-Density Lipoprotein-Triacylglycerol in the Fasted and Fed States. *J Clin Endocrinol Metab* 91, 1446-1452.

Barter, P.J., and Rye, K.A. (2012). Cholesteryl Ester Transfer Protein Inhibition as a Strategy to Reduce Cardiovascular Risk. *J Lipid Res* 53, 1755-1766.

Bates, S.R., Murphy, P.L., Feng, Z.C., Kanazawa, T., and Getz, G.S. (1984). Very Low Density Lipoproteins Promote Triglyceride Accumulation in Macrophages. *Arteriosclerosis* 4, 103-114.

Bays, H.E., Schwartz, S., Littlejohn, T., 3rd, Kerzner, B., Krauss, R.M., Karpf, D.B., Choi, Y.J., Wang, X., Naim, S., and Roberts, B.K. (2011). Mbx-8025, a Novel Peroxisome Proliferator Receptor-Delta Agonist: Lipid and Other Metabolic Effects in Dyslipidemic Overweight Patients Treated with and without Atorvastatin. *J Clin Endocrinol Metab* 96, 2889-2897.

Becker, L., Liu, N.C., Averill, M.M., Yuan, W., Pamir, N., Peng, Y., Irwin, A.D., Fu, X., Bornfeldt, K.E., and Heinecke, J.W. (2012). Unique Proteomic Signatures Distinguish Macrophages and Dendritic Cells. *PLoS One* 7, e33297.

Biddinger, S.B., Hernandez-Ono, A., Rask-Madsen, C., Haas, J.T., Aleman, J.O., Suzuki, R., Scapa, E.F., Agarwal, C., Carey, M.C., Stephanopoulos, G., *et al.* (2008). Hepatic Insulin Resistance Is Sufficient to Produce Dyslipidemia and Susceptibility to Atherosclerosis. *Cell Metab* 7, 125-134.

Blasiolo, D.A., Davis, R.A., and Attie, A.D. (2007). The Physiological and Molecular Regulation of Lipoprotein Assembly and Secretion. *Mol Biosyst* 3, 608-619.

Bojic, L.A., Sawyez, C.G., Telford, D.E., Edwards, J.Y., Hegele, R.A., and Huff, M.W. (2012). Activation of Peroxisome Proliferator-Activated Receptor Delta Inhibits Human Macrophage Foam Cell Formation and the Inflammatory Response Induced by Very Low-Density Lipoprotein. *Arterioscler Thromb Vasc Biol*.

Bonnefont, J.P., Djouadi, F., Prip-Buus, C., Gobin, S., Munnich, A., and Bastin, J. (2004). Carnitine Palmitoyltransferases 1 and 2: Biochemical, Molecular and Medical Aspects. *Mol Aspects Med* 25, 495-520.

Brown, M.S., and Goldstein, J.L. (2008). Selective Versus Total Insulin Resistance: A Pathogenic Paradox. *Cell Metab* 7, 95-96.

Brown, M.S., Ho, Y.K., and Goldstein, J.L. (1980). The Cholesteryl Ester Cycle in Macrophage Foam Cells. Continual Hydrolysis and Re-Esterification of Cytoplasmic Cholesteryl Esters. *J Biol Chem* 255, 9344-9352.

Buhman, K.K., Accad, M., Novak, S., Choi, R.S., Wong, J.S., Hamilton, R.L., Turley, S., and Farese, R.V., Jr. (2000). Resistance to Diet-Induced Hypercholesterolemia and Gallstone Formation in Acat2-Deficient Mice. *Nat Med* 6, 1341-1347.

Cannon, C.P., Braunwald, E., McCabe, C.H., Rader, D.J., Rouleau, J.L., Belder, R., Joyal, S.V., Hill, K.A., Pfeffer, M.A., and Skene, A.M. (2004). Intensive Versus Moderate Lipid Lowering with Statins after Acute Coronary Syndromes. *N Engl J Med* 350, 1495-1504.

Chakravarthy, M.V., Pan, Z., Zhu, Y., Tordjman, K., Schneider, J.G., Coleman, T., Turk, J., and Semenkovich, C.F. (2005). "New" Hepatic Fat Activates Pparalpha to Maintain Glucose, Lipid, and Cholesterol Homeostasis. *Cell Metab* 1, 309-322.

Chatalow, N.A.a.S. (1983). Classics in Arteriosclerosis Research: On Experimental Cholesterin Steatosis and Its Significance in the Origin of Some Pathological Processes by N. Anitschkow and S. Chatalow, Translated by Mary Z. Pelias, 1913. *Arteriosclerosis* 3, 178-182.

Chawla, A., Lee, C.H., Barak, Y., He, W., Rosenfeld, J., Liao, D., Han, J., Kang, H., and Evans, R.M. (2003). Ppardelta Is a Very Low-Density Lipoprotein Sensor in Macrophages. *Proc Natl Acad Sci U S A* 100, 1268-1273.

Chawla, A., Schwarz, E.J., Dimaculangan, D.D., and Lazar, M.A. (1994). Peroxisome Proliferator-Activated Receptor (Ppar) Gamma: Adipose-Predominant Expression and Induction Early in Adipocyte Differentiation. *Endocrinology* 135, 798-800.

Chen, H.C., Stone, S.J., Zhou, P., Buhman, K.K., and Farese, R.V., Jr. (2002). Dissociation of Obesity and Impaired Glucose Disposal in Mice Overexpressing Acyl Coenzyme A:Diacylglycerol Acyltransferase 1 in White Adipose Tissue. *Diabetes* 51, 3189-3195.

Chen, S.H., Habib, G., Yang, C.Y., Gu, Z.W., Lee, B.R., Weng, S.A., Silberman, S.R., Cai, S.J., Deslypere, J.P., Rosseneu, M., *et al.* (1987). Apolipoprotein B-48 Is the Product of a Messenger Rna with an Organ-Specific in-Frame Stop Codon. *Science* 238, 363-366.

Choi, J.H., Banks, A.S., Estall, J.L., Kajimura, S., Bostrom, P., Laznik, D., Ruas, J.L., Chalmers, M.J., Kamenecka, T.M., Bluher, M., *et al.* (2010). Anti-Diabetic Drugs Inhibit Obesity-Linked Phosphorylation of Ppargamma by Cdk5. *Nature* 466, 451-456.

Choi, J.H., Banks, A.S., Kamenecka, T.M., Busby, S.A., Chalmers, M.J., Kumar, N., Kuruvilla, D.S., Shin, Y., He, Y., Bruning, J.B., *et al.* (2011). Antidiabetic Actions of a

Non-Agonist Ppargamma Ligand Blocking Cdk5-Mediated Phosphorylation. *Nature* 477, 477-481.

Choi, Y.J., Roberts, B.K., Wang, X., Geaney, J.C., Naim, S., Wojnoonski, K., Karpf, D.B., and Krauss, R.M. (2012). Effects of the Ppar-Delta Agonist Mbx-8025 on Atherogenic Dyslipidemia. *Atherosclerosis* 220, 470-476.

Crooke, R.M., Graham, M.J., Lemonidis, K.M., Whipple, C.P., Koo, S., and Perera, R.J. (2005). An Apolipoprotein B Antisense Oligonucleotide Lowers Ldl Cholesterol in Hyperlipidemic Mice without Causing Hepatic Steatosis. *J Lipid Res* 46, 872-884.

Curtiss, L.K., Black, A.S., Bonnet, D.J., and Tobias, P.S. (2012). Atherosclerosis Induced by Endogenous and Exogenous Toll-Like Receptor (Tlr)1 or Tlr6 Agonists. *J Lipid Res* 53, 2126-2132.

Cybulsky, M.I., and Jongstra-Bilen, J. (2010). Resident Intimal Dendritic Cells and the Initiation of Atherosclerosis. *Curr Opin Lipidol* 21, 397-403.

DeFronzo, R.A., Okerson, T., Viswanathan, P., Guan, X., Holcombe, J.H., and MacConell, L. (2008). Effects of Exenatide Versus Sitagliptin on Postprandial Glucose, Insulin and Glucagon Secretion, Gastric Emptying, and Caloric Intake: A Randomized, Cross-over Study. *Curr Med Res Opin* 24, 2943-2952.

Dzambo, N., van Denderen, B.J., Hevener, A.L., Jorgensen, S.B., Honeyman, J., Galic, S., Chen, Z.P., Watt, M.J., Campbell, D.J., Steinberg, G.R., *et al.* (2010). Ampk Beta1 Deletion Reduces Appetite, Preventing Obesity and Hepatic Insulin Resistance. *J Biol Chem* 285, 115-122.

Eckel, R.H., Alberti, K.G., Grundy, S.M., and Zimmet, P.Z. (2010). The Metabolic Syndrome. *Lancet* 375, 181-183.

Eferl, R., and Wagner, E.F. (2003). Ap-1: A Double-Edged Sword in Tumorigenesis. *Nat Rev Cancer* 3, 859-868.

Endo, A., Kuroda, M., and Tsujita, Y. (1976). MI-236a, MI-236b, and MI-236c, New Inhibitors of Cholesterologenesis Produced by *Penicillium Citrinium*. *J Antibiot (Tokyo)* 29, 1346-1348.

Engelking, L.J., Kuriyama, H., Hammer, R.E., Horton, J.D., Brown, M.S., Goldstein, J.L., and Liang, G. (2004). Overexpression of Insig-1 in the Livers of Transgenic Mice Inhibits Srebp Processing and Reduces Insulin-Stimulated Lipogenesis. *J Clin Invest* 113, 1168-1175.

Engelking, L.J., Liang, G., Hammer, R.E., Takaishi, K., Kuriyama, H., Evers, B.M., Li, W.P., Horton, J.D., Goldstein, J.L., and Brown, M.S. (2005). Schoenheimer Effect

Explained--Feedback Regulation of Cholesterol Synthesis in Mice Mediated by Insig Proteins. *J Clin Invest* 115, 2489-2498.

Erridge, C., and Samani, N.J. (2009). Saturated Fatty Acids Do Not Directly Stimulate Toll-Like Receptor Signaling. *Arterioscler Thromb Vasc Biol* 29, 1944-1949.

Erwig, L.P., and Henson, P.M. (2008). Clearance of Apoptotic Cells by Phagocytes. *Cell Death Differ* 15, 243-250.

Fazio, S., Major, A.S., Swift, L.L., Gleaves, L.A., Accad, M., Linton, M.F., and Farese, R.V., Jr. (2001). Increased Atherosclerosis in Ldl Receptor-Null Mice Lacking Acat1 in Macrophages. *J Clin Invest* 107, 163-171.

Febbraio, M., Podrez, E.A., Smith, J.D., Hajjar, D.P., Hazen, S.L., Hoff, H.F., Sharma, K., and Silverstein, R.L. (2000). Targeted Disruption of the Class B Scavenger Receptor Cd36 Protects against Atherosclerotic Lesion Development in Mice. *J Clin Invest* 105, 1049-1056.

Fernandez-Hernando, C., Ackah, E., Yu, J., Suarez, Y., Murata, T., Iwakiri, Y., Prendergast, J., Miao, R.Q., Birnbaum, M.J., and Sessa, W.C. (2007). Loss of Akt1 Leads to Severe Atherosclerosis and Occlusive Coronary Artery Disease. *Cell Metab* 6, 446-457.

Fisher, E.A., Feig, J.E., Hewing, B., Hazen, S.L., and Smith, J.D. (2012). High-Density Lipoprotein Function, Dysfunction, and Reverse Cholesterol Transport. *Arterioscler Thromb Vasc Biol* 32, 2813-2820.

Fournier, T., Tsatsaris, V., Handschuh, K., and Evain-Brion, D. (2007). Ppars and the Placenta. *Placenta* 28, 65-76.

Fox, C.S., Coady, S., Sorlie, P.D., D'Agostino, R.B., Sr., Pencina, M.J., Vasan, R.S., Meigs, J.B., Levy, D., and Savage, P.J. (2007). Increasing Cardiovascular Disease Burden Due to Diabetes Mellitus: The Framingham Heart Study. *Circulation* 115, 1544-1550.

Fox, C.S., Coady, S., Sorlie, P.D., Levy, D., Meigs, J.B., D'Agostino, R.B., Sr., Wilson, P.W., and Savage, P.J. (2004). Trends in Cardiovascular Complications of Diabetes. *Jama* 292, 2495-2499.

Fu, S., Watkins, S.M., and Hotamisligil, G.S. (2012). The Role of Endoplasmic Reticulum in Hepatic Lipid Homeostasis and Stress Signaling. *Cell Metab* 15, 623-634.

Gerstein, H.C., Bosch, J., Dagenais, G.R., Diaz, R., Jung, H., Maggioni, A.P., Pogue, J., Probstfield, J., Ramachandran, A., Riddle, M.C., *et al.* (2012). Basal Insulin and Cardiovascular and Other Outcomes in Dysglycemia. *N Engl J Med* 367, 319-328.

Gerstein, H.C., Miller, M.E., Genuth, S., Ismail-Beigi, F., Buse, J.B., Goff, D.C., Jr., Probstfield, J.L., Cushman, W.C., Ginsberg, H.N., Bigger, J.T., *et al.* (2011). Long-Term Effects of Intensive Glucose Lowering on Cardiovascular Outcomes. *N Engl J Med* 364, 818-828.

Getz, G.S., and Reardon, C.A. (2006). Diet and Murine Atherosclerosis. *Arterioscler Thromb Vasc Biol* 26, 242-249.

Ginsberg, H.N. (2000). Insulin Resistance and Cardiovascular Disease. *J Clin Invest* 106, 453-458.

Ginsberg, H.N., Elam, M.B., Lovato, L.C., Crouse, J.R., 3rd, Leiter, L.A., Linz, P., Friedewald, W.T., Buse, J.B., Gerstein, H.C., Probstfield, J., *et al.* (2010). Effects of Combination Lipid Therapy in Type 2 Diabetes Mellitus. *N Engl J Med* 362, 1563-1574.

Glass, C.K., and Witztum, J.L. (2001). Atherosclerosis. The Road Ahead. *Cell* 104, 503-516.

Goldberg, I.J., Eckel, R.H., and McPherson, R. (2011). Triglycerides and Heart Disease: Still a Hypothesis? *Arterioscler Thromb Vasc Biol* 31, 1716-1725.

Goldstein, J.L., and Brown, M.S. (2009). The Ldl Receptor. *Arterioscler Thromb Vasc Biol* 29, 431-438.

Goldstein, J.L., DeBose-Boyd, R.A., and Brown, M.S. (2006). Protein Sensors for Membrane Sterols. *Cell* 124, 35-46.

Graham, T.L., Mookherjee, C., Suckling, K.E., Palmer, C.N., and Patel, L. (2005). The Ppardelta Agonist Gw0742x Reduces Atherosclerosis in Ldlr(-/-) Mice. *Atherosclerosis* 181, 29-37.

Gregor, M.F., and Hotamisligil, G.S. (2011). Inflammatory Mechanisms in Obesity. *Annu Rev Immunol* 29, 415-445.

Group, U. (1998). Intensive Blood-Glucose Control with Sulphonylureas or Insulin Compared with Conventional Treatment and Risk of Complications in Patients with Type 2 Diabetes (Ukpds 33). Uk Prospective Diabetes Study (Ukpds) Group. *Lancet* 352, 837-853.

Haas, J.T., and Biddinger, S.B. (2009). Dissecting the Role of Insulin Resistance in the Metabolic Syndrome. *Curr Opin Lipidol* 20, 206-210.

Haas, J.T., Miao, J., Chanda, D., Wang, Y., Zhao, E., Haas, M.E., Hirschey, M., Vaitheesvaran, B., Farese, R.V., Jr., Kurland, I.J., *et al.* (2012). Hepatic Insulin Signaling Is Required for Obesity-Dependent Expression of Srebp-1c Mrna but Not for Feeding-Dependent Expression. *Cell Metab* 15, 873-884.

Han, S., Liang, C.P., DeVries-Seimon, T., Ranalletta, M., Welch, C.L., Collins-Fletcher, K., Accili, D., Tabas, I., and Tall, A.R. (2006). Macrophage Insulin Receptor Deficiency Increases Er Stress-Induced Apoptosis and Necrotic Core Formation in Advanced Atherosclerotic Lesions. *Cell Metab* 3, 257-266.

Harmon, G.S., Lam, M.T., and Glass, C.K. (2011). Ppars and Lipid Ligands in Inflammation and Metabolism. *Chem Rev* 111, 6321-6340.

Hegele, R.A. (2009). Plasma Lipoproteins: Genetic Influences and Clinical Implications. *Nat Rev Genet* 10, 109-121.

Horton, J.D., Goldstein, J.L., and Brown, M.S. (2002). Srebps: Activators of the Complete Program of Cholesterol and Fatty Acid Synthesis in the Liver. *J Clin Invest* 109, 1125-1131.

Hu, L., van der Hoogt, C.C., Espirito Santo, S.M., Out, R., Kypreos, K.E., van Vlijmen, B.J., Van Berkel, T.J., Romijn, J.A., Havekes, L.M., van Dijk, K.W., *et al.* (2008). The Hepatic Uptake of Vldl in Lrp-Ldlr-/Vldlr-/ Mice Is Regulated by Lpl Activity and Involves Proteoglycans and Sr-Bi. *J Lipid Res* 49, 1553-1561.

Huff, M.W., Evans, A.J., Sawyez, C.G., Wolfe, B.M., and Nestel, P.J. (1991). Cholesterol Accumulation in J774 Macrophages Induced by Triglyceride-Rich Lipoproteins. Comparison of Very Low Density Lipoprotein from Subjects with Type Iii, Iv, and V Hyperlipoproteinemias. *Arterioscler Thromb* 11, 221-233.

Huff, M.W., Pollex, R.L., and Hegele, R.A. (2006). Npc1l1: Evolution from Pharmacological Target to Physiological Sterol Transporter. *Arterioscler Thromb Vasc Biol* 26, 2433-2438.

Hummasti, S., and Hotamisligil, G.S. (2010). Endoplasmic Reticulum Stress and Inflammation in Obesity and Diabetes. *Circ Res* 107, 579-591.

Ikonen, E. (2008). Cellular Cholesterol Trafficking and Compartmentalization. *Nat Rev Mol Cell Biol* 9, 125-138.

Ishibashi, S., Brown, M.S., Goldstein, J.L., Gerard, R.D., Hammer, R.E., and Herz, J. (1993). Hypercholesterolemia in Low Density Lipoprotein Receptor Knockout Mice and Its Reversal by Adenovirus-Mediated Gene Delivery. *J Clin Invest* 92, 883-893.

Janabi, M., Yamashita, S., Hirano, K., Sakai, N., Hiraoka, H., Matsumoto, K., Zhang, Z., Nozaki, S., and Matsuzawa, Y. (2000). Oxidized Ldl-Induced Nf-Kappa B Activation and Subsequent Expression of Proinflammatory Genes Are Defective in Monocyte-Derived Macrophages from Cd36-Deficient Patients. *Arterioscler Thromb Vasc Biol* 20, 1953-1960.

Johnson, A.C., Yabu, J.M., Hanson, S., Shah, V.O., and Zager, R.A. (2003). Experimental Glomerulopathy Alters Renal Cortical Cholesterol, Sr-B1, Abca1, and Hmg Coa Reductase Expression. *Am J Pathol* 162, 283-291.

Kamagate, A., Qu, S., Perdomo, G., Su, D., Kim, D.H., Slusher, S., Meseck, M., and Dong, H.H. (2008). Foxo1 Mediates Insulin-Dependent Regulation of Hepatic Vldl Production in Mice. *J Clin Invest* 118, 2347-2364.

Kannan, Y., Sundaram, K., Aluganti Narasimhulu, C., Parthasarathy, S., and Wewers, M.D. (2012). Oxidatively Modified Low Density Lipoprotein (Ldl) Inhibits Tlr2 and Tlr4 Cytokine Responses in Human Monocytes but Not in Macrophages. *J Biol Chem* 287, 23479-23488.

Karpe, F. (2002). Postprandial Lipemia--Effect of Lipid-Lowering Drugs. *Atheroscler Suppl* 3, 41-46.

Kido, Y., Nakae, J., and Accili, D. (2001). Clinical Review 125: The Insulin Receptor and Its Cellular Targets. *J Clin Endocrinol Metab* 86, 972-979.

Kliwer, S.A., Forman, B.M., Blumberg, B., Ong, E.S., Borgmeyer, U., Mangelsdorf, D.J., Umesono, K., and Evans, R.M. (1994). Differential Expression and Activation of a Family of Murine Peroxisome Proliferator-Activated Receptors. *Proc Natl Acad Sci U S A* 91, 7355-7359.

Koliwad, S.K., Streeper, R.S., Monetti, M., Cornelissen, I., Chan, L., Terayama, K., Naylor, S., Rao, M., Hubbard, B., and Farese, R.V., Jr. (2010). Dgat1-Dependent Triacylglycerol Storage by Macrophages Protects Mice from Diet-Induced Insulin Resistance and Inflammation. *J Clin Invest* 120, 756-767.

Lauber, K., Blumenthal, S.G., Waibel, M., and Wesselborg, S. (2004). Clearance of Apoptotic Cells: Getting Rid of the Corpses. *Mol Cell* 14, 277-287.

Lee, C.H., Chawla, A., Urbiztondo, N., Liao, D., Boisvert, W.A., Evans, R.M., and Curtiss, L.K. (2003). Transcriptional Repression of Atherogenic Inflammation: Modulation by Ppardelta. *Science* 302, 453-457.

Lee, C.H., Kang, K., Mehl, I.R., Nofsinger, R., Alaynick, W.A., Chong, L.W., Rosenfeld, J.M., and Evans, R.M. (2006a). Peroxisome Proliferator-Activated Receptor Delta Promotes Very Low-Density Lipoprotein-Derived Fatty Acid Catabolism in the Macrophage. *Proc Natl Acad Sci U S A* 103, 2434-2439.

Lee, C.H., Olson, P., Hevener, A., Mehl, I., Chong, L.W., Olefsky, J.M., Gonzalez, F.J., Ham, J., Kang, H., Peters, J.M., *et al.* (2006b). Ppardelta Regulates Glucose Metabolism and Insulin Sensitivity. *Proc Natl Acad Sci U S A* 103, 3444-3449.

Lee, D.S., Chiu, M., Manuel, D.G., Tu, K., Wang, X., Austin, P.C., Mattern, M.Y., Mitiku, T.F., Svenson, L.W., Putnam, W., *et al.* (2009). Trends in Risk Factors for Cardiovascular Disease in Canada: Temporal, Socio-Demographic and Geographic Factors. *CMAJ* 181, E55-66.

Lee, J.Y., Zhao, L., Youn, H.S., Weatherill, A.R., Tapping, R., Feng, L., Lee, W.H., Fitzgerald, K.A., and Hwang, D.H. (2004a). Saturated Fatty Acid Activates but Polyunsaturated Fatty Acid Inhibits Toll-Like Receptor 2 Dimerized with Toll-Like Receptor 6 or 1. *J Biol Chem* 279, 16971-16979.

Lee, R.G., Kelley, K.L., Sawyer, J.K., Farese, R.V., Jr., Parks, J.S., and Rudel, L.L. (2004b). Plasma Cholesteryl Esters Provided by Lecithin:Cholesterol Acyltransferase and Acyl-Coenzyme A:Cholesterol Acyltransferase 2 Have Opposite Atherosclerotic Potential. *Circ Res* 95, 998-1004.

Li, A.C., Binder, C.J., Gutierrez, A., Brown, K.K., Plotkin, C.R., Pattison, J.W., Valledor, A.F., Davis, R.A., Willson, T.M., Witztum, J.L., *et al.* (2004). Differential Inhibition of Macrophage Foam-Cell Formation and Atherosclerosis in Mice by Pparalpha, Beta/Delta, and Gamma. *J Clin Invest* 114, 1564-1576.

Li, S., Brown, M.S., and Goldstein, J.L. (2010). Bifurcation of Insulin Signaling Pathway in Rat Liver: Mtorc1 Required for Stimulation of Lipogenesis, but Not Inhibition of Gluconeogenesis. *Proc Natl Acad Sci U S A* 107, 3441-3446.

Li, Y., Schwabe, R.F., DeVries-Seimon, T., Yao, P.M., Gerbod-Giannone, M.C., Tall, A.R., Davis, R.J., Flavell, R., Brenner, D.A., and Tabas, I. (2005). Free Cholesterol-Loaded Macrophages Are an Abundant Source of Tumor Necrosis Factor-Alpha and Interleukin-6: Model of Nf-Kappab- and Map Kinase-Dependent Inflammation in Advanced Atherosclerosis. *J Biol Chem* 280, 21763-21772.

Liang, C.P., Han, S., Li, G., Tabas, I., and Tall, A.R. (2012). Impaired Mek Signaling and Serca Expression Promote Er Stress and Apoptosis in Insulin-Resistant Macrophages and Are Reversed by Exenatide Treatment. *Diabetes* 61, 2609-2620.

Libby, P., Ridker, P.M., and Hansson, G.K. (2011). Progress and Challenges in Translating the Biology of Atherosclerosis. *Nature* 473, 317-325.

Lippi, G., and Favaloro, E.J. (2011). Antisense Therapy in the Treatment of Hypercholesterolemia. *Eur J Intern Med* 22, 541-546.

Liu, Q., Siloto, R.M., Lehner, R., Stone, S.J., and Weselake, R.J. (2012). Acyl-Coa:Diacylglycerol Acyltransferase: Molecular Biology, Biochemistry and Biotechnology. *Prog Lipid Res* 51, 350-377.

Liu, S., Hatano, B., Zhao, M., Yen, C.C., Kang, K., Reilly, S.M., Gangl, M.R., Gorgun, C., Balschi, J.A., Ntambi, J.M., *et al.* (2011). Role of Peroxisome Proliferator-Activated Receptor $\{\Delta\}/\{\beta\}$ in Hepatic Metabolic Regulation. *J Biol Chem* 286, 1237-1247.

Lloyd-Jones, D., Adams, R.J., Brown, T.M., Carnethon, M., Dai, S., De Simone, G., Ferguson, T.B., Ford, E., Furie, K., Gillespie, C., *et al.* (2010). Executive Summary: Heart Disease and Stroke Statistics--2010 Update: A Report from the American Heart Association. *Circulation* 121, 948-954.

Lusis, A.J. (2000). Atherosclerosis. *Nature* 407, 233-241.

Mandard, S., Muller, M., and Kersten, S. (2004). Peroxisome Proliferator-Activated Receptor Alpha Target Genes. *Cell Mol Life Sci* 61, 393-416.

Manning-Tobin, J.J., Moore, K.J., Seimon, T.A., Bell, S.A., Sharuk, M., Alvarez-Leite, J.I., de Winther, M.P., Tabas, I., and Freeman, M.W. (2009). Loss of Sr-a and Cd36 Activity Reduces Atherosclerotic Lesion Complexity without Abrogating Foam Cell Formation in Hyperlipidemic Mice. *Arterioscler Thromb Vasc Biol* 29, 19-26.

Martinet, W., Schrijvers, D.M., and De Meyer, G.R. (2012). Molecular and Cellular Mechanisms of Macrophage Survival in Atherosclerosis. *Basic Res Cardiol* 107, 297.

Matsumoto, M., Han, S., Kitamura, T., and Accili, D. (2006). Dual Role of Transcription Factor Foxo1 in Controlling Hepatic Insulin Sensitivity and Lipid Metabolism. *J Clin Invest* 116, 2464-2472.

Maxfield, F.R., and Tabas, I. (2005). Role of Cholesterol and Lipid Organization in Disease. *Nature* 438, 612-621.

Mazzone, T., Chait, A., and Plutzky, J. (2008). Cardiovascular Disease Risk in Type 2 Diabetes Mellitus: Insights from Mechanistic Studies. *Lancet* 371, 1800-1809.

Meiner, V.L., Cases, S., Myers, H.M., Sande, E.R., Bellosta, S., Schambelan, M., Pitas, R.E., McGuire, J., Herz, J., and Farese, R.V., Jr. (1996). Disruption of the Acyl-Coa:Cholesterol Acyltransferase Gene in Mice: Evidence Suggesting Multiple Cholesterol Esterification Enzymes in Mammals. *Proc Natl Acad Sci U S A* 93, 14041-14046.

Mills, E.J., Rachlis, B., Wu, P., Devereaux, P.J., Arora, P., and Perri, D. (2008). Primary Prevention of Cardiovascular Mortality and Events with Statin Treatments: A Network Meta-Analysis Involving More Than 65,000 Patients. *J Am Coll Cardiol* 52, 1769-1781.

Miyazaki, A., Sakuma, S., Morikawa, W., Takiue, T., Miake, F., Terano, T., Sakai, M., Hakamata, H., Sakamoto, Y., Natio, M., *et al.* (1995). Intravenous Injection of Rabbit Apolipoprotein a-I Inhibits the Progression of Atherosclerosis in Cholesterol-Fed Rabbits. *Arterioscler Thromb Vasc Biol* 15, 1882-1888.

Monetti, M., Levin, M.C., Watt, M.J., Sajan, M.P., Marmor, S., Hubbard, B.K., Stevens, R.D., Bain, J.R., Newgard, C.B., Farese, R.V., Sr., *et al.* (2007). Dissociation of Hepatic Steatosis and Insulin Resistance in Mice Overexpressing Dgat in the Liver. *Cell Metab* 6, 69-78.

Moon, Y.A., Liang, G., Xie, X., Frank-Kamenetsky, M., Fitzgerald, K., Koteliansky, V., Brown, M.S., Goldstein, J.L., and Horton, J.D. (2012). The Scap/Srebp Pathway Is Essential for Developing Diabetic Fatty Liver and Carbohydrate-Induced Hypertriglyceridemia in Animals. *Cell Metab* 15, 240-246.

Moore, K.J., and Freeman, M.W. (2006). Scavenger Receptors in Atherosclerosis: Beyond Lipid Uptake. *Arterioscler Thromb Vasc Biol* 26, 1702-1711.

Moore, K.J., and Tabas, I. (2011). Macrophages in the Pathogenesis of Atherosclerosis. *Cell* 145, 341-355.

Mukundan, L., Odegaard, J.I., Morel, C.R., Heredia, J.E., Mwangi, J.W., Ricardo-Gonzalez, R.R., Goh, Y.P., Eagle, A.R., Dunn, S.E., Awakuni, J.U., *et al.* (2009). Ppar-Delta Senses and Orchestrates Clearance of Apoptotic Cells to Promote Tolerance. *Nat Med* 15, 1266-1272.

Mullick, A.E., Fu, W., Graham, M.J., Lee, R.G., Witchell, D., Bell, T.A., Whipple, C.P., and Crooke, R.M. (2011). Antisense Oligonucleotide Reduction of Apob-Ameliorated Atherosclerosis in Ldl Receptor-Deficient Mice. *J Lipid Res* 52, 885-896.

Mullick, A.E., Tobias, P.S., and Curtiss, L.K. (2005). Modulation of Atherosclerosis in Mice by Toll-Like Receptor 2. *J Clin Invest* 115, 3149-3156.

Musunuru, K. (2010). Atherogenic Dyslipidemia: Cardiovascular Risk and Dietary Intervention. *Lipids* 45, 907-914.

Neaton, J.D., and Wentworth, D. (1992). Serum Cholesterol, Blood Pressure, Cigarette Smoking, and Death from Coronary Heart Disease. Overall Findings and Differences by Age for 316,099 White Men. Multiple Risk Factor Intervention Trial Research Group. *Arch Intern Med* 152, 56-64.

Nicholls, S.J., Gordon, A., Johannson, J., Ballantyne, C.M., Barter, P.J., Brewer, H.B., Kastelein, J.J., Wong, N.C., Borgman, M.R., and Nissen, S.E. (2012). ApoA-I Induction as a Potential Cardioprotective Strategy: Rationale for the Sustain and Assure Studies. *Cardiovasc Drugs Ther* 26, 181-187.

Nyomba, B.L., Ossowski, V.M., Bogardus, C., and Mott, D.M. (1990). Insulin-Sensitive Tyrosine Kinase: Relationship with in Vivo Insulin Action in Humans. *Am J Physiol* 258, E964-974.

Nyomba, B.L., Swinburn, B.A., Ossowski, V.M., Boyce, V.L., Bogardus, C., and Mott, D.M. (1991). Insulin-Sensitive Tyrosine Kinase Activity Changes in Parallel with Plasma Insulin and Glucose Concentrations in Humans. *J Clin Endocrinol Metab* 72, 1212-1219.

O'Neill, H.M., Holloway, G.P., and Steinberg, G.R. (2013). Ampk Regulation of Fatty Acid Metabolism and Mitochondrial Biogenesis: Implications for Obesity. *Mol Cell Endocrinol* 366, 135-151.

Oakhill, J.S., Steel, R., Chen, Z.P., Scott, J.W., Ling, N., Tam, S., and Kemp, B.E. (2011). Ampk Is a Direct Adenylate Charge-Regulated Protein Kinase. *Science* 332, 1433-1435.

Odegaard, J.I., Ricardo-Gonzalez, R.R., Red Eagle, A., Vats, D., Morel, C.R., Goforth, M.H., Subramanian, V., Mukundan, L., Ferrante, A.W., and Chawla, A. (2008). Alternative M2 Activation of Kupffer Cells by Ppardelta Ameliorates Obesity-Induced Insulin Resistance. *Cell Metab* 7, 496-507.

Olson, E.J., Pearce, G.L., Jones, N.P., and Sprecher, D.L. (2012). Lipid Effects of Peroxisome Proliferator-Activated Receptor-Delta Agonist Gw501516 in Subjects with Low High-Density Lipoprotein Cholesterol: Characteristics of Metabolic Syndrome. *Arterioscler Thromb Vasc Biol* 32, 2289-2294.

Ooi, E.M., Watts, G.F., Sprecher, D.L., Chan, D.C., and Barrett, P.H. (2011). Mechanism of Action of a Peroxisome Proliferator-Activated Receptor (Ppar)-Delta Agonist on Lipoprotein Metabolism in Dyslipidemic Subjects with Central Obesity. *J Clin Endocrinol Metab* 96, E1568-1576.

Ozcan, L., Wong, C.C., Li, G., Xu, T., Pajvani, U., Park, S.K., Wronska, A., Chen, B.X., Marks, A.R., Fukamizu, A., *et al.* (2012). Calcium Signaling through Camkii Regulates Hepatic Glucose Production in Fasting and Obesity. *Cell Metab* 15, 739-751.

Ozcan, U., Cao, Q., Yilmaz, E., Lee, A.H., Iwakoshi, N.N., Ozdelen, E., Tuncman, G., Gorgun, C., Glimcher, L.H., and Hotamisligil, G.S. (2004). Endoplasmic Reticulum Stress Links Obesity, Insulin Action, and Type 2 Diabetes. *Science* 306, 457-461.

Pinkosky, S.L., Filippov, S., Srivastava, R.A., Hanselman, J.C., Bradshaw, C.D., Hurley, T.R., Cramer, C.T., Spahr, M.A., Brant, A.F., Houghton, J.L., *et al.* (2013). Amp-Activated Protein Kinase and Atp-Citrate Lyase Are Two Distinct Molecular Targets for Etc-1002, a Novel Small Molecule Regulator of Lipid and Carbohydrate Metabolism. *J Lipid Res* 54, 134-151.

Proctor, S.D., and Mamo, J.C. (1998). Retention of Fluorescent-Labelled Chylomicron Remnants within the Intima of the Arterial Wall--Evidence That Plaque Cholesterol May Be Derived from Post-Prandial Lipoproteins. *Eur J Clin Invest* 28, 497-503.

Prudente, S., Morini, E., and Trischitta, V. (2009). Insulin Signaling Regulating Genes: Effect on T2dm and Cardiovascular Risk. *Nat Rev Endocrinol* 5, 682-693.

Qin, X., Xie, X., Fan, Y., Tian, J., Guan, Y., Wang, X., Zhu, Y., and Wang, N. (2008). Peroxisome Proliferator-Activated Receptor-Delta Induces Insulin-Induced Gene-1 and Suppresses Hepatic Lipogenesis in Obese Diabetic Mice. *Hepatology* 48, 432-441.

Qin, Z. (2012). The Use of Thp-1 Cells as a Model for Mimicking the Function and Regulation of Monocytes and Macrophages in the Vasculature. *Atherosclerosis* 221, 2-11.

Qiu, G., Ho, A.C., Yu, W., and Hill, J.S. (2007). Suppression of Endothelial or Lipoprotein Lipase in Thp-1 Macrophages Attenuates Proinflammatory Cytokine Secretion. *J Lipid Res* 48, 385-394.

Rader, D.J., Alexander, E.T., Weibel, G.L., Billheimer, J., and Rothblat, G.H. (2009). The Role of Reverse Cholesterol Transport in Animals and Humans and Relationship to Atherosclerosis. *J Lipid Res* 50 *Suppl*, S189-194.

Rader, D.J., and Tall, A.R. (2012). The Not-So-Simple Hdl Story: Is It Time to Revise the Hdl Cholesterol Hypothesis? *Nat Med* 18, 1344-1346.

Rapp, J.H., Lespine, A., Hamilton, R.L., Colyvas, N., Chaumeton, A.H., Tweedie-Hardman, J., Kotite, L., Kunitake, S.T., Havel, R.J., and Kane, J.P. (1994). Triglyceride-Rich Lipoproteins Isolated by Selected-Affinity Anti-Apolipoprotein B Immunosorption from Human Atherosclerotic Plaque. *Arterioscler Thromb* 14, 1767-1774.

Rasmussen, B.B., Holmback, U.C., Volpi, E., Morio-Liondore, B., Paddon-Jones, D., and Wolfe, R.R. (2002). Malonyl Coenzyme a and the Regulation of Functional Carnitine Palmitoyltransferase-1 Activity and Fat Oxidation in Human Skeletal Muscle. *J Clin Invest* 110, 1687-1693.

Repa, J.J., and Mangelsdorf, D.J. (2000). The Role of Orphan Nuclear Receptors in the Regulation of Cholesterol Homeostasis. *Annu Rev Cell Dev Biol* 16, 459-481.

Reyes-Soffer, G., Ngai, C.I., Lovato, L., Karmally, W., Ramakrishnan, R., Holleran, S., and Ginsberg, H.N. (2013). Effect of Combination Therapy with Fenofibrate and Simvastatin on Postprandial Lipemia in the Accord Lipid Trial. *Diabetes Care* 36, 422-428.

Riserus, U., Sprecher, D., Johnson, T., Olson, E., Hirschberg, S., Liu, A., Fang, Z., Hegde, P., Richards, D., Sarov-Blat, L., *et al.* (2008). Activation of Peroxisome Proliferator-Activated Receptor (Ppar)Delta Promotes Reversal of Multiple Metabolic Abnormalities, Reduces Oxidative Stress, and Increases Fatty Acid Oxidation in Moderately Obese Men. *Diabetes* 57, 332-339.

Rong, J.X., Blachford, C., Feig, J.E., Bander, I., Mayne, J., Kusunoki, J., Miller, C., Davis, M., Wilson, M., Dehn, S., *et al.* (2013). Acat Inhibition Reduces the Progression of Preexisting, Advanced Atherosclerotic Mouse Lesions without Plaque or Systemic Toxicity. *Arterioscler Thromb Vasc Biol* 33, 4-12.

Rosen, E.D., Sarraf, P., Troy, A.E., Bradwin, G., Moore, K., Milstone, D.S., Spiegelman, B.M., and Mortensen, R.M. (1999). Ppar Gamma Is Required for the Differentiation of Adipose Tissue in Vivo and in Vitro. *Mol Cell* 4, 611-617.

Rosenberg, B.R., Hamilton, C.E., Mwangi, M.M., Dewell, S., and Papavasiliou, F.N. (2011). Transcriptome-Wide Sequencing Reveals Numerous Apobec1 Mrna-Editing Targets in Transcript 3' Utrs. *Nat Struct Mol Biol* 18, 230-236.

Sanders, M.J., Grondin, P.O., Hegarty, B.D., Snowden, M.A., and Carling, D. (2007). Investigating the Mechanism for Amp Activation of the Amp-Activated Protein Kinase Cascade. *Biochem J* 403, 139-148.

Saraswathi, V., and Hasty, A.H. (2006). The Role of Lipolysis in Mediating the Proinflammatory Effects of Very Low Density Lipoproteins in Mouse Peritoneal Macrophages. *J Lipid Res* 47, 1406-1415.

Schwartz, G.G., Olsson, A.G., Abt, M., Ballantyne, C.M., Barter, P.J., Brumm, J., Chaitman, B.R., Holme, I.M., Kallend, D., Leiter, L.A., *et al.* (2012). Effects of Dalcetrapib in Patients with a Recent Acute Coronary Syndrome. *N Engl J Med* 367, 2089-2099.

Seimon, T.A., Wang, Y., Han, S., Senokuchi, T., Schrijvers, D.M., Kuriakose, G., Tall, A.R., and Tabas, I.A. (2009). Macrophage Deficiency of P38alpha Mapk Promotes Apoptosis and Plaque Necrosis in Advanced Atherosclerotic Lesions in Mice. *J Clin Invest* 119, 886-898.

Senokuchi, T., Liang, C.P., Seimon, T.A., Han, S., Matsumoto, M., Banks, A.S., Paik, J.H., DePinho, R.A., Accili, D., Tabas, I., *et al.* (2008). Forkhead Transcription Factors (Foxos) Promote Apoptosis of Insulin-Resistant Macrophages During Cholesterol-Induced Endoplasmic Reticulum Stress. *Diabetes* 57, 2967-2976.

Serrano-Marco, L., Barroso, E., El Kochairi, I., Palomer, X., Michalik, L., Wahli, W., and Vazquez-Carrera, M. (2011). The Peroxisome Proliferator-Activated Receptor (Ppar) Beta/Delta Agonist Gw501516 Inhibits Il-6-Induced Signal Transducer and Activator of Transcription 3 (Stat3) Activation and Insulin Resistance in Human Liver Cells. *Diabetologia* 55, 743-751.

Shah, P.K., Yano, J., Reyes, O., Chyu, K.Y., Kaul, S., Bisgaier, C.L., Drake, S., and Cercek, B. (2001). High-Dose Recombinant Apolipoprotein a-I(Milano) Mobilizes Tissue Cholesterol and Rapidly Reduces Plaque Lipid and Macrophage Content in Apolipoprotein E-Deficient Mice. Potential Implications for Acute Plaque Stabilization. *Circulation* 103, 3047-3050.

Shao, W., and Espenshade, P.J. (2012). Expanding Roles for Srebp in Metabolism. *Cell Metab* 16, 414-419.

Shi, H., Kokoeva, M.V., Inouye, K., Tzameli, I., Yin, H., and Flier, J.S. (2006). Tlr4 Links Innate Immunity and Fatty Acid-Induced Insulin Resistance. *J Clin Invest* 116, 3015-3025.

Smith, S.J., Cases, S., Jensen, D.R., Chen, H.C., Sande, E., Tow, B., Sanan, D.A., Raber, J., Eckel, R.H., and Farese, R.V., Jr. (2000). Obesity Resistance and Multiple Mechanisms of Triglyceride Synthesis in Mice Lacking Dgat. *Nat Genet* 25, 87-90.

Sorci-Thomas, M.G., and Thomas, M.J. (2012). High Density Lipoprotein Biogenesis, Cholesterol Efflux, and Immune Cell Function. *Arterioscler Thromb Vasc Biol* 32, 2561-2565.

Spann, N.J., Garmire, L.X., McDonald, J.G., Myers, D.S., Milne, S.B., Shibata, N., Reichart, D., Fox, J.N., Shaked, I., Heudobler, D., *et al.* (2012). Regulated Accumulation of Desmosterol Integrates Macrophage Lipid Metabolism and Inflammatory Responses. *Cell* 151, 138-152.

Sprecher, D.L., Massien, C., Pearce, G., Billin, A.N., Perlstein, I., Willson, T.M., Hassall, D.G., Ancellin, N., Patterson, S.D., Lobe, D.C., *et al.* (2007). Triglyceride:High-Density Lipoprotein Cholesterol Effects in Healthy Subjects Administered a Peroxisome Proliferator Activated Receptor Delta Agonist. *Arterioscler Thromb Vasc Biol* 27, 359-365.

Stry, H.C. (2000). Natural History and Histological Classification of Atherosclerotic Lesions: An Update. *Arterioscler Thromb Vasc Biol* 20, 1177-1178.

Stry, H.C., Chandler, A.B., Dinsmore, R.E., Fuster, V., Glagov, S., Insull, W., Jr., Rosenfeld, M.E., Schwartz, C.J., Wagner, W.D., and Wissler, R.W. (1995). A Definition of Advanced Types of Atherosclerotic Lesions and a Histological Classification of Atherosclerosis. A Report from the Committee on Vascular Lesions of the Council on Arteriosclerosis, American Heart Association. *Circulation* 92, 1355-1374.

Stry, H.C., Chandler, A.B., Glagov, S., Guyton, J.R., Insull, W., Jr., Rosenfeld, M.E., Schaffer, S.A., Schwartz, C.J., Wagner, W.D., and Wissler, R.W. (1994). A Definition of Initial, Fatty Streak, and Intermediate Lesions of Atherosclerosis. A Report from the Committee on Vascular Lesions of the Council on Arteriosclerosis, American Heart Association. *Arterioscler Thromb* 14, 840-856.

Stewart, C.R., Stuart, L.M., Wilkinson, K., van Gils, J.M., Deng, J., Halle, A., Rayner, K.J., Boyer, L., Zhong, R., Frazier, W.A., *et al.* (2010). Cd36 Ligands Promote Sterile Inflammation through Assembly of a Toll-Like Receptor 4 and 6 Heterodimer. *Nat Immunol* 11, 155-161.

Stollenwerk, M.M., Schiopu, A., Fredrikson, G.N., Dichtl, W., Nilsson, J., and Ares, M.P. (2005). Very Low Density Lipoprotein Potentiates Tumor Necrosis Factor-Alpha Expression in Macrophages. *Atherosclerosis* 179, 247-254.

Stone, S.J., Myers, H.M., Watkins, S.M., Brown, B.E., Feingold, K.R., Elias, P.M., and Farese, R.V., Jr. (2004). Lipopenia and Skin Barrier Abnormalities in Dgat2-Deficient Mice. *J Biol Chem* 279, 11767-11776.

Su, D., Coudriet, G.M., Hyun Kim, D., Lu, Y., Perdomo, G., Qu, S., Slusher, S., Tse, H.M., Piganelli, J., Giannoukakis, N., *et al.* (2009). Foxo1 Links Insulin Resistance to Proinflammatory Cytokine Il-1beta Production in Macrophages. *Diabetes* 58, 2624-2633.

Subramanian, S., Goodspeed, L., Wang, S., Kim, J., Zeng, L., Ioannou, G.N., Haigh, W.G., Yeh, M.M., Kowdley, K.V., O'Brien, K.D., *et al.* (2011). Dietary Cholesterol Exacerbates Hepatic Steatosis and Inflammation in Obese Ldl Receptor-Deficient Mice. *J Lipid Res* 52, 1626-1635.

Subramanian, S., Han, C.Y., Chiba, T., McMillen, T.S., Wang, S.A., Haw, A., 3rd, Kirk, E.A., O'Brien, K.D., and Chait, A. (2008). Dietary Cholesterol Worsens Adipose Tissue Macrophage Accumulation and Atherosclerosis in Obese Ldl Receptor-Deficient Mice. *Arterioscler Thromb Vasc Biol* 28, 685-691.

Sudano, I., Spieker, L.E., Hermann, F., Flammer, A., Corti, R., Noll, G., and Luscher, T.F. (2006). Protection of Endothelial Function: Targets for Nutritional and Pharmacological Interventions. *J Cardiovasc Pharmacol* 47 Suppl 2, S136-150; discussion S172-136.

Sun, L.P., Li, L., Goldstein, J.L., and Brown, M.S. (2005). Insig Required for Sterol-Mediated Inhibition of Scap/Srebp Binding to Copii Proteins in Vitro. *J Biol Chem* 280, 26483-26490.

Swirski, F.K., Pittet, M.J., Kircher, M.F., Aikawa, E., Jaffer, F.A., Libby, P., and Weissleder, R. (2006). Monocyte Accumulation in Mouse Atherogenesis Is Progressive and Proportional to Extent of Disease. *Proc Natl Acad Sci U S A* 103, 10340-10345.

Tabas, I. (2010). The Role of Endoplasmic Reticulum Stress in the Progression of Atherosclerosis. *Circ Res* 107, 839-850.

Tabas, I., and Ron, D. (2011). Integrating the Mechanisms of Apoptosis Induced by Endoplasmic Reticulum Stress. *Nat Cell Biol* 13, 184-190.

Tabas, I., Tall, A., and Accili, D. (2010). The Impact of Macrophage Insulin Resistance on Advanced Atherosclerotic Plaque Progression. *Circ Res* 106, 58-67.

Tabas, I., Williams, K.J., and Boren, J. (2007). Subendothelial Lipoprotein Retention as the Initiating Process in Atherosclerosis: Update and Therapeutic Implications. *Circulation* 116, 1832-1844.

Takata, Y., Liu, J., Yin, F., Collins, A.R., Lyon, C.J., Lee, C.H., Atkins, A.R., Downes, M., Barish, G.D., Evans, R.M., *et al.* (2008). Ppardelta-Mediated Antiinflammatory Mechanisms Inhibit Angiotensin II-Accelerated Atherosclerosis. *Proc Natl Acad Sci U S A* 105, 4277-4282.

Talayero, B.G., and Sacks, F.M. (2011). The Role of Triglycerides in Atherosclerosis. *Curr Cardiol Rep* 13, 544-552.

Tall, A.R., Yvan-Charvet, L., Terasaka, N., Pagler, T., and Wang, N. (2008). Hdl, Abc Transporters, and Cholesterol Efflux: Implications for the Treatment of Atherosclerosis. *Cell Metab* 7, 365-375.

Tanaka, T., Yamamoto, J., Iwasaki, S., Asaba, H., Hamura, H., Ikeda, Y., Watanabe, M., Magoori, K., Ioka, R.X., Tachibana, K., *et al.* (2003). Activation of Peroxisome Proliferator-Activated Receptor Delta Induces Fatty Acid Beta-Oxidation in Skeletal Muscle and Attenuates Metabolic Syndrome. *Proc Natl Acad Sci U S A* 100, 15924-15929.

Tarling, E.J., Bojanic, D.D., Tangirala, R.K., Wang, X., Lovgren-Sandblom, A., Lusis, A.J., Bjorkhem, I., and Edwards, P.A. (2010). Impaired Development of Atherosclerosis in *Abcg1*^{-/-} *ApoE*^{-/-} Mice: Identification of Specific Oxysterols That Both Accumulate in *Abcg1*^{-/-} *ApoE*^{-/-} Tissues and Induce Apoptosis. *Arterioscler Thromb Vasc Biol* 30, 1174-1180.

Thorp, E., Li, G., Seimon, T.A., Kuriakose, G., Ron, D., and Tabas, I. (2009). Reduced Apoptosis and Plaque Necrosis in Advanced Atherosclerotic Lesions of *ApoE*^{-/-} and *Ldlr*^{-/-} Mice Lacking Chop. *Cell Metab* 9, 474-481.

Timmins, J.M., Lee, J.Y., Boudyguina, E., Kluckman, K.D., Brunham, L.R., Mulya, A., Gebre, A.K., Coutinho, J.M., Colvin, P.L., Smith, T.L., *et al.* (2005). Targeted Inactivation of Hepatic *Abca1* Causes Profound Hypoalphalipoproteinemia and Kidney Hypercatabolism of ApoA-I. *J Clin Invest* 115, 1333-1342.

Tobert, J.A. (2003). Lovastatin and Beyond: The History of the Hmg-Coa Reductase Inhibitors. *Nat Rev Drug Discov* 2, 517-526.

Tontonoz, P., Hu, E., and Spiegelman, B.M. (1994). Stimulation of Adipogenesis in Fibroblasts by Ppar Gamma 2, a Lipid-Activated Transcription Factor. *Cell* 79, 1147-1156.

Trigatti, B.L., Krieger, M., and Rigotti, A. (2003). Influence of the Hdl Receptor Sr-Bi on Lipoprotein Metabolism and Atherosclerosis. *Arterioscler Thromb Vasc Biol* 23, 1732-1738.

Tsuchiya, K., Tanaka, J., Shuiqing, Y., Welch, C.L., DePinho, R.A., Tabas, I., Tall, A.R., Goldberg, I.J., and Accili, D. (2012). Foxos Integrate Pleiotropic Actions of Insulin in Vascular Endothelium to Protect Mice from Atherosclerosis. *Cell Metab* 15, 372-381.

Tsuchiya, S., Yamabe, M., Yamaguchi, Y., Kobayashi, Y., Konno, T., and Tada, K. (1980). Establishment and Characterization of a Human Acute Monocytic Leukemia Cell Line (Thp-1). *Int J Cancer* 26, 171-176.

Tsukano, H., Gotoh, T., Endo, M., Miyata, K., Tazume, H., Kadomatsu, T., Yano, M., Iwawaki, T., Kohno, K., Araki, K., *et al.* (2010). The Endoplasmic Reticulum Stress-C/Ebp Homologous Protein Pathway-Mediated Apoptosis in Macrophages Contributes to the Instability of Atherosclerotic Plaques. *Arterioscler Thromb Vasc Biol* 30, 1925-1932.

Vance, D.E., and Van den Bosch, H. (2000). Cholesterol in the Year 2000. *Biochim Biophys Acta* 1529, 1-8.

Vosper, H., Patel, L., Graham, T.L., Khoudoli, G.A., Hill, A., Macphee, C.H., Pinto, I., Smith, S.A., Suckling, K.E., Wolf, C.R., *et al.* (2001). The Peroxisome Proliferator-Activated Receptor Delta Promotes Lipid Accumulation in Human Macrophages. *J Biol Chem* 276, 44258-44265.

Walldius, G., and Jungner, I. (2006). The Apob/Apoa-I Ratio: A Strong, New Risk Factor for Cardiovascular Disease and a Target for Lipid-Lowering Therapy--a Review of the Evidence. *J Intern Med* 259, 493-519.

Walther, T.C., and Farese, R.V., Jr. (2012). Lipid Droplets and Cellular Lipid Metabolism. *Annu Rev Biochem* 81, 687-714.

Wang, Y.X., Lee, C.H., Tjep, S., Yu, R.T., Ham, J., Kang, H., and Evans, R.M. (2003). Peroxisome-Proliferator-Activated Receptor Delta Activates Fat Metabolism to Prevent Obesity. *Cell* 113, 159-170.

Wang, Y.X., Zhang, C.L., Yu, R.T., Cho, H.K., Nelson, M.C., Bayuga-Ocampo, C.R., Ham, J., Kang, H., and Evans, R.M. (2004). Regulation of Muscle Fiber Type and Running Endurance by Ppardelta. *PLoS Biol* 2, e294.

Wasan, K.M., Brocks, D.R., Lee, S.D., Sachs-Barrable, K., and Thornton, S.J. (2008). Impact of Lipoproteins on the Biological Activity and Disposition of Hydrophobic Drugs: Implications for Drug Discovery. *Nat Rev Drug Discov* 7, 84-99.

Weber, C., Zernecke, A., and Libby, P. (2008). The Multifaceted Contributions of Leukocyte Subsets to Atherosclerosis: Lessons from Mouse Models. *Nat Rev Immunol* 8, 802-815.

Whitman, S.C., Argmann, C.A., Sawyez, C.G., Miller, D.B., Hegele, R.A., and Huff, M.W. (1999). Uptake of Type Iv Hypertriglyceridemic Vldl by Cultured Macrophages Is Enhanced by Interferon-Gamma. *J Lipid Res* 40, 1017-1028.

Willner, E.L., Tow, B., Buhman, K.K., Wilson, M., Sanan, D.A., Rudel, L.L., and Farese, R.V., Jr. (2003). Deficiency of Acyl Coa:Cholesterol Acyltransferase 2 Prevents Atherosclerosis in Apolipoprotein E-Deficient Mice. *Proc Natl Acad Sci U S A* 100, 1262-1267.

Yamauchi, T., Kamon, J., Waki, H., Murakami, K., Motojima, K., Komeda, K., Ide, T., Kubota, N., Terauchi, Y., Tobe, K., *et al.* (2001). The Mechanisms by Which Both Heterozygous Peroxisome Proliferator-Activated Receptor Gamma (Ppargamma) Deficiency and Ppargamma Agonist Improve Insulin Resistance. *J Biol Chem* 276, 41245-41254.

Yecies, J.L., Zhang, H.H., Menon, S., Liu, S., Yecies, D., Lipovsky, A.I., Gorgun, C., Kwiatkowski, D.J., Hotamisligil, G.S., Lee, C.H., *et al.* (2011). Akt Stimulates Hepatic Srebp1c and Lipogenesis through Parallel Mtorc1-Dependent and Independent Pathways. *Cell Metab* 14, 21-32.

Yen, C.L., Stone, S.J., Koliwad, S., Harris, C., and Farese, R.V., Jr. (2008). Thematic Review Series: Glycerolipids. Dgat Enzymes and Triacylglycerol Biosynthesis. *J Lipid Res* 49, 2283-2301.

Yvan-Charvet, L., Ranalletta, M., Wang, N., Han, S., Terasaka, N., Li, R., Welch, C., and Tall, A.R. (2007). Combined Deficiency of Abca1 and Abcg1 Promotes Foam Cell Accumulation and Accelerates Atherosclerosis in Mice. *J Clin Invest* 117, 3900-3908.

Zechner, R., Zimmermann, R., Eichmann, T.O., Kohlwein, S.D., Haemmerle, G., Lass, A., and Madeo, F. (2012). Fat Signals--Lipases and Lipolysis in Lipid Metabolism and Signaling. *Cell Metab* 15, 279-291.

Zhang, J., Kelley, K.L., Marshall, S.M., Davis, M.A., Wilson, M.D., Sawyer, J.K., Farese, R.V., Jr., Brown, J.M., and Rudel, L.L. (2012). Tissue-Specific Knockouts of Acat2 Reveal That Intestinal Depletion Is Sufficient to Prevent Diet-Induced Cholesterol Accumulation in the Liver and Blood. *J Lipid Res* 53, 1144-1152.

Zhou, J., Lhotak, S., Hilditch, B.A., and Austin, R.C. (2005). Activation of the Unfolded Protein Response Occurs at All Stages of Atherosclerotic Lesion Development in Apolipoprotein E-Deficient Mice. *Circulation* 111, 1814-1821.

Chapter 2*

Activation of PPAR δ inhibits human macrophage foam cell formation and the inflammatory response induced by very low-density lipoprotein

2.1 INTRODUCTION

Excessive lipid accumulation within macrophages of the arterial intima drives the synthesis and secretion of proinflammatory mediators, potentiating atherogenesis (Hansson, 2005). Canonically, elevated plasma low density lipoprotein (LDL) is considered a major lipoprotein contributing to accelerated atherogenesis. However, epidemiological evidence strongly suggests that hypertriglyceridemia also increases the risk of premature atherosclerosis, especially in the context of metabolic syndrome and type 2 diabetes (Nordestgaard et al., 2007, Reaven, 2005). Plasma triacylglycerol (TG)-carrying very low density lipoprotein (VLDL) has been localized within atherosclerotic lesions from human patients and animal models (Proctor and Mamo, 1998, Rapp et al., 1994), providing rationale for examining the mechanisms by which these lipoproteins induce the development of macrophage foam cells. VLDL readily induces macrophage lipid accumulation (Evans et al., 1993, Whitman et al., 1999, Whitman et al., 1998), which in turn stimulates the synthesis of cytokines such as IL-1 β and MIP-1 α (Saraswathi and Hasty, 2006, Stollenwerk et al., 2005a, Stollenwerk et al., 2005b). The mechanisms regulating these lipid-induced macrophage inflammatory responses have not been fully characterized.

In mouse macrophages, VLDL-induced expression of *Mip-1 α* requires fatty acid liberation by lipoprotein lipase (LPL) and is dependent on the activation of ERK1/2 (Saraswathi and Hasty, 2006). Furthermore, VLDL potentiates LPS-stimulated macrophage IL-1 β secretion via activation of the transcription factor AP-1 (Stollenwerk et

*a version of this chapter is published Bojic et al. (2012) *ATVB* **32(12)**, 2919-28.

al., 2005a). which is known to be regulated by MAP kinases ERK1/2 and p38 (Eferl and Wagner, 2003). The involvement of p38, which is thought to act cooperatively with ERK1/2 in AP-1 associated inflammatory responses (Eferl and Wagner, 2003), has not been established (Saraswathi and Hasty, 2006). In addition, macrophage insulin resistance may potentiate the inflammatory response. Macrophage-specific deletion of the insulin receptor in *Ldlr*^{-/-} mice significantly increased atherosclerosis (Han et al., 2006), an effect attributed to impaired macrophage Akt/FoxO1 signaling (Han et al., 2006). Insulin-resistant macrophages with cholesterol-induced ER-stress display impaired Akt phosphorylation, increased nuclear FoxO1 activity and enhanced apoptosis (Senokuchi et al., 2008). Furthermore, Il-1 β is a FoxO1 target gene in macrophages with insulin resistance (Su et al., 2009). Collectively, these studies highlight the importance of examining the role of AKT/FoxO1 signaling in the VLDL-induced inflammatory response.

The peroxisome proliferator-activated receptors (PPARs) are important regulators of metabolic and inflammatory signaling (Lee et al., 2003b). The three known isoforms, namely PPAR α , PPAR γ and PPAR δ , each exhibit distinct tissue distribution and PPAR-specific regulation of gene transcription (Lee et al., 2003b). In contrast to PPAR α and PPAR γ , expression of PPAR δ is ubiquitous, with high levels in macrophages (Vosper et al., 2001), where its biological role is unclear. Macrophage PPAR δ is activated by VLDL-derived fatty acids (Chawla et al., 2003, Lee et al., 2006), and conflicting reports have demonstrated that synthetic ligands promote either lipid accumulation (Vosper et al., 2001), or fatty acid catabolism (Chawla et al., 2003, Lee et al., 2006). Consequently, the net effect of PPAR δ activation on VLDL-induced TG accumulation is unknown. The anti-inflammatory properties of PPAR δ activation have been linked to the liberation of BCL-6 from unliganded PPAR δ (Lee et al., 2003a), which inhibits expression of AP-1-inducible cytokines by localizing to AP-1 response elements and recruiting co-repressors to these promoter regions (Vasanwala et al., 2002).

Additionally, in adipocytes and cardiomyocytes, PPAR δ agonists inhibit LPS-induced NF κ B regulated cytokine expression (Ding et al., 2006, Rodriguez-Calvo et al., 2008). The mechanism(s) underlying VLDL-induced cytokine expression in macrophages, in the absence of LPS, and the impact of PPAR δ activation have not been elucidated.

In the present study, we report that synthetic ligand activation of PPAR δ attenuates VLDL-stimulated TG accumulation by activating a transcriptional program resulting in attenuation of LPL activity, increased fatty acid uptake and enhanced β -oxidation. VLDL stimulates the expression of proinflammatory cytokines *IL-1 β* , *MIP-1 α* , and *ICAM-1* via both ERK1/2- and AKT/FoxO1-dependent signaling mechanisms. Furthermore, macrophage treatment with synthetic PPAR δ ligands inhibits proinflammatory cytokine expression, by inhibiting VLDL-stimulated ERK1/2 activation and reversing VLDL-mediated inhibition of AKT/FoxO1 phosphorylation.

2.2 MATERIALS AND METHODS

2.2.1 LIPOPROTEINS

Subjects were recruited from the Lipid Clinic at the London Health Sciences Center University Campus (London, Ontario, Canada). The University of Western Ontario Health Science Standing Committee on Human Research approved the studies (IRB reference #15685). VLDL (Sf 20 to 400) was isolated from plasma of type IV hyperlipoproteinemic patients by differential ultracentrifugation using a Beckman 70.1 Ti rotor (16hr, 40,000 rpm, 12°C) as previously described (Whitman et al., 1998).

2.2.2 CELL CULTURE

The human THP-1 macrophage-like cell line was obtained from American Type Culture Collection (ATCC, Manassas, VA). For experiments, cells were cultured at 4.0×10^6 cells/35-mm plate (Falcon Scientific, BD Biosciences) in RPMI 1640 supplemented with 10% fetal bovine serum (Sigma), β -mercaptoethanol (5×10^{-5} mol/L), 100 units/mL penicillin, and 100 μ g/ml streptomycin and differentiated with 300 nmol/L

phorbol 12,13-dibutyrate (PDB, Sigma) for 1 week prior to use in experiments as described (Argmann et al., 2005, Beyea et al., 2007). PPAR δ agonists GW0742 (Sigma) and GW501516 (Alexis Biochemicals, Plymouth, PA) were dissolved in dimethyl sulfoxide (DMSO, Sigma) and incubated with cells at the indicated concentrations. THP-1 macrophages were preincubated (24 hr) in the presence or absence of PPAR δ agonists. Subsequently, cells were incubated with PPAR δ agonists in the presence or absence of lipoproteins or various inhibitors as indicated. HepG2 cells were obtained from ATCC and grown as described previously (Evans et al., 1992). For experiments, HepG2 cells were plated in either 100-mm or six-well (35-mm) culture plates (Falcon, Mississauga, ON) and maintained in minimal essential medium (MEM) containing 10% fetal bovine serum (FBS), but switched to MEM containing 5% human lipoprotein-deficient serum (LPDS) for experimental incubations.

2.2.3 LUCIFERASE REPORTER ASSAYS

Luciferase reporter assays were performed as previously described (Mulvihill et al.). Briefly, HepG2 cells were transfected with 0.01 μ g/mL human PPAR α , γ or δ .SG5 expression vectors and reporter gene plasmids, 0.5 μ g/mL of pTK-PPRE(x3)-Luc and 0.05 μ g/mL of the TK promoter-*Renilla* luciferase construct, (tk.pRL) (provided by Dr. John Capone, McMaster University, Hamilton ON). Cells were incubated for 24 hr with DMSO or the appropriate PPAR agonists: PPAR α (10nmol/L, GW7647, Sigma); PPAR γ (3 μ mol/L, rosiglitazone, Alexis Biochemicals, Cedarlane Laboratories, Burlington, ON), or PPAR δ (GW0742 and GW501516) at a range of concentrations. Cell lysates were prepared and the Luciferase activity (relative light units (RLU)) was measured and normalized to *Renilla* activity, as previously described (Allister et al., 2005, Argmann et al., 2005).

2.2.4 CELLULAR LIPID MASS

THP-1 macrophages were preincubated in the presence of PPAR δ agonists or equal volume of DMSO (not to exceed 0.5% of total medium) for 24 hr in RPMI 1640 supplemented with 10% fetal bovine serum (FBS) and 300nmol/L PDB. Cells were incubated for a further 16 hr with fresh media containing 5% LPDS and compounds in the absence or presence of HTG-VLDL (50 μ g of lipoprotein total cholesterol (TC)/mL medium). Cellular CE, TC, FC, TG, FFA (NEFA) and protein mass were determined using enzymatic colorimetric assays for NEFA, TC and FC (Wako Diagnostics, Richmond, VA) as well as TG (Boehringer Mannheim, Laval, QC) as previously described (Rowe et al., 2003). Cellular CE was determined as the difference between TC and FC (Rowe et al., 2003). Cells were lysed in 1mL of 0.1N NaOH, and aliquots were used to determine protein concentrations (Beyea et al., 2012).

2.2.5 ENZYME-LINKED IMMUNOSORBENT ASSAY

THP-1 macrophages were preincubated in the presence of PPAR δ agonists or equal volume of DMSO (not to exceed 0.5% of total medium) for 24 hr in RPMI 1640 supplemented with 10% fetal bovine serum (FBS) and 300nmol/L PDB. Cells were incubated for a further 16 hr with fresh media containing 5% LPDS and compounds in the absence or presence of hypertriglyceridemic (HTG)-VLDL (50 μ g of lipoprotein total cholesterol (TC)/mL medium). Media was collected and analyzed for IL-1 β secretion via enzyme-linked immunosorbent assay (ELISA) using the BD OptEIA human IL-1 β ELISA kit II (BD Biosciences, Mississauga, ON) as per manufacturer's protocol.

2.2.6 QUANTITATIVE REAL-TIME PCR GENE ABUNDANCE ANALYSIS

THP-1 cells were incubated for 24 hr in RPMI 1640 with 5% LPDS, 300nmol/L PDB, in the presence or absence of PPAR δ agonists, and subsequently total RNA was isolated using TriZol reagent (Invitrogen, Burlington, ON) according to manufacturer's instructions. In experiments examining VLDL-induced inflammatory cytokine expression,

cells were preincubated for 24 hr in RPMI 1640 with 10% FBS, 300nmol/L PDB, in the presence or absence of PPAR δ agonists. Cells were then incubated with fresh 5%-LPDS media and compounds with or without the CPT-1 α inhibitor etomoxir (Sigma, 50 μ mol/L for 0.5 hr, followed by a further 16 hr in the absence or presence of HTG-VLDL (50 μ g-TC/mL) prior to TriZol RNA extraction. Abundance of total RNA (2 μ g) was reverse transcribed using the Applied Biosystems High Capacity cDNA reverse transcription kit according to the manufacturer's protocol. Subsequently, cDNA (10ng) was analyzed in triplicate by quantitative real time RT-PCR (qRT-PCR) on an ABI Prism (model 7900HT) Sequence Detection System (Applied Biosystems, Foster City, CA) according to the manufacturer's instructions and as previously described (Beyea et al., 2007). Primer-probe sets for each gene were obtained from Applied Biosystems (Carlsbad, CA). Abundance of target genes was normalized to *GAPDH* abundance.

2.2.7 LPL ACTIVITY, TG SYNTHESIS, FA β -oxidation, AND FA UPTAKE

LPL activity of THP-1 cells (cell surface and medium) was determined following a 24 hr incubation in RPMI 1640 with 5% human LPDS and 300nmol/L PDB in the presence or absence of selected concentrations of PPAR δ agonists, as the release of free fatty acids from intralipid (an exogenous lipid source) as previously described (Whitman et al., 1999). The synthesis of triacylglycerol was measured in THP-1 cells following a preincubation in 5% LPDS-containing medium for 19 hr in the presence or absence of selected concentrations of PPAR δ agonists. For a subsequent 5 hr incubation, 0.08nCi/mL [14 C]oleic acid (Amersham Biosciences) complexed with fatty acid-free bovine serum albumin in a molar ratio of 5.36:1 (Sigma) was added as described previously (Evans et al., 1993). Cellular lipid extracts were separated by thin layer chromatography (Evans et al., 1993). Fatty acid β -oxidation experiments were performed as described previously (Mulvihill et al.). Briefly, THP-1 cells were preincubated in the presence or absence of PPAR δ agonists in 10% FBS-containing

medium for 24 hr, followed by the addition of 2.0 μ Ci/mL [3 H]-palmitate in 100 μ mol/L palmitate per well for 0.5 hr. The media was removed and 10% trichloroacetic acid was added. Unreacted FAs were extracted from the supernatant with n-hexane and the remaining counts determined by scintillation counting. Data was determined as nmol palmitate oxidized/min/mg cell protein and was corrected for differences in fatty acid uptake in the presence of PPAR δ agonists. Fatty acid uptake experiments were performed as described (Lee et al., 2006). Briefly, THP-1 cells were preincubated in the presence or absence of PPAR δ agonists in 5% LPDS-containing medium for 24 hr, followed by the addition of either [1- 14 C]oleic acid or [3 H]-palmitate (both prepared as described above) for 1min. Ice cold stop solution (200 μ mol/L phloretin in phosphate buffered saline) was added directly to the culture medium. Cells were washed five times with ice cold stop solution. Cells were lysed in 1mL of 0.1N NaOH, and aliquots were used to determine protein concentrations and the amount of unprocessed radiolabelled fatty acid.

2.2.8 IMMUNOBLOT ANALYSIS AND DENSITOMETRY

Total cell lysates were fractionated into cytosolic and nuclear fractions as previously described (Azzout-Marniche et al., 2000). Proteins were separated by SDS-PAGE, transferred to polyvinylidene difluoride membranes and immunoblotted as described previously (Rowe et al., 2003). Cellular cytosolic fractions were probed using antibodies against human phospho (p)-FoxO1, pERK1/2, p-p38, pAKT, FoxO1, ERK1/2, p38, AKT, β -actin (Cell Signaling, Danvers, MA) and nuclear fractions were probed using antibodies against human total-FoxO1 and Lamin A/C (Santa Cruz Biotechnology Inc., Santa Cruz, CA). Quantification analysis of the developed films was performed using an imaging densitometer (Bio-Rad Quantity One Software). Phospho-proteins from cytosolic fractions were normalized to their respective total proteins or β -Actin, whereas nuclear fractions were normalized to lamin A/C. Additionally, cytosolic and nuclear

fractions were immunoblotted for Lamin A/C and β -Actin, respectively, in order to demonstrate complete separation of these fractions.

2.2.9 STATISTICAL ANALYSIS

Data are expressed as means \pm standard error of the mean (SEM). The Shapiro-Wilk normality test was used to test for parametric distributions in each data set. *P* values for observed differences between treatment and control groups were calculated by one-way ANOVA followed by Bonferroni post hoc test or paired student's *t*-test where indicated. *P* values for observed pair-wise comparisons were calculated by one-way ANOVA followed by Tukey's post hoc test. Significance thresholds were *P* values less than 0.05. Statistical analyses were performed with SigmaPlot 11.0 software (Systat, Inc, San Jose, CA).

2.3 RESULTS

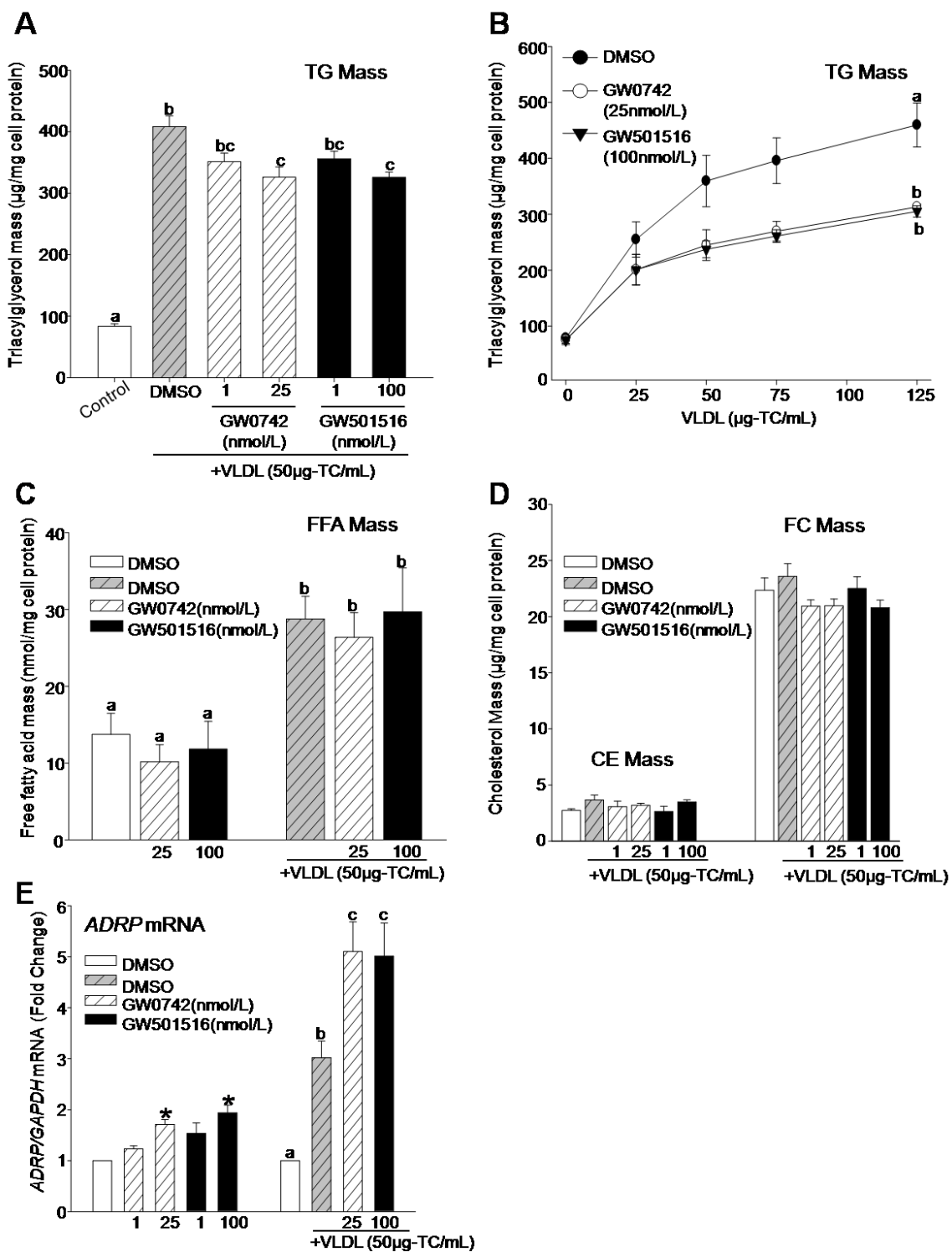
2.3.1 PPAR δ -SPECIFIC ACTIVATION ATTENUATES VLDL-INDUCED MACROPHAGE TRIACYLGLYCEROL ACCUMULATION

THP-1 cells treated with VLDL demonstrated a dose-dependent increase in TG mass achieving a marked 5-fold increase with VLDL at 50 μ g/mL (Figure 2.1A-B). Pre-treatment with PPAR δ agonists for 24 hours modestly but significantly reduced VLDL-induced TG mass by 25-30% (Figure 2.1A-B). VLDL significantly induced intracellular FFA mass, which was unchanged by pre-treatment with PPAR δ agonists (Figure 2.1C). Cellular cholesteryl ester or free cholesterol concentrations were unaffected by VLDL or PPAR δ agonists (Figure 2.1D), indicating that whole particle VLDL uptake was modest. A known PPAR δ -specific target gene, adipocyte differentiation-related protein (*ADRP*) (Chawla et al., 2003), was significantly increased by both agonists (Figure 2.1E), indicating PPAR δ activation.

High doses of PPAR agonists can activate PPAR isoforms non-selectively (Berger et al., 1999, Willson et al., 2000). Therefore, we determined the PPAR δ -

Figure 2.1 PPAR δ -specific activation attenuates VLDL-induced triacylglycerol mass accumulation.

THP-1 cells were pre-incubated with PPAR δ agonists GW0742 and GW501516 for 24hr, followed by a 16hr incubation with or without VLDL (50 μ g-TC/mL). **A,B** TG mass (n=5-7). **C**, Free fatty acid (FFA) mass (n=3-4). **D**, Cholesteryl ester (CE) and free cholesterol (FC) mass (n=6). **E**, *ADRP* mRNA in THP-1 cells following preincubation with PPAR δ agonists for 24hr, and following a 16hr incubation, with or without VLDL (n=4). Data is presented as mean \pm SEM. Different letters indicate significant differences; ANOVA with post-hoc Tukey's test ($P < 0.05$). * indicates significant difference versus DMSO control; ANOVA with post hoc Bonferroni's test ($P < 0.05$)



specificity of the concentrations of agonists employed. PPAR δ -deletion results in derepression of PPAR δ target genes (Lee et al., 2006), and transrepression of inflammatory cytokine expression, creating an experimental confounder for the present studies (Lee et al., 2003a). We therefore assessed agonist-specificity by co-transfecting HepG2 cells with luciferase reporter constructs driven by PPAR response elements and each PPAR isoform (α , γ , δ). We determined dose-responses for each receptor in cells treated with PPAR δ agonists (GW0742 and GW501516), and used agonists for PPAR α (GW7647) and PPAR γ (rosiglitazone) as positive controls. GW0742 at 25nmol/L and GW501516 at 100nmol/L were concentrations at which these ligands maximally activated PPAR δ , without activation of either PPAR α or PPAR γ (Figure 2.2A-D). Furthermore, canonical PPAR α and PPAR γ target genes (*ACOX* and *FABP4*, respectively) were unaffected by either 25nmol/L GW0742 or 100nmol/L GW501516 (Figure 2.2E-F). Although unlikely, these agonists may have effects on non-PPAR targets. However, with respect to PPARs, these data demonstrate selectivity of the agonist concentrations used for PPAR δ .

2.3.2 PPAR δ AGONISTS REGULATE LPL ACTIVITY, FATTY ACID UPTAKE AND FATTY ACID β -OXIDATION

We examined whether PPAR δ activation attenuated VLDL-induced TG mass by regulating lipoprotein hydrolysis, fatty acid uptake or fatty acid esterification. In contrast to rosiglitazone, *LPL* mRNA was unchanged in response to PPAR δ agonists, further demonstrating PPAR δ -specificity (Figure 2.3A and Figure 2.2G). The PPAR δ -target gene, angiopoietin-like 4 (*ANGPTL4*) encodes a protein known to potently inhibit LPL activity (Sukonina et al., 2006). *ANGPTL4* mRNA expression was markedly enhanced by both PPAR δ agonists in the presence or absence of VLDL, which was associated with a 50% inhibition of LPL activity (Figure 2.3B,C). The PPAR δ ligands significantly increased

Figure 2.2 GW0742 and GW501516 are PPAR δ -specific agonists.

Human hepatoma (HepG2) cells were co-transfected with plasmids encoding a PPRE-luciferase construct, a *Renilla* luciferase construct (transfection control) and vectors encoding each individual PPAR isoform as indicated. Cells were incubated with **(A)** PPAR α agonist GW7647, **(B)** PPAR γ agonist rosiglitazone or PPAR δ agonists **(C)** GW0742 or **(D)** GW501516 for 24hr. Cell lysates were isolated and luciferase relative light units (RLU) were measured (n=2-4). In separate experiments, THP-1 cells were incubated with PPAR agonists for 24hr. Total RNA was isolated and **(E)** ACOX, **(F)** *FABP4* and **(G)** *LPL* mRNA abundance was measured by qRT-PCR (n=3-6). Data is presented as mean +/- SEM. * indicates significant difference versus DMSO control; ANOVA with post hoc Bonferroni test ($P<0.05$).

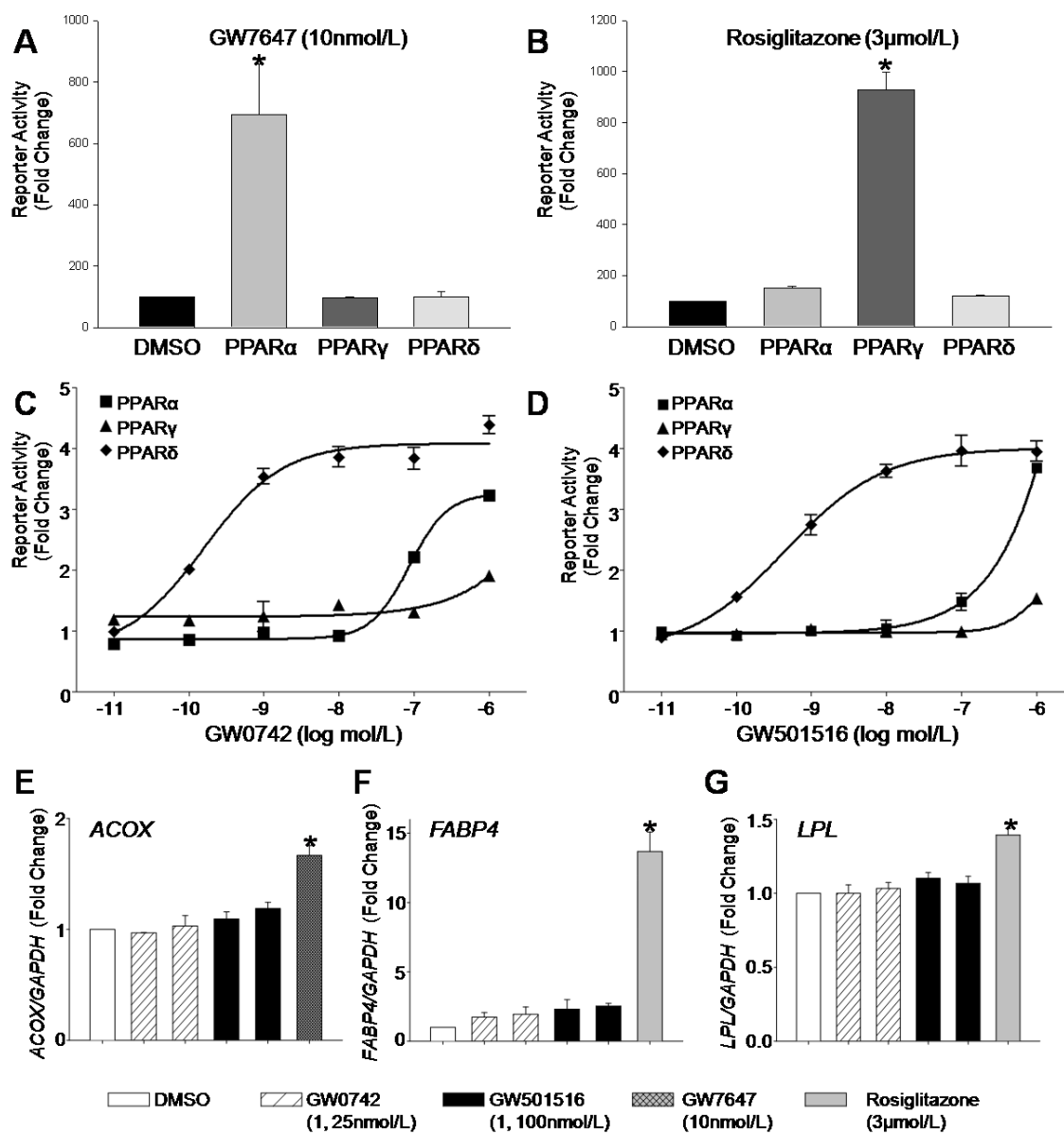
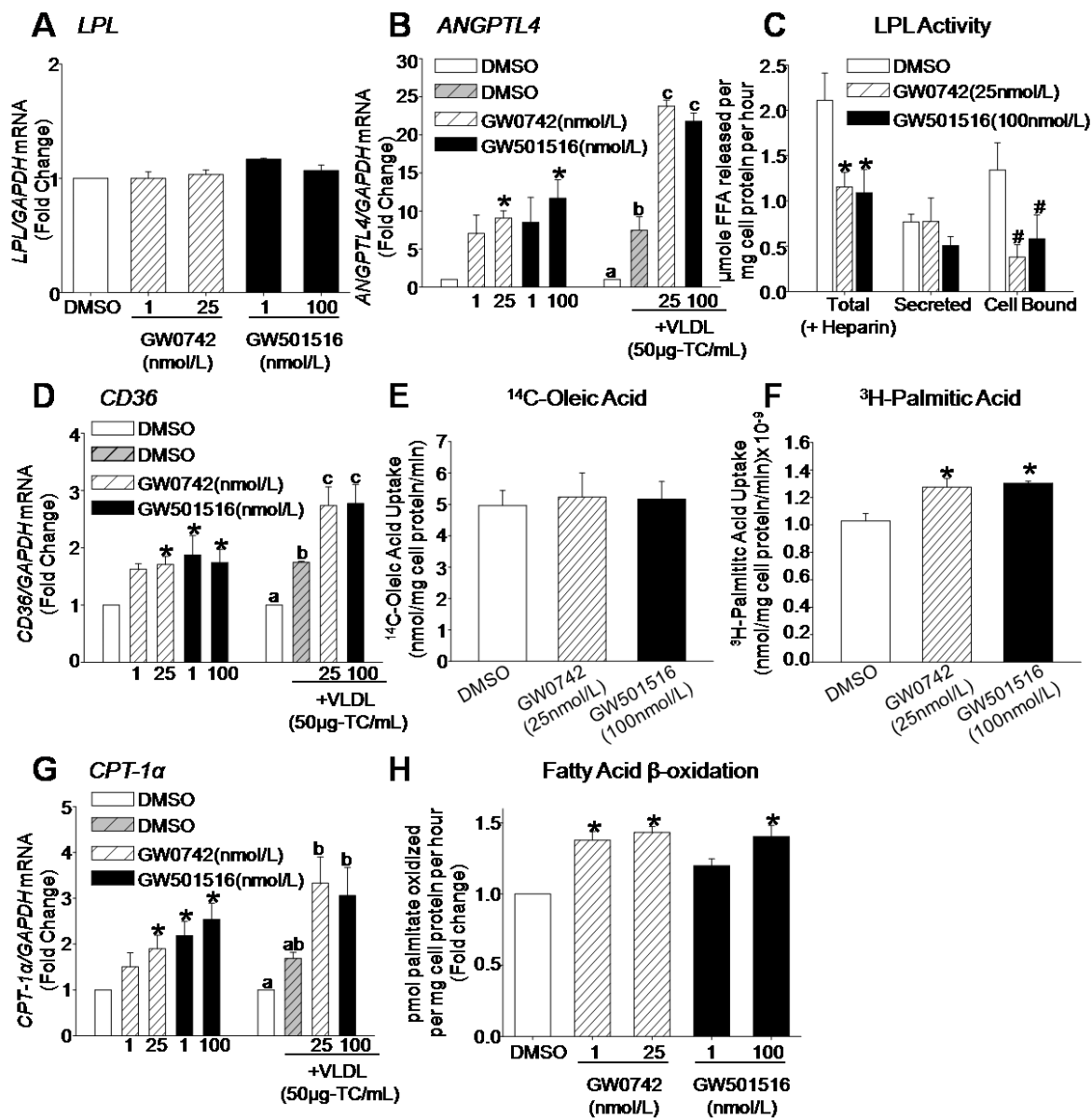


Figure 2.3 PPAR δ activation regulates triglyceride metabolism.

A, *LPL* mRNA in THP-1 cells following preincubation with PPAR δ agonists for 24hr. mRNA abundance of **(B)** *ANGPTL4*, **(D)** *CD36* and **(G)** *CPT-1 α* in THP-1 cells following preincubation with PPAR δ agonists for 24hr, and following a 16hr incubation, with or without VLDL (n=4). **C**, LPL activity (n=4). Cell surface-bound LPL activity = Total activity (heparin) minus secreted activity (without heparin). **E,F** Fatty acid uptake (n=3). **H**, β -oxidation (n=3). Data is presented as mean \pm SEM. Different letters indicate significant differences; ANOVA with post-hoc Tukey's test ($P < 0.05$). *indicates significant difference versus DMSO control. In **C**, # indicates significant difference versus cell bound DMSO control; ANOVA with post hoc Bonferroni's test ($P < 0.05$).



expression of the PPAR-target gene CD36 (Welch et al., 2003) irrespective of lipid load, which was correlated with a 25% increase in palmitate uptake, but not oleate uptake (Figure 2.3D-F). *DGAT1* mRNA, *DGAT2* mRNA, and TG synthesis were unaffected by PPAR δ activation (Figure 2.4). PPAR δ ligands significantly upregulated *CPT-1 α* mRNA, with or without VLDL, which was associated with a 40% increase in fatty acid oxidation (Figure 2.3G,H). Collectively, these results indicate that although PPAR δ activation modestly increases palmitate uptake, the attenuation of LPL-mediated VLDL TG-hydrolysis and the enhancement of fatty acid β -oxidation results in a net reduction of macrophage triglyceride content.

2.3.3 PPAR δ AGONISTS INHIBIT VLDL- AND FREE FATTY ACID-INDUCED CYTOKINE EXPRESSION

Exposure of mouse macrophages to VLDL stimulates *Mip-1 α* expression, an AP-1 mediated inflammatory response (Saraswathi and Hasty, 2006). Here, human VLDL significantly induced macrophage expression of *IL-1 β* , *MIP-1 α* , and *ICAM-1* mRNA. Pre-treatment with PPAR δ ligands significantly inhibited the VLDL-induced expression of all three cytokines (Figure 2.5A-C), without affecting basal cytokine expression (Figure 2.6). Furthermore, media levels of VLDL-induced IL-1 β were significantly decreased by both PPAR δ agonists (Figure 2.7A). Canonical NF κ B-target genes *TNF α* and *IL-6* were unaffected by VLDL treatment (Figure 2.7B). Moreover, parthenolide, an inhibitor of NF κ B signaling, had no effect on VLDL-stimulated expression of *IL-1 β* , *MIP-1 α* and *ICAM-1*, however parthenolide completely inhibited cytokine stimulation by LPS, a known NF κ B activator (Figure 2.7C). Collectively, these data suggest that VLDL-induced macrophage inflammatory responses do not require NF κ B activation

Figure 2.4 Effect of PPAR δ activation on FFA re-esterification mechanisms.

THP-1 cells were incubated with PPAR δ -specific agonists for 24hr. Total RNA was isolated and **(A)** *DGAT1* and **(B)** *DGAT2* mRNA was measured by qRT-PCR (n=4). **C**, Following a 19hr incubation with PPAR δ agonists at indicated concentrations, THP-1 cells were incubated for a further 5hr with PPAR δ agonists and 1-[14 C]oleic acid to measure oleate incorporation into cellular triacylglycerol (n=3). Data is presented as mean +/- SEM.

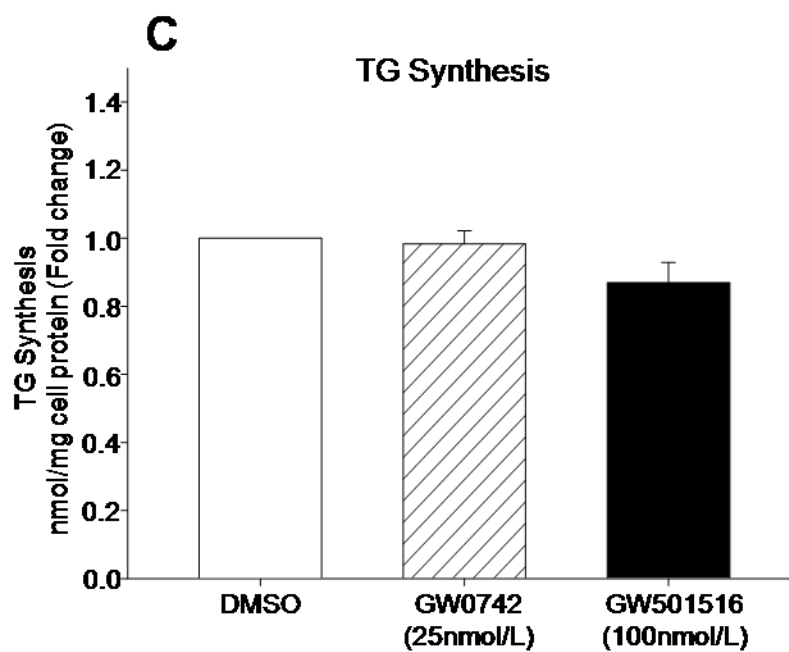
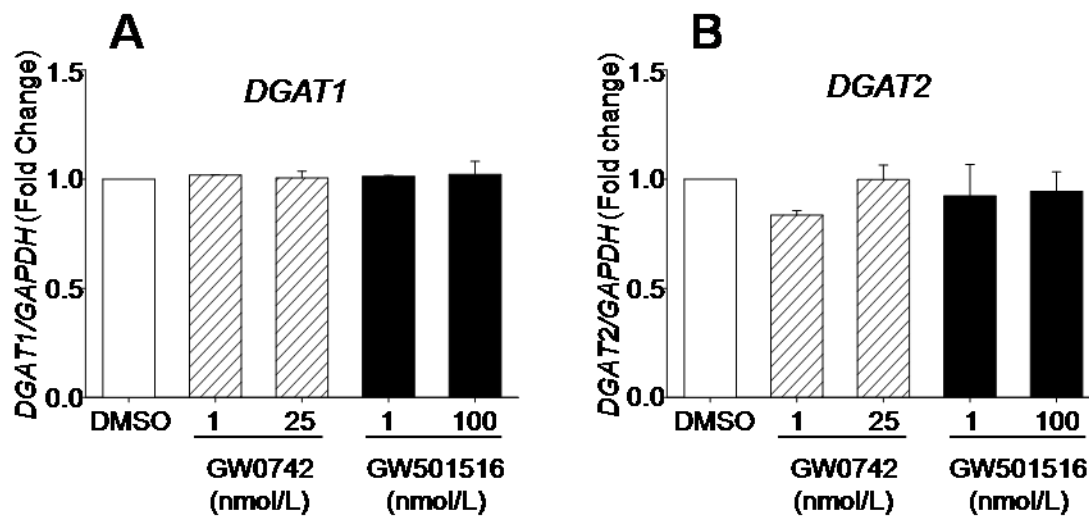


Figure 2.5 PPAR δ agonists attenuate VLDL-stimulated expression of AP-1 associated inflammatory cytokines.

THP-1 cells were pre-incubated with PPAR δ agonists for 24hr, followed by a 16hr incubation with or without VLDL. mRNA abundance for **(A)** *IL-1 β* , **(B)** *MIP-1 α* and **(C)** *ICAM-1* was measured (n=4). **D**, THP-1 cells were incubated with PPAR δ agonists for 24hr, followed by an incubation with Etomoxir (ETO 50 μ mol/L) for 0.5hr and a subsequent incubation with or without VLDL for 16hr. mRNA for *IL-1 β* , *MIP-1 α* and *ICAM-1* mRNA was measured (n=3). Data is presented as mean +/- SEM. Different letters indicate significant differences; ANOVA with post-hoc Tukey's test ($P<0.05$).

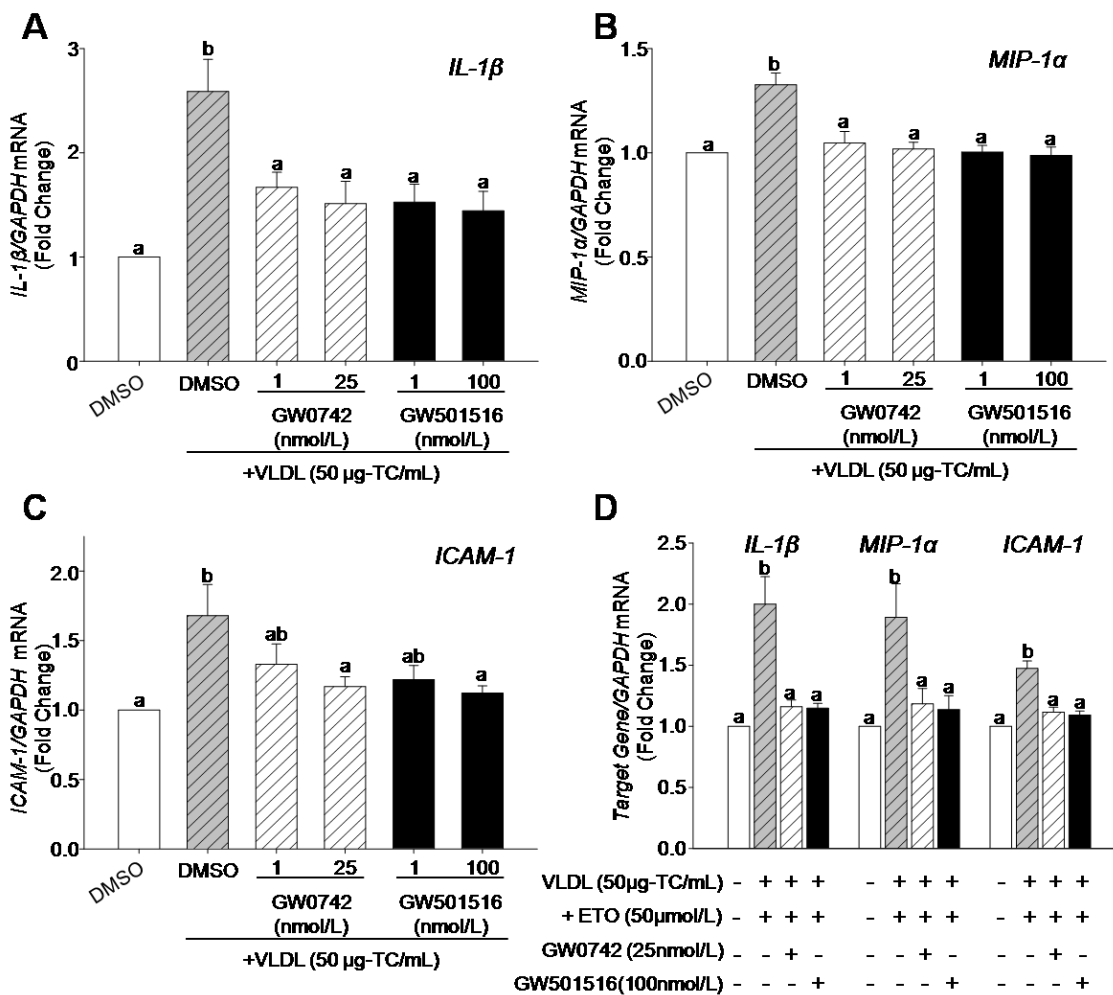


Figure 2.6 PPAR δ activation does not affect basal cytokine expression in THP-1 human macrophages

THP-1 cells were incubated with PPAR δ -specific agonists at the indicated concentrations for 24hr. Total RNA was isolated and *IL-1 β* , *MIP-1 α* and *ICAM-1* mRNA was measured by qRT-PCR (n=4). Data is presented as mean \pm SEM (n=4).

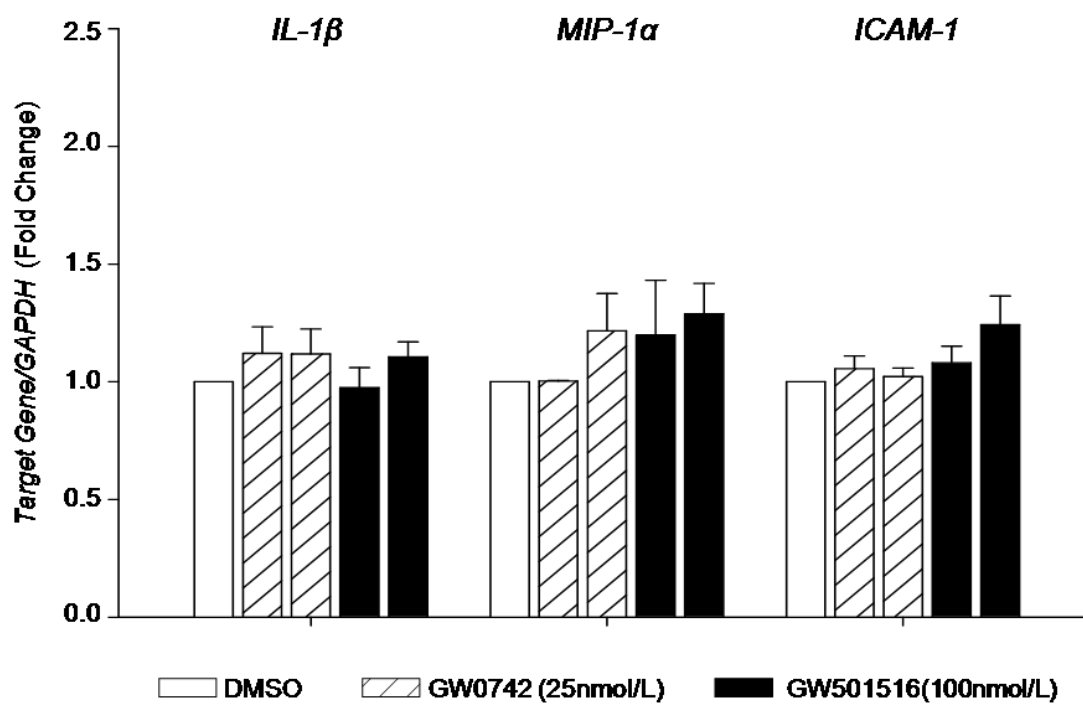
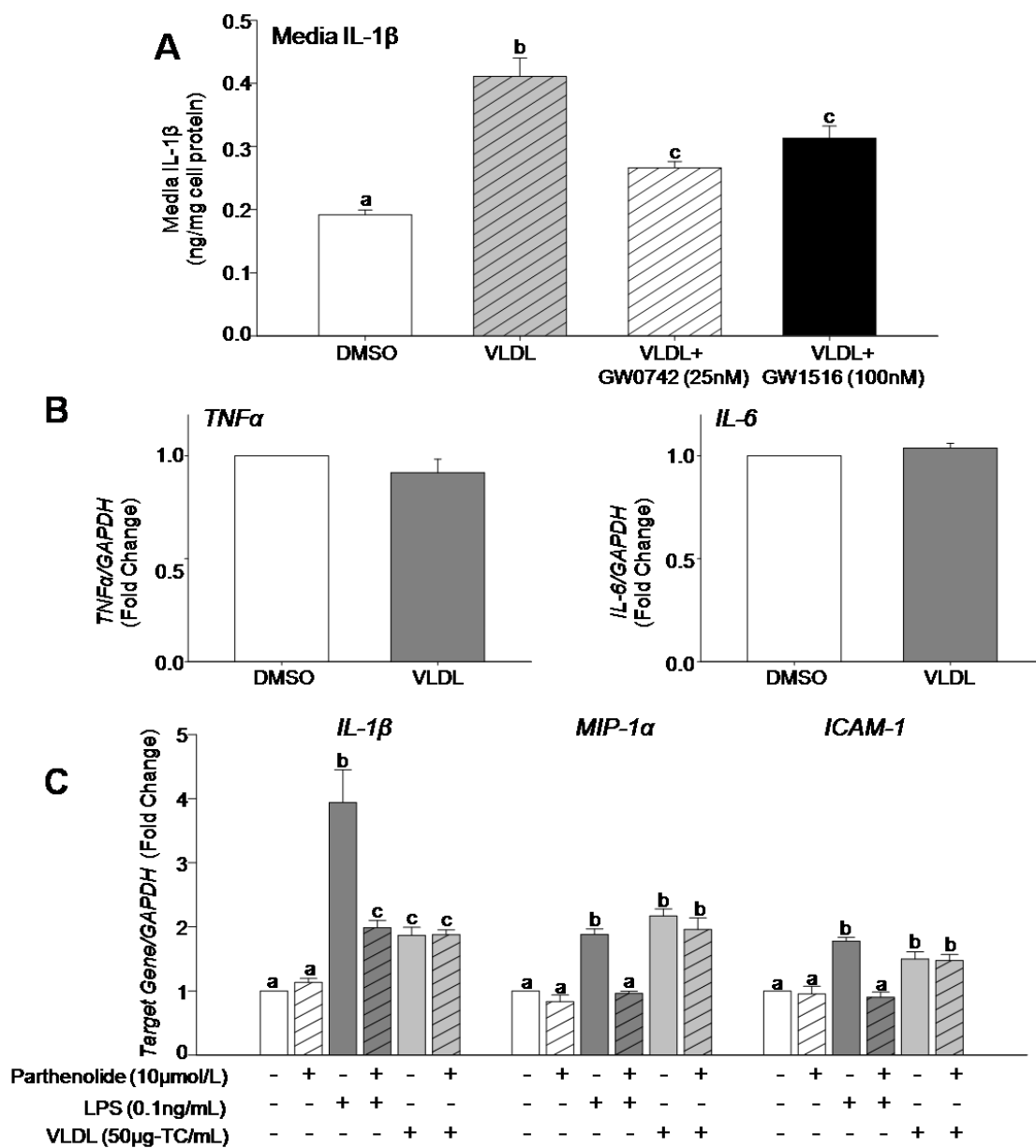


Figure 2.7 The effect of PPAR δ agonists on media *IL-1 β* protein; the effect of VLDL on *TNF α* or *IL-6* expression and the VLDL-induced inflammatory response in the presence of an inhibitor of NF κ B. THP-1 cells were pre-incubated with PPAR δ agonists for 24hr, followed by a 16hr incubation with or without VLDL (50 μ g-TC/mL). **A**, Media was collected and analyzed for *IL-1 β* protein levels by enzyme-linked immunosorbent assay. In separate experiments, THP-1 cells were incubated with or without VLDL (50 μ g-TC/mL) for 16hr. Total RNA was isolated and **(B)** *TNF α* and *IL-6* mRNA were measured by qRT-PCR (n=4). **C**, THP-1 cells were incubated with I κ B kinase inhibitor (Parthenolide 10 μ mol/L) for 0.5hr followed by 16hr incubation with or without VLDL or LPS at the indicated concentrations. Total RNA was isolated and *IL-1 β* , *MIP-1 α* and *ICAM-1* mRNA was measured by qRT-PCR (n=3-4). Data is presented as mean \pm SEM. Different letters indicate significant differences; ANOVA with post-hoc Tukey's test ($P < 0.05$).



2.3.4 INHIBITION OF VLDL-INDUCED INFLAMMATION BY PPAR δ ACTIVATION IS INDEPENDENT OF REDUCED CELLULAR TRIGLYCERIDE

We examined if inhibition of VLDL-induced inflammation by PPAR δ agonists was a consequence of reduced TG accumulation. Complete inhibition of LPL with tetrahydrolipstatin (THL), blocked cellular TG and cytokine expression. However, inhibition of TG accumulation with low-dose THL, to the same extent as that achieved by PPAR δ agonists (~25%), decreased *ICAM-1* expression by 30% but did not affect *MIP-1 α* or *IL-1 β* (Figure 2.8). PPAR δ activation normalized VLDL-induced cytokine expression, even when β -oxidation was inhibited by etomoxir (Figure 2.5D), a CPT-1 α inhibitor (Galic et al., 2011). This data suggests that activated PPAR δ -induced β -oxidation only partially accounts for reduced cytokine expression by PPAR δ activation.

Our results are consistent with the concept that VLDL-derived FAs are the primary mediators of the inflammatory response (Anderson et al., 2012, Saraswathi and Hasty, 2006). Paradoxically, FAs also activate PPAR δ (Chawla et al., 2003). To reconcile this, macrophages were treated with oleic acid, which resulted in a marked induction of TG mass and expression of *IL-1 β* and *MIP-1 α* (Figure 2.9A,B). These effects were significantly attenuated by pre-incubation of cells with GW501516 (Figure 2.9A,B), suggesting that the known ability of FAs to activate PPAR δ (Chawla et al., 2003), is insufficient to prevent macrophage TG accumulation and cytokine expression.

2.3.5 VLDL-STIMULATED EXPRESSION OF INFLAMMATORY CYTOKINES IS DEPENDENT ON MAPK ACTIVATION AND REPRESSION OF AKT/FoxO1 SIGNALING

VLDL-induced *Mip1 α* expression in mouse macrophages involves activation of ERK1/2 (Saraswathi and Hasty, 2006). In THP-1 cells, ERK1/2 phosphorylation increased significantly within 0.5hr of VLDL exposure, which returned to baseline by 1hr

Figure 2.8 Prevention of VLDL-induced TG accumulation and cytokine expression are independent effects of PPAR δ activation.

THP-1 cells were incubated with lipolysis inhibitor (THL) at the indicated concentrations for 0.5hr followed by 16hr incubation with or without VLDL (50 μ g-TC/mL). **A**, TG mass (n=2). **B**, TG mass (n=4). THP-1 cells were incubated with THL at the indicated concentrations for 0.5hr followed by 16hr incubation with or without VLDL (50 μ g-TC/mL) or LPS (0.1ng/mL). Total RNA was isolated and **(C)** *IL-1 β* , *MIP-1 α* and *ICAM-1* mRNA was measured by qRT-PCR (n=3). Data is presented as mean +/- SEM. Different letters indicate significant differences; ANOVA with post-hoc Tukey's test ($P < 0.05$).

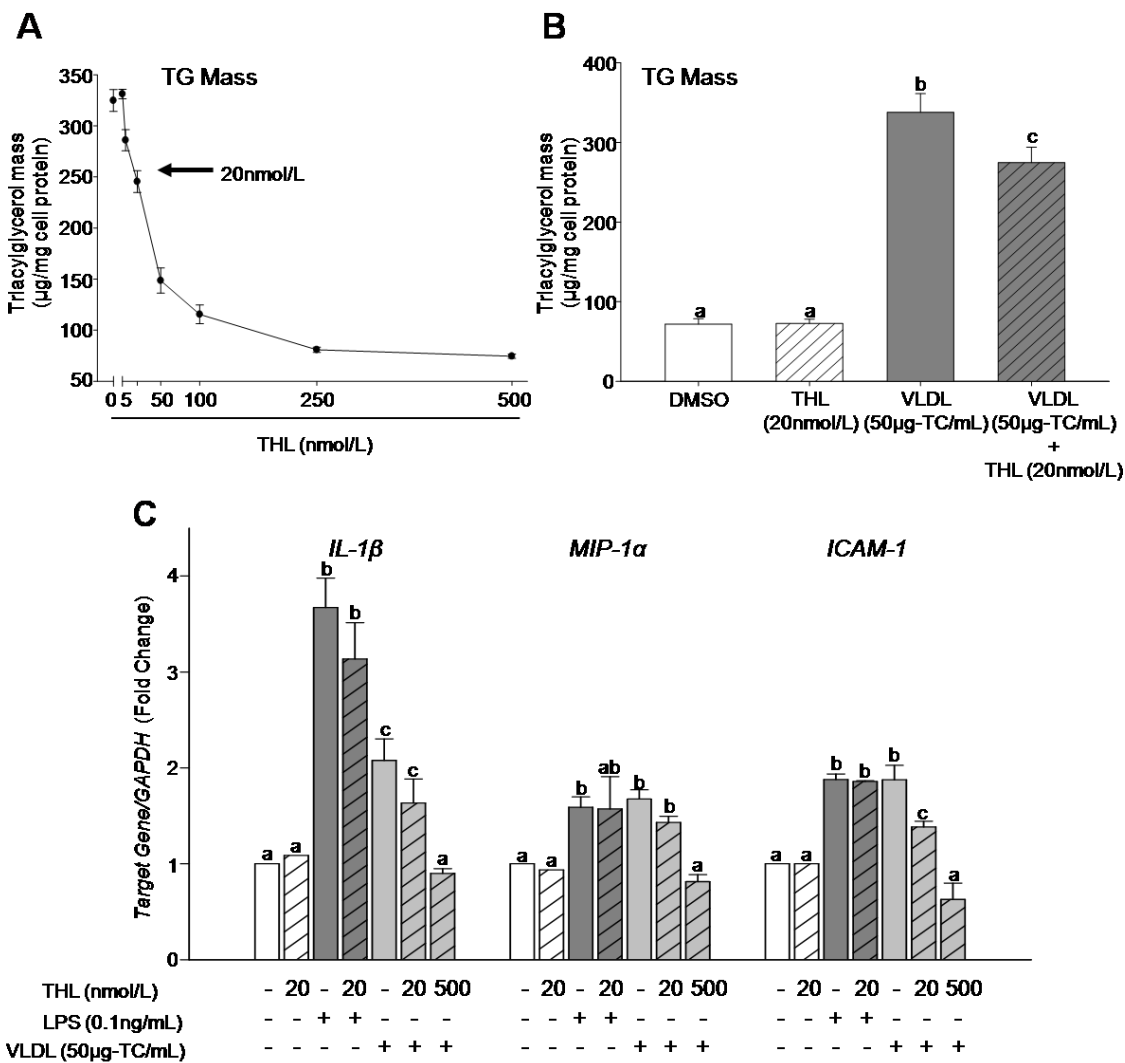
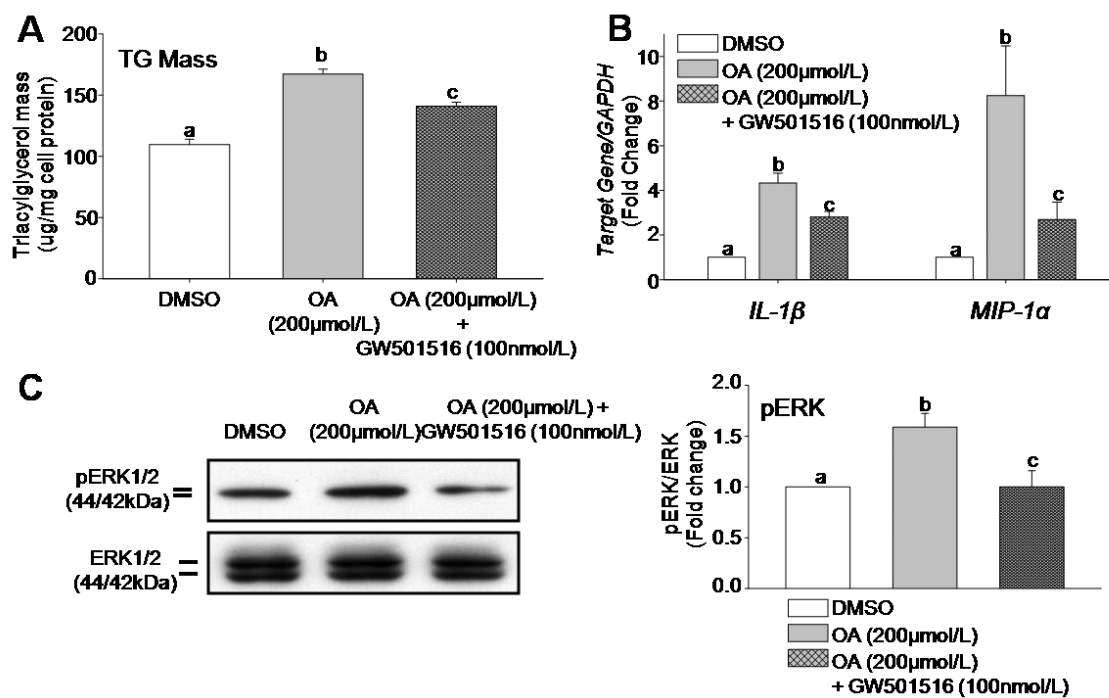


Figure 2.9 Free fatty acids are the primary effectors of the VLDL-induced inflammatory response in human macrophages. THP-1 cells were pre-incubated with PPAR δ agonist GW501516 for 24hr, followed by a 16hr incubation with or without oleic acid (OA, 200 μ mol/L). **A**, TG accumulation (n=4). **B**, Total RNA was isolated and *IL-1 β* and *MIP-1 α* mRNA was measured by qRT-PCR (n=4). **C**, In a separate set of experiments, THP-1 cells were pre-incubated with the PPAR δ agonist at the indicated concentration for 24hr, followed by a 0.5hr incubation with or without 200 μ mol/L OA. Cytosolic fractions were isolated and immunoblotted for ERK1/2. Equal loading was confirmed by total ERK. Representative immunoblots for phosphorylated and total ERK1/2 with quantitation shown (n=4). Data is presented as mean \pm SEM. Different letters indicate significant differences; ANOVA with post-hoc Tukey's test ($P < 0.05$).



(Figure 2.10A and Figure 2.9C). Similarly, VLDL stimulated p38 phosphorylation, reaching peak phosphorylation by 0.5hr, and remained elevated for ~3hr (Figure 2.10B). The MEK1/2 inhibitor, U0126, abrogated VLDL-stimulated expression of all cytokines (Figure 2.10C). In contrast, the p38 inhibitor SB203580 stimulated cytokine expression under basal conditions, and further increased cytokine expression in VLDL-treated cells (Figure 2.10D). Inhibition of p38 resulted in a 5-fold induction in ERK1/2 phosphorylation (Figure 2.11A) suggesting that the MAPK^{erk} signal stimulates cytokine expression, whereas MAPK^{p38} represses the actions of MAPK^{erk}.

The temporal disconnect between VLDL-induced MAPK^{erk} activation/deactivation (1hr) and elevated cytokine expression (16hr), suggests that other macrophage inflammatory signaling pathways are stimulated by VLDL. Given that *IL-1 β* is a target of nuclear FoxO1 in macrophages in the context of fatty acid-induced insulin resistance (Su et al., 2009), we examined the role of AKT/FoxO1 in VLDL-induced inflammation. Exposure of THP-1 cells to VLDL resulted in a time-dependent reduction of phospho-AKT levels for up to 6hr (Figure 2.12A). Reduced phospho-AKT was correlated with attenuated phospho-FoxO1 and increased nuclear-FoxO1 by 3hr (Figure 2.12B, C), demonstrating that VLDL inhibits AKT/FoxO1-signaling. As proof-of-concept, treatment of macrophages with AKT_{inhibitor} IV mimicked VLDL-treatment, resulting in reduced phospho-AKT, reduced phospho-FoxO1 over 6hr (Figure 2.11B) and significant elevations in the expression of *IL-1 β* as well as *MIP-1 α* and *ICAM-1* over 16hr (Figure 2.11C).

Figure 2.10 MAPK signaling in THP-1 human macrophages in response to VLDL.

THP-1 cells were incubated for indicated times with or without VLDL. Representative immunoblots of phosphorylated **(A)** ERK1/2 and **(B)** p38 from cytosolic fractions (n=4). **C**, THP-1 cells were incubated with MEK1/2 inhibitor (U0126 10 μ mol/L) or its inactive form (U0124 10 μ mol/L) for 0.5hr followed by 16hr incubation with or without VLDL. *IL-1 β* , *MIP-1 α* and *ICAM-1* mRNA was measured by qRT-PCR. **D**, THP-1 cells were incubated with p38 inhibitor (SB203580 10 μ mol/L) or its inactive isoform (SB202474 10 μ mol/L) for 0.5hr followed by a 16hr incubation with or without VLDL. mRNA determinations as in **(C)**. Values are mean \pm SEM (n=4). **A,B** * indicates significant difference versus respective DMSO control; ANOVA with post hoc Bonferroni's test ($P<0.05$). Representative bands are from the same immunoblot, cut from different regions. **C,D** Different letters are significantly different; ANOVA with post-hoc Tukey's test ($P<0.05$).

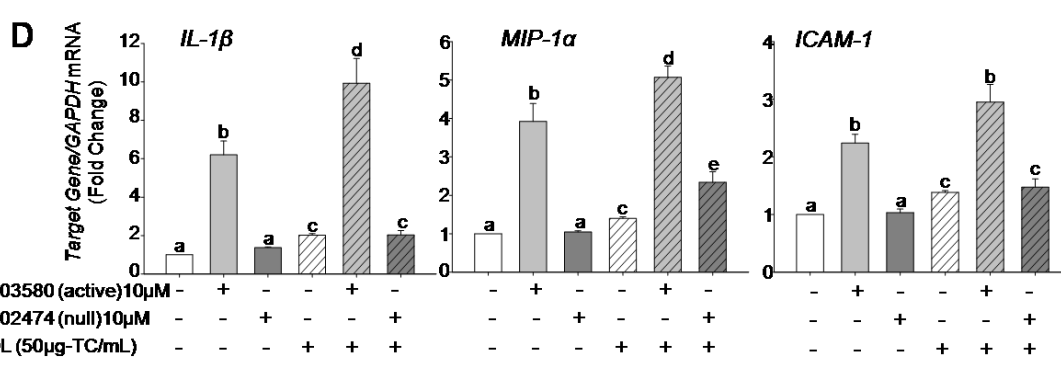
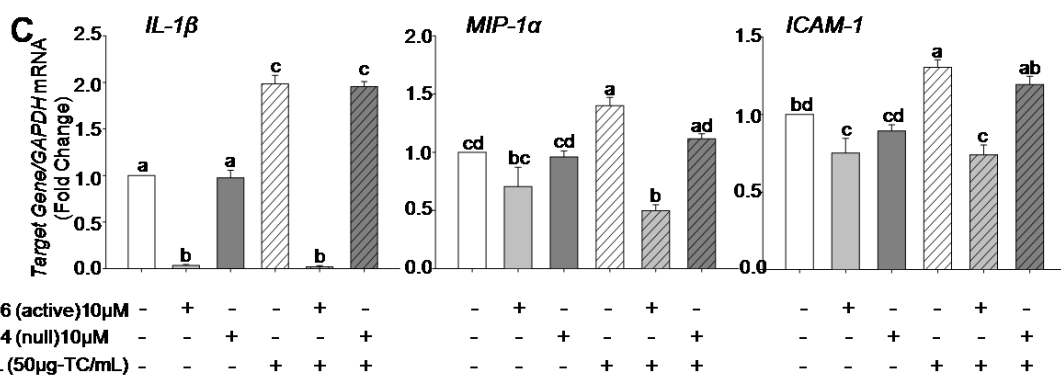
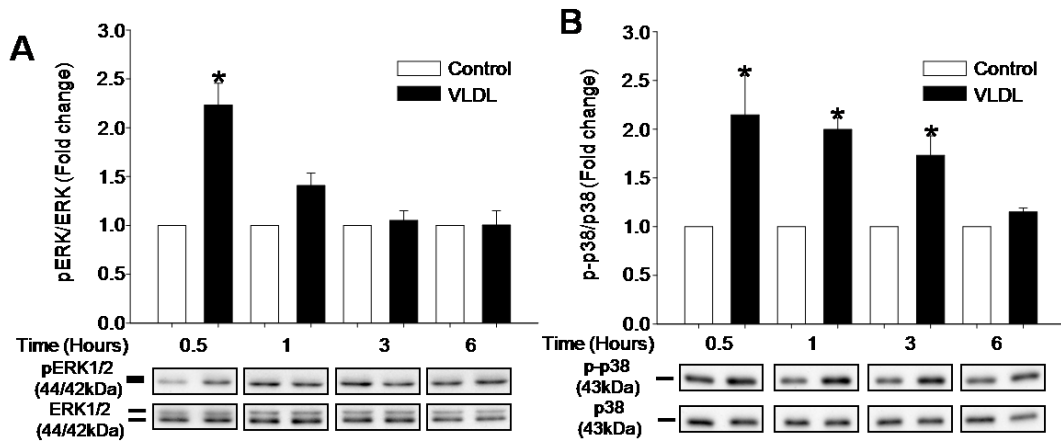


Figure 2.11 Effects of inhibitors on cell signalling cascades. THP-1 cells were incubated with or without p38 inhibitor SB203580 (10 μ mol/L) for 0.5hr. Cytosolic fractions were isolated and immunoblotted for **(A)** pERK1/2 and p-p38. Equal loading was confirmed by total ERK and total p38, respectively (n=3). In a separate experiment, THP-1 cells were incubated for indicated times with or without AKT inhibitor (AKT_i) IV (10 μ mol/L). Levels of **(B)** pAKT and pFoxO1 were determined by immunoblotting of cytosolic fractions. Quantitation was determined relative to total AKT and β -Actin, respectively (n=3). **C**, THP-1 cells incubated for 16hr with or without AKT activity inhibitor (AKT_i IV 10 μ mol/L). mRNA for *IL-1 β* , *MIP-1 α* and *ICAM-1* mRNA was measured by qRT-PCR. Data is presented as mean \pm SEM (n=4). * indicates significant difference versus control; *t*-test ($P < 0.05$). For **A-B**, relative intensities represent the mean ratio of phospho:total protein relative to the respective DMSO control of 3 independent experiments.

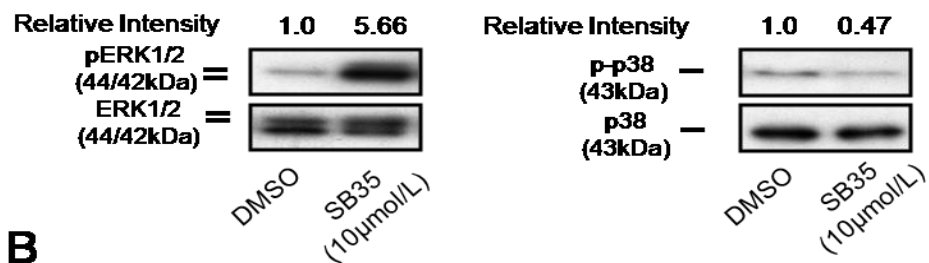
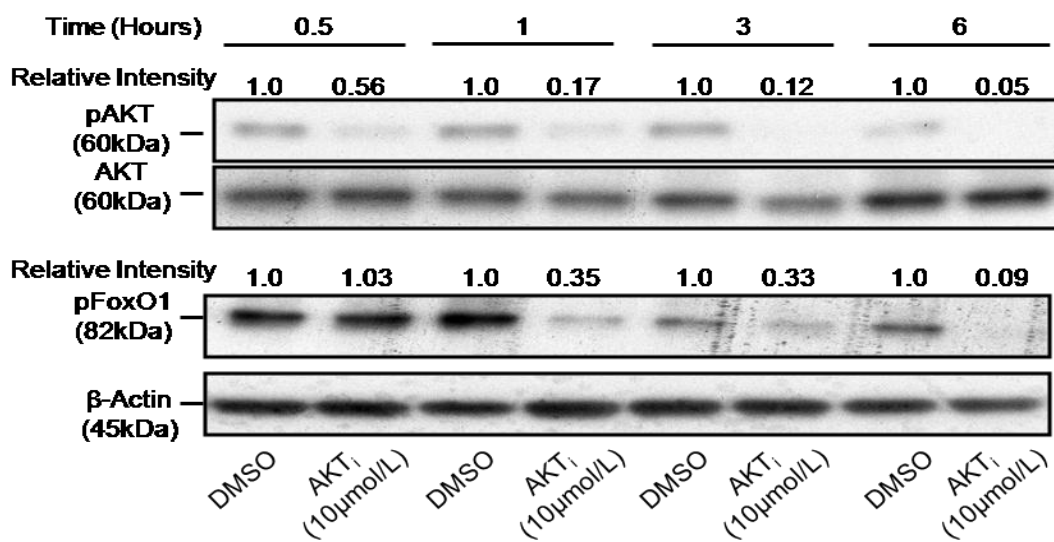
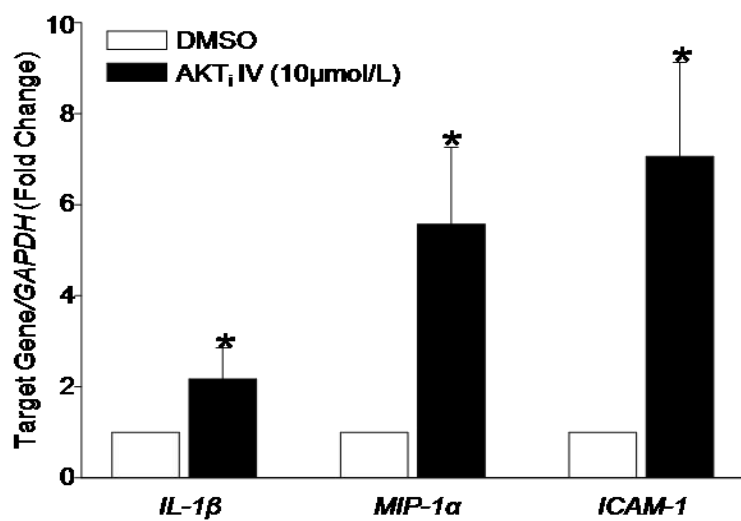
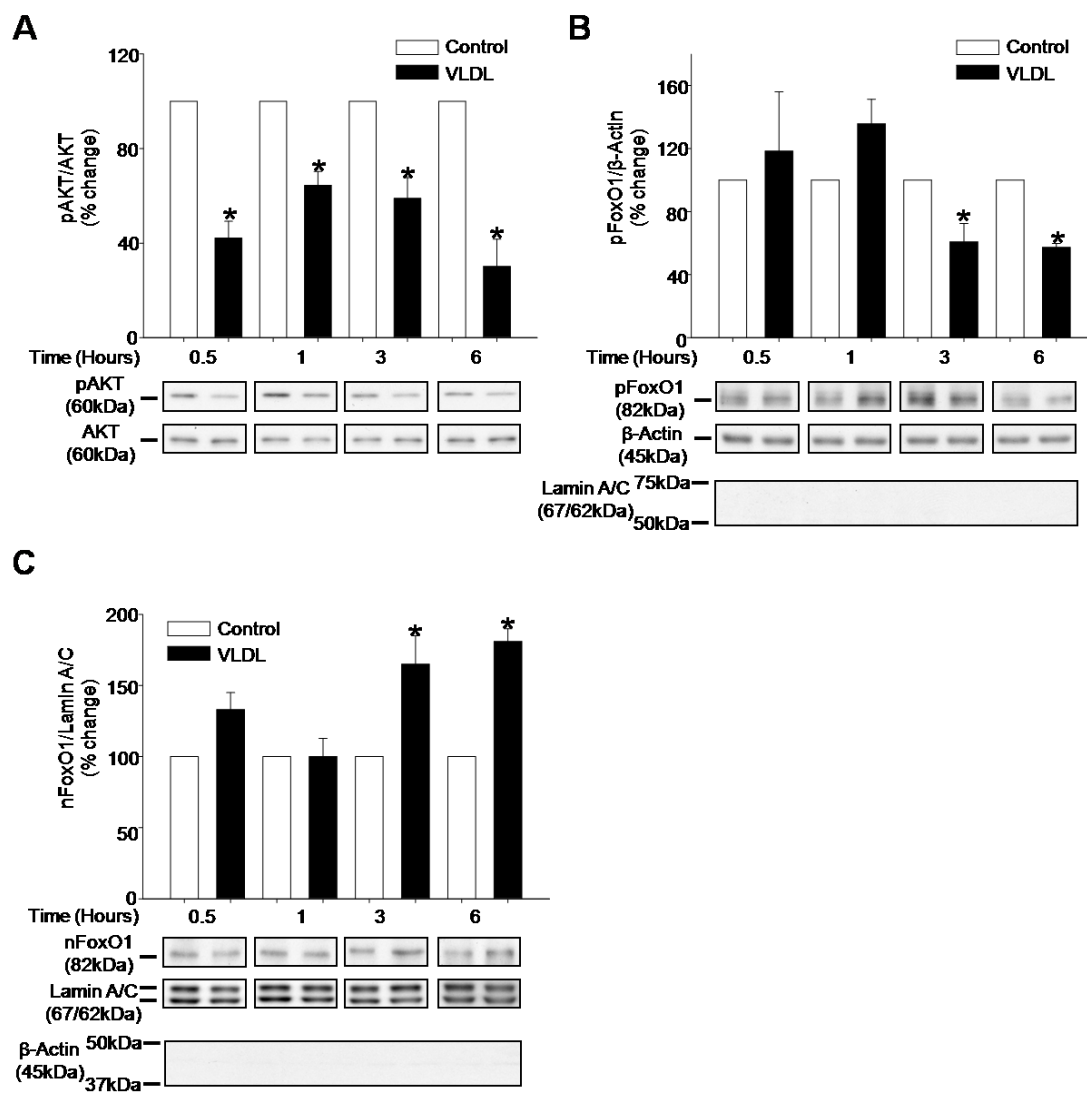
A**B****C**

Figure 2.12 VLDL induces human macrophage inflammation via AKT/FoxO1 signaling.

THP-1 cells were incubated for indicated times with or without VLDL. Representative immunoblots of **(A)** phosphorylated-AKT and **(B)** phosphorylated-FoxO1 from cytosolic fractions. **(C)** nFoxO1 from nuclear fractions. Equal loading was confirmed by total AKT, β -Actin, and Lamin A/C respectively (n=4). The immunoblots for Lamin A/C in **(B)** and for β -Actin in **(C)** show no detectable bands demonstrating complete separation of cytosolic and nuclear fractions, respectively. Data is presented as mean \pm SEM (n=4). * indicates significant difference versus control; *t*-test ($P < 0.05$). Representative bands are from the same immunoblot, cut from different regions.



2.3.6 VLDL-STIMULATED ACTIVATION OF MAPK SIGNALING AND REPRESSION OF AKT/FoxO1 SIGNALING ARE CORRECTED BY PPAR δ ACTIVATION

To determine the mechanism whereby PPAR δ activation attenuates VLDL-induced cytokine expression, we examined the effect of PPAR δ agonists on macrophage MAPK and AKT/FoxO1 signaling. GW0742 and GW501516 significantly attenuated both VLDL-stimulated ERK1/2 and p38 activation (Figure 2.13A, B). Furthermore, both PPAR δ agonists increased phospho-Akt and phospho-FoxO1 in control cells (Figure 2.13C), and reversed the reductions of phospho-Akt and phospho-FoxO1 in VLDL-treated cells (Figure 2.13D, E). Importantly, GW0742 and GW501516 prevented the VLDL-induced increase in nuclear FoxO1 (Figure 2.13F). Inhibition of β -oxidation by etomoxir had no effect on the ability of PPAR δ activation to normalize VLDL-induced MAPK signaling (Figure 2.14A,B) or restore normal AKT/FoxO1 signaling (Figure 2.14C,D). Collectively, these data demonstrate that PPAR δ activation inhibits VLDL-induced inflammatory cytokine expression by inhibiting MAPK signaling and restoring signaling through AKT/FoxO1. Furthermore, the modulation of both signaling pathways by PPAR δ activation was independent of PPAR δ agonist-induced β -oxidation.

Figure 2.13 PPAR δ activation normalizes VLDL-stimulated inflammatory signaling.

THP-1 cells were pre-incubated with PPAR δ agonists for 24hr, followed by a 0.5hr incubation with or without VLDL. Representative immunoblots of phosphorylated **(A)** pERK1/2 and **(B)** p-p38 from cytosolic fractions (n=5-7). THP-1 cells were incubated for 6hr with or without PPAR δ agonists. Levels of **(A)** pAKT and pFoxO1 were determined by immunoblotting cytosolic fractions. Equal loading was confirmed by total AKT and β -Actin, respectively (n=2). Relative intensities represent ratio of phospho:total protein relative to the respective DMSO control of the representative immunoblot. **D-F**, THP-1 cells were pre-incubated with PPAR δ agonists for 24hr, followed by 6hr incubation with or without VLDL. Representative immunoblots of phosphorylated **(C)** pAKT and **(D)** pFoxO1 from cytosolic fractions and **(E)** nFoxO1 from nuclear fractions. Equal loading was confirmed by total AKT, β -Actin, and Lamin A/C respectively (n=5-7). Different letters indicate significant differences; ANOVA with post-hoc Tukey's test ($P < 0.05$).

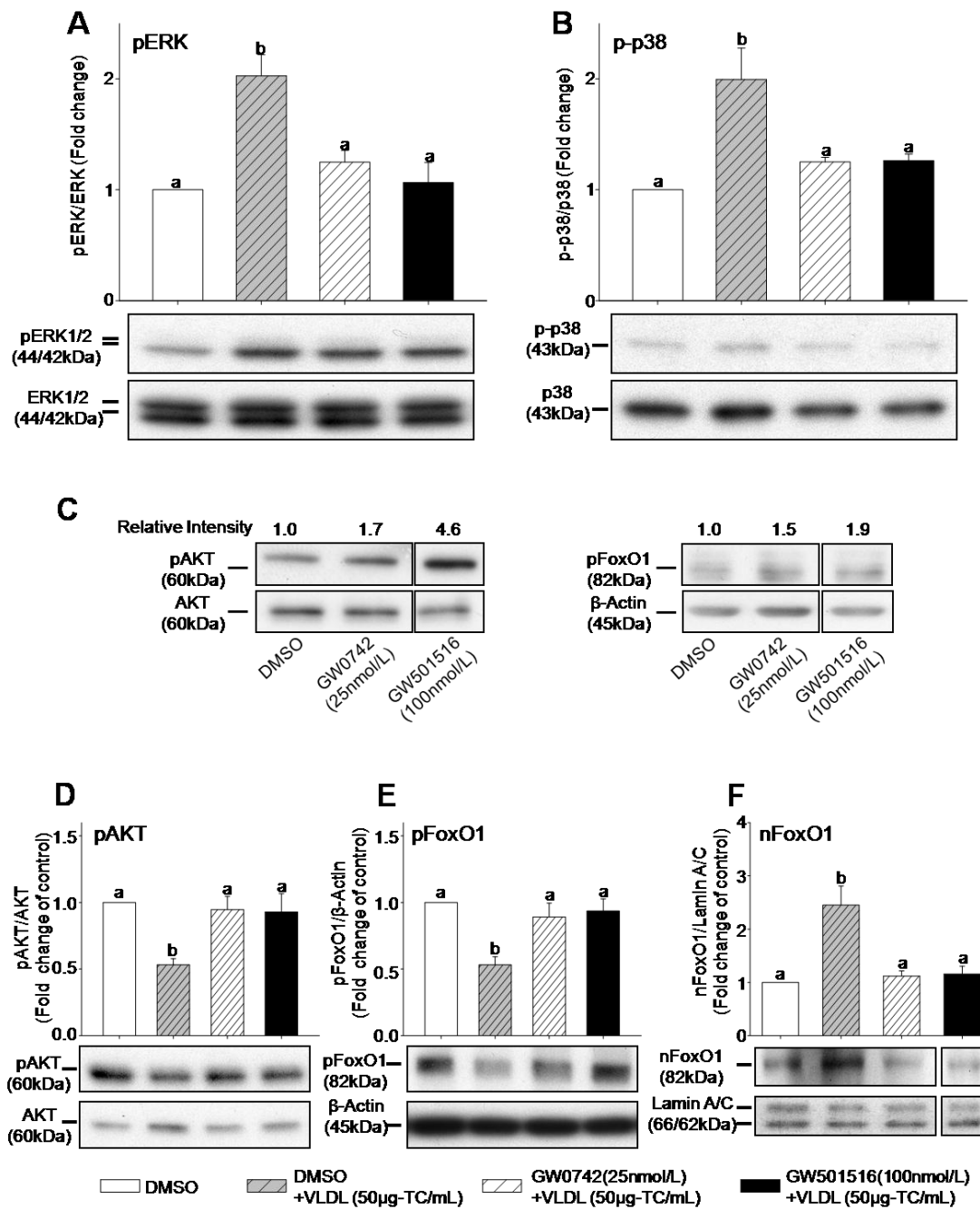
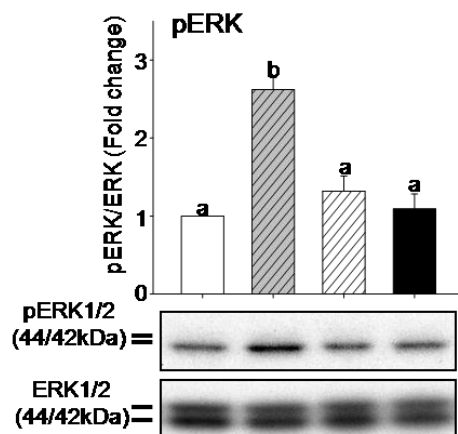
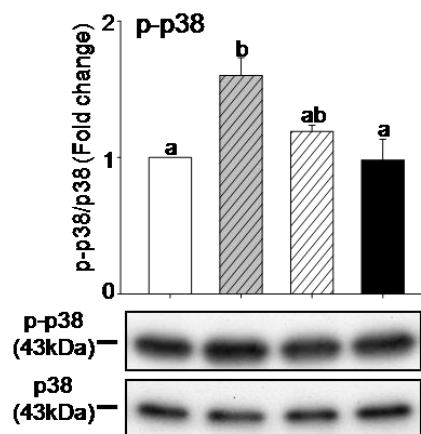
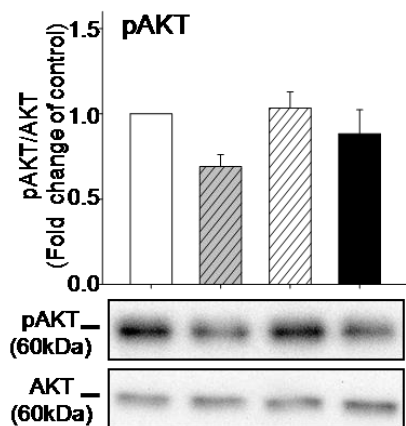
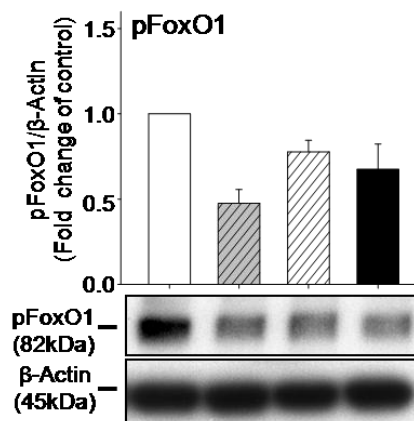


Figure 2.14 Inhibition of β -oxidation had no effect on the ability of PPAR δ activation to correct VLDL-induced inflammatory signalling. THP-1 cells were pre-incubated with PPAR δ agonists for 24hr, followed by a 0.5hr incubation with the CPT-1 α inhibitor etomoxir (ETO). For a subsequent 0.5hr, cells were incubated with or without VLDL. Representative immunoblots of phosphorylated **(A)** pERK1/2 and **(B)** p-p38 from cytosolic fractions (n=3). **C,D**, THP-1 cells were pre-incubated with PPAR δ agonists for 24hr, followed by a 0.5hr incubation with ETO. For a subsequent 6hr, cells were incubated with or without VLDL. Representative immunoblots of phosphorylated **(C)** pAKT and **(D)** pFoxO1 from cytosolic fractions (n=3). Data is presented as mean +/- SEM. Different letters indicate significant differences; ANOVA with post-hoc Tukey's test ($P<0.05$).

A**B****C****D**

DMSO
 VLDL (50µg-TC/mL) + ETO (50µmol/L)
 GW0742 (25nmol/L) + VLDL (50µg-TC/mL) + ETO (50µmol/L)
 GW501516 (100nmol/L) + VLDL (50µg-TC/mL) + ETO (50µmol/L)

2.4 DISCUSSION

Patients with insulin resistant syndromes such as type 2 diabetes and metabolic syndrome have significant elevations of plasma VLDL, which confers increased risk for atherosclerosis (Facchini et al., 2001, Reaven, 2005). Type 2 diabetes, metabolic syndrome and atherosclerosis are interwoven by the commonality of chronic low-grade inflammation (Dandona et al., 2004, Hotamisligil, 2006). However, the molecular processes that link elevated plasma VLDL, atherosclerosis and inflammation require further elucidation. In the present study, we demonstrate that human native VLDL induces both macrophage TG accumulation and expression of proinflammatory cytokines, in the absence of exogenous LPS. Furthermore, we demonstrate that PPAR δ activation attenuates both of these pathogenic macrophage foam cell processes, and define the mechanisms involved. Although VLDL-derived fatty acids are the stimulus for cytokine expression, the ability of PPAR δ agonists to dampen the inflammatory response is independent of agonist-induced LPL inhibition, stimulation of β -oxidation or reduction in cellular TG.

PPAR δ is expressed in abundance in macrophages (Vosper et al., 2001), but its biological role in lipid homeostasis has been controversial (Chawla et al., 2003, Lee et al., 2006, Vosper et al., 2001). In this study, we demonstrate that VLDL-induced TG accumulation is significantly decreased by PPAR δ activation. Hydrolysis of VLDL-TG by macrophage LPL is required for cellular FA uptake and TG resynthesis (Evans et al., 1993). PPAR δ agonists increased *ANGPTL4* expression, which was coupled to a reduction in LPL activity thereby limiting liberated FAs for macrophage uptake. These findings are consistent with recent studies demonstrating that *ANGPTL4* is a PPAR δ target gene, which is expressed in macrophages and irreversibly inactivates LPL by converting active LPL-dimers into inactive LPL-monomers (Adhikary et al., , Sukonina et

al., 2006). PPAR δ activation increased expression of the FA transporter CD36, which resulted in a modest increase in FA uptake, albeit from a smaller FA pool. However, we confirm that PPAR δ agonists upregulate *CPT-1 α* expression (Lee et al., 2006), which enhances FA oxidation. Furthermore, we show for the first time, that PPAR δ activation results in a net depletion of VLDL-induced TG accumulation. These results are consistent with the concept that one role for PPAR δ activation in macrophages is to prevent lipotoxicity by limiting VLDL hydrolysis and enhancing FA catabolism (Chawla et al., 2003, Lee et al., 2006), and contradict the notion that PPAR δ activation promotes lipid accumulation (Vosper et al., 2001). Furthermore, although VLDL-derived FAs activate PPAR δ (Chawla et al., 2003), potent synthetic agonists of PPAR δ are required in order to attenuate VLDL-stimulated macrophage foam cell formation, as well as inhibit the inflammatory response.

VLDL markedly stimulates expression of AP-1-inducible inflammatory cytokines, which occurs in the absence of NF κ B signaling or exogenous LPS. VLDL has been demonstrated to induce *Mip-1 α* in murine macrophages via ERK1/2 activation (Saraswathi and Hasty, 2006). We extend this response to human THP-1 macrophages and to include the induction of *IL-1 β* and *ICAM-1*. In THP-1 macrophages, both ERK1/2 and p38 are activated in response to VLDL, and p38 phosphorylation remains elevated well beyond that of ERK1/2. Inhibition of p38 stimulated ERK1/2 phosphorylation and enhanced cytokine expression. Moreover, the combination of VLDL treatment and p38 inhibition results in additive stimulation of cytokine expression over either treatment alone, suggesting that relieving the p38-induced impediment on ERK1/2 signaling enhances cytokine expression. Although in some cells, p38 activation has no effect or amplifies ERK1/2 signaling, we and others have reported that in hepatoma cells, insulin-induced phosphorylation of p38 also acts as a negative regulator of insulin-stimulated

ERK1/2 activation (Allister et al., 2005, Keeton et al., 2002). The present study supports this paradigm, and demonstrates for the first time, that VLDL-stimulation of macrophage cytokine expression through MAPK^{erk} involves p38 acting as a negative regulator of ERK1/2 signaling.

VLDL-treated macrophages displayed attenuated AKT and FoxO1 phosphorylation which coincided with increased nuclear FoxO1 and increased cytokine expression. Although the mechanism by which VLDL attenuates AKT signaling leading to activation of FoxO1 has not been defined, it is known that FoxO1 is a direct transcriptional activator of *Il-1 β* in mouse macrophages (Su et al., 2009). Several reports indicate that lipid-induced macrophage insulin resistance is associated with impaired AKT/FoxO1 signaling, increased FoxO1 activity, and thus plays a critical role in macrophage inflammation and ER-stress-induced apoptosis (Han et al., 2006, Senokuchi et al., 2008, Su et al., 2009). Some studies have suggested that free fatty acids induce macrophage inflammation through activation of toll-like receptor (TLR) signaling (Nguyen et al., 2007, Shi et al., 2006). However, more recent reports have provided contrary evidence (Anderson et al., 2012, Erridge and Samani, 2009). The present study is consistent with the concept that VLDL-stimulated macrophage inflammatory cytokine expression results from macrophage insulin resistance, rather than elicitation of a TLR-NF κ B response. This is evidenced by: (i) impaired AKT/FoxO1 signaling and enhanced MAPK signaling by VLDL treatment, (ii) canonical NF κ B target genes *TNF α* and *IL-6* being unaffected by VLDL treatment, and (iii) the inability of parthenolide, (an inhibitor of NF κ B signaling) to block VLDL-stimulated expression of *IL-1 β* , *MIP-1 α* and *ICAM-1*.

It is tempting to hypothesize that VLDL-induced inflammatory responses are initially derived from rapid ERK1/2 activation followed by later and sustained AKT

signaling. The ERK1/2 signal is rapidly down-regulated by activated p38, whereas the AKT signal is possibly mitigated by a self-limiting feedback loop (Fan et al., 2010). Furthermore, with time, it is possible that incoming FAs increase the saturated lipid content of the ER membrane, thereby inducing an ER-stress response (Borradaile et al., 2006), and subsequent amplification of nuclear FoxO1 (Ozcan et al., 2004). The exact relationship among time-dependent signaling events governing VLDL-stimulated inflammatory responses requires further study.

VLDL-induced expression of inflammatory cytokines was completely normalized by both PPAR δ agonists, despite a lack of effect on intracellular FFA levels, and even under conditions of inhibited β -oxidation. This suggests that stimulation of β -oxidation by PPAR δ activation is insufficient to explain the anti-inflammatory effects. Additionally, VLDL-stimulated phosphorylation of both ERK1/2 and p38 were normalized by PPAR δ activation, suggesting regulation of a common upstream MAPK factor. This concept is consistent with a previous report that GW0742 inhibited angiotensin II-induced phosphorylation of ERK1/2 and p38 in mouse macrophages, via upregulation of RGS4 and RGS5 (Takata et al., 2008). Whether this mechanism applies to the present study remains to be determined.

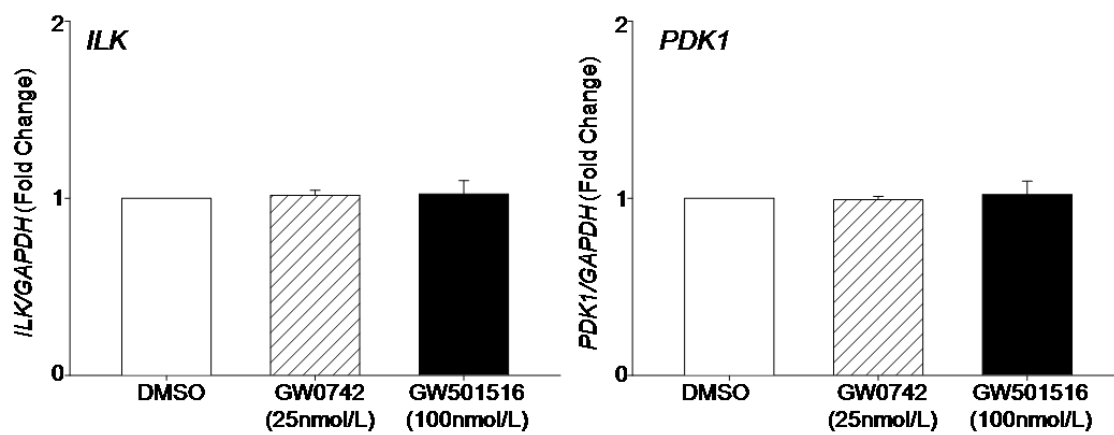
Macrophages exposed to VLDL in the presence of PPAR δ agonists restored levels of phospho-AKT, phospho-FoxO1 and nuclear FoxO1 to those observed in untreated cells, an effect independent of PPAR δ agonist-induced enhanced β -oxidation. Although modulation of AKT activity by PPAR δ activation has been observed in keratinocytes and endothelial cells (Di-Poi et al., 2002, Han et al., 2008), the mechanisms underlying this phenomenon remain unclear. Di-Poi *et al.* demonstrated that PPAR δ ligand L-165041 induced expression of integrin-like kinase (ILK) and 3-phosphoinositide-dependent kinase-1 (PDK1), which led to phosphorylation of AKT and

FoxO1 (Di-Poi et al., 2002). In contrast, Han *et al.* reported that GW501516-treated endothelial progenitor cells displayed marked elevations in phospho-AKT, without increased ILK expression (Han et al., 2008). In our experiments in macrophages, PPAR δ agonists increased phospho-AKT and phospho-FoxO1, without effecting *ILK* or *PDK1* expression (Figure 2.15). This suggests that the anti-inflammatory effect of PPAR δ activation is, in part, due to direct stimulation of AKT/FoxO1 phosphorylation, thereby preventing VLDL from dysregulating this signaling cascade.

In summary, VLDL-induced macrophage lipid accumulation and proinflammatory cytokine synthesis are attenuated by PPAR δ activation, effects which involve ERK1/2- and AKT-dependent signaling mechanisms. These combined reductions of lipid accumulation and inflammatory cytokine expression by PPAR δ ligands reveal a novel mechanism for preventing the deleterious consequences of macrophage foam cell formation.

Figure 2.15 Effects of PPAR δ agonists on expression of *ILK* and *PDK1*.

THP-1 cells were incubated with PPAR δ -specific agonists at the indicated concentrations for 24hr. Total RNA was isolated and *ILK* and *PDK1* mRNA was measured by qRT-PCR (n=4). Data is presented as mean +/- SEM.



2.5 REFERENCES

Adhikary, T., Kaddatz, K., Finkernagel, F., Schonbauer, A., Meissner, W., Scharfe, M., Jarek, M., Blocker, H., Muller-Brusselbach, S., and Muller, R. Genomewide Analyses Define Different Modes of Transcriptional Regulation by Peroxisome Proliferator-Activated Receptor-Beta/Delta (Pparbeta/Delta). *PLoS One* 6, e16344.

Allister, E.M., Borradaile, N.M., Edwards, J.Y., and Huff, M.W. (2005). Inhibition of Microsomal Triglyceride Transfer Protein Expression and Apolipoprotein B100 Secretion by the Citrus Flavonoid Naringenin and by Insulin Involves Activation of the Mitogen-Activated Protein Kinase Pathway in Hepatocytes. *Diabetes* 54, 1676-1683.

Anderson, E.K., Hill, A.A., and Hasty, A.H. (2012). Stearic Acid Accumulation in Macrophages Induces Toll-Like Receptor 4/2-Independent Inflammation Leading to Endoplasmic Reticulum Stress-Mediated Apoptosis. *Arterioscler Thromb Vasc Biol*.

Argmann, C.A., Edwards, J.Y., Sawyez, C.G., O'Neil, C.H., Hegele, R.A., Pickering, J.G., and Huff, M.W. (2005). Regulation of Macrophage Cholesterol Efflux through Hydroxymethylglutaryl-Coa Reductase Inhibition: A Role for Rhoa in Abca1-Mediated Cholesterol Efflux. *J Biol Chem* 280, 22212-22221.

Azzout-Marniche, D., Becard, D., Guichard, C., Foretz, M., Ferre, P., and Foufelle, F. (2000). Insulin Effects on Sterol Regulatory-Element-Binding Protein-1c (Srebp-1c) Transcriptional Activity in Rat Hepatocytes. *Biochem J* 350 Pt 2, 389-393.

Berger, J., Leibowitz, M.D., Doebber, T.W., Elbrecht, A., Zhang, B., Zhou, G., Biswas, C., Cullinan, C.A., Hayes, N.S., Li, Y., *et al.* (1999). Novel Peroxisome Proliferator-Activated Receptor (Ppar) Gamma and Ppardelta Ligands Produce Distinct Biological Effects. *J Biol Chem* 274, 6718-6725.

Beyea, M.M., Heslop, C.L., Sawyez, C.G., Edwards, J.Y., Markle, J.G., Hegele, R.A., and Huff, M.W. (2007). Selective up-Regulation of Lxr-Regulated Genes Abca1, Abcg1, and Apoe in Macrophages through Increased Endogenous Synthesis of 24(S),25-Epoxycholesterol. *J Biol Chem* 282, 5207-5216.

Beyea, M.M., Reaume, S., Sawyez, C.G., Edwards, J.Y., O'Neil, C., Hegele, R.A., Pickering, J.G., and Huff, M.W. (2012). The Oxysterol 24(S),25-Epoxycholesterol Attenuates Human Smooth Muscle-Derived Foam Cell Formation Via Reduced Low-Density Lipoprotein Uptake and Enhanced Cholesterol Efflux. *J Am Heart Assoc* 1, e000810.

Borradaile, N.M., Han, X., Harp, J.D., Gale, S.E., Ory, D.S., and Schaffer, J.E. (2006). Disruption of Endoplasmic Reticulum Structure and Integrity in Lipotoxic Cell Death. *J Lipid Res* 47, 2726-2737.

Chawla, A., Lee, C.H., Barak, Y., He, W., Rosenfeld, J., Liao, D., Han, J., Kang, H., and Evans, R.M. (2003). Ppardelta Is a Very Low-Density Lipoprotein Sensor in Macrophages. *Proc Natl Acad Sci U S A* 100, 1268-1273.

Dandona, P., Aljada, A., and Bandyopadhyay, A. (2004). Inflammation: The Link between Insulin Resistance, Obesity and Diabetes. *Trends Immunol* 25, 4-7.

Di-Poi, N., Tan, N.S., Michalik, L., Wahli, W., and Desvergne, B. (2002). Antiapoptotic Role of Pparbeta in Keratinocytes Via Transcriptional Control of the Akt1 Signaling Pathway. *Mol Cell* 10, 721-733.

Ding, G., Cheng, L., Qin, Q., Frontin, S., and Yang, Q. (2006). Ppardelta Modulates Lipopolysaccharide-Induced Tnfalpha Inflammation Signaling in Cultured Cardiomyocytes. *J Mol Cell Cardiol* 40, 821-828.

Eferl, R., and Wagner, E.F. (2003). Ap-1: A Double-Edged Sword in Tumorigenesis. *Nat Rev Cancer* 3, 859-868.

Erridge, C., and Samani, N.J. (2009). Saturated Fatty Acids Do Not Directly Stimulate Toll-Like Receptor Signaling. *Arterioscler Thromb Vasc Biol* 29, 1944-1949.

Evans, A.J., Sawyez, C.G., Wolfe, B.M., Connelly, P.W., Maguire, G.F., and Huff, M.W. (1993). Evidence That Cholesteryl Ester and Triglyceride Accumulation in J774 Macrophages Induced by Very Low Density Lipoprotein Subfractions Occurs by Different Mechanisms. *J Lipid Res* 34, 703-717.

Evans, A.J., Sawyez, C.G., Wolfe, B.M., and Huff, M.W. (1992). Lipolysis Is a Prerequisite for Lipid Accumulation in Hepg2 Cells Induced by Large Hypertriglyceridemic Very Low Density Lipoproteins. *J Biol Chem* 267, 10743-10751.

Facchini, F.S., Hua, N., Abbasi, F., and Reaven, G.M. (2001). Insulin Resistance as a Predictor of Age-Related Diseases. *J Clin Endocrinol Metab* 86, 3574-3578.

Fan, W., Morinaga, H., Kim, J.J., Bae, E., Spann, N.J., Heinz, S., Glass, C.K., and Olefsky, J.M. (2010). Foxo1 Regulates Tlr4 Inflammatory Pathway Signalling in Macrophages. *EMBO J* 29, 4223-4236.

Galic, S., Fullerton, M.D., Schertzer, J.D., Sikkema, S., Marcinko, K., Walkley, C.R., Izon, D., Honeyman, J., Chen, Z.P., van Denderen, B.J., *et al.* (2011). Hematopoietic Ampk Beta1 Reduces Mouse Adipose Tissue Macrophage Inflammation and Insulin Resistance in Obesity. *J Clin Invest* 121, 4903-4915.

Han, J.K., Lee, H.S., Yang, H.M., Hur, J., Jun, S.I., Kim, J.Y., Cho, C.H., Koh, G.Y., Peters, J.M., Park, K.W., *et al.* (2008). Peroxisome Proliferator-Activated Receptor-Delta

Agonist Enhances Vasculogenesis by Regulating Endothelial Progenitor Cells through Genomic and Nongenomic Activations of the Phosphatidylinositol 3-Kinase/Akt Pathway. *Circulation* 118, 1021-1033.

Han, S., Liang, C.P., DeVries-Seimon, T., Ranalletta, M., Welch, C.L., Collins-Fletcher, K., Accili, D., Tabas, I., and Tall, A.R. (2006). Macrophage Insulin Receptor Deficiency Increases Er Stress-Induced Apoptosis and Necrotic Core Formation in Advanced Atherosclerotic Lesions. *Cell Metab* 3, 257-266.

Hansson, G.K. (2005). Inflammation, Atherosclerosis, and Coronary Artery Disease. *N Engl J Med* 352, 1685-1695.

Hotamisligil, G.S. (2006). Inflammation and Metabolic Disorders. *Nature* 444, 860-867.

Keeton, A.B., Amsler, M.O., Venable, D.Y., and Messina, J.L. (2002). Insulin Signal Transduction Pathways and Insulin-Induced Gene Expression. *J Biol Chem* 277, 48565-48573.

Lee, C.H., Chawla, A., Urbiztondo, N., Liao, D., Boisvert, W.A., Evans, R.M., and Curtiss, L.K. (2003a). Transcriptional Repression of Atherogenic Inflammation: Modulation by Ppardelta. *Science* 302, 453-457.

Lee, C.H., Kang, K., Mehl, I.R., Nofsinger, R., Alaynick, W.A., Chong, L.W., Rosenfeld, J.M., and Evans, R.M. (2006). Peroxisome Proliferator-Activated Receptor Delta Promotes Very Low-Density Lipoprotein-Derived Fatty Acid Catabolism in the Macrophage. *Proc Natl Acad Sci U S A* 103, 2434-2439.

Lee, C.H., Olson, P., and Evans, R.M. (2003b). Minireview: Lipid Metabolism, Metabolic Diseases, and Peroxisome Proliferator-Activated Receptors. *Endocrinology* 144, 2201-2207.

Mulvihill, E.E., Assini, J.M., Lee, J.K., Allister, E.M., Sutherland, B.G., Koppes, J.B., Sawyez, C.G., Edwards, J.Y., Telford, D.E., Charbonneau, A., *et al.* Nobiletin Attenuates Vldl Overproduction, Dyslipidemia, and Atherosclerosis in Mice with Diet-Induced Insulin Resistance. *Diabetes* 60, 1446-1457.

Nguyen, M.T., Favelyukis, S., Nguyen, A.K., Reichart, D., Scott, P.A., Jenn, A., Liu-Bryan, R., Glass, C.K., Neels, J.G., and Olefsky, J.M. (2007). A Subpopulation of Macrophages Infiltrates Hypertrophic Adipose Tissue and Is Activated by Free Fatty Acids Via Toll-Like Receptors 2 and 4 and Jnk-Dependent Pathways. *J Biol Chem* 282, 35279-35292.

Nordestgaard, B.G., Benn, M., Schnohr, P., and Tybjaerg-Hansen, A. (2007). Nonfasting Triglycerides and Risk of Myocardial Infarction, Ischemic Heart Disease, and Death in Men and Women. *JAMA* 298, 299-308.

Ozcan, U., Cao, Q., Yilmaz, E., Lee, A.H., Iwakoshi, N.N., Ozdelen, E., Tuncman, G., Gorgun, C., Glimcher, L.H., and Hotamisligil, G.S. (2004). Endoplasmic Reticulum Stress Links Obesity, Insulin Action, and Type 2 Diabetes. *Science* 306, 457-461.

Proctor, S.D., and Mamo, J.C. (1998). Retention of Fluorescent-Labelled Chylomicron Remnants within the Intima of the Arterial Wall--Evidence That Plaque Cholesterol May Be Derived from Post-Prandial Lipoproteins. *Eur J Clin Invest* 28, 497-503.

Rapp, J.H., Lespine, A., Hamilton, R.L., Colyvas, N., Chaumeton, A.H., Tweedie-Hardman, J., Kotite, L., Kunitake, S.T., Havel, R.J., and Kane, J.P. (1994). Triglyceride-Rich Lipoproteins Isolated by Selected-Affinity Anti-Apolipoprotein B Immunosorption from Human Atherosclerotic Plaque. *Arterioscler Thromb* 14, 1767-1774.

Reaven, G.M. (2005). Insulin Resistance, the Insulin Resistance Syndrome, and Cardiovascular Disease. *Panminerva Med* 47, 201-210.

Rodriguez-Calvo, R., Serrano, L., Coll, T., Moullan, N., Sanchez, R.M., Merlos, M., Palomer, X., Laguna, J.C., Michalik, L., Wahli, W., *et al.* (2008). Activation of Peroxisome Proliferator-Activated Receptor Beta/Delta Inhibits Lipopolysaccharide-Induced Cytokine Production in Adipocytes by Lowering Nuclear Factor-KappaB Activity Via Extracellular Signal-Related Kinase 1/2. *Diabetes* 57, 2149-2157.

Rowe, A.H., Argmann, C.A., Edwards, J.Y., Sawyez, C.G., Morand, O.H., Hegele, R.A., and Huff, M.W. (2003). Enhanced Synthesis of the Oxysterol 24(S),25-Epoxycholesterol in Macrophages by Inhibitors of 2,3-Oxidosqualene:Lanosterol Cyclase: A Novel Mechanism for the Attenuation of Foam Cell Formation. *Circ Res* 93, 717-725.

Saraswathi, V., and Hasty, A.H. (2006). The Role of Lipolysis in Mediating the Proinflammatory Effects of Very Low Density Lipoproteins in Mouse Peritoneal Macrophages. *J Lipid Res* 47, 1406-1415.

Senokuchi, T., Liang, C.P., Seimon, T.A., Han, S., Matsumoto, M., Banks, A.S., Paik, J.H., DePinho, R.A., Accili, D., Tabas, I., *et al.* (2008). Forkhead Transcription Factors (Foxos) Promote Apoptosis of Insulin-Resistant Macrophages During Cholesterol-Induced Endoplasmic Reticulum Stress. *Diabetes* 57, 2967-2976.

Shi, H., Kokoeva, M.V., Inouye, K., Tzameli, I., Yin, H., and Flier, J.S. (2006). Tlr4 Links Innate Immunity and Fatty Acid-Induced Insulin Resistance. *J Clin Invest* 116, 3015-3025.

Stollenwerk, M.M., Lindholm, M.W., Porn-Ares, M.I., Larsson, A., Nilsson, J., and Ares, M.P. (2005a). Very Low-Density Lipoprotein Induces Interleukin-1beta Expression in Macrophages. *Biochem Biophys Res Commun* 335, 603-608.

Stollenwerk, M.M., Schiopu, A., Fredrikson, G.N., Dichtl, W., Nilsson, J., and Ares, M.P. (2005b). Very Low Density Lipoprotein Potentiates Tumor Necrosis Factor-Alpha Expression in Macrophages. *Atherosclerosis* 179, 247-254.

Su, D., Coudriet, G.M., Hyun Kim, D., Lu, Y., Perdomo, G., Qu, S., Slusher, S., Tse, H.M., Piganelli, J., Giannoukakis, N., *et al.* (2009). Foxo1 Links Insulin Resistance to Proinflammatory Cytokine Il-1beta Production in Macrophages. *Diabetes* 58, 2624-2633.

Sukonina, V., Lookene, A., Olivecrona, T., and Olivecrona, G. (2006). Angiopoietin-Like Protein 4 Converts Lipoprotein Lipase to Inactive Monomers and Modulates Lipase Activity in Adipose Tissue. *Proc Natl Acad Sci U S A* 103, 17450-17455.

Takata, Y., Liu, J., Yin, F., Collins, A.R., Lyon, C.J., Lee, C.H., Atkins, A.R., Downes, M., Barish, G.D., Evans, R.M., *et al.* (2008). Ppardelta-Mediated Antiinflammatory Mechanisms Inhibit Angiotensin Ii-Accelerated Atherosclerosis. *Proc Natl Acad Sci U S A* 105, 4277-4282.

Vasanwala, F.H., Kusam, S., Toney, L.M., and Dent, A.L. (2002). Repression of Ap-1 Function: A Mechanism for the Regulation of Blimp-1 Expression and B Lymphocyte Differentiation by the B Cell Lymphoma-6 Protooncogene. *J Immunol* 169, 1922-1929.

Vosper, H., Patel, L., Graham, T.L., Khoudoli, G.A., Hill, A., Macphee, C.H., Pinto, I., Smith, S.A., Suckling, K.E., Wolf, C.R., *et al.* (2001). The Peroxisome Proliferator-Activated Receptor Delta Promotes Lipid Accumulation in Human Macrophages. *J Biol Chem* 276, 44258-44265.

Welch, J.S., Ricote, M., Akiyama, T.E., Gonzalez, F.J., and Glass, C.K. (2003). Ppargamma and Ppardelta Negatively Regulate Specific Subsets of Lipopolysaccharide and Ifn-Gamma Target Genes in Macrophages. *Proc Natl Acad Sci U S A* 100, 6712-6717.

Whitman, S.C., Argmann, C.A., Sawyez, C.G., Miller, D.B., Hegele, R.A., and Huff, M.W. (1999). Uptake of Type Iv Hypertriglyceridemic Vldl by Cultured Macrophages Is Enhanced by Interferon-Gamma. *J Lipid Res* 40, 1017-1028.

Whitman, S.C., Sawyez, C.G., Miller, D.B., Wolfe, B.M., and Huff, M.W. (1998). Oxidized Type Iv Hypertriglyceridemic Vldl-Remnants Cause Greater Macrophage Cholesteryl Ester Accumulation Than Oxidized Ldl. *J Lipid Res* 39, 1008-1020.

Willson, T.M., Brown, P.J., Sternbach, D.D., and Henke, B.R. (2000). The Ppars: From Orphan Receptors to Drug Discovery. *J Med Chem* 43, 527-550.

Chapter 3

Activation of PPAR δ inhibits human macrophage foam cell formation induced by native and modified low-density lipoprotein

3.1 INTRODUCTION

During atherogenesis, excessive macrophage uptake of lipoproteins drives lipid accumulation and the synthesis and secretion of proinflammatory mediators within the arterial wall, events that potentiate lesion progression (Libby et al., 2011). An important risk factor for the development of atherosclerosis is the elevation of plasma lipoproteins, primarily due to their ability to permeate the vessel wall and initiate macrophage foam cell formation as well as maladaptive immune responses (Libby et al., 2011, Moore and Tabas, 2011). Specifically, increased plasma cholesteryl ester (CE)-rich low-density lipoprotein (LDL) is a major foam cell-inducing lipoprotein, and in turn, a significant contributor to accelerated atherogenesis (Libby et al., 2011, Moore and Tabas, 2011). High plasma LDL is also positively correlated with inflammation linked to atherogenesis in both humans and mice (Blake and Ridker, 2003, Getz and Reardon, 2006). Therefore, pharmacological inhibition of LDL-induced macrophage foam cell formation and the linked inflammatory response(s) represent an attractive therapeutic strategy.

Cholesterol homeostasis in macrophages is a dynamic process regulated by uptake, storage and efflux. The predominant LDL uptake pathway in macrophages of the arterial intima is via its modified form through the scavenger receptors cluster of differentiation (CD) 36 and scavenger receptor A I/II (SRAI/II) (Moore and Freeman, 2006). Subendothelial retention of LDL leads to the formation of oxLDL (Steinberg, 2009, Steinberg and Witztum, 2010), a high-affinity scavenger receptor ligand (Moore and Freeman, 2006). Binding of oxLDL to either of these scavenger receptors readily induces macrophage cholesterol accumulation (Argmann et al., 2003). Once internalized, lipoprotein derived CEs are hydrolyzed in the late endosomes to free cholesterol and fatty acids (Maxfield and Tabas, 2005), which are subsequently re-

esterified in the endoplasmic reticulum (ER) by acyl-CoA:cholesterol acyltransferase (ACAT) (Brown et al., 1980, Ikonen, 2008). In macrophages, ACAT1 is the only expressed isoform that generates CE for storage in cytoplasmic lipid droplets (Ikonen, 2008). Collectively, under these circumstances, it is important that cholesterol efflux maintains the rate of cholesterol uptake, to prevent accumulation of cholesterol-laden foam cells within the arterial intima (Libby et al., 2011).

In response to massive cholesterol accumulation, macrophage foam cells also synthesize and secrete proinflammatory mediators that potentiate lesion progression (Tabas, 2010). Although the mechanisms by which cholesterol induces inflammatory responses are not fully understood, one proposed stimulus has been the induction of the endoplasmic reticulum (ER)-stress pathway (Tabas, 2010). As a consequence of excessive lipoprotein-derived cholesterol uptake, free cholesterol (FC) builds up in the ER, causing ER-stress (Tabas, 2010). Subsequently, the C/EBP homologous protein (CHOP) is induced, which in turn stimulates Nfkb signaling to upregulate the expression of tumor necrosis factor (*TNF*) α and interleukin (*IL*)-6 (Li et al., 2005). Therefore, excessive lipoprotein-derived cholesterol delivered to macrophages must be appropriately partitioned, either to storage in cytoplasmic lipid droplets or to cholesterol efflux pathways, in order to prevent the deleterious proinflammatory consequences of FC accrual in the ER (Rong et al., 2013, Tabas, 2010).

In addition to the ER-stress pathway, a growing body of evidence suggests that cell-surface receptor signaling also plays a role in the stimulation of macrophage inflammatory responses. Specifically, a series of studies support the concept that oxLDL stimulates proinflammatory cytokine expression through CD36 in concert with the pattern recognition toll-like receptors (TLR) (Moore and Tabas, 2011). The assembly of CD36-TLR complexes leads to the activation of nuclear factor kappa B (Nfkb) signal transduction to simulate expression of proinflammatory effector molecules, such as *Tnf*

and interleukin *IL-6* (Stewart et al., 2010). Addition of lipopolysaccharide (LPS) to cultured macrophages significantly enhances oxLDL-induced inflammation (Wiesner et al., 2010). In macrophages isolated from CD36 deficient patients, oxLDL fails to stimulate cytokine expression (Janabi et al., 2000). In mice, genetic ablation of either CD36 or various TLRs is linked to protection from diet-induced atherosclerosis and aortic inflammation (Curtiss et al., 2012, Febbraio et al., 2000, Michelsen et al., 2004, Mullick et al., 2005).

Despite the overwhelming positive evidence for oxLDL-induced inflammatory responses, a series of studies have provided contrary evidence (Chung et al., 2000, Kannan et al., 2012, Qiu et al., 2007). LPS-induced expression of the proinflammatory cytokine IL-12 was significantly reduced in macrophages treated with oxLDL (Chung et al., 2000). A subsequent study showed that macrophages treated with oxLDL exhibited lower expression of a panel of proinflammatory cytokines that included *TNF α* and *IL-6* (Qiu et al., 2007). Most recently, oxLDL-treatment of monocytes failed to increase *TNF α* and *IL-6* expression, and protected these cells from LPS-induced proinflammatory responses (Kannan et al., 2012). Collectively, these studies suggest that our understanding of macrophage inflammatory responses in the context of lipoprotein uptake, is not well defined.

The peroxisome proliferator-activated receptors (PPARs) are important regulators of metabolic and inflammatory signaling (Harmon et al., 2011, Lee et al., 2003). There are three known isoforms (PPAR α , γ and δ) which exhibit distinct patterns of tissue distribution and function (Harmon et al., 2011, Lee et al., 2003). In contrast to the predominant expression of PPAR α and PPAR γ in a cell- or tissue-specific manner (Harmon et al., 2011), expression of PPAR δ is ubiquitous. However, the expression of PPAR δ is high in macrophages (Vosper et al., 2001) where its role in cholesterol homeostasis remains unclear. Conflicting reports have demonstrated that synthetic PPAR δ agonists either stimulate cholesterol efflux and reverse cholesterol transport or

promote lipid accumulation (Oliver et al., 2001, Vosper et al., 2001, Wallace et al., 2005). One study suggested that the PPAR δ agonist GW0742 had no effect on cholesterol accumulation in mouse peritoneal macrophages isolated from mice fed a high-fat, high cholesterol diet supplemented with the compound (Li et al., 2004). Consequently, the net effect of PPAR δ activation on oxLDL-induced macrophage cholesterol accumulation has been difficult to define. With regard to inflammation, in adipocytes and cardiomyocytes, PPAR δ agonists inhibit LPS-induced Nfkb-mediated inflammatory responses (Ding et al., 2006, Rodriguez-Calvo et al., 2008). However, the impact of PPAR δ activation on the mechanisms underlying oxLDL-induced inflammatory responses, in the absence of LPS, has not been examined.

In the present study, we report that synthetic ligand activation of PPAR δ in macrophages attenuates LDL- and oxLDL-induced CE accumulation as well as oxLDL-induced FC accumulation. This was at least in part due to promoting ABCA1-mediated cholesterol efflux to apoAI. OxLDL-treated macrophages displayed reduced expression of *TNF α* and *IL-6* compared to untreated cells, which was not further affected by PPAR δ activation. The oxLDL-mediated anti-inflammatory response was associated with increased expression of genes known to be regulated by the liver X receptor (LXR) as well as by PPAR γ and PPAR δ .

3.2 MATERIALS AND METHODS

3.2.1 LIPOPROTEINS

LDL and high-density lipoprotein₃ (HDL₃) were isolated from plasma of human subjects recruited from the Lipid Clinic at the London Health Sciences Centre, University Campus (London, Ontario, Canada). This study was approved by the University of Western Ontario Institutional Review Board (IRB reference #15685). Lipoproteins were separated by differential ultracentrifugation using a Beckman 70.1 Ti rotor (16hr, 40,000 rpm, 12°C) as previously described (Whitman et al., 1997). LDL was oxidized (oxLDL) via the copper sulfate method and the extent of modification was confirmed by alterations in electrophoretic mobility (Whitman et al., 1997).

3.2.2 CELL CULTURE

Human THP-1 macrophages were obtained from American Type Culture Collection (Manassas, VA) and cultured as described previously (Beyea et al., 2007). PPAR δ agonists GW0742 (Sigma) and GW501516 (Alexis Biochemicals, Plymouth, PA) were dissolved in dimethyl sulfoxide (DMSO, Sigma) and incubated with cells at the indicated concentrations. These concentrations have been determined to specifically activate PPAR δ , in the absence of PPAR α or PPAR γ activation (Chapter 2). THP-1 macrophages were preincubated (24 hr) the presence or absence of PPAR δ agonists. Subsequently, cells were incubated with PPAR δ agonists in the presence or absence of lipoproteins as indicated. The ACAT inhibitors Dup-128 (DuPont Merck Pharmaceutical Co.) and CI-1011 (Parke-Davis Pharmaceutical Research) were dissolved in DMSO and applied to THP-1 macrophages 0.5 hr prior to lipoprotein additions. Experimental concentrations of DMSO did not exceed 0.5% of total medium.

3.2.3 CELLULAR LIPID MASS

THP-1 macrophages were preincubated in the presence of PPAR δ agonists or equal volume of DMSO (not to exceed 0.5% of total medium) for 24 hr in RPMI 1640

supplemented with 10% fetal bovine serum (FBS) and 300nmol/L PDB. Cells were incubated for a further 16 hr with fresh media containing 5% LPDS and compounds in the absence or presence of native or oxidatively modified LDL (150 µg of lipoprotein total cholesterol (TC)/mL medium). Cellular TC, FC, TG, and protein mass were determined using enzymatic colorimetric assays for TC and FC (Wako Diagnostics, Richmond, VA) as well as TG (Boehringer Mannheim, Laval, QC) as previously described (Rowe et al., 2003). Cellular CE was determined as the difference between TC and FC (Rowe et al., 2003).

3.2.4 CHOLESTEROL ESTERIFICATION

The esterification of cholesterol was measured in THP-1 cells following a preincubation in 5% LPDS-containing medium for 19 hr in the presence or absence of the indicated concentrations of PPAR δ agonists. For a subsequent 5 hr incubation, 0.08nCi/mL [$1\text{-}^{14}\text{C}$]oleic acid (Amersham Biosciences) complexed with fatty acid-free bovine serum albumin in a molar ratio of 5.36:1 (Sigma) was added with or without LDL or oxLDL as described previously (Beyea et al., 2012). Cellular lipid extracts were separated by thin layer chromatography. Cells were lysed in 1mL of 0.1N NaOH, and aliquots were used to determine protein concentrations (Beyea et al., 2012).

3.2.5 CHOLESTEROL EFFLUX

THP-1 macrophages were incubated with acLDL (5 µg-TC/mL) in medium containing 0.2% FAF:BSA and [$1\alpha,2\alpha$ (n)- ^3H]cholesterol (1 µCi/mL, Amersham Biosciences) for 24 hr. Monolayers were then washed with phosphate buffered saline (PBS) and incubated in fresh medium with GW0742 or GW1516 at the indicated concentrations for 24 hr. Subsequently, macrophages were incubated with fresh compound and medium with 0.2% FAF:BSA alone, apoAI (10 µg/mL, Sigma) or HDL $_3$ (100µg-TC/mL) for a further 16 hr. Cholesterol efflux was expressed as the percentage of [^3H] counts in the media versus total [^3H] cholesterol counts (media plus cell) and

normalized to cell protein determined from 0.1N NaOH lysates as described (Argmann et al., 2003).

3.2.6 QUANTITATIVE REAL-TIME PCR mRNA ABUNDANCE ANALYSIS

THP-1 cells were incubated for 24 hr in RPMI 1640 with 5% LPDS, 300nmol/L PDB, in the presence or absence of PPAR δ agonists, and subsequently total RNA was isolated using TriZol reagent (Invitrogen, Burlington, ON) according to the manufacturer's instructions. In experiments examining oxLDL-induced inflammatory cytokine expression, cells were preincubated for 24 hr in RPMI 1640 with 10% FBS, 300nmol/L PDB, in the presence or absence of PPAR δ agonists. Cells were then incubated with fresh 5%-LPDS media and compounds for a further 16 hr in the absence or presence of oxLDL (150 μ g-TC/mL) prior to TriZol RNA extraction. Abundance of total RNA (2 μ g) was reverse transcribed using the Applied Biosystems High Capacity cDNA reverse transcription kit according to the manufacturer's protocol. Subsequently, cDNA (10ng) was analyzed in triplicate by quantitative real time RT-PCR (qRT-PCR) on an ABI Prism (model 7900HT) Sequence Detection System (Applied Biosystems, Foster City, CA) according to the manufacturer's instructions and as previously described (Chapter 2). Primer-probe sets for each gene (*ABCA1*, *ABCG1*, *ACAT1*, *ACOX*, *ADFP*, *DHCR24*, *FABP4*, *FAS*, *IL-6*, *MYLIP*, *SREBP-1c*, and *TNF α*) were obtained from Applied Biosystems (Carlsbad, CA). Abundance of target genes, calculated using the standard curve method, was normalized to *GAPDH* abundance.

3.2.7 IMMUNOBLOT ANALYSIS AND DENSITOMETRY

Total cell lysates were prepared as previously described (Chapter 2). Proteins were separated by SDS-PAGE, transferred to polyvinylidene difluoride membranes and immunoblotted as described (Rowe et al., 2003). Cellular cytosolic fractions were probed using antibodies against human ABCA1, ABCG1 (Novus Biologicals, Littleton, CO) and β -actin (Cell Signaling, Danvers, MA). Quantification analysis of the developed films was

performed using an imaging densitometer (Bio-Rad Quantity One Software). ABCA1 and ABCG1 from cytosolic fractions were normalized to β -Actin.

3.2.8 STATISTICAL ANALYSES

Data are expressed as means \pm standard error of the mean (SEM). The Shapiro-Wilk normality test was used to test for parametric distributions in each data set. *P* values for observed differences between treatment and control groups were calculated by one-way ANOVA followed by Bonferroni post hoc test. *P* values for observed pair-wise comparisons were calculated by one-way ANOVA followed by Tukey's post hoc test. Significance thresholds were *P* values less than 0.05. Statistical analyses were performed with SigmaPlot 11.0 software (Systat, Inc, San Jose, CA).

3.3 RESULTS

3.3.1 PPAR δ -SPECIFIC ACTIVATION ATTENUATES NATIVE AND OXIDIZED LDL-INDUCED MACROPHAGE CHOLESTERYL ESTER ACCUMULATION

THP-1 cells treated with native LDL (150 μ g-TC/mL) displayed a modest but significant 1.6-fold increase in CE accumulation (Figure 3.1A). Pre-treatment with PPAR δ agonists at concentrations known to be PPAR δ -specific (Chapter 2) for 24 hours almost completely normalized LDL-induced CE mass (Figure 3.1A). Cellular free cholesterol (FC) concentrations were unaffected by LDL or PPAR δ agonist treatment, whereas triglyceride (TG) mass trended towards a reduction in the presence of the PPAR δ ligands (Figure 3.1B). In contrast to the modest induction of foam cell formation by native LDL, oxLDL (150 μ g-TC/mL)-treated macrophages exhibited a marked 5-fold increase in CE mass, which was significantly attenuated (~40%) by 24 hour pre-treatment with PPAR δ agonists (Figure 3.1C). The 1.8-fold increase in FC accumulation induced by oxLDL was reduced (~50%) in the presence of the PPAR δ ligands (Figure 3.1D). Collectively, these results demonstrate that PPAR δ activation attenuates CE-rich lipoprotein induced macrophage foam cell formation.

3.3.2 PPAR δ AGONISTS ENHANCE CHOLESTEROL UPTAKE GENES AND ABCA1-MEDIATED CHOLESTEROL EFFLUX TO APOAI, HAVE NO EFFECT ON ABCG1-MEDIATED EFFLUX TO HDL₃ AND INHIBIT CHOLESTEROL ESTERIFICATION

We hypothesized that the observed attenuation of CE mass mediated by the PPAR δ agonists may be due to reduced lipoprotein uptake. However, PPAR δ activation enhanced both *LDLR* (Figure 3.2A) and *CD36* mRNA abundance (Chapter 2, Figure 2.3D), which would be predicted to enhance native and oxidized LDL uptake, respectively. We next examined cholesterol esterification, and found that *ACAT1* expression was unchanged in response to the PPAR δ ligands (Figure 3.2B). However, both PPAR δ agonists attenuated basal and lipoprotein-induced

Figure 3.1: PPAR δ activation attenuates LDL-induced cholesteryl ester mass accumulation.

THP-1 cells were pre-incubated with PPAR δ agonists at the indicated concentrations for 24h, followed by a 16h incubation with or without LDL. **A**, Total and free cholesterol mass were measured via a colorimetric assay. Cholesteryl ester (CE) is calculated as the difference between total and free cholesterol. Values are expressed as CE mass +/- SEM of duplicate determinations (n=6). **B**, Free cholesterol and triacylglycerol mass were measured via a colorimetric assay. Values are expressed as CE mass +/- SEM and FC mass +/- SEM of duplicate determinations (n=6). **C**, oxLDL-induced CE mass. **D**, oxLDL-induced FC and TG mass. Different letters are significantly different from one another. ANOVA with post hoc Tukey's test ($P < 0.05$).

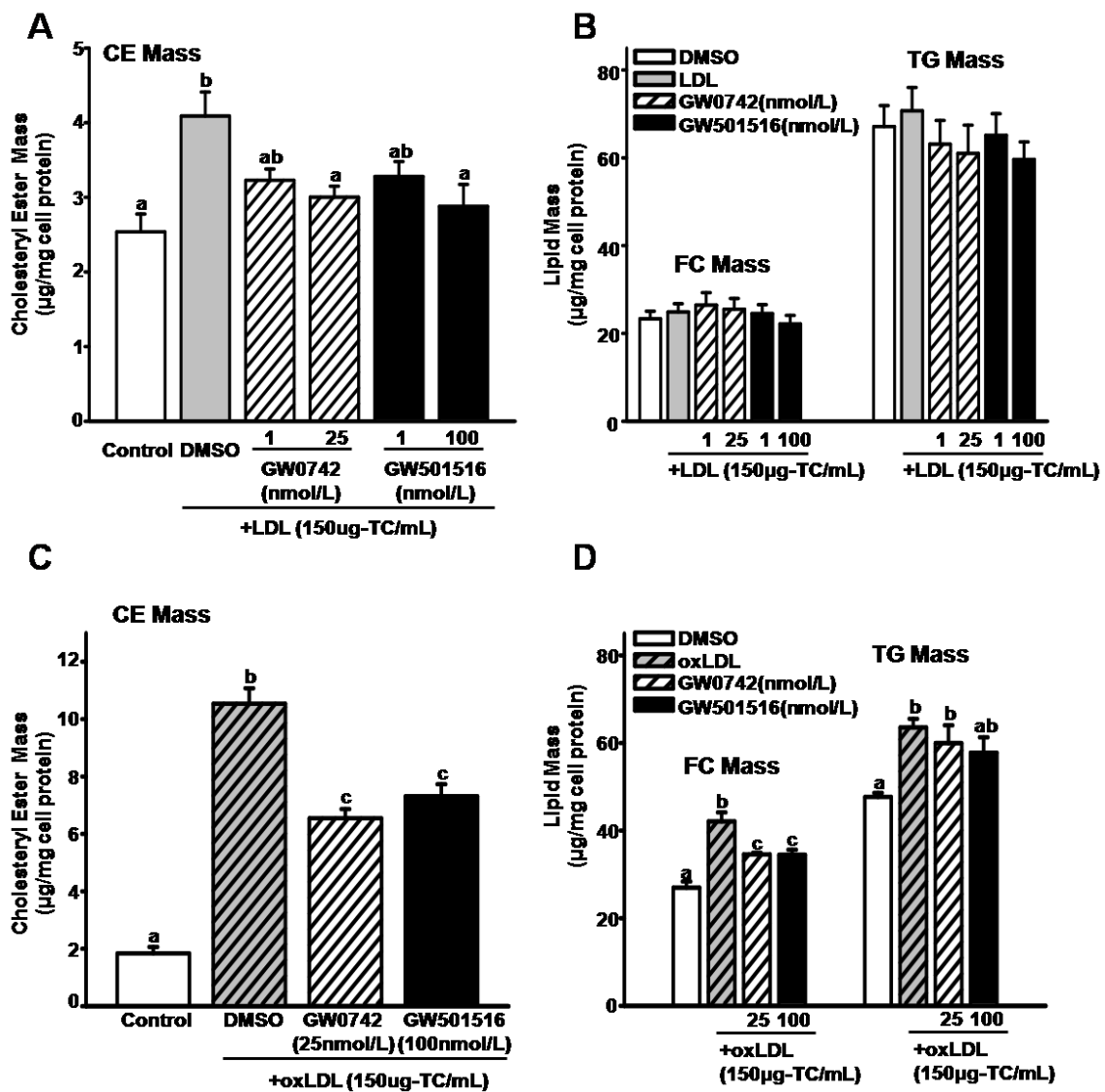
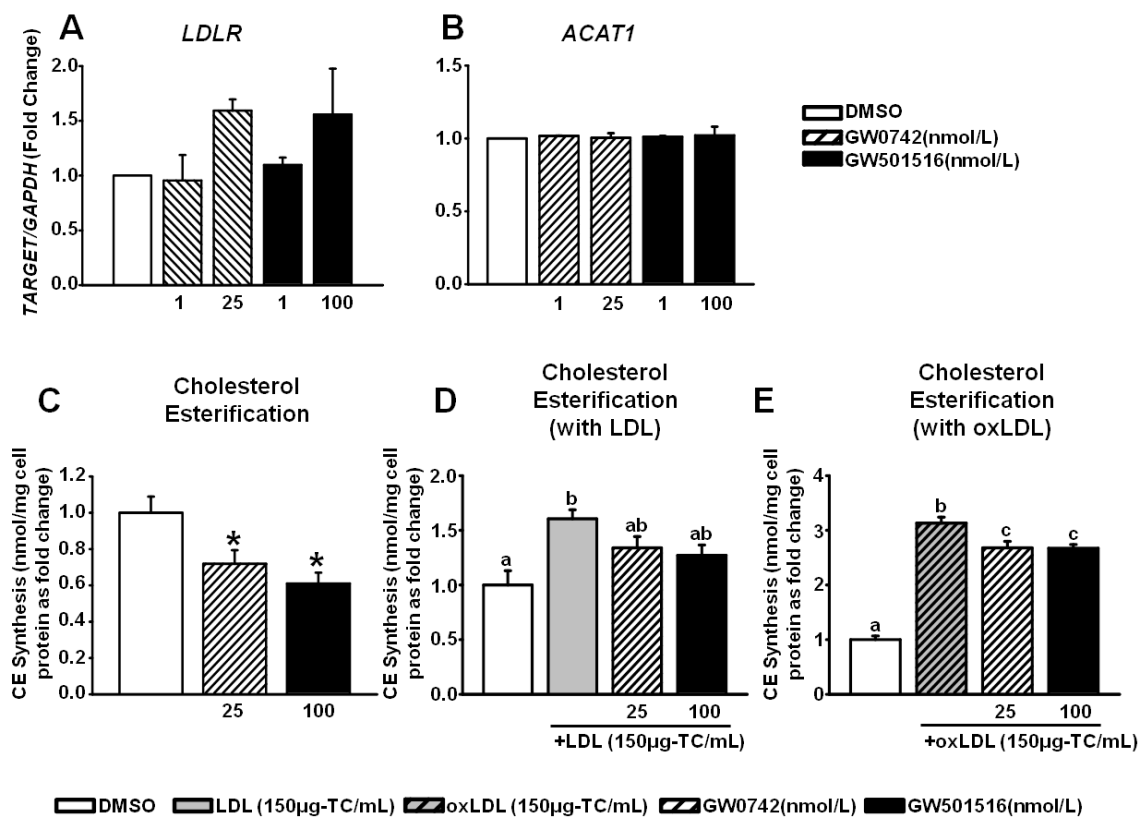


Figure 3.2: Effect of PPAR δ activation on uptake and FFA re-esterification into cholesteryl ester.

THP-1 cells were incubated with PPAR δ -specific agonists at the indicated concentrations for 24h. mRNA was harvested and **(A)** *LDLR* and **(B)** *ACAT1* abundance was measured by qRT-PCR. Values are expressed as a fold change of DMSO control cells normalized to GAPDH +/- SEM of duplicate determinations (n=2-4). In separate experiments, following a 19h incubation with PPAR δ agonists at indicated concentrations, THP-1 cells were incubated for a further 5h with PPAR δ agonists and **(C)** 1-[14 C]oleic acid, **(D)** with or without LDL and **(E)** with or without oxLDL to measure oleate incorporation into cellular cholesteryl ester. Values are expressed as a fold change of DMSO control cells +/- SEM of duplicate determinations (n=3-4). Different letters are significantly different from one another. ANOVA with post hoc Tukey's test ($P < 0.05$).



cholesterol esterification, as evidenced by reduced incorporation of ^{14}C -oleic acid into CE (Figure 3.2C-E).

Regarding cholesterol efflux, abundance of ABCA1 mRNA and protein was significantly increased in THP-1 cells treated with either PPAR δ agonist (Figure 3.3A, B). Moreover, cells treated with GW0742 (25nmol/L) displayed a marked 2-fold increase in ABCG1 mRNA, and significantly increased ABCG1 protein, effects which were not observed with GW501516 (Figure 3.3C, D). Increased ABCA1 mRNA and protein was associated with a significant 1.8-fold increase in cholesterol efflux to apoAI (Figure 3.3E). Although there was a trend towards increased cholesterol efflux to HDL $_3$, this did not achieve statistical significance (Figure 3.3C). Collectively these results suggest that PPAR δ activation stimulates ABCA1- but not ABCG1-mediated cholesterol efflux, which likely contributes to a net reduction in macrophage CE content.

3.3.3 PPAR δ ACTIVATION DOES NOT FURTHER AFFECT THE OXLDL-MEDIATED REDUCTION IN PROINFLAMMATORY CYTOKINE EXPRESSION

Exposure of macrophages to oxLDL has been shown to stimulate Nfkb-mediated proinflammatory responses (Janabi et al., 2000, Stewart et al., 2010), and macrophages loaded with FC are thought to stimulate expression the canonical Nfkb-target genes, *TNF α* and *IL-6* (Li et al., 2005). Here, oxLDL-treated macrophages exhibited reduced expression of *TNF α* (-50%) and *IL-6* (-30%) (Figure 3.4A, B). Pre-treatment with the PPAR δ agonists had no further effect on expression of these cytokines (Figure 3.4A, B). We reasoned that the observed 1.8-fold increase in macrophage FC content in response to oxLDL (Figure 3.1D) was perhaps insufficient to stimulate ER-stress and induce an inflammatory response (Li et al., 2005). Treatment of macrophages with ACAT inhibitors Dup-128 or CI-1011 in the presence of oxLDL resulted in a further 1.3- and 1.5-fold increase in macrophage FC content, respectively (Figure 3.4C). CE mass

Figure 3.3: PPAR δ activation enhances ABCA1 and ABCG1 mRNA and protein, leading to increased cholesterol efflux.

THP-1 cells were incubated with PPAR δ agonists for 24h. Total RNA was analyzed for **(A)** *ABCA1* and **(C)** *ABCG1* mRNA by qRT-PCR. Values are expressed as a fold change of DMSO control cells normalized to *GAPDH* +/- SEM of duplicate samples. ANOVA with post hoc Bonferroni correction, * $P < 0.05$ versus control (n=4). **B,E**, ABCA1 and ABCG1 protein; representative immunoblots of 4 independent experiments shown. **D**, Cholesterol efflux from macrophages was measured following incubation with [3 H]cholesterol and acetylated LDL (5 μ g of total cholesterol/mL, 24h) in 0.2% (w/v) fatty acid-free bovine serum albumin medium followed by 24h with vehicle or PPAR δ agonists at the indicated concentrations, and a final 16h incubation with vehicle or PPAR δ agonists in the presence of FAF:BSA alone or apoAI (10 μ g/mL) or HDL $_3$ (100 μ g/mL). Cholesterol efflux is expressed as the percentage of [3 H]cholesterol in the medium relative to total [3 H]cholesterol (medium plus cell) normalized to total cell protein and plotted as a ratio of apoAI with vehicle alone (mean +/- SEM, n=4). ANOVA with post hoc Tukey's test, different letters are statistically different ($P < 0.05$).

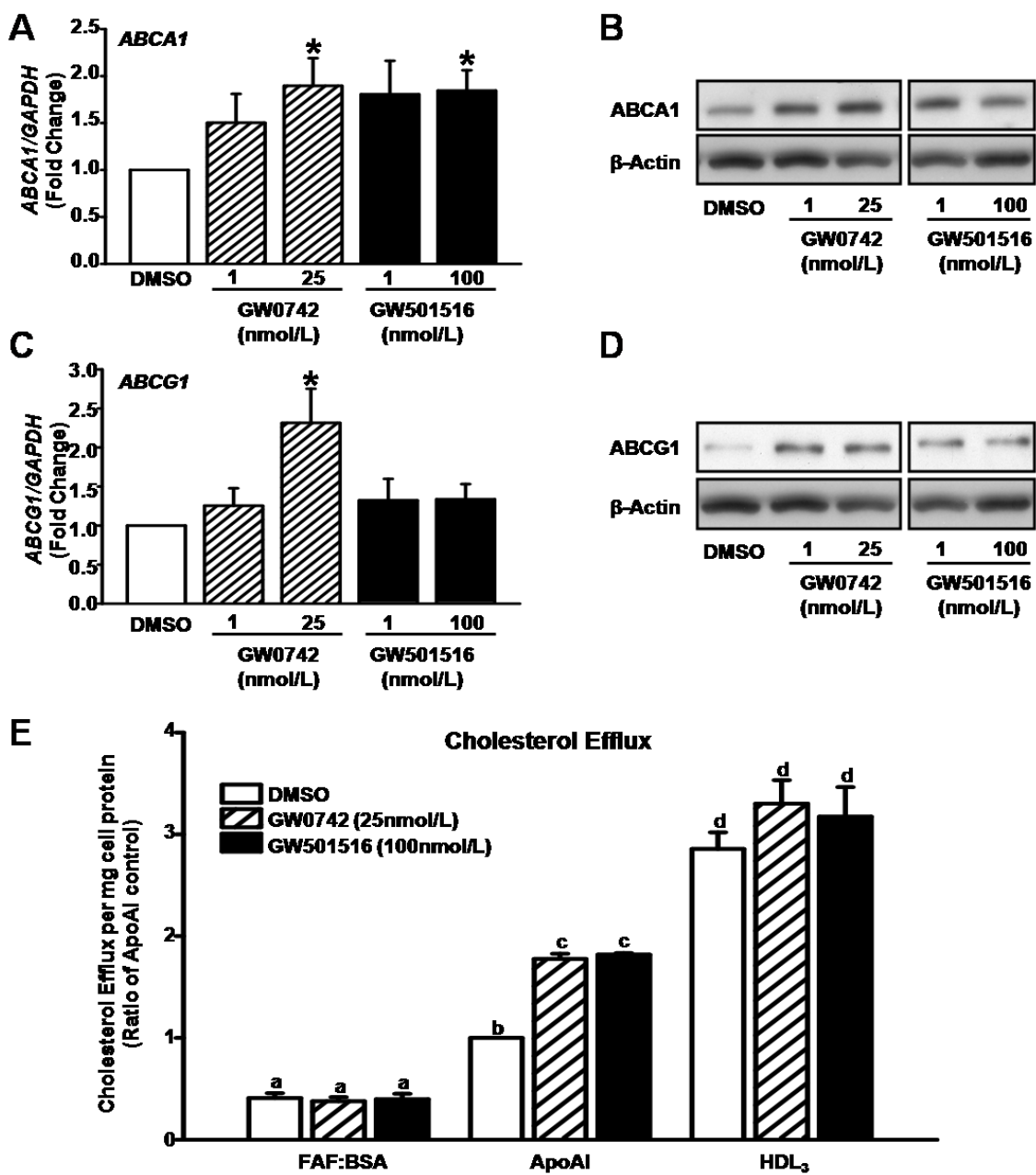
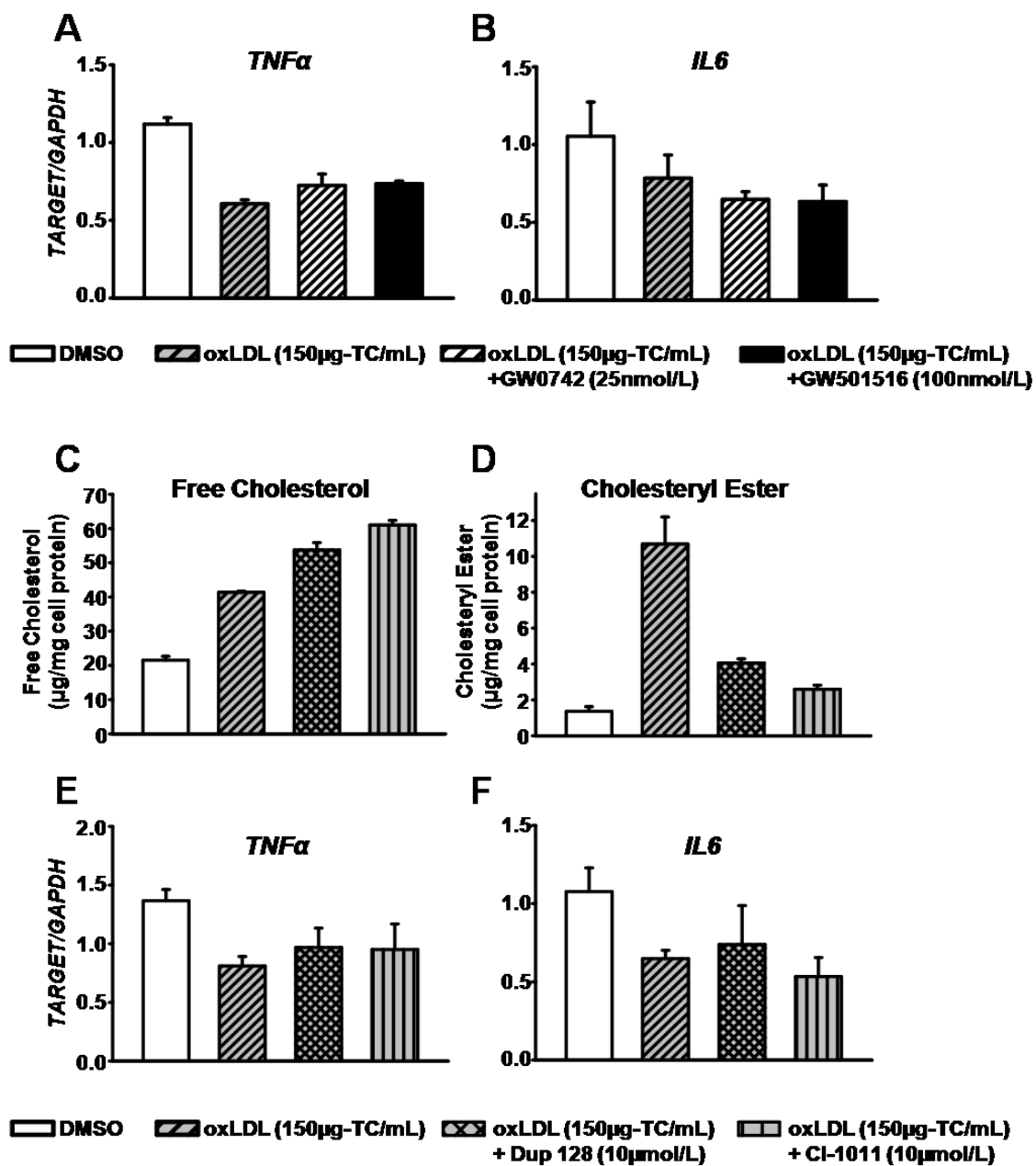


Figure 3.4: PPAR δ agonists and ACAT inhibitors do not further affect the oxLDL-mediated reduction in proinflammatory cytokine expression.

THP-1 cells were pre-incubated with PPAR δ agonists at the indicated concentrations for 24h, followed by a 16h incubation with or without oxLDL (150 μ g-TC/mL) for 16h. Total RNA was analyzed for the proinflammatory cytokines **(A)** *TNF α* and **(B)** *IL-6* by qRT-PCR and normalized to *GAPDH*. In a separate set of experiments, THP-1 cells were pre-incubated with or without ACAT inhibitors at the indicated concentration for 0.5h, followed by a 16h incubation with or without oxLDL (150 μ g-TC/mL) for 16h. **C**, Free cholesterol mass. **D**, Cholesteryl Ester mass. *TNF α* **(E)** and *IL-6* **(F)** mRNA abundance normalized to *GAPDH*. Data is presented as mean \pm SEM of duplicate samples (n=2).



was significantly reduced by the presence of the ACAT inhibitors (Figure 3.4D). Despite the further induction of cellular FC by ACAT inhibition, the suppression of *TNF α* or *IL-6* expression by oxLDL was unaffected (Figure 3.4E, F). These data suggest that oxLDL treatment or FC accumulation in macrophages does not stimulate the inflammatory response.

3.3.4 OXLDL-TREATED MACROPHAGES DISPLAY INCREASED EXPRESSION OF LXR, PPAR γ AND PPAR δ TARGET GENES

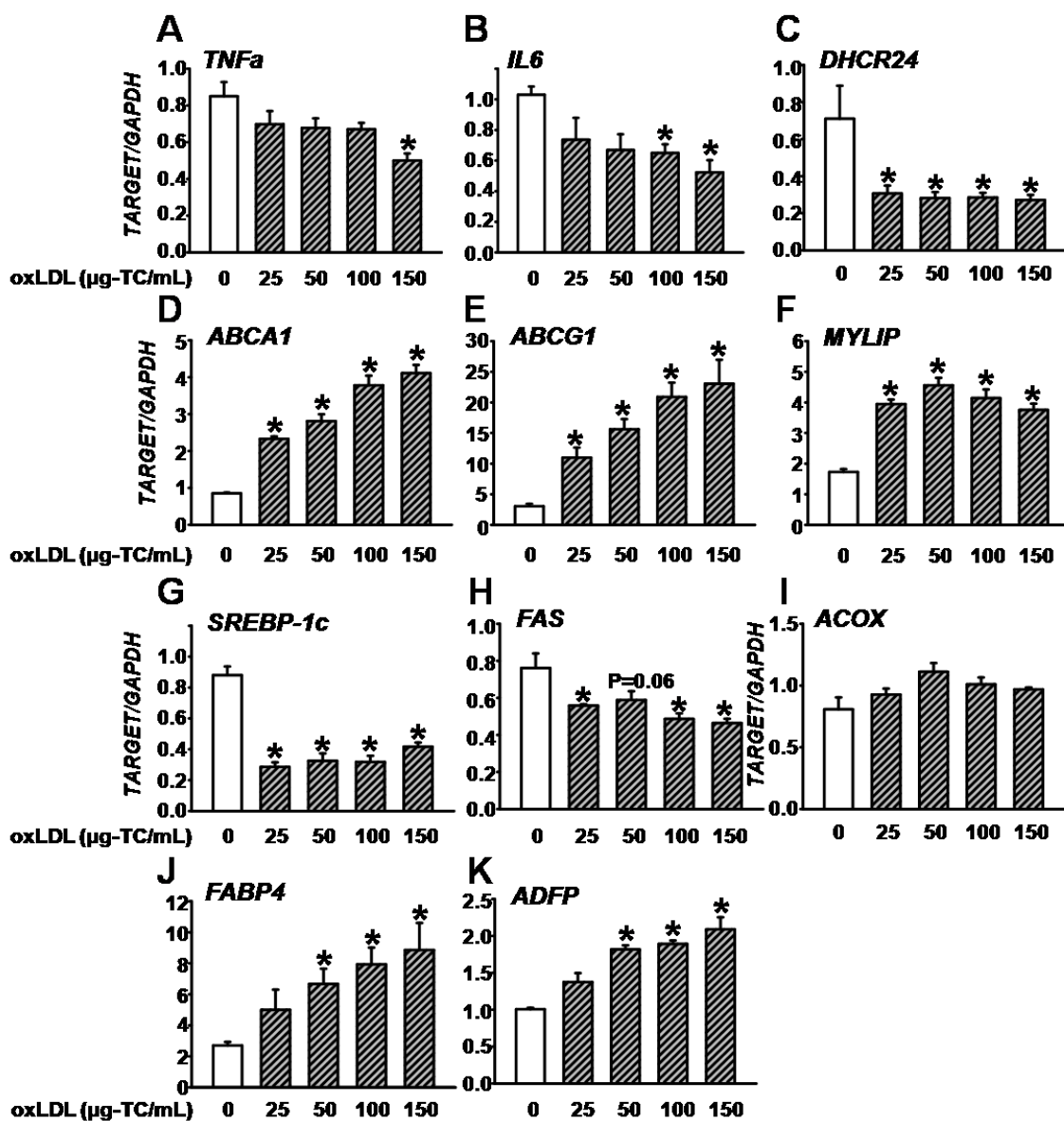
It has recently been reported that peritoneal macrophages isolated from high-fat, high cholesterol fed *Ldlr*^{-/-} mice display significant enrichment of cholesterol, coupled to substantially reduced dehydrocholesterol reductase (*DHCR*) 24 expression (Spann et al., 2012). The *DHCR24* transcript encodes the enzyme responsible for catalyzing the conversion of lanosterol to 24,25-dihydrolanosterol in the Kandutsch-Russel cholesterol biosynthetic pathway, as well as the conversion of desmosterol to cholesterol in the Bloch pathway (Spann et al., 2012). Accordingly, a significant accumulation of the potent LXR-ligand desmosterol was observed in cholesterol-rich peritoneal macrophages. As LXR activation is known to negatively regulate the inflammatory response, increased desmosterol was associated with a marked reduction in the expression of proinflammatory genes (Spann et al., 2012). We hypothesized that this phenomenon might reconcile the data observed in Figure 3.4 of the current study. THP-1 cells exposed to increasing concentrations of oxLDL exhibited a dose-dependent decrease in *TNF α* and *IL-6* expression (Figure 3.5A, B). Reduced cytokine expression was associated with a significant decrease in *DHCR24* mRNA abundance (Figure 3.5C). Moreover, expression of the LXR-target genes *ABCA1*, *ABCG1* and *MYLIP* was substantially enhanced in oxLDL-treated macrophages (Figure 3.5D-F). Macrophages abundant in oxysterols, like desmosterol, are known to exhibit reduced processing of SREBP-1c, resulting in reduced expression of SREBP-1c target genes (Beyea et al.,

2007). Here, *SREBP-1c* and *FAS* expression were significantly reduced in oxLDL-treated THP-1 macrophages (Figure 3.5G, H). Taken together these data support the notion that cholesterol-loaded macrophages down-regulate *DHCR24* expression and activity, which results in an anti-inflammatory response mediated partially through LXR activation.

Given that PPARs are known to regulate anti-inflammatory responses (Harmon et al., 2011), and that oxLDL-treatment of macrophages can activate PPAR γ transcriptional activity (Nagy et al., 1998), we examined whether there was any evidence of PPAR activation in oxLDL-loaded THP-1 cells. OxLDL had no effect on the PPAR α -specific target gene *ACOX* (Figure 3.5I). In contrast, macrophage oxLDL-treatment significantly increased expression of the PPAR γ - and PPAR δ -specific target genes *FABP4* and *ADFP*, respectively (Figure 3.5J, K). These results suggest that PPAR γ and PPAR δ activation may contribute to part of the oxLDL-mediated anti-inflammatory response.

Figure 3.5: oxLDL dose-dependently reduces proinflammatory cytokine expression which is associated with a dose-dependent increase in LXR, PPAR γ and PPAR δ target genes

THP-1 cells were incubated with oxLDL (25-150 μ g-TC/mL) for 16h. Total RNA was analyzed for the proinflammatory cytokines **(A)** *TNF α* and **(B)** *IL-6*, for the cholesterol biosynthesis regulatory gene **(C)** *DHCR24*, the LXR-target genes **(D)** *ABCA1*, **(E)** *ABCG1* and **(F)** *MYLIP*, the SREBP-1c target genes **(G)** *SREBP-1c* and **(H)** *FAS* and the PPAR α -, γ -, and δ -specific target genes **(I)** *ACOX* **(J)** *FABP4* and **(K)** *ADFP*, respectively, by qRT-PCR and normalized to *GAPDH*. Data is presented as mean \pm SEM of duplicate samples. Asterisk (*) indicates $P < 0.05$ versus control; ANOVA with post hoc Bonferroni test.



3.4 DISCUSSION

High circulating LDL significantly increases the risk for the development of atherosclerotic cardiovascular disease (Libby et al., 2011). A strong positive correlation exists between high plasma LDL, inflammation and atherosclerosis (Blake and Ridker, 2003, Getz and Reardon, 2006, Libby et al., 2011). However, the molecular processes of atherosclerosis-associated inflammation as a consequence of high plasma LDL require further elucidation. Here, we demonstrate that oxLDL induces both CE and FC accumulation in THP-1 human macrophages, which are significantly attenuated by PPAR δ activation. Additionally, we show that in response to oxLDL, proinflammatory cytokine expression is decreased, rather than activated, and is not further affected by synthetic PPAR δ agonists or ACAT inhibitors. The anti-inflammatory response observed in oxLDL-treated macrophages was associated with decreased *DHCR24* expression, and increased expression of LXR-, PPAR γ - and PPAR δ -target genes.

PPAR δ is expressed in abundance in macrophages (Vosper et al., 2001), but its biological role in cholesterol homeostasis has been controversial (Li et al., 2004, Oliver et al., 2001, Vosper et al., 2001, Wallace et al., 2005). In this study, we demonstrate that oxLDL-induced CE and FC accumulation are significantly decreased by PPAR δ activation. We confirm that PPAR δ activation increases *ABCA1* mRNA and protein, which enhances cholesterol efflux to apoAI (Ogata et al., 2009, Oliver et al., 2001). Furthermore, our results imply that the PPAR δ agonist-induced increase in macrophage *ABCA1* expression is greater than that induced by downregulation of *DHCR24* in response to oxLDL alone. With regard to *ABCG1* activation, the effects of PPAR δ have not been reported. Although GW0742 enhanced *ABCG1* mRNA and protein, functionally, this did not enhance cholesterol efflux to HDL₃. Nevertheless, both PPAR δ agonists used in this study reduced LDL- and oxLDL-induced CE and FC accumulation. Deletion of *Abca1* but not *Abcg1* in mice, results in increased atherosclerotic plaque

development (Yvan-Charvet et al., 2007). Furthermore, *Abcg1*^{-/-} mice crossed to an *apolipoprotein E* knockout background are protected from diet-induced atherosclerosis (Tarling et al., 2010). These studies suggest that ABCA1, rather than ABCG1, is a critical efflux transporter for the regulation of cholesterol homeostasis in hematopoietic cells of the arterial intima. The findings reported here, at least with respect to macrophages, support this concept.

Given that oxLDL-uptake is mediated, in part, by CD36, and that PPAR δ activation is known to increase *CD36* expression (Chapter 2, Figure 2.3D) it would be predicted the PPAR δ ligands would promote oxLDL uptake. Our laboratory has previously demonstrated that macrophages treated with PPAR γ activators, which also activate *CD36* expression, increased oxLDL uptake, yet increased ABCA1-mediated cholesterol efflux, resulting in a net depletion of CE and FC (Argmann et al., 2003). The data reported here suggest that PPAR δ activation may promote a similar mechanism of macrophage cholesterol homeostasis in response to oxLDL. Furthermore, the results in the current study contradict the notion that PPAR δ activation has either no effect, or a stimulatory effect, on cholesterol accumulation (Li et al., 2004, Vosper et al., 2001).

Cholesterol esterification under basal and lipoprotein-stimulated conditions was attenuated by PPAR δ activation. The apparent reduction in ACAT activity is likely a secondary effect of the PPAR δ agonist's ability to increase cholesterol efflux, thereby preventing cholesterol from reaching the ACAT-accessible pool. Pharmacological and genetic manipulations that increase cholesterol efflux pathways are known to reduce cholesterol esterification by virtue of shuttling cholesterol away from the ER esterification pool, and towards the plasma membrane for efflux (Beyea et al., 2012, Yamauchi et al., 2004). Although further studies would be required to determine the specific effects of PPAR δ agonists on cholesterol trafficking in macrophages, our results support the

paradigm that increasing cholesterol efflux leads to a secondary reduction in cholesterol esterification (Francis and Perry, 1999, Wang et al., 2001).

Several studies have suggested that oxLDL stimulates macrophage inflammatory responses through elicitation of TLR-Nfkb signaling (Curtiss et al., 2012, Febbraio et al., 2000, Janabi et al., 2000, Michelsen et al., 2004, Mullick et al., 2005, Stewart et al., 2010). Additionally, ACAT inhibition leading to FC-loading of macrophages is thought to activate the ER-stress-Nkb cascade, resulting in the stimulation of *TNF α* and *IL-6* expression (Li et al., 2005). However, recent reports have provided contrary evidence to both of these paradigms (Anderson et al., 2012, Kannan et al., 2012, Qiu et al., 2007). oxLDL not only reduces monocyte and macrophage basal expression of *TNF α* and *IL-6*, but it also inhibits LPS-stimulated expression of both these cytokines (Kannan et al., 2012, Qiu et al., 2007). Furthermore, lipotoxicity-induced inflammation can occur in the absence of ER-stress (Anderson et al., 2012). The findings reported here are in support of these latter studies. In our hands, oxLDL-treated macrophages displayed attenuated expression of *TNF α* and *IL-6*, which was unaffected by treatment with the PPAR δ agonists. Furthermore, inhibition of ACAT activity to significantly increase FC accumulation, did not induce a pro-inflammatory phenotype in oxLDL-treated macrophages. Collectively, the present study is consistent with the concept that macrophages loaded with cholesterol are anti-inflammatory (Spann et al., 2012, Suzuki et al., 2012), rather than proinflammatory, and that PPAR δ agonists are incapable of further suppression.

Cholesterol-loaded mouse peritoneal macrophages display significant accumulation of desmosterol, a known potent activator of LXR (Spann et al., 2012). It is well characterized that activation of LXR is anti-inflammatory, as liganded LXR recruits corepressor complexes to promoter regions of proinflammatory genes (Im and Osborne, 2011). This recruitment event results in protein-protein interactions between Nfkb and

the LXR-bound corepressors, which prevents Nfkb from stimulating transcription of proinflammatory cytokines (Im and Osborne, 2011). PPAR γ activation exerts anti-inflammatory effects through a similar mechanism (Straus and Glass, 2007). Whether oxLDL-treatment increases corepressor occupancy of the *TNF α* and *IL-6* promoters in THP-1 macrophages remains to be determined. Nevertheless, our studies support the concept that desmosterol accumulation within macrophages is associated with suppression of pro-inflammatory gene expression (Spann et al., 2012).

Given that oxLDL stimulated the expression of the PPAR δ -specific target gene *ADFP*, it is tempting to hypothesize that PPAR δ ligands accumulate in response to cholesterol loading. Fatty acids are known to activate PPAR δ (Chawla et al., 2003). In cholesterol-loaded or desmosterol-treated mouse peritoneal macrophages, Spann et al. observed increases in cellular oleic acid in the picomolar range (Spann et al., 2012). In the micromolar range, oleic acid induces macrophage inflammatory responses (Chapter 2). However, picomolar concentrations of oleic acid may be sufficient to activate PPAR δ but insufficient to stimulate the inflammatory response. The possibility that PPAR δ activation plays a role in the oxLDL-mediated anti-inflammatory response of macrophages requires further study.

In summary, oxLDL-induced foam cell formation is attenuated by PPAR δ activation, supporting the use of synthetic PPAR δ agonists as a macrophage-targeted therapeutic strategy in the treatment of atherosclerosis. Furthermore, our studies suggest that macrophages of the arterial intima are not proinflammatory in response to cholesterol loading, *per se*. Rather we support the shift in paradigm that under conditions of high plasma LDL, immune cells of the arterial intima, such as dendritic cells (Becker et al., 2012), are the inflammatory effectors that secrete extrinsic factors to promote proinflammatory macrophage activation (Spann et al., 2012).

3.5 REFERENCES

Anderson, E.K., Hill, A.A., and Hasty, A.H. (2012). Stearic Acid Accumulation in Macrophages Induces Toll-Like Receptor 4/2-Independent Inflammation Leading to Endoplasmic Reticulum Stress-Mediated Apoptosis. *Arterioscler Thromb Vasc Biol* 32, 1687-1695.

Argmann, C.A., Sawyez, C.G., McNeil, C.J., Hegele, R.A., and Huff, M.W. (2003). Activation of Peroxisome Proliferator-Activated Receptor Gamma and Retinoid X Receptor Results in Net Depletion of Cellular Cholesteryl Esters in Macrophages Exposed to Oxidized Lipoproteins. *Arterioscler Thromb Vasc Biol* 23, 475-482.

Becker, L., Liu, N.C., Averill, M.M., Yuan, W., Pamir, N., Peng, Y., Irwin, A.D., Fu, X., Bornfeldt, K.E., and Heinecke, J.W. (2012). Unique Proteomic Signatures Distinguish Macrophages and Dendritic Cells. *PLoS One* 7, e33297.

Beyea, M.M., Heslop, C.L., Sawyez, C.G., Edwards, J.Y., Markle, J.G., Hegele, R.A., and Huff, M.W. (2007). Selective up-Regulation of Lxr-Regulated Genes *Abca1*, *Abcg1*, and *ApoE* in Macrophages through Increased Endogenous Synthesis of 24(S),25-Epoxycholesterol. *J Biol Chem* 282, 5207-5216.

Beyea, M.M., Reaume, S., Sawyez, C.G., Edwards, J.Y., O'Neil, C., Hegele, R.A., Pickering, J.G., and Huff, M.W. (2012). The Oxysterol 24(S),25-Epoxycholesterol Attenuates Human Smooth Muscle-Derived Foam Cell Formation Via Reduced Low-Density Lipoprotein Uptake and Enhanced Cholesterol Efflux. *J Am Heart Assoc* 1, e000810.

Blake, G.J., and Ridker, P.M. (2003). C-Reactive Protein and Other Inflammatory Risk Markers in Acute Coronary Syndromes. *J Am Coll Cardiol* 41, 37S-42S.

Brown, M.S., Ho, Y.K., and Goldstein, J.L. (1980). The Cholesteryl Ester Cycle in Macrophage Foam Cells. Continual Hydrolysis and Re-Esterification of Cytoplasmic Cholesteryl Esters. *J Biol Chem* 255, 9344-9352.

Chawla, A., Lee, C.H., Barak, Y., He, W., Rosenfeld, J., Liao, D., Han, J., Kang, H., and Evans, R.M. (2003). PPARdelta Is a Very Low-Density Lipoprotein Sensor in Macrophages. *Proc Natl Acad Sci U S A* 100, 1268-1273.

Chung, S.W., Kang, B.Y., Kim, S.H., Pak, Y.K., Cho, D., Trinchieri, G., and Kim, T.S. (2000). Oxidized Low Density Lipoprotein Inhibits Interleukin-12 Production in Lipopolysaccharide-Activated Mouse Macrophages Via Direct Interactions between Peroxisome Proliferator-Activated Receptor-Gamma and Nuclear Factor-Kappa B. *J Biol Chem* 275, 32681-32687.

Curtiss, L.K., Black, A.S., Bonnet, D.J., and Tobias, P.S. (2012). Atherosclerosis Induced by Endogenous and Exogenous Toll-Like Receptor (Tlr)1 or Tlr6 Agonists. *J Lipid Res* 53, 2126-2132.

Ding, G., Cheng, L., Qin, Q., Frontin, S., and Yang, Q. (2006). Ppar δ Modulates Lipopolysaccharide-Induced Tnf α Inflammation Signaling in Cultured Cardiomyocytes. *J Mol Cell Cardiol* 40, 821-828.

Febbraio, M., Podrez, E.A., Smith, J.D., Hajjar, D.P., Hazen, S.L., Hoff, H.F., Sharma, K., and Silverstein, R.L. (2000). Targeted Disruption of the Class B Scavenger Receptor Cd36 Protects against Atherosclerotic Lesion Development in Mice. *J Clin Invest* 105, 1049-1056.

Francis, G.A., and Perry, R.J. (1999). Targeting Hdl-Mediated Cellular Cholesterol Efflux for the Treatment and Prevention of Atherosclerosis. *Clin Chim Acta* 286, 219-230.

Getz, G.S., and Reardon, C.A. (2006). Diet and Murine Atherosclerosis. *Arterioscler Thromb Vasc Biol* 26, 242-249.

Harmon, G.S., Lam, M.T., and Glass, C.K. (2011). Ppars and Lipid Ligands in Inflammation and Metabolism. *Chem Rev* 111, 6321-6340.

Ikonen, E. (2008). Cellular Cholesterol Trafficking and Compartmentalization. *Nat Rev Mol Cell Biol* 9, 125-138.

Im, S.S., and Osborne, T.F. (2011). Liver X Receptors in Atherosclerosis and Inflammation. *Circ Res* 108, 996-1001.

Janabi, M., Yamashita, S., Hirano, K., Sakai, N., Hiraoka, H., Matsumoto, K., Zhang, Z., Nozaki, S., and Matsuzawa, Y. (2000). Oxidized Ldl-Induced Nf-Kappa B Activation and Subsequent Expression of Proinflammatory Genes Are Defective in Monocyte-Derived Macrophages from Cd36-Deficient Patients. *Arterioscler Thromb Vasc Biol* 20, 1953-1960.

Kannan, Y., Sundaram, K., Aluganti Narasimhulu, C., Parthasarathy, S., and Wewers, M.D. (2012). Oxidatively Modified Low Density Lipoprotein (Ldl) Inhibits Tlr2 and Tlr4 Cytokine Responses in Human Monocytes but Not in Macrophages. *J Biol Chem* 287, 23479-23488.

Lee, C.H., Olson, P., and Evans, R.M. (2003). Minireview: Lipid Metabolism, Metabolic Diseases, and Peroxisome Proliferator-Activated Receptors. *Endocrinology* 144, 2201-2207.

Li, A.C., Binder, C.J., Gutierrez, A., Brown, K.K., Plotkin, C.R., Pattison, J.W., Villedor, A.F., Davis, R.A., Willson, T.M., Witztum, J.L., *et al.* (2004). Differential Inhibition of Macrophage Foam-Cell Formation and Atherosclerosis in Mice by Ppar α , Beta/Delta, and Gamma. *J Clin Invest* 114, 1564-1576.

Li, Y., Schwabe, R.F., DeVries-Seimon, T., Yao, P.M., Gerbod-Giannone, M.C., Tall, A.R., Davis, R.J., Flavell, R., Brenner, D.A., and Tabas, I. (2005). Free Cholesterol-

Loaded Macrophages Are an Abundant Source of Tumor Necrosis Factor-Alpha and Interleukin-6: Model of Nf-Kappab- and Map Kinase-Dependent Inflammation in Advanced Atherosclerosis. *J Biol Chem* 280, 21763-21772.

Libby, P., Ridker, P.M., and Hansson, G.K. (2011). Progress and Challenges in Translating the Biology of Atherosclerosis. *Nature* 473, 317-325.

Maxfield, F.R., and Tabas, I. (2005). Role of Cholesterol and Lipid Organization in Disease. *Nature* 438, 612-621.

Michelsen, K.S., Wong, M.H., Shah, P.K., Zhang, W., Yano, J., Doherty, T.M., Akira, S., Rajavashisth, T.B., and Ardit, M. (2004). Lack of Toll-Like Receptor 4 or Myeloid Differentiation Factor 88 Reduces Atherosclerosis and Alters Plaque Phenotype in Mice Deficient in Apolipoprotein E. *Proc Natl Acad Sci U S A* 101, 10679-10684.

Moore, K.J., and Freeman, M.W. (2006). Scavenger Receptors in Atherosclerosis: Beyond Lipid Uptake. *Arterioscler Thromb Vasc Biol* 26, 1702-1711.

Moore, K.J., and Tabas, I. (2011). Macrophages in the Pathogenesis of Atherosclerosis. *Cell* 145, 341-355.

Mullick, A.E., Tobias, P.S., and Curtiss, L.K. (2005). Modulation of Atherosclerosis in Mice by Toll-Like Receptor 2. *J Clin Invest* 115, 3149-3156.

Nagy, L., Tontonoz, P., Alvarez, J.G., Chen, H., and Evans, R.M. (1998). Oxidized Ldl Regulates Macrophage Gene Expression through Ligand Activation of Ppargamma. *Cell* 93, 229-240.

Ogata, M., Tsujita, M., Hossain, M.A., Akita, N., Gonzalez, F.J., Staels, B., Suzuki, S., Fukutomi, T., Kimura, G., and Yokoyama, S. (2009). On the Mechanism for Ppar Agonists to Enhance Abca1 Gene Expression. *Atherosclerosis* 205, 413-419.

Oliver, W.R., Jr., Shenk, J.L., Snaith, M.R., Russell, C.S., Plunket, K.D., Bodkin, N.L., Lewis, M.C., Winegar, D.A., Sznajdman, M.L., Lambert, M.H., *et al.* (2001). A Selective Peroxisome Proliferator-Activated Receptor Delta Agonist Promotes Reverse Cholesterol Transport. *Proc Natl Acad Sci U S A* 98, 5306-5311.

Qiu, G., Ho, A.C., Yu, W., and Hill, J.S. (2007). Suppression of Endothelial or Lipoprotein Lipase in Thp-1 Macrophages Attenuates Proinflammatory Cytokine Secretion. *J Lipid Res* 48, 385-394.

Rodriguez-Calvo, R., Serrano, L., Coll, T., Moullan, N., Sanchez, R.M., Merlos, M., Palomer, X., Laguna, J.C., Michalik, L., Wahli, W., *et al.* (2008). Activation of Peroxisome Proliferator-Activated Receptor Beta/Delta Inhibits Lipopolysaccharide-Induced Cytokine Production in Adipocytes by Lowering Nuclear Factor-Kappab Activity Via Extracellular Signal-Related Kinase 1/2. *Diabetes* 57, 2149-2157.

Rong, J.X., Blachford, C., Feig, J.E., Bander, I., Mayne, J., Kusunoki, J., Miller, C., Davis, M., Wilson, M., Dehn, S., *et al.* (2013). Acat Inhibition Reduces the Progression of Preexisting, Advanced Atherosclerotic Mouse Lesions without Plaque or Systemic Toxicity. *Arterioscler Thromb Vasc Biol* 33, 4-12.

Rowe, A.H., Argmann, C.A., Edwards, J.Y., Sawyez, C.G., Morand, O.H., Hegele, R.A., and Huff, M.W. (2003). Enhanced Synthesis of the Oxysterol 24(S),25-Epoxycholesterol in Macrophages by Inhibitors of 2,3-Oxidosqualene:Lanosterol Cyclase: A Novel Mechanism for the Attenuation of Foam Cell Formation. *Circ Res* 93, 717-725.

Spann, N.J., Garmire, L.X., McDonald, J.G., Myers, D.S., Milne, S.B., Shibata, N., Reichart, D., Fox, J.N., Shaked, I., Heudobler, D., *et al.* (2012). Regulated Accumulation of Desmosterol Integrates Macrophage Lipid Metabolism and Inflammatory Responses. *Cell* 151, 138-152.

Steinberg, D. (2009). The Ldl Modification Hypothesis of Atherogenesis: An Update. *J Lipid Res* 50 *Suppl*, S376-381.

Steinberg, D., and Witztum, J.L. (2010). Oxidized Low-Density Lipoprotein and Atherosclerosis. *Arterioscler Thromb Vasc Biol* 30, 2311-2316.

Stewart, C.R., Stuart, L.M., Wilkinson, K., van Gils, J.M., Deng, J., Halle, A., Rayner, K.J., Boyer, L., Zhong, R., Frazier, W.A., *et al.* (2010). Cd36 Ligands Promote Sterile Inflammation through Assembly of a Toll-Like Receptor 4 and 6 Heterodimer. *Nat Immunol* 11, 155-161.

Straus, D.S., and Glass, C.K. (2007). Anti-Inflammatory Actions of Ppar Ligands: New Insights on Cellular and Molecular Mechanisms. *Trends Immunol* 28, 551-558.

Suzuki, M., Becker, L., Pritchard, D.K., Gharib, S.A., Wijsman, E.M., Bammler, T.K., Beyer, R.P., Vaisar, T., Oram, J.F., and Heinecke, J.W. (2012). Cholesterol Accumulation Regulates Expression of Macrophage Proteins Implicated in Proteolysis and Complement Activation. *Arterioscler Thromb Vasc Biol* 32, 2910-2918.

Tabas, I. (2010). The Role of Endoplasmic Reticulum Stress in the Progression of Atherosclerosis. *Circ Res* 107, 839-850.

Tarling, E.J., Bojanic, D.D., Tangirala, R.K., Wang, X., Lovgren-Sandblom, A., Lusis, A.J., Bjorkhem, I., and Edwards, P.A. (2010). Impaired Development of Atherosclerosis in *Abcg1*^{-/-} *Apoe*^{-/-} Mice: Identification of Specific Oxysterols That Both Accumulate in *Abcg1*^{-/-} *Apoe*^{-/-} Tissues and Induce Apoptosis. *Arterioscler Thromb Vasc Biol* 30, 1174-1180.

Vosper, H., Patel, L., Graham, T.L., Khoudoli, G.A., Hill, A., Macphee, C.H., Pinto, I., Smith, S.A., Suckling, K.E., Wolf, C.R., *et al.* (2001). The Peroxisome Proliferator-

Activated Receptor Delta Promotes Lipid Accumulation in Human Macrophages. *J Biol Chem* 276, 44258-44265.

Wallace, J.M., Schwarz, M., Coward, P., Houze, J., Sawyer, J.K., Kelley, K.L., Chai, A., and Rudel, L.L. (2005). Effects of Peroxisome Proliferator-Activated Receptor Alpha/Delta Agonists on Hdl-Cholesterol in Vervet Monkeys. *J Lipid Res* 46, 1009-1016.

Wang, W.Q., Moses, A.S., and Francis, G.A. (2001). Cholesterol Mobilization by Free and Lipid-Bound Apoai(Milano) and Apoai(Milano)-Apoaii Heterodimers. *Biochemistry* 40, 3666-3673.

Whitman, S.C., Miller, D.B., Wolfe, B.M., Hegele, R.A., and Huff, M.W. (1997). Uptake of Type Iii Hypertriglyceridemic Vldl by Macrophages Is Enhanced by Oxidation, Especially after Remnant Formation. *Arterioscler Thromb Vasc Biol* 17, 1707-1715.

Wiesner, P., Choi, S.H., Almazan, F., Benner, C., Huang, W., Diehl, C.J., Gonen, A., Butler, S., Witztum, J.L., Glass, C.K., *et al.* (2010). Low Doses of Lipopolysaccharide and Minimally Oxidized Low-Density Lipoprotein Cooperatively Activate Macrophages Via Nuclear Factor Kappa B and Activator Protein-1: Possible Mechanism for Acceleration of Atherosclerosis by Subclinical Endotoxemia. *Circ Res* 107, 56-65.

Yamauchi, Y., Chang, C.C., Hayashi, M., Abe-Dohmae, S., Reid, P.C., Chang, T.Y., and Yokoyama, S. (2004). Intracellular Cholesterol Mobilization Involved in the Abca1/Apolipoprotein-Mediated Assembly of High Density Lipoprotein in Fibroblasts. *J Lipid Res* 45, 1943-1951.

Yvan-Charvet, L., Ranalletta, M., Wang, N., Han, S., Terasaka, N., Li, R., Welch, C., and Tall, A.R. (2007). Combined Deficiency of Abca1 and Abcg1 Promotes Foam Cell Accumulation and Accelerates Atherosclerosis in Mice. *J Clin Invest* 117, 3900-3908.

Chapter 4*
PPAR δ agonist GW1516 attenuates diet-induced aortic inflammation, insulin resistance and atherosclerosis in *Ldlr*^{-/-} mice

4.1 INTRODUCTION

The principal cause of mortality in type 2 diabetic patients is atherosclerosis (Grundy et al., 2002, Libby et al., 2009), a chronic inflammatory disease that is the primary precursor underlying most cardiovascular events (Tabas et al., 2007). Although the molecular and pathophysiological links between type 2 diabetes and atherosclerosis are not fully understood, a crucial factor is likely insulin resistance (DeFronzo, 2010, Rewers et al., 2004). This is in part due to promotion of multiple independent risk factors associated with cardiovascular disease including obesity, hypertension and dyslipidemia (DeFronzo, 2010, Ginsberg, 2000). Atherogenic dyslipidemia associated with insulin resistance is characterized by increased plasma concentrations of triglyceride (TG)-rich very low-density lipoprotein (VLDL) and cholesteryl ester (CE)-rich LDL, both of which can permeate a compromised endothelium and initiate atherogenesis (Ginsberg, 2000, Tabas et al., 2010). Therapeutic strategies to reduce plasma LDL have proven effective in reducing cardiovascular events (Kearney et al., 2008). However, a significant unmet medical need persists in cardioprotective therapy, making VLDL-lowering strategies an attractive therapeutic target.

Subendothelial retention of atherogenic lipoproteins leads to a series of maladaptive immune responses, culminating in the development of macrophage foam cells (Tabas et al., 2010, Tabas et al., 2007). Macrophages of the arterial intima also play a critical role in the evolution of fatty streaks towards progression of complex lesions. In particular, M1 macrophages secrete inflammatory effector cytokines such as

*a version of this chapter has been submitted

interleukin (IL)-1 β and tumor necrosis factor alpha (TNF α), driven predominantly by MAPK and NF- κ B signaling (Moore and Tabas, 2011, Stollenwerk et al., 2005). However, insulin signaling, namely the Akt/forkhead box O1 (FoxO1) pathway, may also play an important role in atherogenic inflammation (Tabas et al., 2010). *In vitro*, *Il-1 β* is a FoxO1 target gene in macrophages with fatty acid-induced insulin resistance (Su et al., 2009). Although not consistent across all experimental models, a growing body of evidence suggests that *in vivo*, arterial insulin resistance directly promotes atherosclerosis (Tabas et al., 2010). In fat-fed apolipoprotein E knockout mice (*apoE*^{-/-}) mice, insulin receptor (IR) deletion (*Insr*^{-/-}) in myeloid cells decreased lesion size (Baumgartl et al., 2006). In contrast, global loss of the major insulin signaling mediator Akt1 in *apoE*^{-/-} mice resulted in accelerated coronary artery disease and aortic atherosclerosis, concomitant with significant aortic inflammation (Fernandez-Hernando et al., 2007). Hematopoietic deletion of the insulin receptor in LDL receptor knockout (*Ldlr*^{-/-}) mice significantly increased atherosclerosis, an effect attributed to impaired macrophage Akt signaling (Han et al., 2006). Furthermore, increased areas of apoptotic macrophages and necrotic core have been visualized in atherosclerotic lesions from patients with type 2 diabetes (Burke et al., 2004). Collectively, these studies highlight that arterial insulin resistance and inflammation may amplify atherogenesis.

Peroxisome proliferator-activated receptors (PPARs) are a class of ligand-dependant transcription factors involved in regulation of metabolic and inflammatory signaling (Wahli and Michalik, 2012). Three isoforms exist (α , γ , δ) which exhibit overlapping but distinct patterns of tissue distribution and function (Evans et al., 2004). Although PPAR δ has been considered the most enigmatic of the PPARs, this receptor has emerged as an important regulator of cellular lipid homeostasis and the inflammatory response (Barish et al., 2006). In cultured macrophages, PPAR δ inhibits

both macrophage lipid accumulation and pro-inflammatory cytokine expression in response to human VLDL (Chapter 2). Furthermore, TG accumulation was decreased via inhibition of extracellular lipolytic activity through angiopoietin-like (ANGPTL) 4-mediated inhibition of lipoprotein lipase (LPL) and enhanced carnitine palmitoyltransferase (CPT) 1 α -stimulated fatty acid β -oxidation, whereas attenuated cytokine expression was mediated through both inhibition of ERK1/2 and activation of Akt/FoxO1 signaling (Chapter 2). *In vivo*, Lee *et al.* demonstrated that macrophage deletion of *Ppar δ* in *Ldlr*^{-/-} mice paradoxically suppressed atherogenesis, attributed to the suppression of atherogenic inflammation by liberation of the inflammatory repressor protein BCL-6, as BCL-6 is normally sequestered by the PPAR δ /RXR co-repressor complex (Lee *et al.*, 2003). These studies elegantly highlighted that deletion of *Ppar δ* mimicked the liganded state of the receptor, suggesting that ligand-activation may be atheroprotective. However, the studies that have examined the effects of synthetic PPAR δ agonists using prevention protocols in mouse models of atherosclerosis have produced a spectrum of results (Barish *et al.*, 2008, Graham *et al.*, 2005, Li *et al.*, 2004). In the first study, administration of the PPAR δ agonist GW0742 to male *Ldlr*^{-/-} mice on a high-fat, high cholesterol diet for 14 weeks had no effect on lesion size (Li *et al.*, 2004). In a second study, 16 weeks of treatment with GW0742 reduced lesion development in female *Ldlr*^{-/-} mice (Graham *et al.*, 2005), however, the doses used yielded serum drug levels 2-fold higher than the reported EC₅₀ values for murine PPAR α and PPAR γ (Barish *et al.*, 2008), raising the possibility that the atheroprotective effects of GW0742 were not PPAR δ -specific. In *Ldlr*^{-/-} mice fed a high-fat diet, low doses of GW0742, prevented the development of angiotensin II-accelerated atherosclerosis (Takata *et al.*, 2008). Barish *et al.* reported that a next generation PPAR δ agonist (GW1516) at PPAR δ -specific doses, prevented the development of atherosclerosis in *apoE*^{-/-} mice fed a high-fat diet,

concomitant with reduced aortic inflammatory cytokine expression (Barish et al., 2008). Although on balance these studies indicate that PPAR δ -specific agonists prevent the development of atherosclerosis and arterial inflammation, it is unknown whether PPAR δ agonists are atheroprotective in an intervention model with pre-established insulin resistance. Furthermore, the impact of PPAR δ activation on lesion pathology, as well as aortic inflammatory signaling cascades, insulin resistance and ER-stress has not been examined.

In the present study we use C57BL/6J *Ldlr*^{-/-} mice fed a high-fat, cholesterol containing (HFHC) diet, a model of diet-induced dyslipidemia and insulin resistance. We demonstrate that following an induction phase, intervention with the addition of the PPAR δ -specific agonist GW1516 to the HFHC diet resulted in regression of metabolic dysregulation including reduced plasma lipids, glucose and insulin, and improved glucose and insulin tolerance. Intervention with GW1516 inhibited aortic MAPK and NF- κ B signaling, attenuated aortic inflammation, improved indices of aortic insulin signaling, reduced aortic ER-stress, and collectively attenuated the progression of pre-established atherosclerosis.

4.2 MATERIALS AND METHODS

4.2.1 ANIMALS AND DIETS

Male *Ldlr*^{-/-} mice on the C57BL/6 background were obtained from the Jackson Laboratory and housed in pairs in standard cages at 23°C. The animals were cared for in accordance with the Canadian Guide for the Care and Use of Laboratory Animals, and all experimental procedures were approved by the Animal Care Committee at the University of Western Ontario. Mice 10-12 weeks of age were fed *ad libitum*, a purified rodent chow diet (14% of calories from fat, Harlan Teklad TD8604, Madison WI) for 12 weeks. Another group of mice were fed a high-fat cholesterol-containing western diet (HFHC - 42% of calories from fat, 0.2% cholesterol, Harlan Teklad TD09268) for 4 weeks, followed by segregation of half of these mice to intervention to the HFHC with 3mg/kg/day GW1516 (Enzo Life Sciences, Ann Arbor, MI) for an additional 8 weeks. In previously published reports, this dose administered by oral gavage rendered a plasma concentration of GW1516 that was more selective for PPAR δ over PPAR α or PPAR γ by >1,000-fold (Barish et al., 2008, Barroso et al., 2011, Narkar et al., 2008). Animals were fasted for 4h prior to analyses or sacrifice. For fasting/re-feeding studies, animals were either fasted for 16h prior to sacrifice or fasted for 16h followed by 2h of acute re-feeding of experimental diets prior to sacrifice (Lu et al., 2012). Blood samples were obtained and the heart and aorta were excised as previously described (Covey et al., 2003, Mulvihill et al., 2009, Mulvihill et al., 2010).

4.2.2 PLASMA LIPID, BLOOD GLUCOSE AND PLASMA INSULIN DETERMINATIONS

Plasma TG, total cholesterol (TC), non-esterified fatty acids (NEFA), and blood glucose were determined as previously described (Mulvihill et al., 2009). Plasma insulin concentrations were determined by ELISA (Alpco Diagnostics, Salem, NH) on EDTA-

plasma as per manufacturer's instructions. Fast Performance Liquid Chromatography (FPLC) was performed on unfrozen EDTA-plasma using an AKTA purifier and Superose 6 column (Mulvihill et al., 2009).

4.2.3 GLUCOSE TOLERANCE AND INSULIN TOLERANCE

A glucose tolerance test (GTT) was performed following *i.p.* injection with 15% glucose in 0.9% NaCl (1 g/kg of body weight). Blood for glucose measurements (Ascensia Elite glucometer, Bayer Healthcare, Toronto, Canada) was taken up to 120 min post-injection. Insulin tolerance test (ITT) was conducted by *i.p.* injection with 0.6 IU/kg Novolin ge Toronto (Novo Nordisk, Cooksville, ON). Blood for glucose measurements was obtained up to 60 min post-injection. Insulin sensitivity and glucose utilization were calculated based on the area under the curve (AUC).

4.2.4 TISSUE HISTOLOGY AND IMMUNOHISTOCHEMISTRY

Histological and morphometric analyses were performed as described previously (Mulvihill et al., 2010). Briefly, at sacrifice, hearts were mounted in OCT and frozen. For quantitation of lesion area in the aortic sinus, oil red-O-stained sections were measured. Frozen serial sections (70-100 per heart, 10 μ m) of the aortic sinus, initiating at the origin of the aortic valves, were prepared using a Leica CM 3050S cryostat. Slides were stained with modified Verhoff's and Masson's trichrome at the Robarts Research Institute Molecular Pathology Core facility. Immunohistochemistry staining for macrophages by MOMA-2 (Accurate Chemical and Scientific Corporation #MCA519G, Westbury, NY) and smooth muscle α -actin (monoclonal anti- α -smooth muscle actin, Clone 1AH, Sigma) was performed. Briefly, slides were fixed in acetone and blocked in 2% bovine serum albumin. After incubation with primary antibody, a goat biotinylated secondary antibody was used. Slides were then incubated in peroxidase blocking reagent, followed by incubation with the ABC reagent (ABC Elite Standard Kit, Vector

Laboratories, Burlington, ON). Slides were then exposed to the DAB substrate (Peroxidase substrate kit, Vector Laboratories) followed by counterstain in hematoxylin and mounting in xylene. Photomicrographs were obtained using an Olympus BX50 microscope and a QImaging Retiga EXi FAST camera. In the aortic sinus, lesion area of four serial sections (100 μ m apart) were quantified using Axiovision computer software. Morphometric analysis of plaques in mice from each dietary group was also performed on serial sections. The relative area of the atherosclerotic plaque positive for MOMA-2, collagen or smooth muscle α -actin staining was determined as the area of positive staining divided by the area of the respective plaque. Quantitation was determined using Axiovision software. To ensure that a standard region was measured in each mouse, lesion analysis began at the origin of the aortic valves.

4.2.5 IMMUNOBLOTTING AND DENSITOMETRY

Total cell lysates were isolated from full-length aortae of mice as previously described (Beyea et al., 2007, Rowe et al., 2003). Proteins were separated by SDS-PAGE, transferred to polyvinylidene difluoride membranes and immunoblotted (Rowe et al., 2003). Lysates were probed using antibodies against mouse phospho and total Akt, FoxO1, ERK1/2, p38, IKK α , and I κ B α , as well as GRP78, CHOP, SHP-1 and β -actin (Cell Signaling, Danvers, MA). Protein levels were determined by densitometry as described (Beyea et al., 2007, Rowe et al., 2003).

4.2.6 QUANTITATIVE REAL-TIME PCR GENE ABUNDANCE ANALYSIS

Total RNA was isolated from full-length aortae of mice via standard TRIzol[®] reagent (Life Technologies, Burlington, ON) as per manufacturer's instructions. Specific mRNA abundances (*Ccl3*, *Il1b*, *Icam1*, *Tnf*, *Il6*, *Ccl2*, *Arg1*, *iNos*, *Ptpn6*, *Trib3*, *Adfp*, *Angptl4*, *Cpt1a*, *Acox*, *Lpl*, *Rgs4*, *Rgs5*, and *Gapdh*) were measured via quantitative real-time PCR (qRT-PCR) using an ABI Prism (7900HT) Sequence Detection System

(Applied Biosystems, Foster City, CA) as previously described (Beyea et al., 2012, Mulvihill et al., 2009).

4.2.7 STATISTICAL ANALYSES

Data are expressed as means \pm SEM. One-way ANOVA followed by the Bonferroni test was used to determine significant differences between two groups. One-way ANOVA followed by pair-wise comparisons by the Tukey's test was used to determine differences between three or more groups. For fasting/re-feeding experiments, two-way ANOVA followed by pair-wise comparisons by the Tukey's test was used to determine differences and interactions between diet groups and fasted/re-fed state. Significance thresholds were *P* values less than 0.05 and indicated by different upper case or lower case letters as well as asterisks as indicated in the figure legends.

4.3 RESULTS

4.3.1 GW1516 IMPROVES HFHC-INDUCED METABOLIC DYSREGULATION IN *LDLR*^{-/-} MICE

Male C57BL/6 *Ldlr*^{-/-} mice were administered a Western diet with 0.2% cholesterol (HFHC diet) for 4 weeks. The metabolic effects of intervention with the PPAR δ agonist GW1516 were evaluated following an additional 8 weeks (Figure 4.1A). Addition of GW1516 to the HFHC diet significantly attenuated HFHC-induced weight gain without affecting caloric intake (Figure 4.2A,B). GW1516 decreased fasting plasma cholesterol, TG and NEFAs compared to 4-week baseline levels, whereas the dyslipidemia of animals remaining on the HFHC diet alone continued to progress (Figure 4.1B). FPLC analyses demonstrated that reduced fasting plasma cholesterol in GW1516-treated mice, was due to a significant reduction in the VLDL-C fraction and a modest but not statistically significant reduction in LDL-C (Figure 4.1C). GW1516 increased HDL-C by 35% (Figure 4.1C). Furthermore, the GW1516-mediated reduction in plasma TG levels was due to a substantial 63% reduction in VLDL-TG (Figure 4.1D). GW1516 intervention decreased epididymal fat mass by 11% compared to 4-week baseline, and by 35% compared to mice remaining on the HFHC diet alone (Figure 4.2C) thus contributing to the attenuation in the rate of weight gain.

GW1516-intervention maintained blood glucose and significantly decreased plasma insulin compared to levels in HFHC-fed mice at 4-weeks. Relative to mice remaining on the HFHC diet, GW1516 intervention completely prevented the significant increase in fasting blood glucose and markedly attenuated the induction of fasting hyperinsulinemia (Figure 4.3A,B). In addition, GW1516 intervention improved whole body insulin sensitivity, as evidenced by improved glucose and insulin tolerance tests (Figure 4.3 C,D).

Figure 4.1: GW1516 regresses diet-induced dyslipidemia.

Ldlr^{-/-} mice were fed standard chow, or a high-fat, high-cholesterol diet (HFHC) for 4 weeks. For a subsequent 8 weeks, chow-fed mice remained on chow; the HFHC-fed mice either remained on HFHC alone or HFHC supplemented with GW501516 (GW1516) (3mg/kg/day). **A**, Experimental timeline for all studies performed. **B**, Plasma cholesterol, triglyceride, and non-esterified fatty acid (NEFA) concentrations were measured at week 0, 4 and 12 (8-12/group). **C and D**, Plasma was subjected to FPLC analysis at week 12, and cholesterol and triglyceride were measured in the eluted fractions (n=3-5/group). Arrows indicate time of GW1516 intervention. Data is presented as mean +/- SEM. Different letters indicate significant differences; ANOVA with post-hoc Tukey's test ($P<0.05$). * indicates significant difference versus HFHC at the end of the study; ANOVA with post hoc Bonferroni's test ($P<0.05$).

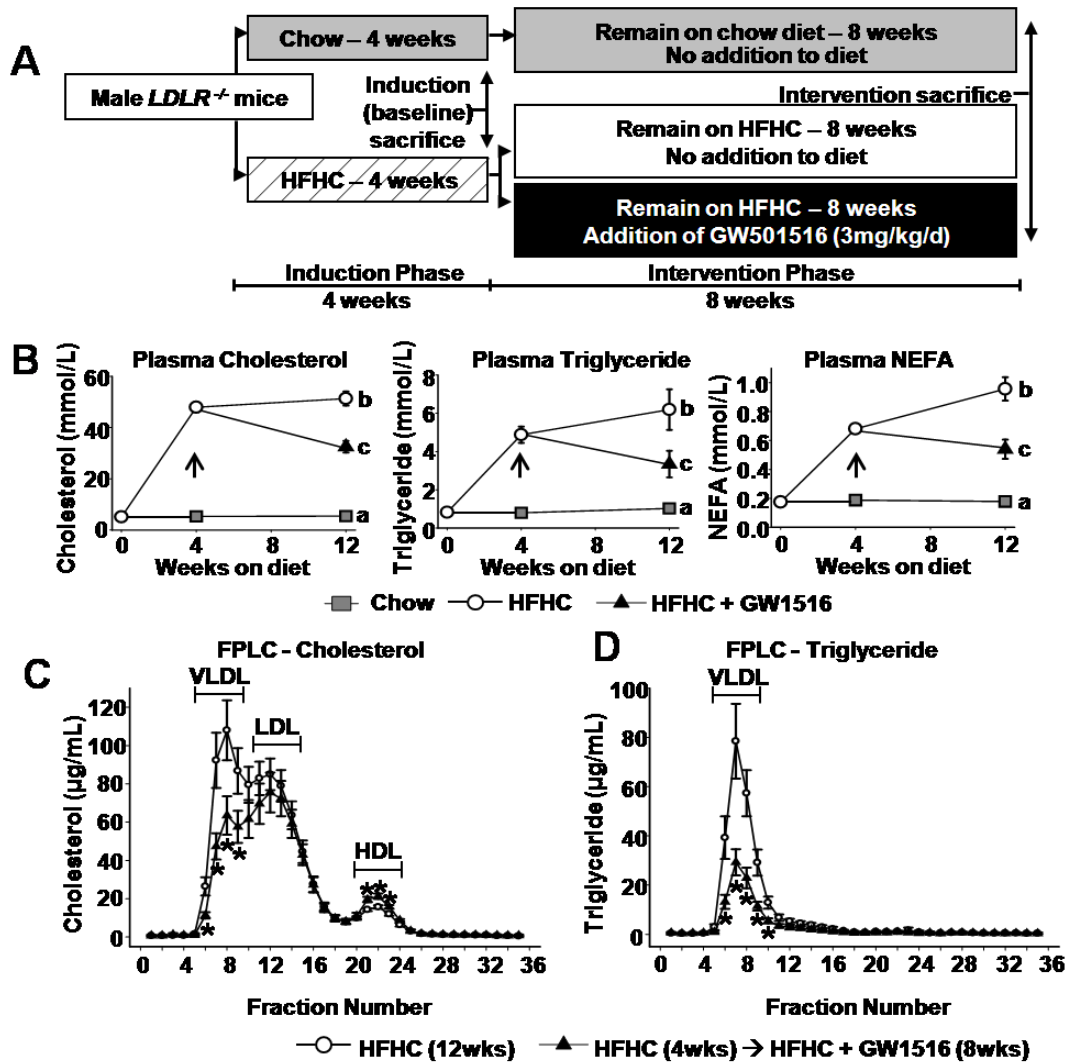


Figure 4.2: GW1516-treatment attenuates rate of body weight gain and epididymal fat mass. *Ldlr*^{-/-} mice were fed a standard lab chow, or a high-fat, high-cholesterol diet (HFHC) for 4 weeks. For a subsequent 8 weeks, chow-fed mice remained on chow; the HFHC-fed mice either remained on HFHC alone or HFHC supplemented with GW501516 (GW1516) (3mg/kg/day). **A**, Body weight. Arrow indicates time of GW1516 intervention. **B**, Caloric intake expressed as kcal per gram body weight per day of study. **C**, Epididymal fat mass in grams. Data is presented as mean +/- SEM (n=8-12/group). Different letters indicate significant differences; ANOVA with post-hoc Tukey's test ($P < 0.05$).

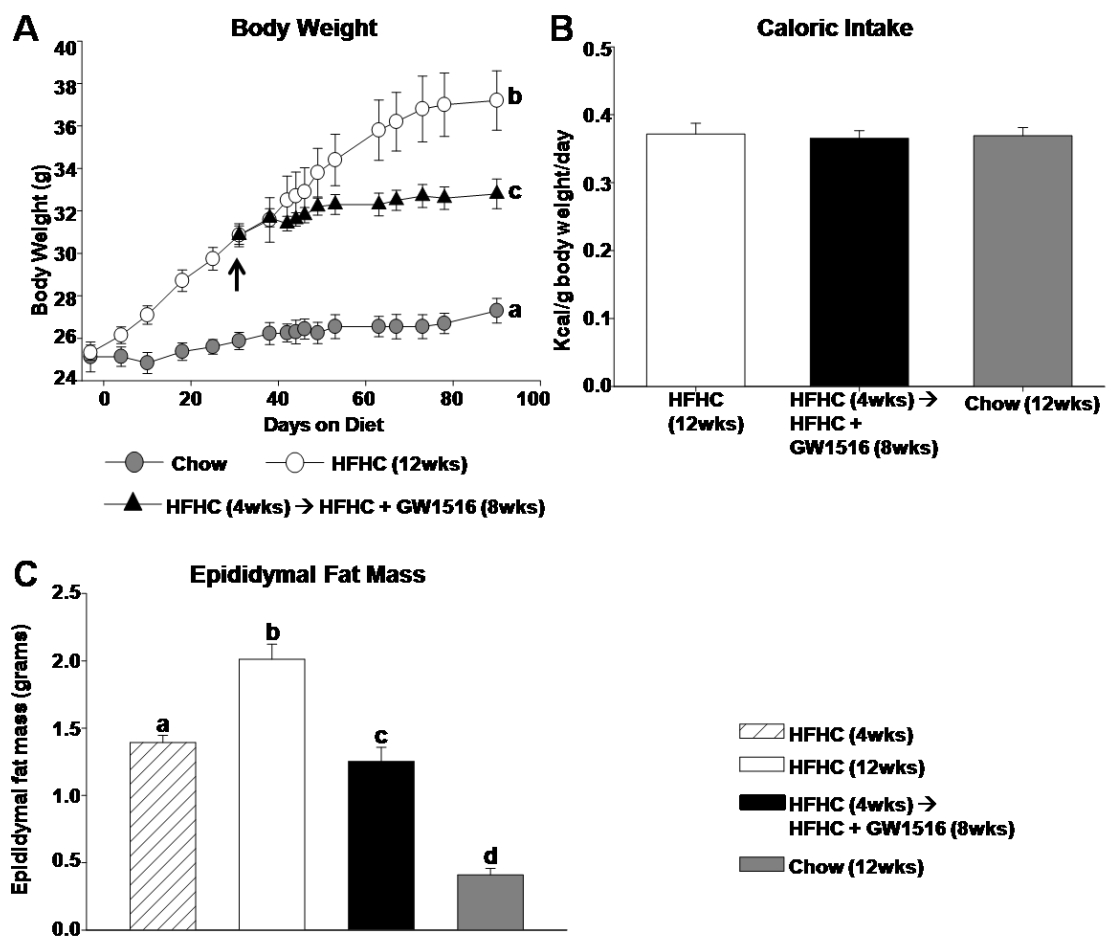
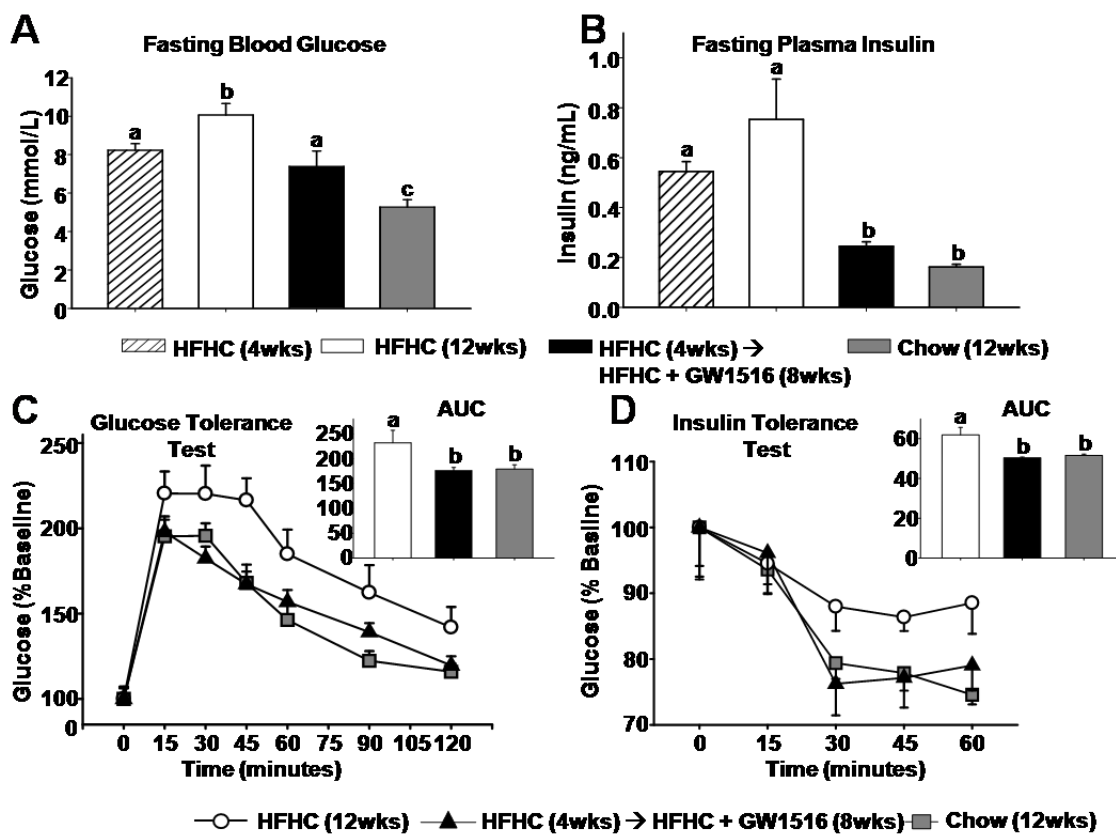


Figure 4.3: GW1516 improves diet-induced dysregulation of metabolic indices.

Ldlr^{-/-} mice were fed standard chow, or a high-fat, high-cholesterol diet (HFHC) for 4 weeks. For a subsequent 8 weeks, chow-fed mice remained on chow; the HFHC-fed mice either remained on HFHC alone or HFHC supplemented with GW501516 (GW1516) (3mg/kg/day). **A**, Fasting blood glucose levels. **B**, Fasting plasma insulin concentrations. **C**, Intraperitoneal glucose tolerance test at 12 weeks. **Inset graph**, absolute area under the curve (glucose mmol/Lx120min). **D**, Intraperitoneal insulin tolerance test at 12 weeks. **Inset graph**, absolute AUC (glucose mmol/Lx60min). Data is presented as mean +/- SEM (n=8-12/group). Different letters indicate significant differences; $P < 0.05$.



4.3.2 GW1516 ATTENUATES AORTIC SINUS ATHEROSCLEROSIS AND AORTIC INFLAMMATION IN HFHC-FED *LDLR*^{-/-} MICE

Examination of aortic sinus atherosclerosis revealed that oil red-O stained lesion area of HFHC-fed mice at 4 weeks progressed significantly (~6-fold) over the subsequent 8 weeks (Figure 4.4). In contrast, although lesion area continued to increase, the area was significantly attenuated in the GW1516-intervention cohort by ~33% compared to animals remaining on the HFHC diet alone (Figure 4.4). Dietary GW1516 influenced lesion composition. As a percent of total area, lesions of HFHC-fed animals for either 4- or 12-weeks displayed infiltration of MOMA-2-positive macrophages, which was significantly attenuated by intervention with GW1516 (Figure 4.4). No appreciable smooth muscle cell (SMC) infiltration or collagen deposition was observed in lesions of HFHC-fed mice at 4 weeks (Figure 4.4). However, smooth muscle α -actin occupied 40% of lesion area in HFHC-mice at 12 weeks, which was similar to that of GW1516-intervention mice. On the other hand, 12 weeks of the HFHC diet resulted in collagen deposition comprising 25% of lesion area, which was further increased (to 35%) in GW1516 intervention mice, despite no further effect on percent lesion SMC content (Figure 4.4). Lipid analyses of full-length aortae from HFHC-fed mice at 12 weeks revealed that aortic TG and TC mass increased 1.4-fold and 1.6-fold, compared to HFHC-mice at 4 weeks (Figure 4.5A,B). GW1516 supplementation decreased aortic TG by 60% compared to the 12-week HFHC-fed cohort, and by 40% compared to the 4-week HFHC-fed mice. GW1516 supplementation decreased aortic TC by 27% compared to HFHC-mice at 12 weeks, but values remained elevated (30%) compared to HFHC-mice at 4 weeks. Collectively, these analyses indicate that intervention to the HFHC diet with GW1516, results in the attenuation of lesion progression and the development of smaller, more stable atherosclerotic lesions.

Figure 4.4: GW1516 attenuates HFHC-induced atherosclerosis.

A, Representative examples are given for oil red-O and Hematoxylin, MOMA-2, SM α -actin and Trichrome stained aortic sinus sections. **B**, Quantitation of Oil-red-O, MOMA-2, collagen and SM α -actin stained areas expressed as lesion area or % of lesion area (n=6-9/group). SM α -actin and collagen were undetectable in 4-week baseline aortic sinus sections. Data is presented as mean +/- SEM. Different letters indicate significant differences; ANOVA with post-hoc Tukey's test ($P < 0.05$).

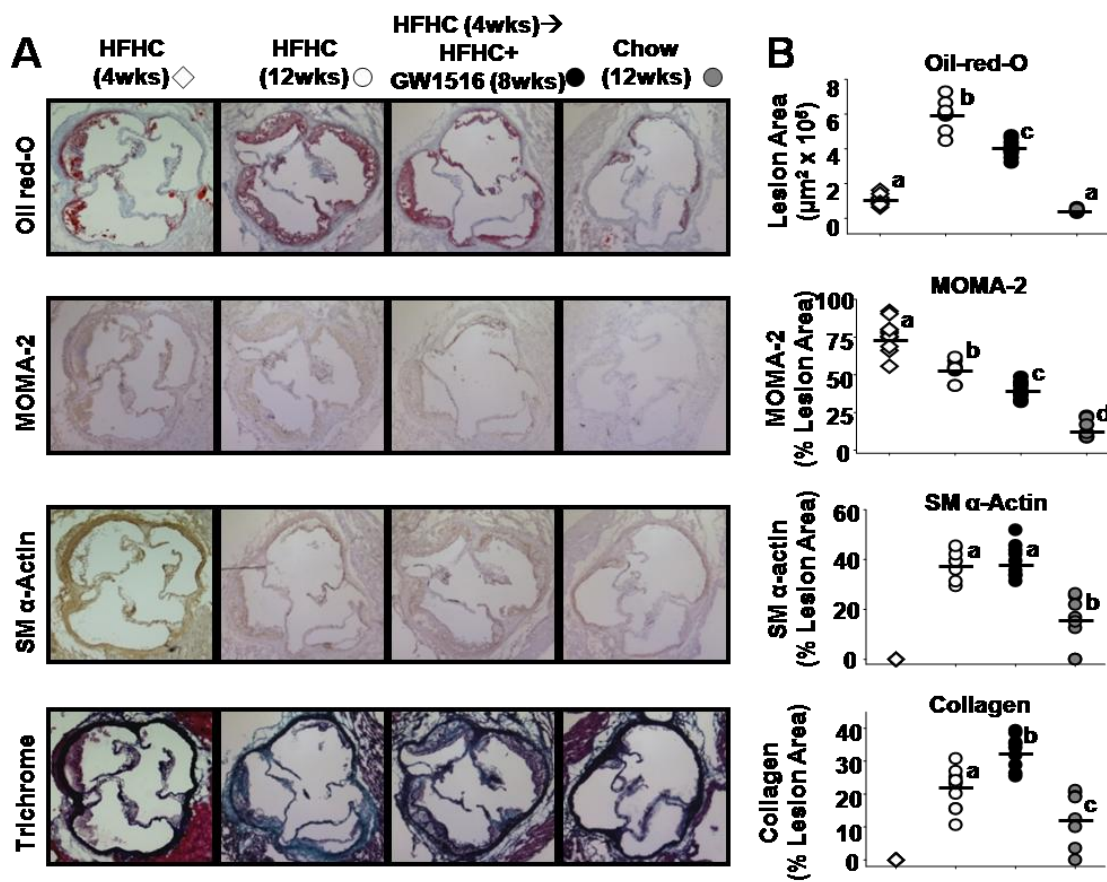
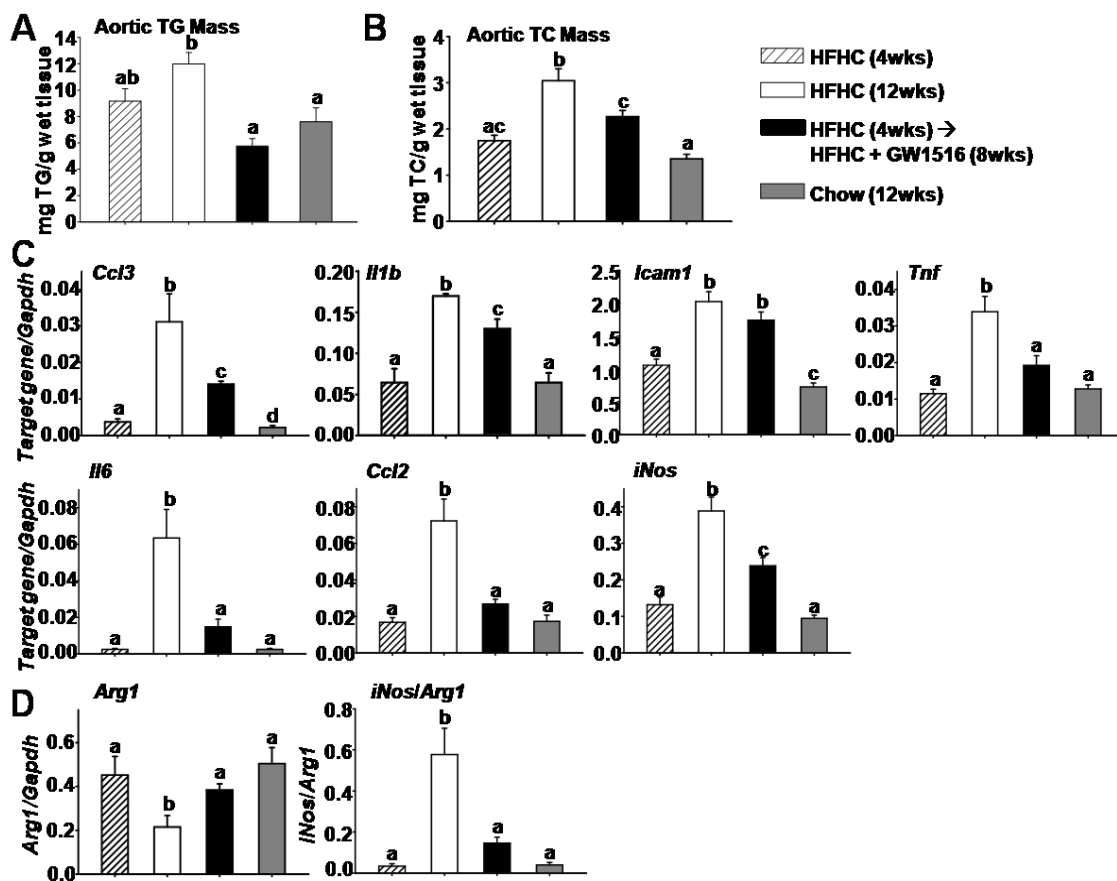


Figure 4.5: GW1516 attenuates lipid accumulation, M1 macrophage markers and induces a shift towards M2 macrophage markers in full length aortae.

A, Triglyceride (TG) and **(B)** cholesterol (TC) concentrations were determined in aortic extracts (n=5-7/group). **C**, mRNA abundance of the indicated proinflammatory M1 cytokines and **(D)** the anti-inflammatory M2 cytokine *Arg1* and the *Arg1/iNos* ratio, determined in full length aortae dissected free of fat and connective tissue (n=4-6/group). Data is presented as mean +/- SEM. Different letters indicate significant differences; ANOVA with post-hoc Tukey's test ($P < 0.05$).



To further assess disease progression, we examined a panel of cytokines known to modulate atherogenesis. In the full length aorta, following 4 weeks of HFHC feeding, only *Ccl3* and *Icam1* expression were increased compared to chow-fed controls, indicative of monocyte recruitment without overt inflammation (Figure 4.5C). However, expression of pro-inflammatory M1 cytokines, *Ccl3*, *Il1b*, *Icam1*, *Tnf*, *Il6*, and *Ccl2* were markedly induced (2-to 25-fold) in the aortae of mice fed the HFHC diet for 12 weeks. In contrast, although all cytokines were elevated in GW1516-treated mice compared to HFHC-fed mice at baseline (4 weeks), cytokine expression was significantly lower (-25 to -85%, mean -60%) compared to HFHC-fed mice at 12 weeks (Figure 4.5C). Although lesion MOMA-2 stained macrophages decreased ~25% in GW1516-treated mice, the greater reduction in cytokine expression suggests that macrophages remaining in lesions of the intervention mice were less inflammatory. Furthermore, 12 week HFHC-feeding significantly increased aortic expression of the M1 marker *iNos* and suppressed aortic expression of the anti-inflammatory M2 marker *Arg1*, resulting in a greatly exacerbated *iNos/Arg1* ratio, compared to HFHC-fed mice at 4 weeks (Figure 4.5C,D). GW1516 intervention completely reversed this expression pattern. Together, these data suggest that although lesion macrophage content is lower (Figure 4.4), there is a shift from M1 to M2 cytokine expression in aortae from PPAR δ -agonist treated mice.

We examined the cell signaling cascades known to regulate the macrophage inflammatory response (Moore and Tabas, 2011, Stollenwerk et al., 2005). Significant activation of MAP kinases ERK1/2 and p38 was observed in full-length aortae of HFHC-fed mice at 12 weeks, compared to chow-fed controls (Figure 4.6A). In addition, we observed a marked induction of NF- κ B activation in HFHC-mice at 12 weeks, as demonstrated by increased phospho-IKK and phospho-I κ B α (Figure 4.6B). In contrast, intervention with GW1516 abrogated HFHC-induced activation of both MAPK and NF- κ B

Figure 4.6: GW1516 corrects aberrant MAPK and NF- κ B signaling in full-length aortae of HFHC-fed mice.

A, Immunoblots of MAPK signaling markers including pERK1/2 and p-p38 and **(B)** NF- κ B signaling markers pIKK and I κ B α in full length aortae dissected free of fat and connective tissue. Representative immunoblots of aortic lysates from two mice from each treatment group with quantitations of 4-6 mice/group are shown. Data is presented as mean \pm SEM. Different letters indicate significant differences; ANOVA with post-hoc Tukey's test ($P < 0.05$). Representative bands are from the same immunoblot, cut from different regions due to loading of multiple replicate lanes.

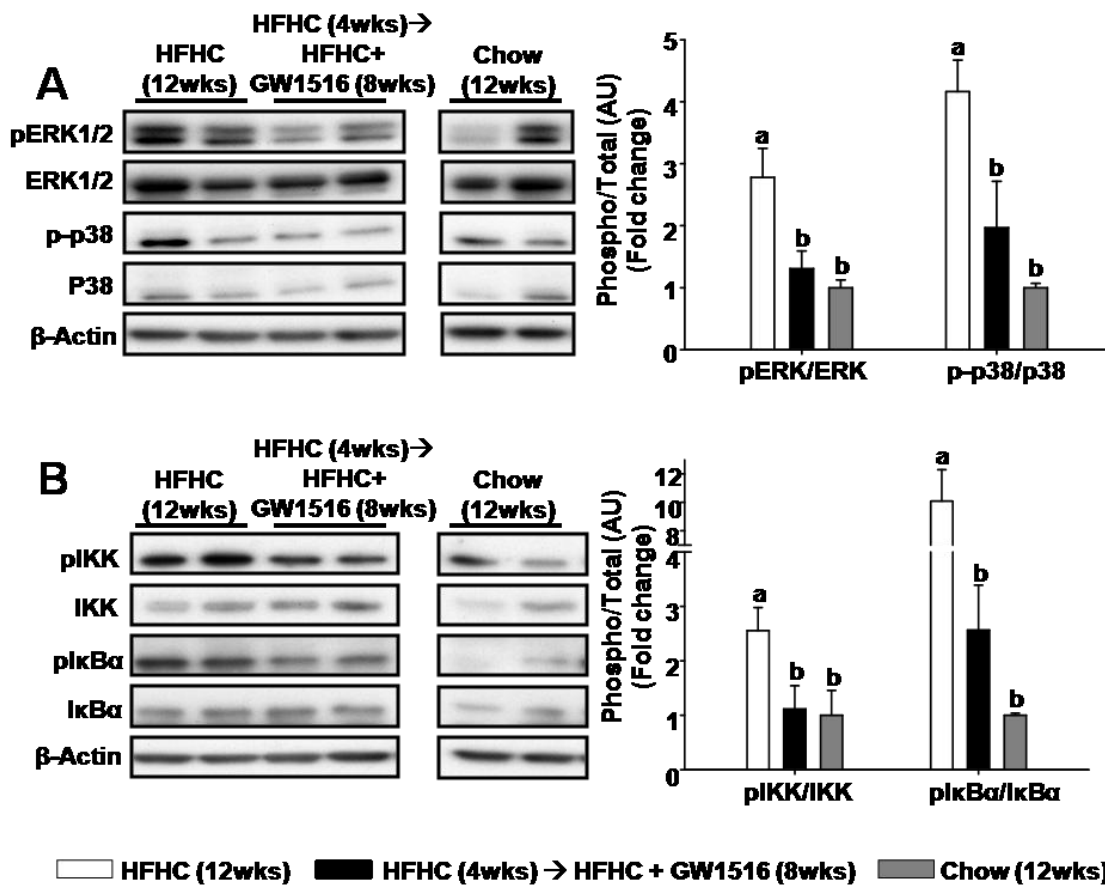


(Figure 4.6A,B). These results suggest that PPAR δ activation diminishes aortic inflammation, in part, by attenuating diet-induced inflammatory signaling.

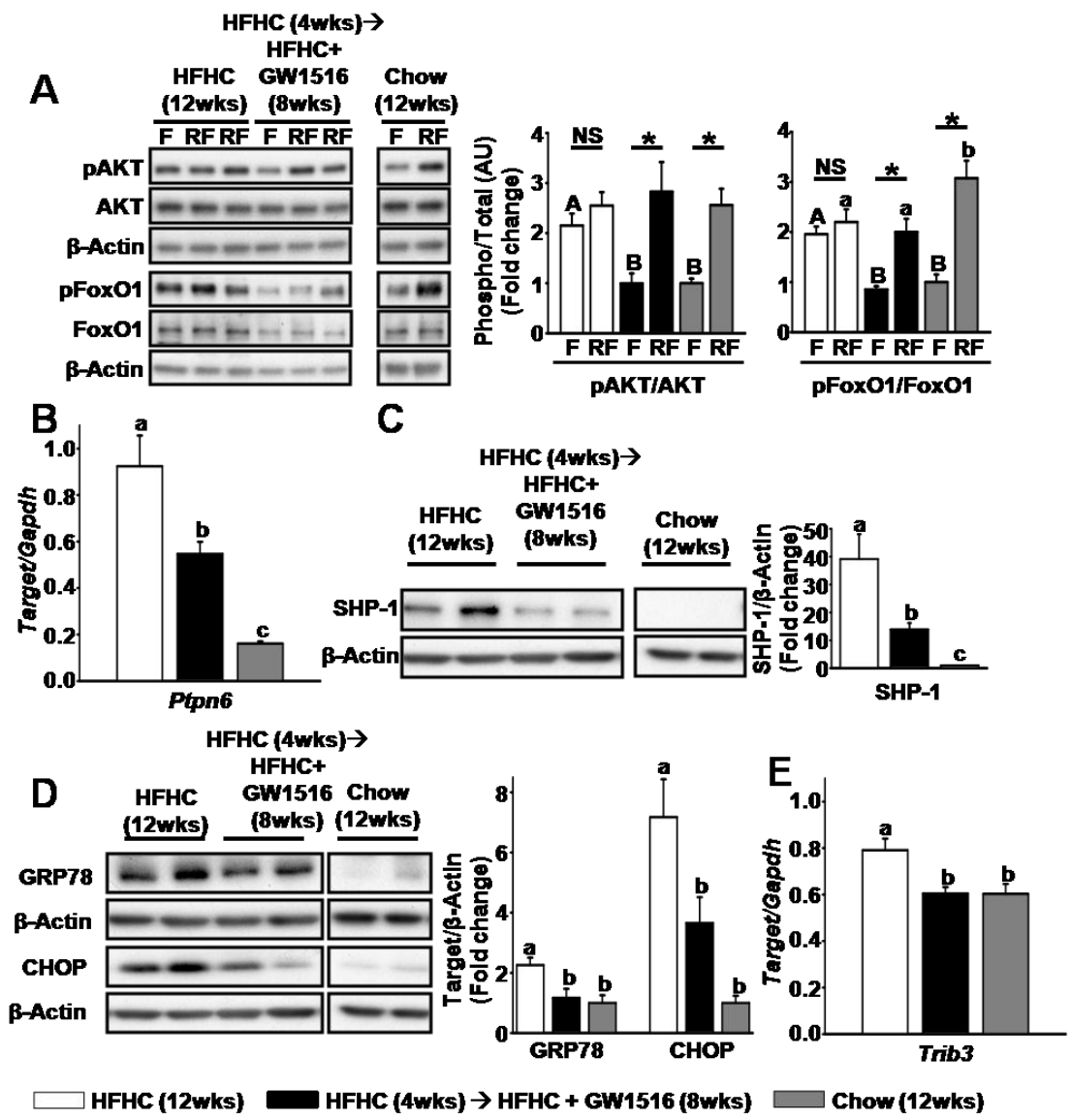
4.3.3 GW1516-INTERVENTION CORRECTS DIET-INDUCED AORTIC INSULIN SIGNALING AND ER-STRESS, AND EXERTS PPAR δ -SPECIFIC VESSEL WALL EFFECTS

Genetic manipulations resulting in impaired insulin signaling in hematopoietic cells exacerbate atherosclerosis, due in part to increased aortic inflammation and ER-stress (Fernandez-Hernando et al., 2007, Han et al., 2006, Tabas et al., 2010). Given the pro-inflammatory phenotype of aortae isolated from insulin-resistant HFHC-fed mice, we hypothesized that this was mediated in part by impaired aortic insulin signaling. To test this, we examined aortic phospho-Akt and phospho-FoxO1 in fasted and acutely re-fed mice at the end of the 8-week intervention phase. Compared to chow-fed mice, Akt and FoxO1 phosphorylation was higher in the aortae excised from fasted HFHC-fed mice, and not further increased in response to re-feeding (Figure 4.7A). In contrast, GW1516-intervention restored the fasting-to-feeding dynamic regulation of Akt and FoxO1 phosphorylation to chow-fed controls (Figure 4.7A). The Src homology 2 domain-containing phosphatase (SHP)-1 is a protein tyrosine phosphatase (PTP) primarily expressed by hematopoietic cells, and is a known negative regulator of hepatic insulin signaling (Dubois et al., 2006). We observed that aortae excised from HFHC-fed mice at 12 weeks were significantly enriched for the SHP-1 transcript (*Ptpn6*) and SHP-1 protein, 5- and 30-fold, respectively, both of which were strongly attenuated by intervention with GW1516 (Figure 4.7B,C).

Coupled to dysregulated aortic insulin signaling was a significant increase in ER-stress markers GRP78 and CHOP (Figure 4.7D). The known CHOP-target gene and negative regulator of insulin signaling, *Trib3* (Du et al., 2003), was elevated in aortae of

Figure 4.7: GW1516 corrects aberrant insulin signaling, the UPR and ER-stress in aortae of HFHC-fed mice.

Western blotting or qRT-PCR were performed on full length aortae dissected free of fat and connective tissue. **A**, Immunoblots of insulin signaling proteins phosphorylated (p) AKT and pFoxO1 in aortae excised from mice fasted for 16h (designated F) and fasted for 16h followed by a 2h re-feeding period (designated RF) (n=6-8/group). **B**, mRNA abundance of negative regulator of insulin signaling *Ptpn6* (n=4-6/group). **C**, Immunoblots of SHP-1 (the protein product of *Ptpn6*) (n=4-6/group). **D**, ER-stress markers GRP78 and CHOP (n=4-6/group). **E**, mRNA abundance of negative regulator of insulin signaling *Trib3* (n=4-6/group). Data is presented as mean +/- SEM. Representative immunoblots with quantitations shown. For **A**, different upper case letters indicate statistical significance among fasted animals, different lower case letters indicate statistical significance among re-fed animals, and asterisk (*) indicates statistical significance between fasted and re-fed within the same diet ($P < 0.05$); two-way ANOVA with post-hoc Tukey's test ($P < 0.05$). For **B-E** different letters indicate significant differences; one-way ANOVA with post-hoc Tukey's test ($P < 0.05$). Representative bands are from the same immunoblot, cut from different regions due to loading of multiple replicate lanes.

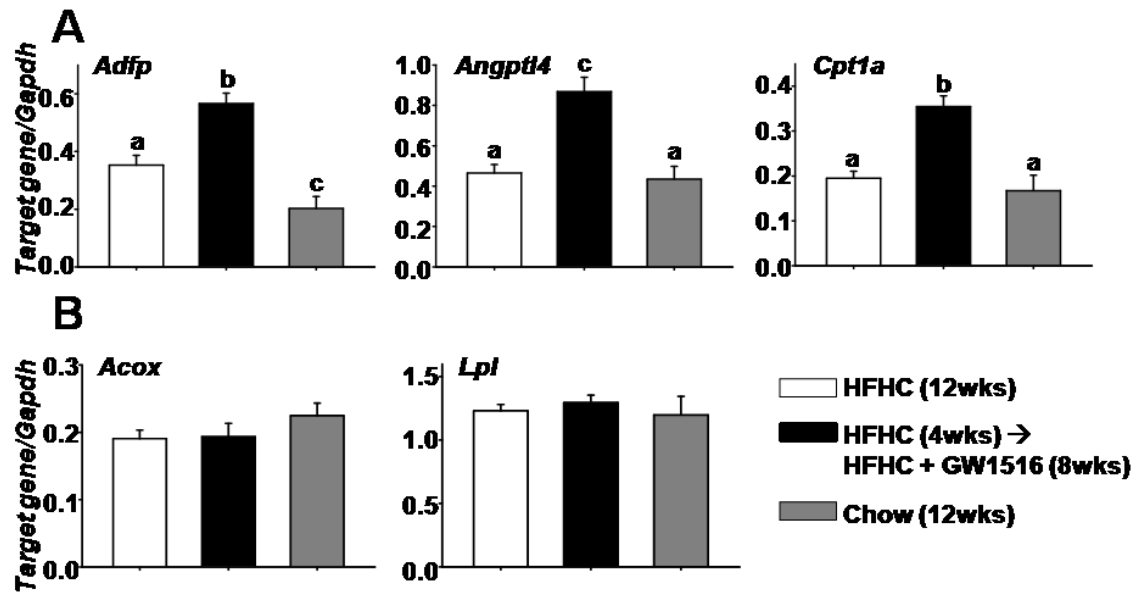


HFHC-fed 12 week mice (Figure 4.7E). GW1516 intervention attenuated GRP78, CHOP and *Trib3* to levels observed in 12-week chow-fed controls (Figure 4.7D,E).

To determine whether GW1516 exerted effects directly at the level of the aorta, we examined aortic expression of known PPAR δ target genes. Expression of *Adfp*, *Angptl4* and *Cpt1a* was significantly increased in aortae of GW1516-treated mice compared to HFHC-fed mice or chow-fed controls at 12 weeks (Figure 4.8A). Expression of the PPAR α - and PPAR γ -specific target genes (*Acox* and *Lpl*, respectively) were unaffected by GW1516-treatment (Figure 4.8B). Similar results were observed in liver (Chapter 5, Figure 5.1). These results suggest that GW1516 exerts a direct effect on the arterial wall, which likely contributes to the attenuation of inflammation, insulin resistance, ER-stress and diet-induced lesion progression. These results further indicate that with respect to PPARs, the aortic effects of GW1516 are PPAR δ -specific.

Figure 4.8: GW1516 activates aortic PPAR δ but not PPAR α or PPAR γ .

A, mRNA abundance of PPAR δ -target genes *Aadp*, *Angtpl4* and *Cpt1a* and **B**, PPAR α - and PPAR γ -target genes *Acox* and *Lpl*, respectively in full length aortae dissected free of fat and connective tissue (n=4-6/group). Data is presented as mean \pm SEM. Different letters indicate significant differences; ANOVA with post-hoc Tukey's test ($P < 0.05$).



4.4 DISCUSSION

Risk of atherosclerotic cardiovascular disease is elevated up to 4-fold in adults with type 2 diabetes (Fox et al., 2007, Fox et al., 2004). Despite this, therapeutic strategies to alleviate atherosclerosis associated with insulin resistant syndromes have remained sparse. Reports have speculated that PPAR δ agonists may confer atheroprotection in settings of insulin resistance (Coll et al., 2010). The present study is the first to demonstrate that intervention with a synthetic PPAR δ agonist in the context of diet-induced dyslipidemia and insulin resistance attenuates progression of early stage lesions to more complex lesions. Furthermore, we show that in HFHC-fed mice, the inflammatory response and insulin signaling within the aorta are impaired, which are completely reversed by PPAR δ activation.

Atherogenic dyslipidemia in the setting of insulin resistance is characterized by elevated plasma VLDL and LDL, concomitant with reduced plasma HDL (Ginsberg, 2000, Grundy, 2004). Statins are the current standard of therapy and effectively lower plasma LDL concentrations, reducing the relative risk of cardiovascular disease by ~30% (Bays et al., 2011, Kearney et al., 2008). However, statins do not fully correct other features of atherosclerosis risk, namely elevated plasma VLDL, decreased HDL, insulin resistance, and body fat composition, resulting in a substantial unmet therapeutic need (Sattar et al., 2010). The present study demonstrates that intervention with a synthetic PPAR δ agonist to a HFHC diet corrects previously established metabolic disturbances. Although plasma LDL was modestly reduced, our results suggest that PPAR δ activation primarily targets plasma VLDL and HDL. This is consistent with recent human studies demonstrating that synthetic PPAR δ agonists correct mixed dyslipidemia in patients with the metabolic syndrome (Bays et al., 2011, Ooi et al., 2011). The present study

contributes to the plausibility of PPAR δ agonists as therapeutic agents for metabolic dysregulation associated with insulin resistance.

We recently demonstrated in cultured macrophages that PPAR δ activation attenuates VLDL-induced triglyceride accumulation and pro-inflammatory cytokine expression (Chapter 2). We extend these *in vitro* findings, demonstrating that intervention with GW1516-treatment induces regression of aortic TG content associated with significant induction of the PPAR δ -target genes *Angptl4* and *Cpt1a*. These results suggest that GW1516 may stimulate aortic fatty acid β -oxidation and inhibit aortic lipoprotein lipase activity, thus contributing to reduced atherogenesis. We provide evidence that inflammatory cells within the aortae of HFHC-fed animals were polarized to the classically activated pro-inflammatory M1 phenotype (Goerdts et al., 1999, Mills et al., 2000). Furthermore, intervention with GW1516 resulted in polarization towards the anti-inflammatory M2 state (Gordon, 2003), consistent with reports demonstrating that alternative M2 activation of adipose tissue macrophages and hepatic Kupffer cells is, in part, mediated by PPAR δ (Kang et al., 2008, Odegaard et al., 2008). M2 macrophages are thought to contribute to tissue remodelling and repair (Gordon, 2003), and are increased in lesions undergoing regression (Feig et al., 2011). Although GW1516 did not induce regression of early lesions, the M2 phenotype was associated with significant slowing of lesion progression. Longer-term studies would be required to assess whether PPAR δ agonists can induce regression of more complex lesions. Nevertheless, the present study demonstrates the ability of PPAR δ activation to alleviate aortic lipid accumulation and inflammation, thus contributing to attenuated lesion development.

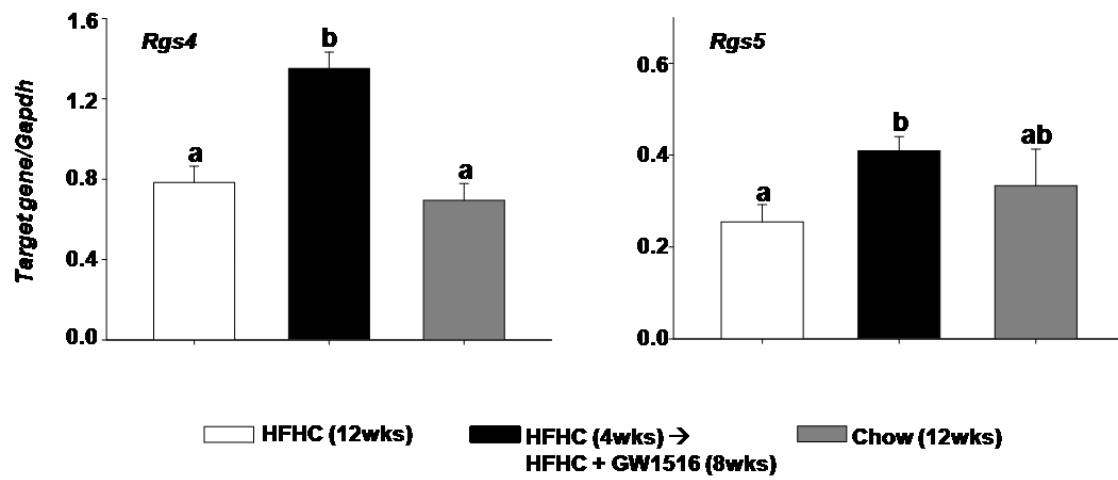
That GW1516 increased lesion collagen deposition without altering lesion SMC content is possibly due to PPAR δ activation having a direct effect on plaque SMCs, enhancing their capacity to synthesize and deposit extracellular matrix. This hypothesis

is consistent with a report that PPAR δ activation in cultured vascular (v) SMCs inhibits IL-1 β -induced matrix metalloproteinase (MMP)-2 and MMP-9 expression (Kim et al., 2010). Although reduced lipid deposition in VSMCs restores their capacity to synthesize extracellular matrix (Beyea et al., 2012, Frontini et al., 2009), the ability of PPAR δ agonists to improve VSMC function in response to a lipid load requires further study.

The MAPK and NF- κ B signaling pathways are critical regulators of inflammatory cytokine expression (Moore and Tabas, 2011, Stollenwerk et al., 2005). In the aortae of HFHC-fed animals, we observed marked activation of both of these cascades. Intervention with GW1516 almost completely normalized both MAPK and NF- κ B activation. In cardiac myocytes, the PPAR δ agonist GW0742 has been shown to attenuate lipopolysaccharide-induced NF- κ B activation through increased I κ B expression, thereby inhibiting nuclear translocation of NF- κ B (Ding et al., 2006). We did not observe any appreciable changes in total aortic I κ B protein. Thus, the mechanism by which PPAR δ inhibits NF- κ B activation in the context of aortic inflammation remains to be determined. With respect to MAPK activation, GW0742 inhibited angiotensin II-induced phosphorylation of ERK1/2 and p38 in mouse macrophages, via upregulation of *Rgs4* and *Rgs5* (Takata et al., 2008). Consistent with this report, we observed a significant upregulation of both *Rgs4* and *Rgs5* in aortae of GW1516-treated animals compared to aortae from HFHC-fed mice (Figure 4.9). Taken together, these results suggest that PPAR δ activation in the aorta attenuates inflammatory signaling, leading to the attenuation of aortic inflammatory cytokine expression.

Impaired insulin signaling in the vasculature has recently emerged as a major contributor to lesion progression (Tabas et al., 2010). *Ldlr*^{-/-} mice receiving *Insr*^{-/-} bone marrow developed larger more complex lesions, attributed to enhanced ER-stress and apoptosis-induced necrotic core formation (Han et al., 2006). Insulin-resistant

Figure 4.9: GW1516 stimulates aortic expression of regulators of G-protein coupled receptor signaling *Rgs4* and *Rgs5*. *Ldlr*^{-/-} mice were fed a standard lab chow, or a high-fat, high-cholesterol diet (HFHC) for 4 weeks. For a subsequent 8 weeks, chow-fed mice remained on chow; the HFHC-fed mice either remained on HFHC alone or HFHC supplemented with GW501516 (GW1516) (3mg/kg/day). Mice were fasted for 4h prior to sacrifice. Analyses were performed on samples of full length aortae dissected free of fat and connective tissue. The indicated cytokines were measured by qRT-PCR. Target genes were normalized to *Gapdh*. Expression relative to chow depicted for each cytokine as mean +/- SEM (n=4-6/group). Different letters indicate significant differences; ANOVA with post-hoc Tukey's test ($P < 0.05$).



macrophages with cholesterol-induced ER-stress display impaired Akt phosphorylation, increased nuclear FoxO1 activity and enhanced apoptosis (Senokuchi et al., 2008). In addition to macrophages, aberrant insulin signaling in vascular endothelial cells can also play a role in atherogenesis, as deletion of three *Foxo* isoforms in these cells resulted in atheroprotection, attributed in part to an anti-inflammatory effect (Tsuchiya et al., 2012). Although these proof-of-concept gene-deletion models highlight the significance of vascular insulin signaling in atherogenesis, these studies do not identify whether insulin signaling becomes dysregulated during lesion development (Bornfeldt and Tabas, 2011). Here we demonstrate that mice with diet-induced atherosclerosis exhibit impaired aortic insulin signaling, as evidenced by the loss of dynamic fasting-to-feeding regulation of both Akt and FoxO1 phosphorylation, coupled to a marked induction of negative regulators of insulin signaling, SHP-1 and *Trib3* (Du et al., 2003, Dubois et al., 2006). Our data suggests that the loss of insulin regulation of both Akt and FoxO1 results in FoxO1 target genes such as *I1b* (Su et al., 2009), to be chronically transcribed, rather than dynamically regulated during states of fasting and re-feeding. We propose that this mechanism contributes to the accumulation of pro-inflammatory mediators in the vessel wall, inducing a state of chronic low-grade inflammation. Moreover, this impairment of aortic insulin signaling is correlated with significant elevations in ER-stress markers CHOP and GRP78. We further demonstrate that activation of PPAR δ restores dynamic insulin signaling responses within the aorta and attenuates ER-stress. It is important to note that the presence of arterial insulin resistance did not impair the ability of GW1516 to attenuate pre-established lesion progression. Thus, although difficult to quantify, it remains possible that improved insulin signaling within GW1516-treated aortae contributes to protection from lesion progression.

In this study, a major factor in the attenuation of lesion development by intervention with GW1516 is reduction of plasma lipids, particularly VLDL/IDL, thereby reducing the atherogenic stimulus. However, the data presented here clearly demonstrate that in the aorta, GW1516 stimulates PPAR δ -specific target genes, which are known to improve macrophage lipid homeostasis and attenuate the inflammatory response. Although these effects likely contribute to the observed reduction in atherosclerosis, further studies are required to elucidate the extent to which improved metabolic parameters, as compared to direct vessel wall effects contribute to PPAR δ -mediated atheroprotection. Nevertheless, the current study provides strong evidence that intervention to a HFHC diet with a PPAR δ agonist delays the HFHC diet-induced progression of early lesions. It will be important to determine if intervention by PPAR δ activation improves the pathology of more advanced lesions and whether extended treatment is able to achieve regression. We conclude that PPAR δ activation remains a viable therapeutic target for atherosclerosis prevention and treatment.

4.5 REFERENCES

Barish, G.D., Atkins, A.R., Downes, M., Olson, P., Chong, L.W., Nelson, M., Zou, Y., Hwang, H., Kang, H., Curtiss, L., *et al.* (2008). Ppar δ Regulates Multiple Proinflammatory Pathways to Suppress Atherosclerosis. *Proc Natl Acad Sci U S A* 105, 4271-4276.

Barish, G.D., Narkar, V.A., and Evans, R.M. (2006). Ppar Δ : A Dagger in the Heart of the Metabolic Syndrome. *J Clin Invest* 116, 590-597.

Barroso, E., Rodriguez-Calvo, R., Serrano-Marco, L., Astudillo, A.M., Balsinde, J., Palomer, X., and Vazquez-Carrera, M. (2011). The Ppar β /Delta Activator Gw501516 Prevents the Down-Regulation of Ampk Caused by a High-Fat Diet in Liver and Amplifies the Pgc-1 α -Lipin 1-Ppar α Pathway Leading to Increased Fatty Acid Oxidation. *Endocrinology* 152, 1848-1859.

Baumgartl, J., Baudler, S., Scherner, M., Babaev, V., Makowski, L., Suttles, J., McDuffie, M., Tobe, K., Kadowaki, T., Fazio, S., *et al.* (2006). Myeloid Lineage Cell-Restricted Insulin Resistance Protects Apolipoprotein-E-Deficient Mice against Atherosclerosis. *Cell Metab* 3, 247-256.

Bays, H.E., Schwartz, S., Littlejohn, T., 3rd, Kerzner, B., Krauss, R.M., Karpf, D.B., Choi, Y.J., Wang, X., Naim, S., and Roberts, B.K. (2011). Mbx-8025, a Novel Peroxisome Proliferator Receptor-Delta Agonist: Lipid and Other Metabolic Effects in Dyslipidemic Overweight Patients Treated with and without Atorvastatin. *J Clin Endocrinol Metab* 96, 2889-2897.

Beyea, M.M., Heslop, C.L., Sawyez, C.G., Edwards, J.Y., Markle, J.G., Hegele, R.A., and Huff, M.W. (2007). Selective up-Regulation of Lxr-Regulated Genes Abca1, Abcg1, and ApoE in Macrophages through Increased Endogenous Synthesis of 24(S),25-Epoxycholesterol. *J Biol Chem* 282, 5207-5216.

Beyea, M.M., Reaume, S., Sawyez, C.G., Edwards, J.Y., O'Neil, C., Hegele, R.A., Pickering, J.G., and Huff, M.W. (2012). The Oxysterol, 24(S), 25-Epoxycholesterol Attenuates Human Smooth Muscle-Derived Foam Cell Formation Via Reduced Ldl Uptake and Enhanced Cholesterol Efflux. *J Am Heart Assoc* 1, 4e000810.

Bornfeldt, K.E., and Tabas, I. (2011). Insulin Resistance, Hyperglycemia, and Atherosclerosis. *Cell Metab* 14, 575-585.

Burke, A.P., Kolodgie, F.D., Zieske, A., Fowler, D.R., Weber, D.K., Varghese, P.J., Farb, A., and Virmani, R. (2004). Morphologic Findings of Coronary Atherosclerotic Plaques in Diabetics: A Postmortem Study. *Arterioscler Thromb Vasc Biol* 24, 1266-1271.

Coll, T., Barroso, E., Alvarez-Guardia, D., Serrano, L., Salvado, L., Merlos, M., Palomer, X., and Vazquez-Carrera, M. (2010). The Role of Peroxisome Proliferator-Activated Receptor Beta/Delta on the Inflammatory Basis of Metabolic Disease. *PPAR Res* 2010.

Covey, S.D., Krieger, M., Wang, W., Penman, M., and Trigatti, B.L. (2003). Scavenger Receptor Class B Type I-Mediated Protection against Atherosclerosis in Ldl Receptor-Negative Mice Involves Its Expression in Bone Marrow-Derived Cells. *Arterioscler Thromb Vasc Biol* 23, 1589-1594.

DeFronzo, R.A. (2010). Insulin Resistance, Lipotoxicity, Type 2 Diabetes and Atherosclerosis: The Missing Links. The Claude Bernard Lecture 2009. *Diabetologia* 53, 1270-1287.

Ding, G., Cheng, L., Qin, Q., Frontin, S., and Yang, Q. (2006). Ppardelta Modulates Lipopolysaccharide-Induced Tnfalpha Inflammation Signaling in Cultured Cardiomyocytes. *J Mol Cell Cardiol* 40, 821-828.

Du, K., Herzig, S., Kulkarni, R.N., and Montminy, M. (2003). Trb3: A Tribbles Homolog That Inhibits Akt/Pkb Activation by Insulin in Liver. *Science* 300, 1574-1577.

Dubois, M.J., Bergeron, S., Kim, H.J., Dombrowski, L., Perreault, M., Fournes, B., Faure, R., Olivier, M., Beauchemin, N., Shulman, G.I., *et al.* (2006). The Shp-1 Protein Tyrosine Phosphatase Negatively Modulates Glucose Homeostasis. *Nat Med* 12, 549-556.

Evans, R.M., Barish, G.D., and Wang, Y.X. (2004). Ppars and the Complex Journey to Obesity. *Nat Med* 10, 355-361.

Feig, J.E., Parathath, S., Rong, J.X., Mick, S.L., Vengrenyuk, Y., Grauer, L., Young, S.G., and Fisher, E.A. (2011). Reversal of Hyperlipidemia with a Genetic Switch Favorably Affects the Content and Inflammatory State of Macrophages in Atherosclerotic Plaques. *Circulation* 123, 989-998.

Fernandez-Hernando, C., Ackah, E., Yu, J., Suarez, Y., Murata, T., Iwakiri, Y., Prendergast, J., Miao, R.Q., Birnbaum, M.J., and Sessa, W.C. (2007). Loss of Akt1 Leads to Severe Atherosclerosis and Occlusive Coronary Artery Disease. *Cell Metab* 6, 446-457.

Fox, C.S., Coady, S., Sorlie, P.D., D'Agostino, R.B., Sr., Pencina, M.J., Vasan, R.S., Meigs, J.B., Levy, D., and Savage, P.J. (2007). Increasing Cardiovascular Disease Burden Due to Diabetes Mellitus: The Framingham Heart Study. *Circulation* 115, 1544-1550.

Fox, C.S., Coady, S., Sorlie, P.D., Levy, D., Meigs, J.B., D'Agostino, R.B., Sr., Wilson, P.W., and Savage, P.J. (2004). Trends in Cardiovascular Complications of Diabetes. *JAMA* 292, 2495-2499.

Frontini, M.J., O'Neil, C., Sawyez, C., Chan, B.M., Huff, M.W., and Pickering, J.G. (2009). Lipid Incorporation Inhibits Src-Dependent Assembly of Fibronectin and Type I Collagen by Vascular Smooth Muscle Cells. *Circ Res* 104, 832-841.

Ginsberg, H.N. (2000). Insulin Resistance and Cardiovascular Disease. *J Clin Invest* 106, 453-458.

Goerdts, S., Politz, O., Schledzewski, K., Birk, R., Gratchev, A., Guillot, P., Hakiy, N., Klemke, C.D., Dippel, E., Kodolja, V., *et al.* (1999). Alternative Versus Classical Activation of Macrophages. *Pathobiology* 67, 222-226.

Gordon, S. (2003). Alternative Activation of Macrophages. *Nat Rev Immunol* 3, 23-35.

Graham, T.L., Mookherjee, C., Suckling, K.E., Palmer, C.N., and Patel, L. (2005). The Ppardelta Agonist Gw0742x Reduces Atherosclerosis in Ldlr(-/-) Mice. *Atherosclerosis* 181, 29-37.

Grundey, S.M. (2004). Obesity, Metabolic Syndrome, and Cardiovascular Disease. *J Clin Endocrinol Metab* 89, 2595-2600.

Grundey, S.M., Howard, B., Smith, S., Jr., Eckel, R., Redberg, R., and Bonow, R.O. (2002). Prevention Conference VI: Diabetes and Cardiovascular Disease: Executive Summary: Conference Proceeding for Healthcare Professionals from a Special Writing Group of the American Heart Association. *Circulation* 105, 2231-2239.

Han, S., Liang, C.P., DeVries-Seimon, T., Ranalletta, M., Welch, C.L., Collins-Fletcher, K., Accili, D., Tabas, I., and Tall, A.R. (2006). Macrophage Insulin Receptor Deficiency Increases ER Stress-Induced Apoptosis and Necrotic Core Formation in Advanced Atherosclerotic Lesions. *Cell Metab* 3, 257-266.

Kang, K., Reilly, S.M., Karabacak, V., Gangl, M.R., Fitzgerald, K., Hatano, B., and Lee, C.H. (2008). Adipocyte-Derived Th2 Cytokines and Myeloid Ppardelta Regulate Macrophage Polarization and Insulin Sensitivity. *Cell Metab* 7, 485-495.

Kearney, P.M., Blackwell, L., Collins, R., Keech, A., Simes, J., Peto, R., Armitage, J., and Baigent, C. (2008). Efficacy of Cholesterol-Lowering Therapy in 18,686 People with Diabetes in 14 Randomised Trials of Statins: A Meta-Analysis. *Lancet* 371, 117-125.

Kim, H.J., Kim, M.Y., Hwang, J.S., Kim, H.J., Lee, J.H., Chang, K.C., Kim, J.H., Han, C.W., Kim, J.H., and Seo, H.G. (2010). Ppardelta Inhibits IL-1beta-Stimulated

Proliferation and Migration of Vascular Smooth Muscle Cells Via up-Regulation of Il-1ra. *Cell Mol Life Sci* 67, 2119-2130.

Lee, C.H., Chawla, A., Urbiztondo, N., Liao, D., Boisvert, W.A., Evans, R.M., and Curtiss, L.K. (2003). Transcriptional Repression of Atherogenic Inflammation: Modulation by Ppardelta. *Science* 302, 453-457.

Li, A.C., Binder, C.J., Gutierrez, A., Brown, K.K., Plotkin, C.R., Pattison, J.W., Valledor, A.F., Davis, R.A., Willson, T.M., Witztum, J.L., *et al.* (2004). Differential Inhibition of Macrophage Foam-Cell Formation and Atherosclerosis in Mice by Pparalpha, Beta/Delta, and Gamma. *J Clin Invest* 114, 1564-1576.

Libby, P., Ridker, P.M., and Hansson, G.K. (2009). Inflammation in Atherosclerosis: From Pathophysiology to Practice. *J Am Coll Cardiol* 54, 2129-2138.

Lu, M., Wan, M., Leavens, K.F., Chu, Q., Monks, B.R., Fernandez, S., Ahima, R.S., Ueki, K., Kahn, C.R., and Birnbaum, M.J. (2012). Insulin Regulates Liver Metabolism in Vivo in the Absence of Hepatic Akt and Foxo1. *Nat Med* 18, 388-395.

Mills, C.D., Kincaid, K., Alt, J.M., Heilman, M.J., and Hill, A.M. (2000). M-1/M-2 Macrophages and the Th1/Th2 Paradigm. *J Immunol* 164, 6166-6173.

Moore, K.J., and Tabas, I. (2011). Macrophages in the Pathogenesis of Atherosclerosis. *Cell* 145, 341-355.

Mulvihill, E.E., Allister, E.M., Sutherland, B.G., Telford, D.E., Sawyez, C.G., Edwards, J.Y., Markle, J.M., Hegele, R.A., and Huff, M.W. (2009). Naringenin Prevents Dyslipidemia, Apolipoprotein B Overproduction, and Hyperinsulinemia in Ldl Receptor-Null Mice with Diet-Induced Insulin Resistance. *Diabetes* 58, 2198-2210.

Mulvihill, E.E., Assini, J.M., Sutherland, B.G., DiMattia, A.S., Khami, M., Koppes, J.B., Sawyez, C.G., Whitman, S.C., and Huff, M.W. (2010). Naringenin Decreases Progression of Atherosclerosis by Improving Dyslipidemia in High-Fat-Fed Low-Density Lipoprotein Receptor-Null Mice. *Arterioscler Thromb Vasc Biol* 30, 742-748.

Narkar, V.A., Downes, M., Yu, R.T., Emblar, E., Wang, Y.X., Banayo, E., Mihaylova, M.M., Nelson, M.C., Zou, Y., Juguilon, H., *et al.* (2008). Ampk and Ppardelta Agonists Are Exercise Mimetics. *Cell* 134, 405-415.

Odegaard, J.I., Ricardo-Gonzalez, R.R., Red Eagle, A., Vats, D., Morel, C.R., Goforth, M.H., Subramanian, V., Mukundan, L., Ferrante, A.W., and Chawla, A. (2008). Alternative M2 Activation of Kupffer Cells by Ppardelta Ameliorates Obesity-Induced Insulin Resistance. *Cell Metab* 7, 496-507.

Ooi, E.M., Watts, G.F., Sprecher, D.L., Chan, D.C., and Barrett, P.H. (2011). Mechanism of Action of a Peroxisome Proliferator-Activated Receptor (Ppar)-Delta Agonist on Lipoprotein Metabolism in Dyslipidemic Subjects with Central Obesity. *J Clin Endocrinol Metab* 96, E1568-1576.

Rewers, M., Zaccaro, D., D'Agostino, R., Haffner, S., Saad, M.F., Selby, J.V., Bergman, R., and Savage, P. (2004). Insulin Sensitivity, Insulinemia, and Coronary Artery Disease: The Insulin Resistance Atherosclerosis Study. *Diabetes Care* 27, 781-787.

Rowe, A.H., Argmann, C.A., Edwards, J.Y., Sawyez, C.G., Morand, O.H., Hegele, R.A., and Huff, M.W. (2003). Enhanced Synthesis of the Oxysterol 24(S),25-Epoxycholesterol in Macrophages by Inhibitors of 2,3-Oxidosqualene:Lanosterol Cyclase: A Novel Mechanism for the Attenuation of Foam Cell Formation. *Circ Res* 93, 717-725.

Sattar, N., Preiss, D., Murray, H.M., Welsh, P., Buckley, B.M., de Craen, A.J., Seshasai, S.R., McMurray, J.J., Freeman, D.J., Jukema, J.W., *et al.* (2010). Statins and Risk of Incident Diabetes: A Collaborative Meta-Analysis of Randomised Statin Trials. *Lancet* 375, 735-742.

Senokuchi, T., Liang, C.P., Seimon, T.A., Han, S., Matsumoto, M., Banks, A.S., Paik, J.H., DePinho, R.A., Accili, D., Tabas, I., *et al.* (2008). Forkhead Transcription Factors (Foxos) Promote Apoptosis of Insulin-Resistant Macrophages During Cholesterol-Induced Endoplasmic Reticulum Stress. *Diabetes* 57, 2967-2976.

Stollenwerk, M.M., Lindholm, M.W., Porn-Ares, M.I., Larsson, A., Nilsson, J., and Ares, M.P. (2005). Very Low-Density Lipoprotein Induces Interleukin-1beta Expression in Macrophages. *Biochem Biophys Res Commun* 335, 603-608.

Su, D., Coudriet, G.M., Hyun Kim, D., Lu, Y., Perdomo, G., Qu, S., Slusher, S., Tse, H.M., Piganelli, J., Giannoukakis, N., *et al.* (2009). Foxo1 Links Insulin Resistance to Proinflammatory Cytokine Il-1beta Production in Macrophages. *Diabetes* 58, 2624-2633.

Tabas, I., Tall, A., and Accili, D. (2010). The Impact of Macrophage Insulin Resistance on Advanced Atherosclerotic Plaque Progression. *Circ Res* 106, 58-67.

Tabas, I., Williams, K.J., and Boren, J. (2007). Subendothelial Lipoprotein Retention as the Initiating Process in Atherosclerosis: Update and Therapeutic Implications. *Circulation* 116, 1832-1844.

Takata, Y., Liu, J., Yin, F., Collins, A.R., Lyon, C.J., Lee, C.H., Atkins, A.R., Downes, M., Barish, G.D., Evans, R.M., *et al.* (2008). Ppardelta-Mediated Antiinflammatory Mechanisms Inhibit Angiotensin II-Accelerated Atherosclerosis. *Proc Natl Acad Sci U S A* 105, 4277-4282.

Tsuchiya, K., Tanaka, J., Shuiqing, Y., Welch, C.L., DePinho, R.A., Tabas, I., Tall, A.R., Goldberg, I.J., and Accili, D. (2012). Foxos Integrate Pleiotropic Actions of Insulin in Vascular Endothelium to Protect Mice from Atherosclerosis. *Cell Metab* 15, 372-381.

Wahli, W., and Michalik, L. (2012). Ppars at the Crossroads of Lipid Signaling and Inflammation. *Trends Endocrinol Metab* 23, 351-363.

Chapter 5*

PPAR δ -specific activation in liver attenuates triglyceride accumulation via enhanced fatty acid oxidation, reduced fatty acid synthesis and improved insulin sensitivity

5.1 INTRODUCTION

The prevalence of the metabolic syndrome has reached an epidemic proportion which has significantly increased the incidence of type 2 diabetes and atherosclerotic cardiovascular disease (Eckel et al., 2010). It represents a constellation of metabolic abnormalities that include obesity, hypertension, glucose intolerance and a dyslipidemia characterized by low plasma high-density lipoprotein (HDL) and high plasma very low-density lipoprotein (VLDL) (Eckel et al., 2010). Insulin resistance can explain most, if not all of the metabolic syndrome and is defined as the inability of the hormone to maintain blood glucose homeostasis (Eckel et al., 2010, Haas and Biddinger, 2009). During insulin resistance hepatic lipogenesis persists which promotes hepatic steatosis, dyslipidemia and consequently cardiovascular disease risk (DeFronzo, 2010). Despite the prevalence of insulin resistant conditions and their significant morbidity and mortality, few therapeutic strategies exist that effectively correct these metabolic disorders.

Hepatic steatosis, defined as excessive lipid accumulation in the liver, is a major clinical manifestation of insulin resistance observed in greater than 40% of patients with type 2 diabetes (Farese et al., 2012, Williamson et al., 2011). Although a causal relationship between hepatic steatosis and insulin resistance has been difficult to define (Farese et al., 2012), inflammation and endoplasmic reticulum (ER)-stress have been implicated as contributing factors to dysregulated hepatic insulin signaling (Hummasti and Hotamisligil, 2010, Ozcan et al., 2004). As a consequence, hyperinsulinemia-mediated lipogenesis ensues which contributes to ectopic lipid deposition (Brown and

*a version of this chapter has been submitted

Goldstein, 2008). At a molecular level, insulin binding to its cognate receptor leads to receptor-mediated tyrosine phosphorylation of IRS-1 and/or IRS-2, which in turn activates PI3-K to stimulate the phosphorylation and activation of Akt (Kido et al., 2001). Normally, the downstream consequences of insulin-stimulated Akt activation include suppression of hepatic gluconeogenesis due to phosphorylation and inactivation of forkhead box (Fox) O1, and promotion of *de novo* lipogenesis due to phosphorylation and activation of the mammalian target of rapamycin complex (mTORC1) (Li et al., 2010). However, in the insulin resistant liver, Akt loses its ability to effectively inactivate FoxO1, but paradoxically maintains its ability to activate mTORC1 (Li et al., 2010). Consequently, mTORC1-driven transcription of the master regulator of lipogenesis, sterol regulatory element binding protein (SREBP)-1c, remains chronically active. In addition, insulin increases the amount of proteolytically processed active SREBP-1c through mechanisms that remain poorly understood (Yecies et al., 2011). Coupled to hyperinsulinemia, these actions of insulin during hepatic insulin resistance lead to continuous activation of genes required for fatty acid synthesis, thus contributing to excessive hepatic lipid accumulation.

In addition to unregulated lipogenesis, decreased fatty acid oxidation often contributes to exacerbation of lipid content in the insulin resistant liver (Assini et al., 2013, Mulvihill et al., 2009, Mulvihill et al., 2011). The adenosine monophosphate-activated protein kinase (AMPK) is an evolutionarily conserved serine/threonine kinase that controls cellular and whole body energy metabolism (Dzamko and Steinberg, 2009, Fullerton et al., 2013). Specifically, hepatic AMPK is a pivotal regulator of fat oxidation and lipogenesis, primarily via direct phosphorylation and inhibition of acetyl-CoA carboxylase (ACC) (Fullerton et al., 2013, Kemp et al., 2003). Biochemically, this reduces malonyl CoA levels in the liver which (1) depletes fatty acid synthase (FAS) of substrate in the lipogenic pathway and (2) results in the de-repression of CPT1 α in the

fatty acid oxidation pathway (Carlson and Kim, 1973, Saggerson, 2008). Thus, activation of AMPK represents a potential mechanism for the attenuation of hepatic steatosis.

Peroxisome proliferator-activated receptors (PPAR α , γ and δ) are a class of ligand-dependent transcription factors involved in regulation of glucose and lipid homeostasis (Evans et al., 2004). In contrast to PPAR α and PPAR γ , synthetic agonists for PPAR δ have yet to reach the clinical arena, despite a number of studies having highlighted a potential role for this receptor in the treatment of metabolic disease (Reilly and Lee, 2008). In mice, genetic manipulations of *Ppar δ* as well as prevention experiments involving administration of PPAR δ agonists have revealed that activation of this receptor attenuates dyslipidemia and hyperglycemia, improves whole-body insulin sensitivity and prevents diet-induced obesity (Lee et al., 2006, Tanaka et al., 2003, Wang et al., 2003).

With respect to PPAR δ and hepatic lipid metabolism in mice, there are seemingly conflicting and controversial reports. Supplementation of mice with the PPAR δ agonist GW1516 attenuated diet-induced hepatic steatosis; however the 2-fold increase in hepatic *Acox* expression suggested a PPAR α -dependent effect (Nagasawa et al., 2006). Tanaka et al. reported that increased expression of genes involved in hepatic fat oxidation resulted in reduced hepatic TG in high-fat fed mice treated with GW1516 (Tanaka et al., 2003). In *db/db* mice injected with adenoviral PPAR δ (*adPPAR δ*), liver TG content was reduced as a result of decreased SREBP-1c-mediated lipogenesis (Qin et al., 2008). Despite reports suggesting reduced hepatic steatosis, studies also demonstrated that PPAR δ activation exerts either no effect (Barroso et al., 2011), or induction of liver TG accumulation (Lee et al., 2006, Liu et al., 2011). In *db/db* mice, GW1516-treatment resulted in accrual of hepatic TG as a result of direct transcriptional activation of *ACC β* , and in turn, enhanced fatty acid synthesis (Lee et al., 2006). *adPPAR δ* gene delivery to *Ldlr*^{-/-} increased hepatic *de novo* lipogenesis and hepatic TG

(Liu et al., 2011). Of significance, none of these studies actually measured hepatic fatty acid oxidation.

That PPAR δ activation increases hepatic steatosis is counterintuitive since PPAR δ agonists are known to improve whole-body insulin sensitivity and lipid homeostasis, and stimulate Cpt1a-mediated fatty acid oxidation in a variety of cell types and tissues (Lee et al., 2006, Tanaka et al., 2003, Wang et al., 2003). Furthermore, in muscle, GW1516 stimulated fatty acid oxidation, in part, through increased AMPK activity (Kramer et al., 2007, Kramer et al., 2005). Additionally, in a model of hepatic steatosis, GW1516 prevented the diet induced inactivation of hepatic AMPK (Barroso et al., 2011). This suggests that AMPK activation by PPAR δ agonists has the ability to regulate hepatic β -oxidation and/or fatty acid synthesis.

The objective of this study was to determine whether intervention to a high-fat, cholesterol containing diet (HFHC) with a selective PPAR δ agonist can reverse hepatic steatosis. We demonstrate that GW1516 inhibited hepatic lipid deposition, a result of attenuated lipogenesis and increased fatty acid oxidation. Decreased fatty acid synthesis was due to GW1516-mediated correction of selective hepatic insulin resistance. We discovered that AMPK activation was required for the PPAR δ -mediated attenuation of *de novo* lipogenesis, but was not required for PPAR δ -mediated induction of fatty acid oxidation. The reduced liver TG content was coupled to attenuated hepatic inflammation and ER-stress.

5.2 MATERIALS AND METHODS

5.2.1 ANIMALS AND DIETS

Male *Ldlr*^{-/-} mice on the C57BL/6 background were obtained from the Jackson Laboratory and housed in pairs in standard cages at 23°C. The animals were cared for in accordance with the Canadian Guide for the Care and Use of Laboratory Animals, and all experimental procedures were approved by the Animal Care Committee at the University of Western Ontario. Mice 10-12 weeks of age (n=16) were fed *ad libitum*, a purified rodent chow diet (14% of calories from fat, Harlan Teklad TD8604, Madison WI) for 12 weeks. Another group of mice (10-12 weeks of age, n=48) were fed a high-fat cholesterol-containing western diet (HFHC - 42% of calories from fat, 0.2% cholesterol, Harlan Teklad TD09268) for 4 weeks. For the subsequent 8 weeks, half of these mice (n=24) remained on the HFHC diet, whereas the other half (n=24) were fed the HFHC diet supplemented with 3mg/kg/day GW1516 (Enzo Life Sciences, Ann Arbor, MI). In previously published reports, this dose administered by oral gavage produced plasma concentrations of GW1516 (106nmol/L) that was >1,000-fold more selective for PPAR δ , compared to PPAR α or PPAR γ (Barish et al., 2008, Barroso et al., 2011, Narkar et al., 2008). Animals were fasted for 4h prior to analyses or sacrifice. For fasting/re-feeding studies, animals were either fasted for 16h prior to sacrifice or fasted for 16h followed by a 2h acute re-feeding period of the experimental diets prior to sacrifice (Lu et al., 2012). Blood samples were obtained as previously described (Mulvihill et al., 2009, Mulvihill et al., 2010).

5.2.2 ACTIVATION OF AMPK *IN VIVO*

Activation of AMPK *in vivo* was assessed following intraperitoneal injection of GW1516 or A-769662. Analysis of respiratory exchange ratio (RER) was performed using the Oxymax Columbus Instruments Comprehensive Lab Animal Monitoring System (CLAMS) (Columbus Instruments, Columbus, OH); mice were acclimatized to

the system for 24hr prior to data collection. Animals were fasted overnight (15:00-07:00) to synchronize RER to ~ 0.7 , followed by a period of free access to food (experimental diets) and water at 07:00 for 2hrs to re-synchronize RER to ~ 1 . At 09:00, chow was removed and mice were injected with vehicle (5% dimethyl sulfoxide in phosphate-buffered saline), 3mg/kg GW1516 or 30mg/kg A-769662 (SelleckBio, Houston, TX), a synthetic activator of AMPK (Cool et al., 2006). Metabolic measurements were collected until 15:30. Carbohydrate ($4.58 \cdot \text{VCO}_2 - 3.23 \cdot \text{VO}_2$) and fat ($1.70 \cdot \text{VO}_2 - 1.69 \cdot \text{VCO}_2$) utilization were calculated as previously described (Hawley et al., 2012). Analyses of *in vivo* phosphorylation of AMPK and ACC were performed in liver samples isolated at sacrifice by freeze-clamp method 90min after injection of the respective treatment and stored at -80°C until analysis as described (Hawley et al., 2012).

5.2.3 ENERGY EXPENDITURE

In the induction/intervention studies, analyses of energy expenditure (EE) and (RER) was performed using the Oxymax Columbus Instruments CLAMS; mice were acclimatized to the system for 24hr prior to a 24hr data collection period.

5.2.4 PRIMARY MOUSE HEPATOCYTE ISOLATION, LIPOGENESIS AND FATTY ACID OXIDATION

Primary mouse hepatocytes were isolated from WT or AMPK $\beta 1^{-/-}$ C57Bl/6J mice by the collagenase perfusion method as described (Dzamko et al., 2010). Experiments were performed the day following hepatocyte isolation. For mRNA expression analyses hepatocytes were incubated with either vehicle, GW1516 or A-769662 (at the indicated concentrations) for 6hrs prior to lysis in TRIzol[®] reagent. For lipogenesis and fatty acid oxidation experiments, cells were washed with PBS and incubated in serum-free Medium 199 for 3hrs. Lipogenesis was assessed by incubating cells with serum-free Medium 199 containing [$1\text{-}^{14}\text{C}$]acetate (0.5 $\mu\text{Ci/ml}$) (Amersham Biosciences) and 0.5 mM unlabeled sodium acetate. After a 4hr incubation, cells were washed twice with PBS

and harvested by scraping cells into PBS. Lipids were extracted using the Bligh and Dyer method as described (Steinberg et al., 2006, Watt et al., 2006). For fatty acid oxidation, cells were incubated for 4hrs with serum-free Medium 199 containing [1-¹⁴C]palmitic acid (0.5 μ Ci/ml) (Amersham Biosciences) and 0.5 mM unlabeled palmitate. Fatty acid oxidation was determined by measuring labelled CO₂ and acid-soluble metabolites as described (Chen et al., 2005).

5.2.5 PLASMA, BLOOD AND TISSUE ANALYSES

Plasma insulin concentrations were determined by ELISA (Alpco Diagnostics, Salem, NH) in EDTA-plasma as per manufacturer's instructions as described previously (Mulvihill et al., 2011). Blood glucose was determined using an Ascensia Elite glucometer (Bayer Healthcare, Toronto, Canada) (Mulvihill et al., 2011). Liver lipids were extracted from 100mg of tissue using the method of Folch et al. and quantitated as described previously (Assini et al., 2013, Folch et al., 1957). Fatty acid synthesis was measured following intraperitoneal injection of [1-¹⁴C]acetic acid as described (Mulvihill et al., 2009). Hepatic fatty acid oxidation was determined in tissue homogenates of fresh liver by conversion of [³H]palmitate to ³H₂O (Mulvihill et al., 2009).

5.2.6 IMMUNOBLOTTING AND DENSITOMETRY

Total cell lysates were isolated from livers or primary mouse hepatocytes of mice as previously described (Beyea et al., 2007, Rowe et al., 2003). Proteins were separated by SDS-PAGE, transferred to polyvinylidene difluoride membranes and immunoblotted (Rowe et al., 2003). Lysates were probed using antibodies against mouse phospho and total Akt, FoxO1, mTORC1, AMPK and ACC as well as GRP78, CHOP and β -actin (Cell Signaling, Danvers, MA). Quantitation of protein was determined by densitometry as described (Beyea et al., 2007, Rowe et al., 2003).

5.2.7 QUANTITATIVE REAL-TIME PCR GENE ABUNDANCE ANALYSIS

Total RNA was isolated from livers or primary mouse hepatocytes via TRIzol[®] reagent (Life Technologies, Burlington, ON) as per manufacturer's instructions. Specific mRNA abundances (*Pgc1a*, *Ppara*, *Acox*, *Cpt1a*, *Afp*, *Srebp1c*, *Fasn*, *Pck1*, *Tnf*, *Icam1*, *Il1b*, *Ccl2*, *Ccl3*, *iNos*, *Arg1* and *Gapdh*) were measured via quantitative real-time PCR (qRT-PCR) using an ABI Prism (7900HT) Sequence Detection System (Applied Biosystems, Foster City, CA) as previously described (Beyea et al., 2012, Mulvihill et al., 2009). mRNA abundances were calculated using the standard curve method

5.2.8 STATISTICAL ANALYSES

Data are expressed as means +/- SEM. One-way ANOVA followed by the Bonferroni test was used to determine significant differences between two groups. One-way ANOVA followed by pair-wise comparisons by the Tukey's test was used to determine differences between three or more groups. For fasting/re-feeding experiments and experiments involving WT or AMPK β 1^{-/-} primary mouse hepatocytes, two-way ANOVA followed by pair-wise comparisons by the Tukey's test was used to determine statistically significant differences and interactions. Significance thresholds were *P* values less than 0.05 and marked by different upper case or lower case letters as well as asterisks as indicated in the figure legends.

5.3 RESULTS

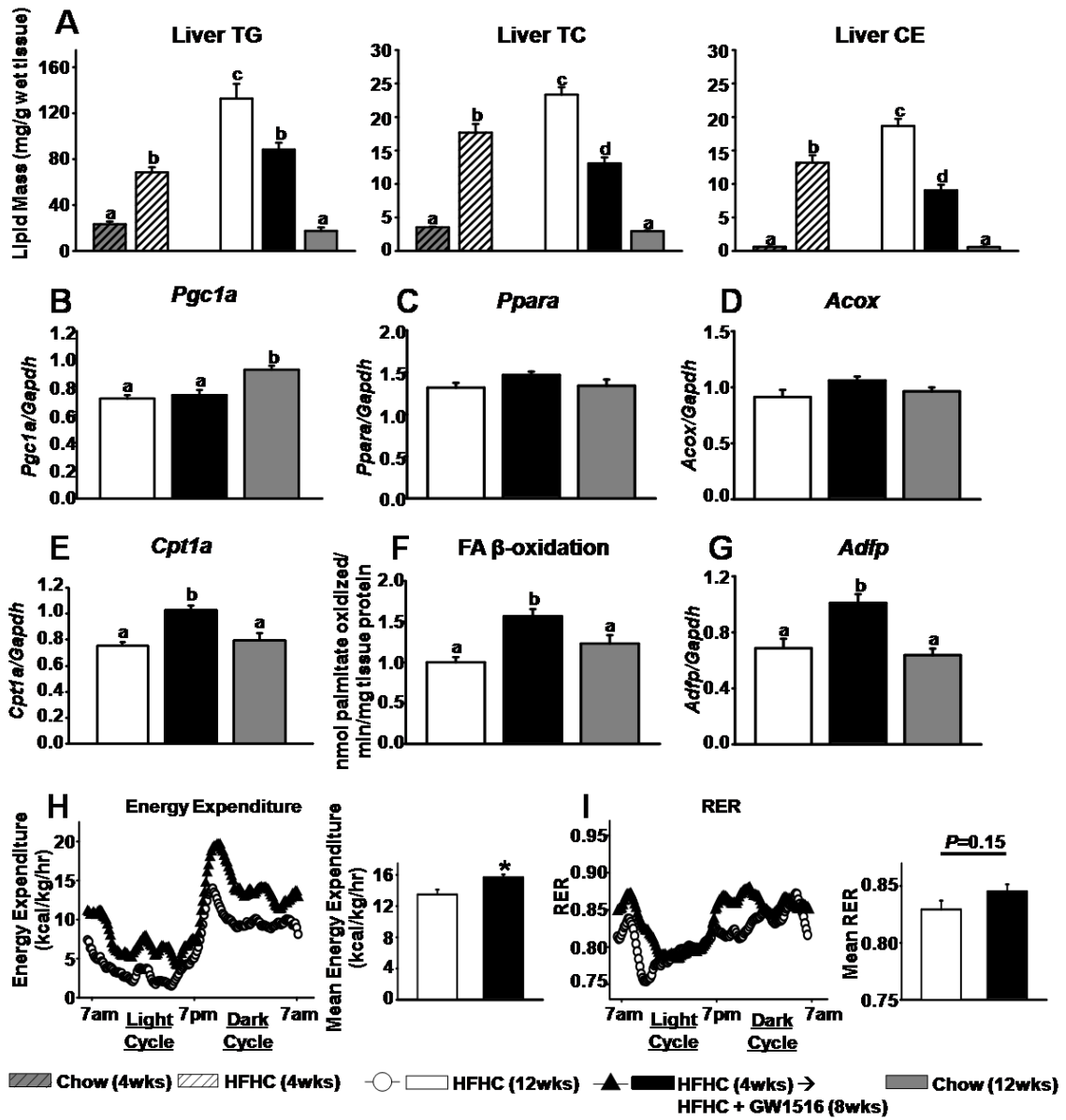
5.3.1 GW1516-TREATMENT ATTENUATES HEPATIC TG ACCUMULATION, IN PART, BY STIMULATING FATTY ACID β -OXIDATION

To examine the role of PPAR δ activation in hepatic lipid metabolism, male C57BL/6 *Ldlr*^{-/-} mice were administered a HFHC diet for 4 weeks to induce hepatic steatosis. Subsequently, mice were fed the HFHC diet supplemented with either vehicle or GW1516 (3mg/kg/day) for an additional 8 weeks. In mice fed the HFHC diet, prominent hepatic steatosis developed at the end of the 4-weeks, as evidenced by significantly increased TC, CE and TG (Figure 5.1A). These lipids continued to increase over the subsequent 8 weeks on the HFHC diet. In contrast the addition of GW1516 to HFHC diet for 8 weeks decreased hepatic lipids by 30-50% demonstrating a significant slowing of steatosis progression (Figure 5.1A).

We reasoned that GW1516 attenuates liver TG accumulation via increased fatty acid (FA) β -oxidation and/or reduced fatty acid synthesis. With respect to FA oxidation, *Pgc1a* expression was suppressed in livers of mice fed the HFHC-diet for 12 weeks (-20% compared to chow-fed mice), which was not further affected by GW1516-treatment (Figure 5.1B). Furthermore, at 12 weeks, the expression of *Ppara* and the PPAR α -target gene *Acox* were unaffected by any diet (Figure 5.1C,D). In contrast, *Cpt1a* mRNA abundance was significantly enhanced (35%) in livers isolated from GW1516-treated animals, which was associated with a 50% increase in FA oxidation as compared to HFHC-fed animals (Figure 5.1E,F). We next examined the expression of the PPAR δ -specific target gene *Adfp* to determine whether hepatic PPAR δ was activated in response to GW1516-treatment. Indeed, expression of *Adfp* was significantly increased (2-fold) in liver from GW1516-treated animals (Figure 5.1G). Collectively, these results suggest that GW1516 attenuates liver TG accumulation partly due to increased hepatic

Figure 5.1: GW1516 attenuates diet-induced hepatic steatosis, in part, via increased fatty acid oxidation.

Ldlr^{-/-} mice were fed a high-fat, cholesterol-containing diet (HFHC) for 4 weeks. For a subsequent 8 weeks, mice remained on HFHC alone or supplemented with GW50516 (GW1516) (3mg/kg/day) (n=12/group). **A**, Hepatic triglyceride (TG), total cholesterol (TC) and cholesteryl ester (CE) mass. Abundance of hepatic *Pgc1a* (**B**) *Ppara* (**C**) *Acox* (**D**) *Cpt1a* (**E**) and *Adfp* (**G**) was measured via qRT-PCR and normalized to *Gapdh*. **F**, Hepatic fatty acid β -oxidation was determined as conversion of [³H]palmitate to ³H₂O. Energy expenditure (**H**) and respiratory exchange ratio (**I**) (RER=VO₂/VCO₂) were measured by indirect calorimetry (CLAMS system) during a 24hr period. Measurements were collected every 10 min. Mean of each parameter during the 24hr period shown. Data is presented as mean \pm SEM. Different letters indicate significant differences; ANOVA with post-hoc Tukey's test ($P < 0.05$). Asterisk (*) indicates significant different between two groups; student's paired *t*-test ($P < 0.05$)



FA β -oxidation, which does not involve the activation of PGC1 α or PPAR α .

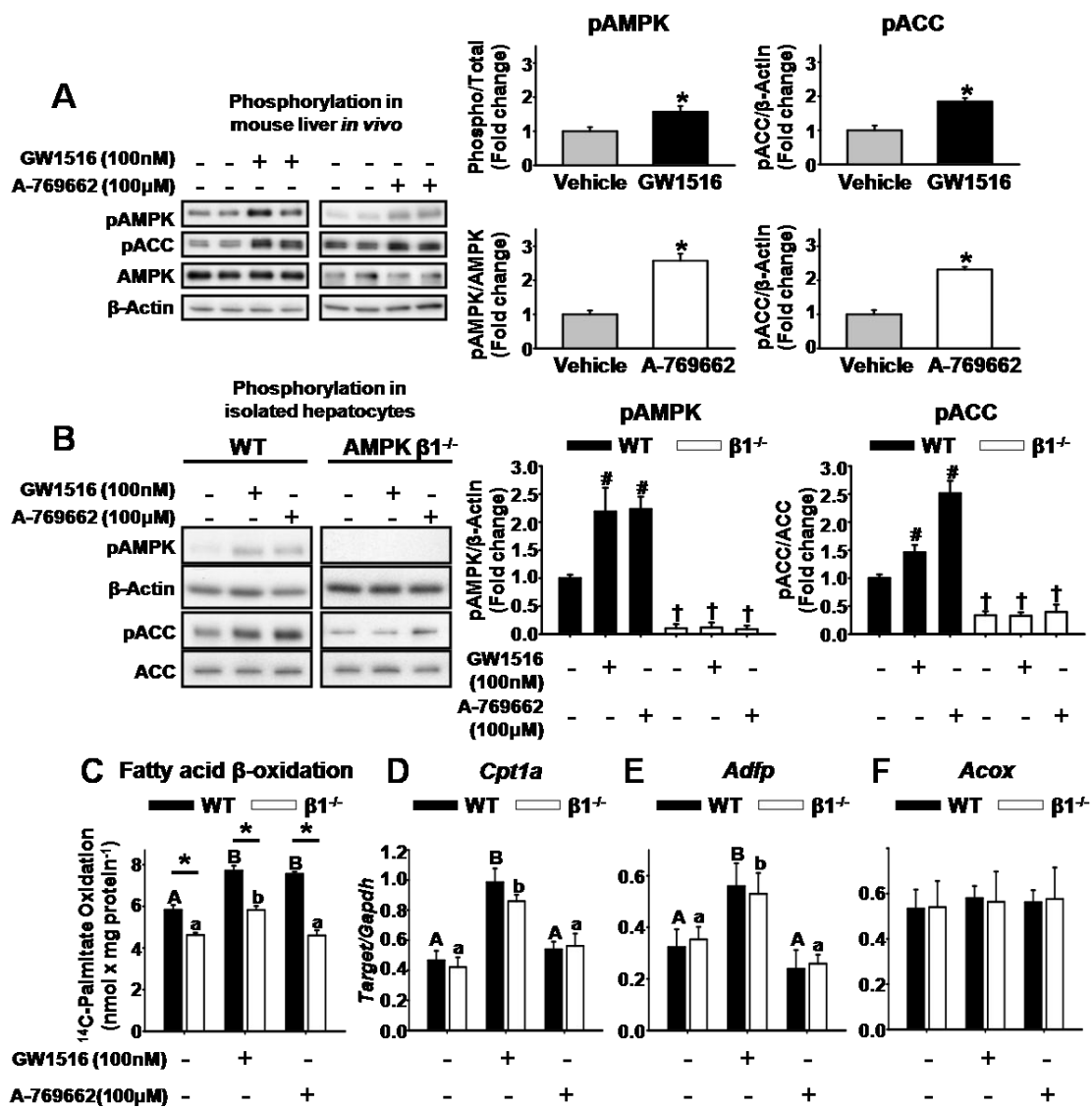
To further investigate the increase in hepatic FA oxidation by GW1516-treatment, we assessed energy balance in an animal metabolic monitoring system. Total energy expenditure (EE) was significantly higher (16%) in mice receiving GW1516 compared to mice remaining on the HFHC diet alone (Figure 5.1H). As there was no significant difference in caloric intake between the diet groups (Chapter 4, Figure 4.2B) increased energy expenditure likely contributed to the significant 30% attenuation of body weight gain observed in Chapter 4 (Figure 4.2A). Nevertheless, the respiratory exchange ratio (RER) profiles, which reflect the relative utilization of carbohydrate (RER \sim 1) versus fat (RER \sim 0.7), were similar between the HFHC-fed and GW1516-intervention groups (Figure 5.1I). Given the significant increase in total EE in GW1516-treated mice, the lack of difference in RER profiles suggests that both carbohydrate and fat utilization are increased by PPAR δ activation.

5.3.2 AMPK ACTIVATION IS NOT REQUIRED FOR THE GW1516-MEDIATED INCREASE IN FAT OXIDATION

AMPK is a cellular energy sensor that regulates fat oxidation, in part, through phosphorylation of its downstream substrate ACC (O'Neill et al., 2012). Given that PPAR δ activation stimulated hepatic FA oxidation *in vivo*, we hypothesized that AMPK activation may be involved. To evaluate the ability of GW1516 to directly stimulate acute hepatic AMPK activation *in vivo*, we employed a fasting, feeding, injection and re-fasting protocol (Hawley et al., 2012). In livers isolated 90min after the injection of GW1516, we observed a significant 2-fold increase in phosphorylation of AMPK and ACC (Figure 5.2A). Mice were also injected with the potent synthetic AMPK activator A-769662 (Cool et al., 2006), which increased AMPK and ACC phosphorylation \sim 2.5-fold (Figure 5.2A).

Figure 5.2: GW1516 increases AMPK and ACC phosphorylation, which is not required for fatty acid oxidation.

Eight to ten week-old *Ldlr*^{-/-} mice fed a standard laboratory chow were fasted overnight, fed at 0700 for 2hrs and re-fasted at 0900. Intraperitoneal injection of vehicle, GW1516 (3mg/kg) or A-769662 (30mg/kg) (n=6/group) occurred at the beginning of the re-fasting period at 0900. **A**, Immunoblots of AMPK and ACC in freeze-clamped liver lysates 90-min post-injection. Representative immunoblots with quantitations shown. **B-F**, Primary hepatocytes isolated from WT and $\beta 1^{-/-}$ mice. Cells were incubated for 1hr with or without GW1516 or A-769662 and lysates were immunoblotted for phosphorylated (p)AMPK and pACC (**B**). Representative immunoblots with quantitations are shown. **C**, Isolated hepatocytes were treated with 0.5mM palmitate (0.5 μ Ci/mL [¹⁴C]palmitate) for 4hrs with or without GW1516 or A-769662 prior to determination of fatty acid oxidation. In isolated hepatocytes treated with or without GW1516 or A-769662 for 6hrs, mRNA abundances of *Cpt1a* (**D**), *Afp* (**E**) and *Acox* (**F**) were measured by qRT-PCR and normalized to *Gapdh*. Data is presented as mean \pm SEM (n=3-4 from at least 3 independent experiments). In (**A**) asterisk (*) indicates significant difference between vehicle and treatment; student's paired *t*-test ($P < 0.05$). In (**B**) # and † indicate significant difference versus WT control; two-way ANOVA with post-hoc Bonferroni's test ($P < 0.05$). In (**C-F**) different upper case letters indicate statistical significance among treatments in WT hepatocytes, different lower case letters indicate statistical significance among treatments in $\beta 1^{-/-}$ hepatocytes, and an asterisk (*) indicates statistical significance between WT and $\beta 1^{-/-}$ within the same treatment group ($P < 0.05$); two-way ANOVA with post-hoc Tukey's test ($P < 0.05$).

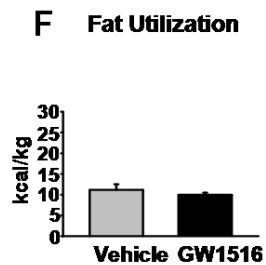
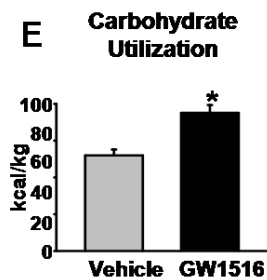
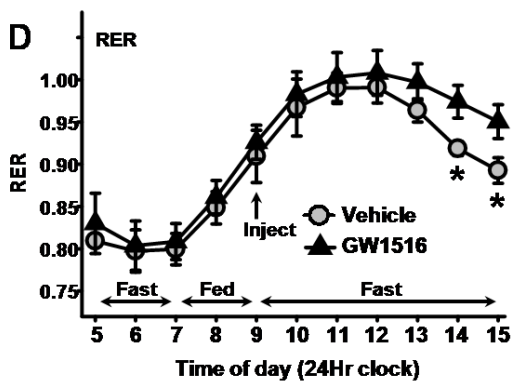
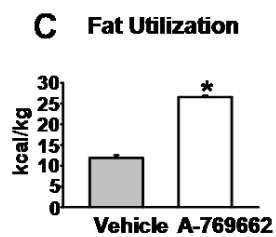
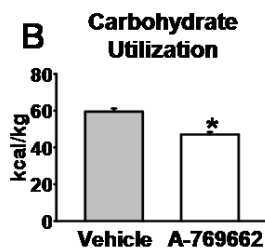
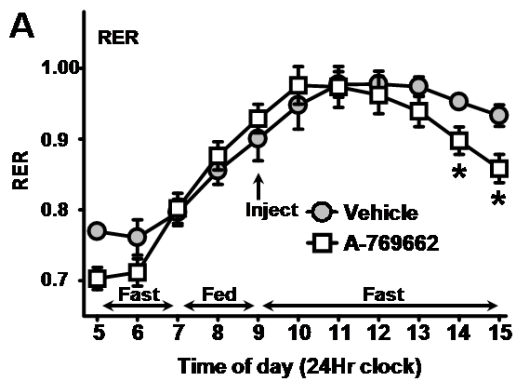


To investigate the requirement of AMPK in the GW1516-mediated stimulation of FA oxidation, we isolated primary mouse hepatocytes from wild type (WT) or AMPK β 1^{-/-} mice (referred to as β 1^{-/-} mice). Deletion of the β 1 subunit of AMPK results in 90% loss of hepatic AMPK activity (Dzamko et al., 2010). As depicted in Figure 5.2B, both GW1516 and A-769662 increased phosphorylation of AMPK and ACC in isolated WT primary mouse hepatocytes but not β 1^{-/-} hepatocytes. Furthermore, GW1516 and A-769662 stimulated a modest but significant 30% increase in FA oxidation in isolated WT hepatocytes (Figure 5.2C). The effect of A-769662 was lost in β 1^{-/-} hepatocytes, consistent with an AMPK-dependent effect (Hawley et al., 2012). However, in β 1^{-/-} hepatocytes GW1516 stimulated fat oxidation to the same extent as in WT cells (Figure 5.2C). To reconcile this, we examined *Cpt1a* expression in WT and β 1^{-/-} hepatocytes and found that GW1516-treatment significantly enhanced *Cpt1a* expression (~2-fold) irrespective of genotype (Figure 5.2D). A-769662 treatment had no effect on *Cpt1a* mRNA abundance in WT or β 1^{-/-} hepatocytes (Figure 5.2D). The PPAR δ -specific target gene *Adfp* was increased 2-fold in isolated hepatocytes from either genotype, whereas the PPAR α -specific target *Acox* was unaffected by genotype or treatment (Figure 5.2E,F). Taken together, these results provide evidence that the ability of GW1516 to increase FA oxidation does not require AMPK activation. Rather, GW1516 stimulates *Cpt1a*, an effect that does not require AMPK. Furthermore, the selected concentration of GW1516 does not activate PPAR α .

To evaluate whether increased hepatic FA oxidation would be reflected in a more rapid switch to fat utilization, we examined RER profiles in the fasting, acute feeding, injection and re-fasting protocol outlined above. Consistent with a faster switch to post-prandial fat utilization, A-769662-injected mice exhibited more rapid depression of RER at 5 and 6 hours post-injection (Figure 5.3A). Accordingly, the calculated oxidation of carbohydrate was significantly decreased (~30%) during this period, whereas oxidation

Figure 5.3: GW1516 activates hepatic AMPK *in vivo*, yet stimulates carbohydrate utilization.

Eight to ten week-old *Ldlr*^{-/-} mice fed a standard laboratory chow were fasted overnight, fed at 0700 for 2hrs and re-fasted at 0900. Intraperitoneal injection of vehicle, GW1516 (3mg/kg) or A-769662 (30mg/kg) (n=6/group) occurred at the beginning of the re-fasting period at 0900. **A**, Respiratory exchange ratio (RER) measured during a fasting, feeding, injection and re-fasting protocol with A-769662. **B-C**, Carbohydrate and fatty acid utilization, respectively, calculated from data shown in **(A)**. **D**, Respiratory exchange ratio (RER) measured during a fasting, feeding, injection with GW1516 and re-fasting protocol. **E-F**, Carbohydrate and fatty acid utilization, respectively, calculated from data shown in **(C)**. Data is presented as mean +/- SEM. * indicates significant difference versus vehicle; student's paired t-test ($P < 0.05$).



of fat was markedly increased by 2.5-fold (Figure 5.3B,C). On the other hand, injection of GW1516 resulted in a slower depression of RER (Figure 5.3D), which is consistent with enhanced post-prandial carbohydrate utilization (Figure 5.3E). In contrast to the mutual inhibition of substrate utilization observed in A-769662-injected mice, GW1516-injection did not suppress post-prandial fat utilization (Figure 5.3F). Collectively, these data suggest that the ability of PPAR δ activation by GW1516 to increase total body glucose oxidation is greater than its ability to increase liver FA oxidation.

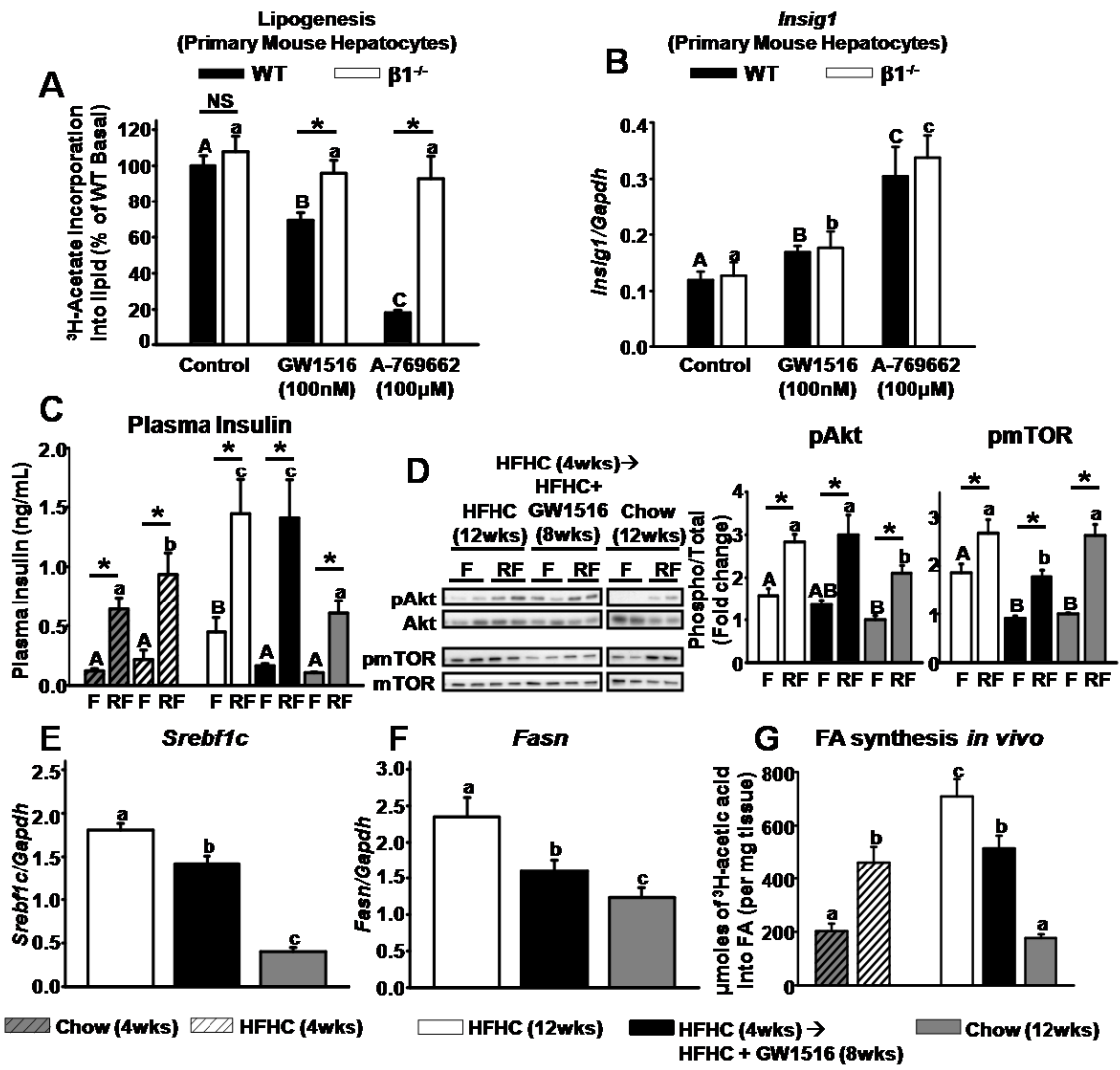
5.3.3 GW1516-TREATMENT ATTENUATES *DE NOVO* LIPOGENESIS, IN PART, VIA ACTIVATION OF AMPK AS WELL AS CORRECTION OF SELECTIVE HEPATIC INSULIN RESISTANCE

In addition to regulating FA oxidation, AMPK is a critical regulator of *de novo* lipogenesis (Dzamko et al., 2010). We thus hypothesized that PPAR δ activation inhibits FA synthesis via activation of AMPK. When incubated with WT hepatocytes, GW1516 significantly inhibited *de novo* lipogenesis by ~30% (Figure 5.4A). This effect was strongly attenuated in $\beta 1^{-/-}$ hepatocytes, in which the suppression was only 11% and not statistically significant (Figure 5.4A). Consistent with an AMPK-specific effect, the 80% reduction in lipogenesis by A-769662 in WT hepatocytes was lost in $\beta 1^{-/-}$ hepatocytes (Figure 5.4A). Both compounds increased expression of *Insig1* (Figure 5.4B), a known negative regulator of SREBP-1c (Qin et al., 2008). The induction of *Insig1* by GW1516 and A-769662 may have contributed to the residual 10% reduction in lipogenesis observed in $\beta 1^{-/-}$ hepatocytes. Nevertheless, in primary mouse hepatocytes GW1516 inhibits *de novo* lipogenesis, in part, through activation of AMPK.

During selective hepatic insulin resistance, hyperinsulinemia drives mTORC1 activation, resulting in enhanced SREBP-1c-mediated lipogenesis (Brown and Goldstein, 2008). Thus, another possible mechanism for reduced hepatic steatosis in GW1516-treated mice is correction of the mTORC1 branch of insulin signaling.

Figure 5.4: GW1516 inhibits hepatic fatty acid synthesis as a consequence of AMPK activation and correction of selective hepatic insulin resistance.

A, Primary mouse hepatocytes isolated from WT and $\beta 1^{-/-}$ mice were incubated with 0.5mM sodium acetate (0.5 μ Ci/mL 14 C-acetate) for 4hrs with or without GW1516 or A-769662 prior to determination of lipogenesis (n=3-4 from at least 3 independent experiments). In isolated hepatocytes treated with or without GW1516 or A-769662 for 6hrs abundance of *Insig1* (**B**) was measured by qRT-PCR and normalized to *Gapdh*. **C**, Plasma insulin at the end of the induction and intervention phases in *Ldlr* $^{-/-}$ mice fasted overnight (designated F) and fasted overnight followed by a 2hr re-feeding period (designated RF). **D**, Immunoblots of insulin signaling proteins phosphorylated (p) AKT and pmTOR in liver lysates from F and RF mice. Representative immunoblots with quantitations shown. mRNA abundance of *Srebf1c* (**E**) and *Fasn* (**F**) in liver lysates isolated from animals fasted for 4hrs (n=6-8/group). **G**, Synthesis of fatty acid in liver obtained 60 min post injection (i.p.) with [14 C]acetic acid (n=6-8/group). Data is presented as mean +/- SEM. In (**A**) different upper case letters indicate statistical significance among WT treatments, different lower case letters indicate statistical significance among $\beta 1^{-/-}$ treatments, and asterisk (*) indicates statistical significance between WT and $\beta 1^{-/-}$ within the same treatment group ($P < 0.05$); two-way ANOVA with post-hoc Tukey's test ($P < 0.05$). In (**C,D**) different upper case letters indicate statistical significance among fasted animals, different lower case letters indicate statistical significance among re-fed animals, and asterisk (*) indicates statistical significance between fasted and re-fed within the same diet ($P < 0.05$); two-way ANOVA with post-hoc Tukey's test ($P < 0.05$). In (**E-G**) different letters indicate significant differences; one-way ANOVA with post-hoc Tukey's test ($P < 0.05$).



In contrast to chow-fed animals, HFHC-feeding resulted in continued progression of fasting hyperinsulinemia (Figure 5.4C). Fasting hyperinsulinemia in the HFHC-fed animals was strongly attenuated by intervention with GW1516 to the HFHC diet (Figure 5.4C). Fasting hyperinsulinemia in the HFHC-fed animals was associated with increased phosphorylation of hepatic Akt and mTORC1 compared to chow-fed animals (Figure 5.4D). In contrast, GW1516-intervention restored fasting phospho-Akt (partially) and phospho-mTORC1 (completely) to levels observed in chow-fed controls (Figure 5.4D). In all three diet groups, re-feeding elicited enhanced phosphorylation of Akt and mTORC1 (Figure 5.4D). This is consistent with increased sensitivity in the lipogenic mTORC1 branch of the insulin signaling cascade in HFHC-fed mice and its normalization following GW1516 treatment (Brown and Goldstein, 2008).

Compared to chow-fed controls, the fasting hyperinsulinemia and increased phospho-mTORC1 observed in HFHC-fed mice at 12 weeks was associated with increased expression of *Srebp1c* and *Fasn* (Figure 5.4E,F), as well as markedly enhanced fasting FA synthesis (Figure 5.4G). In contrast, the GW1516-intervention cohort exhibited significant attenuation of *Srebp1c* and *Fasn* expression (Figure 5.4E,F), which was coupled to a complete inhibition of the HFHC-induced progression of FA synthesis from 4- to 12-weeks of feeding (Figure 5.4G). Together with results in primary mouse hepatocytes, these data suggest that PPAR δ activation inhibits hepatic lipogenesis through activation of AMPK as well as correction of selective hepatic insulin resistance, both of which contribute to the attenuation of ectopic liver TG accrual.

5.3.4 PPAR δ ACTIVATION RESTORES DYNAMIC REGULATION OF HEPATIC FoxO1 WHICH SLOWS THE DEVELOPMENT OF OF HYPERGLYCEMIA

Given that PPAR δ plays a role in hepatic insulin sensitivity (Lee et al., 2006), we hypothesized that this was perhaps a result of correcting the bifurcation in the insulin signaling cascade induced by the HFHC diet. At 12 weeks, livers isolated from HFHC-

fed mice lost the ability to suppress *Pck1* expression and stimulate FoxO1 phosphorylation in the fasting-to-feeding transition (Figure 5.5A,B). This is consistent with previous hyperinsulinemic euglycemic clamp studies in which the liver of *Ldlr*^{-/-} mice fed a high fat diet were insulin resistant (Mulvihill et al., 2011). In contrast, animals receiving the GW1516-intervention retained the ability to dynamically regulate fasting/re-feeding *Pck1* expression and FoxO1 phosphorylation, similar to that observed in chow-fed mice (Figure 5.5A,B). We examined fasting blood glucose levels and found a significant 1.5-fold increase in fasting hyperglycemia in mice fed the HFHC for 12 weeks, which was partially attenuated by GW1516-intervention (Figure 5.5C). These data suggest that PPAR δ activation corrects the gluconeogenic branch of insulin signaling during selective hepatic insulin resistance, which prevents exacerbation of diet-induced dysglycemia.

5.3.5 GW1516 INHIBITS HEPATIC INFLAMMATION AND INDUCTION OF ER STRESS

Inflammation is a prominent feature of hepatic insulin resistance and steatosis (Hummasti and Hotamisligil, 2010). Given that GW1516-intervention attenuated hepatic steatosis and corrected selective hepatic insulin resistance, we postulated that this would be associated with reduced hepatic inflammation. As shown in Figure 5.6A, expression of the proinflammatory M1 cytokines *Tnf*, *Icam1*, *Il1b*, *Ccl2*, *Ccl3* and *iNos* were markedly induced (2- to 15-fold) in livers of mice fed the HFHC diet at 12 weeks. In contrast, these cytokines were significantly attenuated (-50- to -65%) in livers excised from the GW1516-intervention group (Figure 5.6A). Furthermore, HFHC-feeding strongly suppressed hepatic expression of the M2 anti-inflammatory marker *Arg1*, resulting in greatly exacerbated *iNos/Arg1* ratio compared to chow-fed control mice (Figure 5.6B). GW1516 intervention completely prevented this expression pattern (Figure 5.6B). Together these data suggest that PPAR δ activation promotes an anti-inflammatory

Figure 5.5: GW1516 corrects the gluconeogenic branch of insulin signalling during selective hepatic insulin resistance which improves fasting hyperglycemia.

A, mRNA abundance of *Pck1* in liver lysates isolated from fasted (F) and re-fed (RF) animals (n=6-8/group). **B**, Immunoblots of insulin signaling protein pFoxO1 in liver lysates from F and RF mice (n=6-8/group). Representative immunoblots with quantitations shown. **C**, Blood glucose levels in F and RF mice (n=6-8/group). Data is presented as mean +/- SEM. Different upper case letters indicate statistical significance among fasted animals, different lower case letters indicate statistical significance among re-fed animals, and asterisk (*) indicates statistical significance between fasted and re-fed within the same diet ($P < 0.05$); two-way ANOVA with post-hoc Tukey's test ($P < 0.05$).

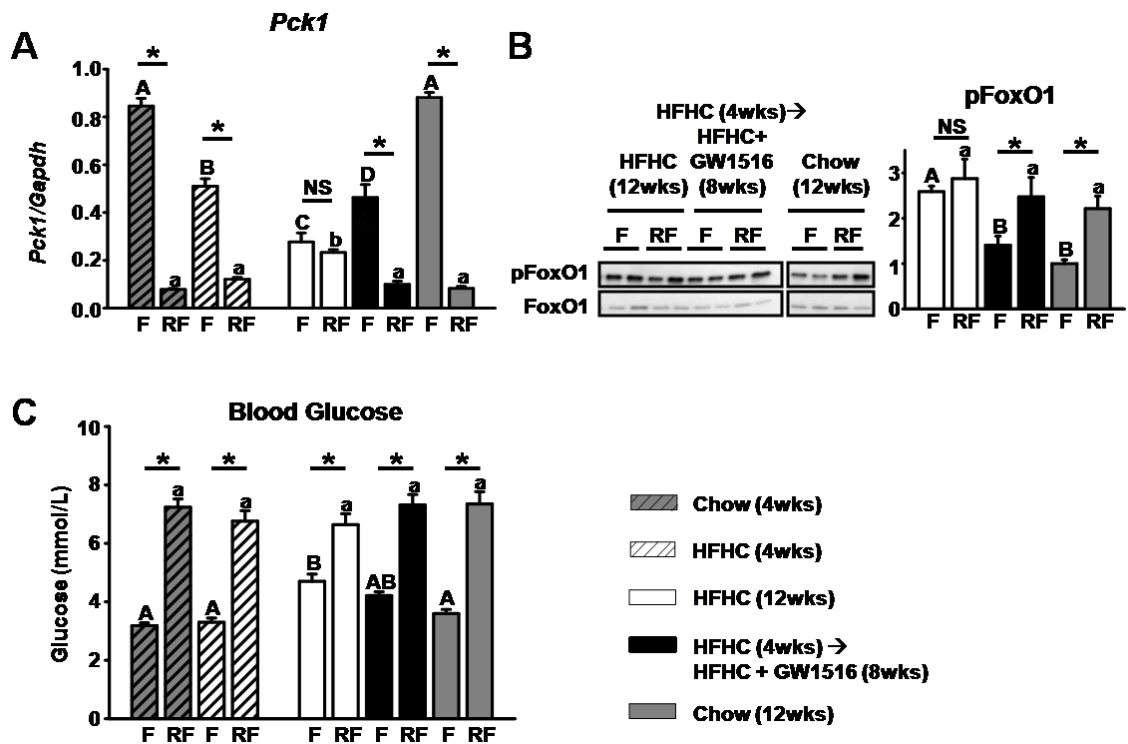
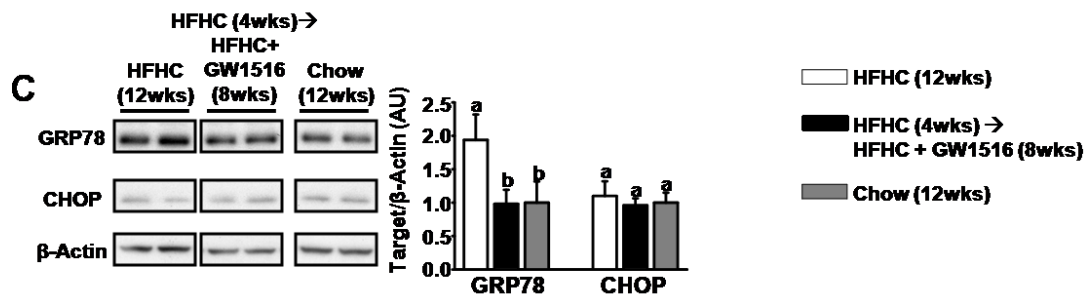
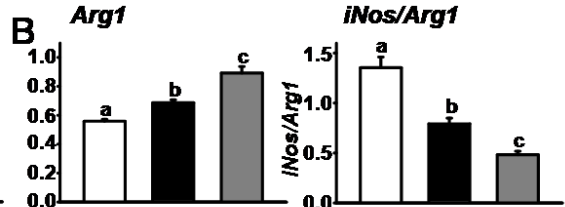
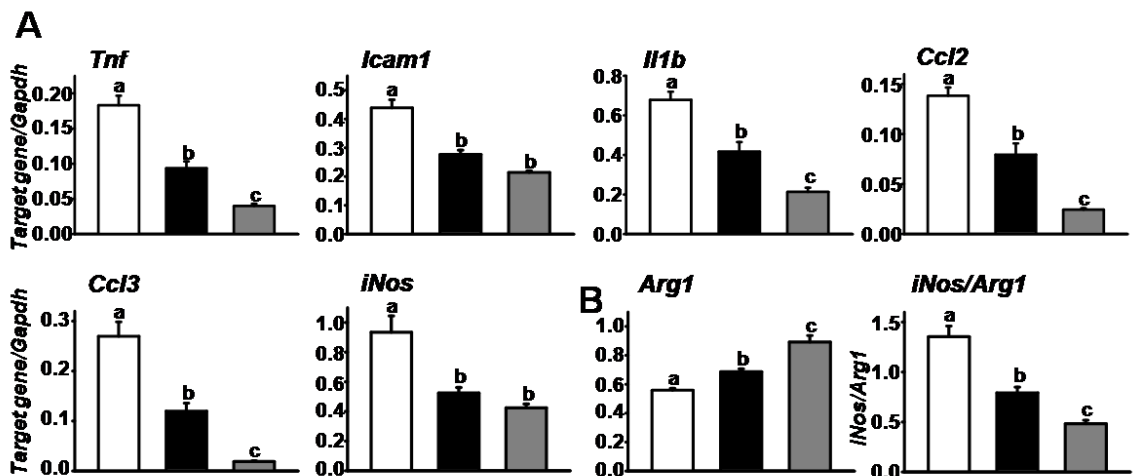


Figure 5.6: GW1516 attenuates hepatic inflammation and ER-stress.

Ldlr^{-/-} mice were fed a high-fat, cholesterol-containing diet (HFHC) for 4 weeks. For a subsequent 8 weeks, mice remained on HFHC alone or supplemented with GW50516 (GW1516) (3mg/kg/day) (n=12/group). **A,B** Hepatic abundance of cytokines was determined at 12 weeks by qRT-PCR, and expression was normalized to *Gapdh* +/- SEM (n=8-12/group). **C**, Immunoblots of GRP78 and CHOP in liver lysates at 12 weeks. Representative immunoblots with quantitations shown. Data is presented as mean +/- SEM (8-12/group). Different letters indicate significant differences; one-way ANOVA with post-hoc Tukey's test ($P < 0.05$).



M2 cytokine milieu in the liver.

Inflammation is commonly interwoven with ER-stress in the development of hepatic insulin resistance (Hummasti and Hotamisligil, 2010, Van Beek et al., 2012). Accordingly, HFHC-feeding significantly increased hepatic GRP78 (Figure 5.6C), a marker of the unfolded protein response (UPR), which is the precursor to the ER-stress response (Kaplowitz et al., 2007). GW1516-intervention completely normalized the diet-induced increase in GRP78 (Figure 5.6C). However, CHOP, the effector of the ER-stress response was unaffected by any diet (Figure 5.6C) suggesting that although the UPR has been initiated, the ER-stress response has not. Nevertheless, PPAR δ activation attenuates this diet-induced hepatic pathology

5.4 DISCUSSION

In the current study, we evaluated the ability of intervention to a HFHC diet with a PPAR δ agonist to attenuate the progression of hepatic steatosis. We show that GW1516-intervention inhibits the progression of diet-induced liver TG accumulation. Mechanistically, attenuation of hepatic steatosis was a result of reduced FA synthesis and increased FA oxidation. The loss of hepatic AMPK activity did not mitigate the ability of PPAR δ activation to induce FA oxidation, whereas loss of AMPK partially prevented PPAR δ agonist-mediated inhibition of lipogenesis. Selective hepatic insulin resistance was corrected by PPAR δ activation, which was associated with reduced hepatic inflammation and ER-stress.

The role of PPAR δ activation in liver TG metabolism has been controversial (Lee et al., 2006, Liu et al., 2011, Nagasawa et al., 2006, Qin et al., 2008). One study showed that GW1516 prevented diet-induced suppression of hepatic AMPK activation, which was associated with increased expression of genes involved in FA oxidation and increased plasma β -hydroxybutyrate. In spite of these observations, GW1516 had no effect on hepatic TG content (Barroso et al., 2011). Another study showed that injection of adPPAR δ into *Ldlr*^{-/-} mice significantly increased AMPK phosphorylation in the liver, which was thought to contribute to glucose lowering (Liu et al., 2011). The impact of increased hepatic AMPK activation on lipid metabolism was not explored (Liu et al., 2011). Here we provide direct evidence that PPAR δ activation increases AMPK and ACC phosphorylation *in vivo* as well as in primary mouse hepatocytes. The GW1516-mediated increase in phospho-ACC was AMPK dependent as this effect was lost in β 1^{-/-} hepatocytes. With regard to lipid metabolism, we demonstrate that PPAR δ activation *in vivo* stimulates hepatic FA oxidation through PPAR δ -specific activation of *Cpt1a*. We recapitulated these results in primary mouse hepatocytes, and identified that AMPK

activation is not a requirement for GW1516 to stimulate FA oxidation, as enhanced *Cpt1a* expression and FA oxidation persisted in $\beta 1^{-/-}$ hepatocytes.

Carbohydrate oxidation and fat oxidation are thought to be mutually inhibitory (Randle, 1998). Thus, an agent that induces liver fat oxidation would be predicted to stimulate a faster switch in post-prandial substrate utilization from carbohydrate to fat (Hawley et al., 2012). In the current study we show that in an acute setting, GW1516-injection increased carbohydrate oxidation, yet fat oxidation during this period was not suppressed. Furthermore, in a setting of prolonged PPAR δ activation, we demonstrate that intervention to the HFHC diet with GW1516 increases total EE, yet has no further effect on average RER through a 24hr period. Previous work has generated the hypothesis that PPAR δ activation stimulates carbohydrate and fat utilization simultaneously (Kramer et al., 2007, Lee et al., 2006). The findings reported here are consistent with this hypothesis, and contribute direct evidence for simultaneous oxidation of both fuel sources in response to a synthetic PPAR δ ligand. The increased oxidation of fat likely contributes to reduced liver TG accumulation.

Studies which have examined the role PPAR δ activation in hepatic *de novo* lipogenesis have yielded both positive and negative results (Lee et al., 2006, Liu et al., 2011, Qin et al., 2008). On one hand, both adPPAR δ injection and GW1516-treatment have been shown to increase hepatic expression of genes involved in lipogenesis, and consequently increase liver TG accumulation (Lee et al., 2006, Liu et al., 2011). On the other hand, delivery of adPPAR δ or the synthetic PPAR δ agonist GW0742 have demonstrated reduced SREBP-1c processing, reduced lipogenic gene expression and prevention of hepatic steatosis (Qin et al., 2008). The data presented here are consistent with, and extend this latter concept, as we provide evidence that intervention to a HFHC diet with GW1516 in mice, corrects selective hepatic insulin resistance, reduces lipogenic gene expression and prevents any further increase in fasting fatty acid

synthesis. Furthermore, GW1516 reduced *de novo* lipogenesis in WT primary mouse hepatocytes, but not in $\beta 1^{-/-}$ hepatocytes, which demonstrated that a component of the inhibition of FA synthesis was AMPK-dependent. Given that two different mechanisms may contribute to the observed reduction in lipogenesis by GW1516-treatment, the relative contributions of these pathways requires further study.

During selective hepatic insulin resistance, Akt loses its ability to phosphorylate and inactivate FoxO1, while maintaining its ability to phosphorylate and activate mTORC1 (Li et al., 2010). Coupled to hyperinsulinemia, this bifurcation in the insulin signaling cascade contributes to hepatic steatosis, dyslipidemia and hyperglycemia (Brown and Goldstein, 2008). In the present study, we provide evidence that hepatic insulin signaling does in fact bifurcate in a model of diet-induced insulin resistance. Importantly, we demonstrate that PPAR δ activation attenuates the progression of the selective hepatic insulin resistant phenotype, as dynamic regulation of fasting-to-feeding phospho-FoxO1 and *Pck1* expression was restored in the GW1516-intervention cohort. These data elaborate on the body of evidence that supports a role for PPAR δ activation in protection from metabolic disease (Lee et al., 2006, Tanaka et al., 2003, Wang et al., 2003), and further support the use of PPAR δ agonists in management of insulin resistance.

Liver inflammation has been linked to hepatic steatosis and insulin resistance (Gregor and Hotamisligil, 2011, Hummasti and Hotamisligil, 2010). Vascular chronic low-grade inflammation is in part mediated by aortic lipid accumulation and insulin resistance (Chapter 2, Chapter 4, (Liang et al., 2007, Tabas et al., 2010)). Given the selective insulin resistant phenotype and TG acquisition in livers of HFHC-fed animals and correction by GW1516-intervention, it is tempting to hypothesize that similar mechanisms govern induction and attenuation of vascular and hepatic inflammation. Moreover, Kupffer cell-specific deletion of *Ppar δ* resulted in increased proinflammatory

cytokine expression and reduced anti-inflammatory cytokine expression, which was coupled to increased liver TG accumulation and hepatic dysfunction (Odegaard et al., 2008). Therefore, our results are consistent with an anti-inflammatory role for PPAR δ activation in the liver. The relative impact of reduced inflammation versus correction of insulin sensitivity to the attenuation of hepatic steatosis cannot be discerned from the present experiments and requires further elucidation.

In summary, the data reported here provide physiological and molecular evidence that intervention with PPAR δ -specific activation in the liver alleviates diet-induced hepatic steatosis, insulin resistance, inflammation and ER-stress. We conclude that PPAR δ agonists may serve as therapeutic options for the treatment of patients with hepatic steatosis.

5.5 REFERENCES

Assini, J.M., Mulvihill, E.E., Sutherland, B.G., Telford, D.E., Sawyez, C.G., Felder, S.L., Chhoker, S., Edwards, J.Y., Gros, R., and Huff, M.W. (2013). Naringenin Prevents Cholesterol-Induced Systemic Inflammation, Metabolic Dysregulation, and Atherosclerosis in Ldlr(-)/(-) Mice. *J Lipid Res* 54, 711-724.

Barish, G.D., Atkins, A.R., Downes, M., Olson, P., Chong, L.W., Nelson, M., Zou, Y., Hwang, H., Kang, H., Curtiss, L., *et al.* (2008). Ppardelta Regulates Multiple Proinflammatory Pathways to Suppress Atherosclerosis. *Proc Natl Acad Sci U S A* 105, 4271-4276.

Barroso, E., Rodriguez-Calvo, R., Serrano-Marco, L., Astudillo, A.M., Balsinde, J., Palomer, X., and Vazquez-Carrera, M. (2011). The Pparbeta/Delta Activator Gw501516 Prevents the Down-Regulation of Ampk Caused by a High-Fat Diet in Liver and Amplifies the Pgc-1alpha-Lipin 1-Pparalpha Pathway Leading to Increased Fatty Acid Oxidation. *Endocrinology* 152, 1848-1859.

Beyea, M.M., Heslop, C.L., Sawyez, C.G., Edwards, J.Y., Markle, J.G., Hegele, R.A., and Huff, M.W. (2007). Selective up-Regulation of Lxr-Regulated Genes Abca1, Abcg1, and Apoe in Macrophages through Increased Endogenous Synthesis of 24(S),25-Epoxycholesterol. *J Biol Chem* 282, 5207-5216.

Beyea, M.M., Reaume, S., Sawyez, C.G., Edwards, J.Y., O'Neil, C., Hegele, R.A., Pickering, J.G., and Huff, M.W. (2012). The Oxysterol 24(S),25-Epoxycholesterol Attenuates Human Smooth Muscle-Derived Foam Cell Formation Via Reduced Low-Density Lipoprotein Uptake and Enhanced Cholesterol Efflux. *J Am Heart Assoc* 1, e000810.

Brown, M.S., and Goldstein, J.L. (2008). Selective Versus Total Insulin Resistance: A Pathogenic Paradox. *Cell Metab* 7, 95-96.

Carlson, C.A., and Kim, K.H. (1973). Regulation of Hepatic Acetyl Coenzyme a Carboxylase by Phosphorylation and Dephosphorylation. *J Biol Chem* 248, 378-380.

Chen, M.B., McAinch, A.J., Macaulay, S.L., Castelli, L.A., O'Brien P, E., Dixon, J.B., Cameron-Smith, D., Kemp, B.E., and Steinberg, G.R. (2005). Impaired Activation of Amp-Kinase and Fatty Acid Oxidation by Globular Adiponectin in Cultured Human Skeletal Muscle of Obese Type 2 Diabetics. *J Clin Endocrinol Metab* 90, 3665-3672.

Cool, B., Zinker, B., Chiou, W., Kifle, L., Cao, N., Perham, M., Dickinson, R., Adler, A., Gagne, G., Iyengar, R., *et al.* (2006). Identification and Characterization of a Small Molecule Ampk Activator That Treats Key Components of Type 2 Diabetes and the Metabolic Syndrome. *Cell Metab* 3, 403-416.

DeFronzo, R.A. (2010). Insulin Resistance, Lipotoxicity, Type 2 Diabetes and Atherosclerosis: The Missing Links. The Claude Bernard Lecture 2009. *Diabetologia* 53, 1270-1287.

Dzambo, N., van Denderen, B.J., Hevener, A.L., Jorgensen, S.B., Honeyman, J., Galic, S., Chen, Z.P., Watt, M.J., Campbell, D.J., Steinberg, G.R., *et al.* (2010). Ampk Beta1 Deletion Reduces Appetite, Preventing Obesity and Hepatic Insulin Resistance. *J Biol Chem* 285, 115-122.

Dzambo, N.L., and Steinberg, G.R. (2009). Ampk-Dependent Hormonal Regulation of Whole-Body Energy Metabolism. *Acta Physiol (Oxf)* 196, 115-127.

Eckel, R.H., Alberti, K.G., Grundy, S.M., and Zimmet, P.Z. (2010). The Metabolic Syndrome. *Lancet* 375, 181-183.

Evans, R.M., Barish, G.D., and Wang, Y.X. (2004). Ppars and the Complex Journey to Obesity. *Nat Med* 10, 355-361.

Farese, R.V., Jr., Zechner, R., Newgard, C.B., and Walther, T.C. (2012). The Problem of Establishing Relationships between Hepatic Steatosis and Hepatic Insulin Resistance. *Cell Metab* 15, 570-573.

Folch, J., Lees, M., and Sloane Stanley, G.H. (1957). A Simple Method for the Isolation and Purification of Total Lipides from Animal Tissues. *J Biol Chem* 226, 497-509.

Fullerton, M.D., Steinberg, G.R., and Schertzer, J.D. (2013). Immunometabolism of Ampk in Insulin Resistance and Atherosclerosis. *Mol Cell Endocrinol* 366, 224-234.

Gregor, M.F., and Hotamisligil, G.S. (2011). Inflammatory Mechanisms in Obesity. *Annu Rev Immunol* 29, 415-445.

Haas, J.T., and Biddinger, S.B. (2009). Dissecting the Role of Insulin Resistance in the Metabolic Syndrome. *Curr Opin Lipidol* 20, 206-210.

Hawley, S.A., Fullerton, M.D., Ross, F.A., Schertzer, J.D., Chevtzoff, C., Walker, K.J., Peggie, M.W., Zibrova, D., Green, K.A., Mustard, K.J., *et al.* (2012). The Ancient Drug Salicylate Directly Activates Amp-Activated Protein Kinase. *Science* 336, 918-922.

Hummasti, S., and Hotamisligil, G.S. (2010). Endoplasmic Reticulum Stress and Inflammation in Obesity and Diabetes. *Circ Res* 107, 579-591.

Kaplowitz, N., Than, T.A., Shinohara, M., and Ji, C. (2007). Endoplasmic Reticulum Stress and Liver Injury. *Semin Liver Dis* 27, 367-377.

Kemp, B.E., Stapleton, D., Campbell, D.J., Chen, Z.P., Murthy, S., Walter, M., Gupta, A., Adams, J.J., Katsis, F., van Denderen, B., *et al.* (2003). Amp-Activated Protein Kinase, Super Metabolic Regulator. *Biochem Soc Trans* 31, 162-168.

Kido, Y., Nakae, J., and Accili, D. (2001). Clinical Review 125: The Insulin Receptor and Its Cellular Targets. *J Clin Endocrinol Metab* 86, 972-979.

Kramer, D.K., Al-Khalili, L., Guigas, B., Leng, Y., Garcia-Roves, P.M., and Krook, A. (2007). Role of Amp Kinase and Ppardelta in the Regulation of Lipid and Glucose Metabolism in Human Skeletal Muscle. *J Biol Chem* 282, 19313-19320.

Kramer, D.K., Al-Khalili, L., Perrini, S., Skogsberg, J., Wretenberg, P., Kannisto, K., Wallberg-Henriksson, H., Ehrenborg, E., Zierath, J.R., and Krook, A. (2005). Direct Activation of Glucose Transport in Primary Human Myotubes after Activation of Peroxisome Proliferator-Activated Receptor Delta. *Diabetes* 54, 1157-1163.

Lee, C.H., Olson, P., Hevener, A., Mehl, I., Chong, L.W., Olefsky, J.M., Gonzalez, F.J., Ham, J., Kang, H., Peters, J.M., *et al.* (2006). Ppardelta Regulates Glucose Metabolism and Insulin Sensitivity. *Proc Natl Acad Sci U S A* 103, 3444-3449.

Li, S., Brown, M.S., and Goldstein, J.L. (2010). Bifurcation of Insulin Signaling Pathway in Rat Liver: Mtorc1 Required for Stimulation of Lipogenesis, but Not Inhibition of Gluconeogenesis. *Proc Natl Acad Sci U S A* 107, 3441-3446.

Liang, C.P., Han, S., Senokuchi, T., and Tall, A.R. (2007). The Macrophage at the Crossroads of Insulin Resistance and Atherosclerosis. *Circ Res* 100, 1546-1555.

Liu, S., Hatano, B., Zhao, M., Yen, C.C., Kang, K., Reilly, S.M., Gangl, M.R., Gorgun, C., Balschi, J.A., Ntambi, J.M., *et al.* (2011). Role of Peroxisome Proliferator-Activated Receptor {Delta}/{Beta} in Hepatic Metabolic Regulation. *J Biol Chem* 286, 1237-1247.

Lu, M., Wan, M., Leavens, K.F., Chu, Q., Monks, B.R., Fernandez, S., Ahima, R.S., Ueki, K., Kahn, C.R., and Birnbaum, M.J. (2012). Insulin Regulates Liver Metabolism in Vivo in the Absence of Hepatic Akt and Foxo1. *Nat Med* 18, 388-395.

Mulvihill, E.E., Allister, E.M., Sutherland, B.G., Telford, D.E., Sawyez, C.G., Edwards, J.Y., Markle, J.M., Hegele, R.A., and Huff, M.W. (2009). Naringenin Prevents Dyslipidemia, Apolipoprotein B Overproduction, and Hyperinsulinemia in Ldl Receptor-Null Mice with Diet-Induced Insulin Resistance. *Diabetes* 58, 2198-2210.

Mulvihill, E.E., Assini, J.M., Lee, J.K., Allister, E.M., Sutherland, B.G., Koppes, J.B., Sawyez, C.G., Edwards, J.Y., Telford, D.E., Charbonneau, A., *et al.* (2011). Nobiletin Attenuates Vldl Overproduction, Dyslipidemia, and Atherosclerosis in Mice with Diet-Induced Insulin Resistance. *Diabetes* 60, 1446-1457.

Mulvihill, E.E., Assini, J.M., Sutherland, B.G., DiMattia, A.S., Khami, M., Koppes, J.B., Sawyez, C.G., Whitman, S.C., and Huff, M.W. (2010). Naringenin Decreases Progression of Atherosclerosis by Improving Dyslipidemia in High-Fat-Fed Low-Density Lipoprotein Receptor-Null Mice. *Arterioscler Thromb Vasc Biol* 30, 742-748.

Nagasawa, T., Inada, Y., Nakano, S., Tamura, T., Takahashi, T., Maruyama, K., Yamazaki, Y., Kuroda, J., and Shibata, N. (2006). Effects of Bezafibrate, Ppar Pan-Agonist, and Gw501516, Ppardelta Agonist, on Development of Steatohepatitis in Mice Fed a Methionine- and Choline-Deficient Diet. *Eur J Pharmacol* 536, 182-191.

Narkar, V.A., Downes, M., Yu, R.T., Emblar, E., Wang, Y.X., Banayo, E., Mihaylova, M.M., Nelson, M.C., Zou, Y., Juguilon, H., *et al.* (2008). Ampk and Ppardelta Agonists Are Exercise Mimetics. *Cell* 134, 405-415.

O'Neill, H.M., Holloway, G.P., and Steinberg, G.R. (2012). Ampk Regulation of Fatty Acid Metabolism and Mitochondrial Biogenesis: Implications for Obesity. *Mol Cell Endocrinol*.

Odegaard, J.I., Ricardo-Gonzalez, R.R., Red Eagle, A., Vats, D., Morel, C.R., Goforth, M.H., Subramanian, V., Mukundan, L., Ferrante, A.W., and Chawla, A. (2008). Alternative M2 Activation of Kupffer Cells by Ppardelta Ameliorates Obesity-Induced Insulin Resistance. *Cell Metab* 7, 496-507.

Ozcan, U., Cao, Q., Yilmaz, E., Lee, A.H., Iwakoshi, N.N., Ozdelen, E., Tuncman, G., Gorgun, C., Glimcher, L.H., and Hotamisligil, G.S. (2004). Endoplasmic Reticulum Stress Links Obesity, Insulin Action, and Type 2 Diabetes. *Science* 306, 457-461.

Qin, X., Xie, X., Fan, Y., Tian, J., Guan, Y., Wang, X., Zhu, Y., and Wang, N. (2008). Peroxisome Proliferator-Activated Receptor-Delta Induces Insulin-Induced Gene-1 and Suppresses Hepatic Lipogenesis in Obese Diabetic Mice. *Hepatology* 48, 432-441.

Randle, P.J. (1998). Regulatory Interactions between Lipids and Carbohydrates: The Glucose Fatty Acid Cycle after 35 Years. *Diabetes Metab Rev* 14, 263-283.

Reilly, S.M., and Lee, C.H. (2008). Ppar Delta as a Therapeutic Target in Metabolic Disease. *FEBS Lett* 582, 26-31.

Rowe, A.H., Argmann, C.A., Edwards, J.Y., Sawyez, C.G., Morand, O.H., Hegele, R.A., and Huff, M.W. (2003). Enhanced Synthesis of the Oxysterol 24(S),25-Epoxycholesterol in Macrophages by Inhibitors of 2,3-Oxidosqualene:Lanosterol Cyclase: A Novel Mechanism for the Attenuation of Foam Cell Formation. *Circ Res* 93, 717-725.

Saggerson, D. (2008). Malonyl-Coa, a Key Signaling Molecule in Mammalian Cells. *Annu Rev Nutr* 28, 253-272.

Steinberg, G.R., Michell, B.J., van Denderen, B.J., Watt, M.J., Carey, A.L., Fam, B.C., Andrikopoulos, S., Proietto, J., Gorgun, C.Z., Carling, D., *et al.* (2006). Tumor Necrosis Factor Alpha-Induced Skeletal Muscle Insulin Resistance Involves Suppression of Amp-Kinase Signaling. *Cell Metab* 4, 465-474.

Tabas, I., Tall, A., and Accili, D. (2010). The Impact of Macrophage Insulin Resistance on Advanced Atherosclerotic Plaque Progression. *Circ Res* 106, 58-67.

Tanaka, T., Yamamoto, J., Iwasaki, S., Asaba, H., Hamura, H., Ikeda, Y., Watanabe, M., Magoori, K., Ioka, R.X., Tachibana, K., *et al.* (2003). Activation of Peroxisome Proliferator-Activated Receptor Delta Induces Fatty Acid Beta-Oxidation in Skeletal Muscle and Attenuates Metabolic Syndrome. *Proc Natl Acad Sci U S A* 100, 15924-15929.

Van Beek, M., Oravec-Wilson, K.I., Delekta, P.C., Gu, S., Li, X., Jin, X., Apel, I.J., Konkle, K.S., Feng, Y., Teitelbaum, D.H., *et al.* (2012). Bcl10 Links Saturated Fat Overnutrition with Hepatocellular Nf-Kb Activation and Insulin Resistance. *Cell Rep* 1, 444-452.

Wang, Y.X., Lee, C.H., Tjep, S., Yu, R.T., Ham, J., Kang, H., and Evans, R.M. (2003). Peroxisome-Proliferator-Activated Receptor Delta Activates Fat Metabolism to Prevent Obesity. *Cell* 113, 159-170.

Watt, M.J., Dzamko, N., Thomas, W.G., Rose-John, S., Ernst, M., Carling, D., Kemp, B.E., Febbraio, M.A., and Steinberg, G.R. (2006). Cntf Reverses Obesity-Induced Insulin Resistance by Activating Skeletal Muscle Ampk. *Nat Med* 12, 541-548.

Williamson, R.M., Price, J.F., Glancy, S., Perry, E., Nee, L.D., Hayes, P.C., Frier, B.M., Van Look, L.A., Johnston, G.I., Reynolds, R.M., *et al.* (2011). Prevalence of and Risk Factors for Hepatic Steatosis and Nonalcoholic Fatty Liver Disease in People with Type 2 Diabetes: The Edinburgh Type 2 Diabetes Study. *Diabetes Care* 34, 1139-1144.

Yecies, J.L., Zhang, H.H., Menon, S., Liu, S., Yecies, D., Lipovsky, A.I., Gorgun, C., Kwiatkowski, D.J., Hotamisligil, G.S., Lee, C.H., *et al.* (2011). Akt Stimulates Hepatic Srebp1c and Lipogenesis through Parallel Mtorc1-Dependent and Independent Pathways. *Cell Metab* 14, 21-32.

Chapter 6 Discussion

6.1 SUMMARY OF FINDINGS

Cardiovascular disease due to accelerated atherosclerosis is the primary cause of death in patients with dyslipidemia, insulin resistance and type 2 diabetes. Central to atherogenesis is the development of lipid-laden macrophage foam cells, which occurs in response to retention of apoB-containing lipoproteins within the arterial intima (Moore and Tabas, 2011). In addition to the accrual of lipid, macrophage foam cells synthesize and secrete proinflammatory effector molecules that potentiate lesion development (Libby et al., 2011). Therefore, a macrophage-targeted treatment that inhibits foam cell formation and the associated inflammatory responses would be desirable. In this thesis, two synthetic agonists for PPAR δ were examined *in vitro*, one of which was extended to *in vivo* experiments. These studies were undertaken to: (1) identify the molecular mechanisms involved in macrophage foam cell-associated inflammatory responses, and (2) define the mechanism of action and therapeutic potential of PPAR δ activation in the regulation of lipid metabolism, inflammatory signaling and protection from atherosclerosis in states of metabolic disturbance such as insulin resistance and dyslipidemia.

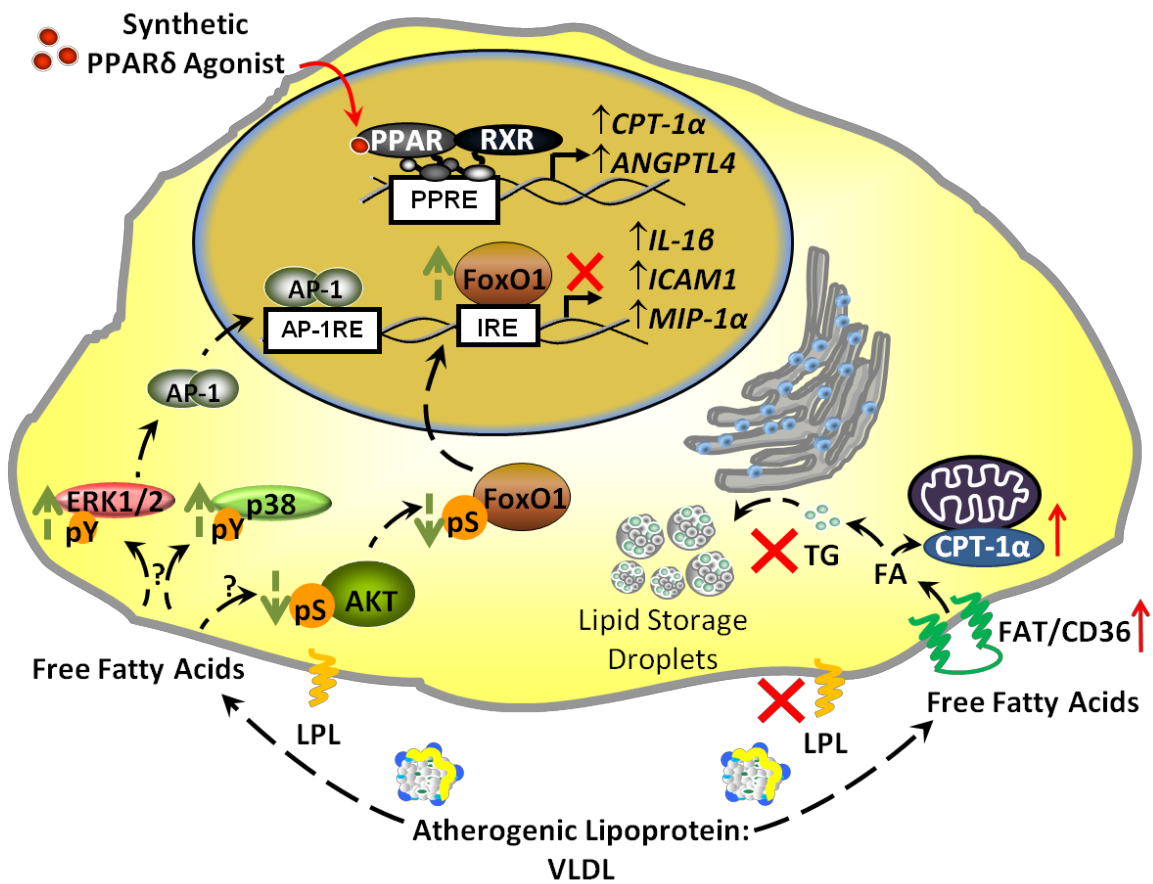
Elevated plasma TG-rich VLDL is an independent risk factor for the development of CVD, and can readily stimulate the development of macrophage foam cells (Evans et al., 1993, Whitman et al., 1999a, Whitman et al., 1999b). Paradoxically, VLDL-derived fatty acids also activate macrophage PPAR δ resulting in up-regulation of genes involved in fatty acid and TG metabolism (Chawla et al., 2003). Thus, from an evolutionary standpoint, PPAR δ serves as a fatty acid sensor in cells of the vasculature to prevent arterial lipid accumulation under normolipidemic conditions. The experiments described in Chapter 2 tested the hypothesis that synthetic ligand activation of PPAR δ would

attenuate VLDL-induced macrophage foam cell formation in the context of hypertriglyceridemia. These *in vitro* studies confirmed that VLDL and synthetic PPAR δ agonists each individually activated similar transcriptional programs (Chawla et al., 2003). However, the VLDL-stimulated PPAR δ -target gene expression was insufficient to prevent the 5-fold increase in VLDL-induced macrophage TG deposition. In contrast, macrophages incubated with VLDL in the presence of the potent synthetic PPAR δ agonists GW0742 and GW1516 resulted in the attenuation of VLDL-induced TG accumulation. Mechanistically, the PPAR δ ligands reduced TG accumulation, at least in part, by increasing expression of *ANGPTL4*, *CD36* and *CPT1 α* above VLDL-treatment alone, which resulted in: (1) reduced lipolysis, (2) enhanced FA uptake, albeit from a smaller FA pool, and (3) increased FA oxidation, respectively. Collectively, the net effect of synthetic ligand activation of PPAR δ was to reduce intracellular TG accumulation (Figure 6.1). It is important to note that the concentrations of the PPAR δ agonists used in these studies were specific for activating PPAR δ , in the absence of activating PPAR α or PPAR γ .

In addition to increasing lipid accumulation, previous work has suggested that VLDL or VLDL-derived FAs can also stimulate or potentiate macrophage inflammatory responses (Saraswathi and Hasty, 2006, Stollenwerk et al., 2005, Su et al., 2009). The second hypothesis tested in Chapter 2 was that PPAR δ agonists could attenuate VLDL-induced macrophage inflammatory responses. In VLDL-treated macrophages, expression of the proinflammatory mediators *IL-1 β* , *MIP-1 α* and *ICAM-1* was significantly enhanced, which was associated with increased MAPK activation as well as dysregulation of the insulin signaling cascade as evidenced by reduced phosphorylation of Akt and FoxO1 (Figure 6.1). In contrast, incubation with the PPAR δ agonists almost completely inhibited VLDL-induced cytokine expression and MAPK activation, and restored the dysregulation of the insulin signaling cascade. These studies also revealed

Figure 6.1: PPAR δ activation inhibits macrophage foam cell formation and the inflammatory response.

PPAR δ activation attenuates VLDL-induced triglyceride (TG) accumulation by activating a transcriptional program resulting in enhanced CPT-1 α -mediated fatty acid β -oxidation and ANGPTL4-mediated inhibition of lipoprotein lipase (LPL) activity. Furthermore, macrophage treatment with synthetic PPAR δ ligands inhibits proinflammatory cytokine expression, by inhibiting VLDL-stimulated ERK1/2 activation and reversing VLDL-mediated inhibition of Akt/FoxO1 phosphorylation.



Bojic and Huff (2013) *Curr Opin Lipidol* **24(2)**, 171-177.

that the PPAR δ -mediated inhibition of the inflammatory response was not a consequence of increased FA oxidation, as both of the PPAR δ agonists normalized VLDL-induced cytokine expression, MAPK activation and dysregulated insulin signaling even in the presence of etomoxir, a potent inhibitor of CPT1 α (Galic et al., 2011).

Although hypertriglyceridemia is an independent risk factor for the development of CVD, the canonical foam cell-inducing lipoprotein is CE-rich LDL in both its native and modified forms. The studies in Chapter 3 addressed the ability of PPAR δ activation to attenuate native and modified LDL-induced macrophage foam cell formation and the associated inflammatory response(s). Cellular CE accumulation in response to native and oxLDL was significantly attenuated by both GW0742 and GW1516. With regard to oxLDL, both PPAR δ agonists increased *CD36* mRNA abundance (Chapter 2), which would be predicted to enhance particle uptake (Moore and Freeman, 2006). However, PPAR δ activation also increased ABCA1-mediated cholesterol efflux to apoAI, likely owing to increased ABCA1 mRNA and protein, which contributed to a net inhibition of CE-rich lipoprotein-induced macrophage foam cell formation.

Previous studies examining oxLDL-induced inflammatory responses have yielded both positive and negative results (Curtiss et al., 2012, Febbraio et al., 2000, Janabi et al., 2000, Kannan et al., 2012, Michelsen et al., 2004, Mullick et al., 2005, Qiu et al., 2007). The studies in Chapter 3 contribute to the notion that cholesterol-loaded macrophages exhibit a dampened inflammatory phenotype, as evidence by reduced expression of *TNF α* and *IL-6*, which was not further affected by synthetic ligand activation of PPAR δ . The anti-inflammatory effect of oxLDL was coupled to reduced *DHCR24* expression, which is known to result in the accumulation of desmosterol, a known activator of LXR. Accumulation of desmosterol within cholesterol-loaded mouse peritoneal macrophages has recently been shown to have potent anti-inflammatory effects (Spann et al., 2012). Thus, the studies conducted in Chapter 3 agree with the

concept that cholesterol-loaded macrophages do not exhibit a proinflammatory phenotype, suggesting that other immune cells of the arterial intima are responsible for the atherosclerosis-associated inflammation observed *in vivo*.

The studies in Chapter 4 were undertaken to determine whether the ability of the PPAR δ agonists to attenuate macrophage foam cell formation translated into reduced foam cell formation *in vivo*, and in turn, protection from diet-induced atherosclerosis. These studies tested the hypothesis that PPAR δ activation attenuates the progression of diet-induced atherosclerosis and aortic inflammation in *Ldlr*^{-/-} mice. Previous studies involving prevention protocols, in which the PPAR δ agonist is administered at the same time as the atherogenic stimulus (a high-fat diet), have reported a preventative effect of PPAR δ activation on atherogenesis (Barish et al., 2008, Graham et al., 2005). The studies in Chapter 4 involved an intervention approach, whereby *Ldlr*^{-/-} mice were fed the HFHC diet for 4 weeks to induce dyslipidemia and insulin resistance, which predisposes the animals to atherosclerosis development. Subsequently, HFHC-fed animals either remained on the atherogenic diet, or were supplemented with GW1516 for a subsequent 8 weeks. A subset of animals was fed standard laboratory chow for the 12-week period. The continued progression of dyslipidemia and hyperinsulinemia in HFHC-fed mice contributed to extensive lipid deposition within atherosclerotic plaques. In concert with increased lipid accumulation, HFHC-fed animals had significant enrichment of lesion macrophage, smooth muscle cell and collagen content. In contrast to the continued progression of dyslipidemia, insulin resistance and plaque development in HFHC-fed mice, GW1516-intervention induced regression of elevated plasma lipid and plasma insulin levels, which contributed to slowed progression of plaque lipid deposition. GW1516-intervention also reduced macrophage infiltration, yet had no effect on lesion smooth muscle cell content. Despite this, collagen deposition was increased in lesions of

GW1516-treated animals, suggesting the development of smaller, more stable atherosclerotic lesions.

Examination of cytokine expression in full-length aortae revealed that HFHC-feeding stimulated a proinflammatory phenotype in the aorta, as the M1 cytokines, *Ccl3*, *Il1b*, *Icam1*, *Tnf*, *Il6*, *iNos* and *Ccl2* were all markedly elevated. Additionally, the M2 anti-inflammatory mediator *Arg1* was substantially lower and the *iNos/Arg1* ratio was greatly exacerbated in aortae excised from HFHC-fed animals as compared to those isolated from chow-fed animals. In contrast, GW1516-intervention attenuated the progression of aortic inflammation, as M1 cytokines were reduced, *Arg1* expression was restored and the *iNos/Arg1* ratio was reverted back to levels in chow-fed mice.

To further build on the translation of findings from Chapters 2 and 3 into the *in vivo* setting, aortic analyses of the signaling cascades known to regulate cytokine expression were performed. HFHC-feeding significantly increased aortic MAPK activation. Furthermore, Nfkb activation was also enhanced, which was correlated with the increased expression of aortic *Tnf*, *Il6* and *Ccl2*. Both MAPK and Nfkb activation were attenuated by intervention with GW1516. To assess aortic insulin signaling, aortae excised from fasted and re-fed mice were examined for phosphorylated Akt and FoxO1. In contrast to the dynamic fasting-to-feeding regulation of pAkt and pFoxO1 observed in aortae isolated from chow-fed animals, this effect was lost in aortae from HFHC-fed mice. GW1516-intervention corrected aortic insulin signaling, which likely contributed to reduced aortic inflammation.

In addition to exerting atheroprotective effects, the studies in Chapter 4 identified that PPAR δ activation also corrects dyslipidemia and peripheral insulin resistance. Coupled to the fact that hepatic steatosis is a major clinical manifestation of insulin resistance that contributes to dyslipidemia (Farese et al., 2012), the studies in Chapter 5 were undertaken to determine whether PPAR δ activation inhibits diet-induced liver lipid

accumulation. To assess this, the same induction/intervention protocol used in Chapter 4 was employed. The Chapter 5 studies demonstrated that the further 2-fold increase hepatic TG accrual in animals remaining on the HFHC diet was significantly attenuated by intervention with GW1516. The PPAR δ agonist reduced cellular TG, in part, through increased FA oxidation, which was unrelated to activation of PGC1 α , PPAR α or PPAR γ . This was evidenced by GW1516 having no effect on hepatic *Pgc1a*, *Ppara*, *Acox* or *Fabp4* expression. Furthermore, the studies conducted in Chapter 5 identified that the stimulation of FA oxidation by a synthetic PPAR δ agonist does not require the activation of AMPK. β -oxidation persisted in PPAR δ agonist-treated primary mouse hepatocytes isolated from AMPK β 1^{-/-} mice.

Compared to chow-fed controls, the HFHC-fed animals were hyperinsulinemic, which was coupled to increased hepatic phosphorylation of the insulin signaling mediators Akt and mTORC1. Accordingly, *Srebf1c* and *Fasn* expression were significantly upregulated. Functionally, increased phospho-mTORC1, *Srebf1c* and *Fasn* expression was associated with significantly enhanced fasting FA synthesis. All of these parameters were markedly attenuated by intervention with GW1516 to the HFHC diet. These experiments demonstrated that part of the mechanism by which PPAR δ activation attenuates hepatic steatosis is through correction of the lipogenic branch of the insulin signaling bifurcation.

The studies in Chapter 5 also revealed that another mechanism by which PPAR δ activation reduces FA synthesis is through increased AMPK activity. Treatment of isolated WT primary mouse hepatocytes with GW1516 resulted in a 30% reduction in basal *de novo* lipogenesis. This effect was lost in β 1^{-/-} hepatocytes. Consistent with an AMPK effect, the synthetic AMPK activator A-769662 reduced rates of lipid synthesis in hepatocytes isolated from WT mice. However, A-769662 was ineffective at inhibiting lipogenesis in β 1^{-/-} hepatocytes.

In addition to stimulating the development of hepatic steatosis and hyperinsulinemia, HFHC-feeding also induced a state of fasting hyperglycemia. The hyperglycemia observed in HFHC-fed animals was at least partially a result of the inability of insulin to elicit further phosphorylation of FoxO1 during re-feeding. Reduced dynamic regulation of FoxO1 activity was associated with a loss of fasting-to-feeding suppression of *Pck1* expression, as hepatic *Pck1* in the 12-week HFHC cohort was similar between fasted and re-fed animals. Importantly, GW1516-intervention to the HFHC diet prevented the progression of resistance in the gluconeogenic FoxO1 branch of the insulin signaling cascade, which likely contributed to the attenuated progression of dysglycemia.

Previous work has suggested that inflammation in the liver is linked to hepatic steatosis and insulin resistance (Gregor and Hotamisligil, 2011, Hummasti and Hotamisligil, 2010). The Chapter 5 studies confirmed a proinflammatory state of the liver during insulin resistance, and showed that intervention to the HFHC-diet with a PPAR δ agonist was able to completely prevent progression of this inflammatory phenotype. Moreover, HFHC-feeding induced the UPR, which is the precursor to ER-stress often linked to inflammation and progression of insulin resistance (Gregor and Hotamisligil, 2011, Hummasti and Hotamisligil, 2010). Importantly, UPR induction was completely normalized by GW1516-intervention.

6.2 CONCLUSIONS AND FUTURE DIRECTIONS

6.2.1 CHAPTER 2 CONCLUSIONS

The studies in Chapter 2 demonstrated that although VLDL-derived FAs activate PPAR δ , potent synthetic agonists for this receptor are required to attenuate VLDL-induced macrophage lipid accumulation and the associated inflammatory responses. Moreover, these studies revealed that the anti-inflammatory and lipid lowering

capabilities of PPAR δ are discrete. That PPAR δ activation was associated with reduced LPL activity and increased β -oxidation would suggest that the normalization of the VLDL-induced inflammatory response by the PPAR δ agonists was a result of reduced TG accumulation. However, inhibition of TG accumulation with low-dose tetrahydropyridolipstatin to the same extent as that achieved by PPAR δ activation failed to normalize VLDL-induced cytokine expression. Furthermore, GW0742 and GW1516 completely inhibited VLDL-induced cytokine expression, even when β -oxidation was inhibited by etomoxir. Whether PPAR δ activation can attenuate VLDL-induced inflammatory responses in *ANGPTL4*^{-/-}, *CPT1 α* ^{-/-} or *ANGPTL4/CPT1 α* double knockout macrophages would be the more definitive experiment to confirm the findings here. However, the data presented in Chapter 2 strongly suggest that the anti-inflammatory and lipid lowering properties of PPAR δ activation are distinct.

A growing body of evidence indicates that lipid-induced macrophage inflammation is a consequence of increased MAPK signaling as well as impaired signaling through the Akt/FoxO1 pathway (Han et al., 2006, Saraswathi and Hasty, 2006, Senokuchi et al., 2008, Su et al., 2009). It is also thought that VLDL-derived FAs can stimulate macrophage inflammation through TLR-Nfkb signaling (Nguyen et al., 2007, Shi et al., 2006). However, this hypothesis has more recently been challenged (Anderson et al., 2012, Erridge and Samani, 2009). The studies conducted in Chapter 2, performed in the complete absence of LPS, contribute to the paradigm that VLDL-derived FAs themselves stimulate macrophage inflammatory responses are a consequence of macrophage insulin resistance, rather than activation of the TLR-Nfkb pathway. This is supported by: (1) reduced pAkt and pFoxO1, increased nuclear FoxO1 and enhanced MAPK signaling by VLDL treatment, (2) canonical Nfkb target genes *TNF α* and *IL-6* being unaffected by VLDL treatment, and (3) the inability of parthenolide (an inhibitor of Nfkb signaling) to block VLDL-stimulated expression of *IL-1 β* , *MIP-1 α* ,

and *ICAM-1*. Importantly, we found that PPAR δ activation blocks VLDL-induced MAPK activation as well as the VLDL-mediated inhibition of the insulin signaling cascade.

6.2.2 CHAPTER 2 FUTURE DIRECTIONS

Going forward, it will be important to identify the mechanism(s) by which VLDL induces MAPK activation and the mechanism(s) by which PPAR δ activation normalizes VLDL-induced MAPK signaling. It has been suggested that PPAR δ activation stimulates the expression of *Rgs4* and *Rgs5* in mouse macrophages, which reduces angiotensin II-induced phosphorylation of ERK1/2 and p38 (Takata et al., 2008). It remains unknown whether this mechanism applies to prevention of VLDL-induced MAPK activation and downstream inflammation. If this were the mechanism, it would imply that VLDL-induced inflammation through the MAPK pathway involves activation of G-protein coupled receptor signaling, which may uncover novel candidates in the inhibition of macrophage inflammation and atherogenesis. We propose to examine *RGS4* and *RGS5* expression in macrophages treated with PPAR δ agonists. Concurrently, we propose studies in which the ability of GW0742 and GW1516 to inhibit VLDL-induced MAPK activation will be compared in PPAR δ agonist treated control, *RGS4*, *RGS5* and combined *RGS4/RGS5* knockdown macrophages. We hypothesize that the ability of PPAR δ activation to attenuate VLDL-induced MAPK activation and cytokine expression will be strongly attenuated in the absence of *RGS4* and/or *RGS5*.

Another important avenue of investigation will be to identify how VLDL-treatment dysregulates insulin signaling, and the mechanism(s) by which the PPAR δ agonists restore this VLDL-induced dysregulation. One possibility is that VLDL induces negative regulators of one or more steps of the cascade. For example, the suppressor of cytokine signaling (SOCS)-3 negatively regulates insulin signaling by targeting IRS-1 and IRS-2 for proteosomal degradation, thereby diminishing signaling to PI3-K and to Akt (Emanuelli et al., 2000, Rui et al., 2002). Another example is the c-Jun N-terminal kinase

(JNK), which phosphorylates the insulin receptor on serine residues, and in doing so, inhibits the intrinsic autophosphorylation of insulin receptor tyrosine residues. In turn, JNK-mediated serine-phosphorylation of the insulin receptor dampens the propagation of the insulin signal through the IRS-proteins, PI3-K and Akt (Ozcan et al., 2004). The hypotheses that SOCS-3 and/or JNK play a role in the impairment of insulin signaling during VLDL-induced macrophage inflammation can be tested using knockdown experiments for SOCS-3 and inhibitor studies for JNK.

Regarding the mechanism by which PPAR δ activation restores VLDL-mediated impairment of insulin signaling, both PPAR δ agonists used in the Chapter 2 studies stimulated enhanced Akt and FoxO1 phosphorylation in the absence of VLDL. We concluded from these experiments that PPAR δ activation primes the insulin signaling cascade to prevent its downregulation by VLDL-treatment. It has been suggested that PPAR δ activation can directly activate Akt activity through the induction of integrin-like kinase (*ILK*) and 3-phosphoinositide-dependent kinase 1 expression (*PDK1*) (Di-Poi et al., 2002). These transcripts encode kinases that are known to directly phosphorylate Akt and, in turn, FoxO1. However, we and others have observed PPAR δ activation-induced enhancement of Akt and FoxO1 phosphorylation, without increased *ILK* or *PDK1* expression (Chapter 2, (Han et al., 2008)). Another series of candidates may be phosphatases that are known to downregulate the insulin signaling. One such example is the phosphatase and tensin homolog (*PTEN*), which catalyses the dephosphorylation of the 3' phosphate of PIP₃, resulting in the biphosphate product PIP₂. This dephosphorylation event inhibits PI3-K activity, thereby mitigating signaling to Akt (Nicholson and Anderson, 2002). In keratinocytes, PPAR δ plays a role in the downregulation of *PTEN*, thus relieving the impediment on the PI3-K to Akt signal (Di-Poi et al., 2002). Whether this mechanism applies to the GW0742 and GW1516-mediated reversal of VLDL-induced insulin resistance in macrophages is unknown. If this

were the case, one would hypothesize that macrophages treated with PPAR δ agonists would exhibit reduced *PTEN* expression. Additionally, one would hypothesize that VLDL and PPAR δ agonist treatment of macrophages transfected with constitutively active PTEN, would attenuate the ability of PPAR δ activation to reverse VLDL-induced downregulation of Akt and FoxO1 phosphorylation, resulting in sustained proinflammatory cytokine expression. If the converse were true, this would identify that activation of insulin signaling by the PPAR δ agonists occurs downstream of PI3-K. This latter scenario would warrant experiments involving treatment of macrophages expressing dominant-negative Akt or phosphorylation-resistant FoxO1, with or without PPAR δ agonists.

6.2.3 CHAPTER 3 CONCLUSIONS

The studies in Chapter 3 showed that PPAR δ activation attenuates both native and oxLDL-induced macrophage foam cell formation. Although the PPAR δ agonists increased *LDLR* and *CD36* expression (Chapter 2), these compounds also increased cholesterol efflux. We concluded from these studies that PPAR δ agonists, similar to PPAR γ ligands (Argmann et al., 2003), induce a transcriptional program that increases cholesterol uptake and concomitantly increases cholesterol efflux, which collectively leads to a net depletion of cellular CE and FC. Induction of cholesterol efflux to apoAI was significantly increased, whereas efflux to HDL₃ was not. The fact that macrophage foam cell formation was reduced despite no apparent increase in ABCG1 activity agrees with the paradigm that ABCA1 is a more critical efflux transporter in the regulation of cholesterol homeostasis in hematopoietic cells of the arterial intima (Tarling et al., 2010, Yvan-Charvet et al., 2007).

With regard to CE-rich lipoprotein-induced inflammatory responses, we observed decreased cytokine expression in macrophages treated with oxLDL compared to vehicle controls. Reduced cytokine expression was not further affected by the PPAR δ agonists.

One interpretation of these data is that the PPAR δ agonists require the induction of cytokine expression in order to exert their inhibitory effects. In Chapter 2, we observed no change in basal cytokine mRNA abundance when macrophages were treated with GW0742 or GW1516, yet a complete inhibition of cytokine expression by these compounds in the presence of the VLDL-stimulus. A study that supports this hypothesis demonstrated that in adipocytes, GW1516 had no effect on basal IL-6 mRNA and protein but completely inhibited LPS-induced IL-6 synthesis and secretion (Rodriguez-Calvo et al., 2008). Another line of evidence that supports this interpretation is that GW0742 had no effect on the inhibitors of Nfkb ($I\kappa B\alpha$ and $I\kappa B\beta$) in cardiomyocytes unless an LPS-stimulus was present (Ding et al., 2006).

Previous studies have suggested that oxLDL-treated macrophages or FC-loaded macrophages exhibit a proinflammatory phenotype, characterized by increased TLR and/or Nfkb signaling (Curtiss et al., 2012, Febbraio et al., 2000, Janabi et al., 2000, Li et al., 2005, Michelsen et al., 2004, Mullick et al., 2011, Stewart et al., 2010). However, other studies have provided contrary evidence (Kannan et al., 2012, Qiu et al., 2007, Spann et al., 2012). In our hands, oxLDL treatment reduced cytokine expression, and inhibition of ACAT activity to significantly increase FC accumulation failed to reverse the anti-inflammatory phenotype of oxLDL-treated macrophages. These results suggest that oxLDL treatment or FC accumulation in macrophages is not a stimulus for the inflammatory response. Furthermore, oxLDL-mediated reduction in cytokine expression was coupled to markers of (1) oxysterol accumulation (reduced *SREBP-1c* and *FAS* expression), (2) LXR activation (increased *ABCA1*, *ABCG1* and *MYLIP*), (3) PPAR γ activation (*FABP4*), and (4) PPAR δ activation (*ADFP*). The activation of LXR, PPAR γ or PPAR δ is known to be anti-inflammatory (Im and Osborne, 2011, Straus and Glass, 2007). Therefore, oxLDL-mediated activation of all three of these nuclear receptors may elicit a combination of effects that contributes to reduced cytokine expression.

6.2.4 CHAPTER 3 FUTRE DIRECTIONS

The association between oxLDL treatment, increased expression of LXR-target genes and reduced inflammatory cytokine expression is most likely linked to desmosterol accumulation as a consequence of reduced *DHCR24* expression. However, it will be critical to determine whether desmosterol does in fact accumulate in THP-1 macrophages exposed to oxLDL. We propose to conduct experiments in which oxLDL-treated macrophages with or without the PPAR δ agonists are examined for intracellular desmosterol concentrations by liquid chromatography tandem mass spectrometry (Honda et al., 2009, Honda et al., 2008). We hypothesize that oxLDL-treatment will stimulate an increase in desmosterol accumulation, which will not be further enhanced by the PPAR δ agonists. The latter portion of this hypothesis is driven by the fact that the PPAR δ agonists did not further suppress *TNF α* and *IL-6* expression beyond oxLDL-treatment alone.

Although enhanced intracellular desmosterol is the most likely driving factor behind the oxLDL-mediated anti-inflammatory response, other mechanisms are certainly possible. In fact, Spann et al. reported that in mouse peritoneal macrophages elicited from LXR-double knockout mice, the anti-inflammatory phenotype was attenuated, but not eliminated, compared to macrophages elicited from LXR-wild type mice (Spann et al., 2012). Thus, LXR-independent anti-inflammatory mechanisms must also play a role in this context. In the Chapter 3 studies, oxLDL stimulated the expression of the PPAR δ -specific target gene *ADFP*, implying that oxLDL may induce the accumulation of PPAR δ ligands. Fatty acids are known to activate PPAR δ (Chawla et al., 2003). Spann et al. observed increases in oleic acid accumulation in cholesterol-loaded and desmosterol-treated mouse peritoneal macrophages which were in the picomolar range (Spann et al., 2012). The studies in Chapter 2 revealed that in the micromolar range, oleic acid

induces macrophage inflammatory responses. However, picomolar concentrations of oleic acid may be sufficient to activate PPAR δ but insufficient to stimulate the inflammatory response.

The hypothesis that oxLDL-mediated anti-inflammatory responses are partially the result of PPAR δ activation can be tested by examining cytokine expression in macrophages treated with oxLDL in the presence or absence of PPAR δ antagonists (GSK0660 or GSK3787). It is important to note that genetic ablation of *PPAR δ* would not be an appropriate model system for these experiments, as *PPAR δ* deletion mimics the liganded state of the receptor. This is due to genetic ablation of *PPAR δ* resulting in the transrepression of inflammatory cytokine expression and derepression of PPAR δ target genes (Lee et al., 2003, Lee et al., 2006a). Hence, this would create an experimental confounder for the proposed studies. Continuing with the proposed PPAR δ inhibitor experiments, one would hypothesize that antagonizing PPAR δ would result in partial reversal of the oxLDL-mediated reduction of *TNF α* and *IL-6*. If this hypothesis is correct, another series of experiments could perhaps determine whether oleic acid or other fatty acid ligands for PPAR δ accumulate in oxLDL-treated macrophages. Subsequently, experiments may also include, but are not limited to, determining the expression of cytokines under the following conditions: (1) oxLDL in the presence of both PPAR δ and LXR antagonists, (2) exogenous addition of the determined fatty acid PPAR δ ligand, (3) in the presence or absence of PPAR δ antagonist(s). The proposed experiments would determine the relative contribution of LXR and PPAR δ activation to the oxLDL-mediated anti-inflammatory response in macrophages, and possibly identify a novel mechanism responsible for the reduced proinflammatory responses observed in oxLDL-treated macrophages.

Given that *TNF α* and *IL-6* expression is regulated, at least in part, by Nfkb signaling (Ding et al., 2006, Li et al., 2005, Rodriguez-Calvo et al., 2008), one would be

inclined to hypothesize reduced phosphorylation of the Nfkb signaling mediators IKK and I κ B in oxLDL-treated macrophages. However, the anti-inflammatory effects of LXR occur as a result of ligand-induced small ubiquitin-like modifier (SUMO)-dependent modification of the receptor. The SUMOylation of LXR results in the recruitment of co-repressor complexes to promoter regions of proinflammatory genes, which inhibit Nfkb from binding to its response elements within these targets (Im and Osborne, 2011). Hence, it is unlikely that oxLDL-treated macrophages would display reduced phospho-IKK and I κ B. On the other hand, PPAR δ inhibits Nfkb signaling through increased expression of the I κ B proteins, suggesting that oxLDL-treated macrophages may exhibit higher I κ B α and I κ B β than untreated controls. In oxLDL-treated macrophages with or without LXR and PPAR δ antagonists, we propose to examine nuclear co-repressor occupancy of the *TNF α* and *IL-6* promoters via chromatin immunoprecipitation (Ghisletti et al., 2007), as well as phospho- (as a control) and total-IKK, I κ B α and I κ B β via immunoblotting. These experiments would expand on the mechanism by which oxLDL mediates reduced *TNF α* and *IL-6* expression.

6.2.5 CHAPTER 4 CONCLUSIONS

The studies in Chapter 4 revealed that, intervention with a synthetic PPAR δ agonist to a diet-induced setting of pre-established dyslipidemia and insulin resistance attenuates the progression of early stage lesions to more complex lesions. A significant contributor to this effect was likely the reduction in plasma lipids, thus reducing the atherogenic stimulus. However, aortae excised from GW1516-treated mice exhibited significantly increased expression of the PPAR δ -target genes *Adrp*, *Angptl4* and *Cpt1a*, which we showed in Chapter 2 are important regulators of VLDL-induced macrophage foam cell formation. Coupled to the fact that aortic TG in mice receiving the GW1516-intervention regressed from the 4-week baseline levels, these data suggest that this

compound has direct vessel wall effects that contribute to the PPAR δ -mediated reduction in lesion lipid deposition.

In HFHC-fed animals, the markedly increased aortic expression of *Ccl3*, *I11b*, *Icam1*, *Tnf*, *Il6*, *iNos* and *Ccl2* coupled to substantially lower *Arg1* and a greatly exacerbated *iNos/Arg1* ratio strongly suggests the polarization of these aortae towards the M1 proinflammatory phenotype. That GW1516-intervention attenuated the progression of this M1 polarization demonstrates that PPAR δ activation exerts anti-inflammatory effects in the aorta, which likely contribute to protection from lesion progression. Furthermore, GW1516 prevented the induction of aortic MAPK, which was associated with increased *Rgs4* and *Rgs5* expression. Additionally, the PPAR δ agonist inhibited HFHC diet-induced aortic Nfkb activation, through mechanisms that remain to be elucidated.

The studies in Chapter 4 also revealed that dynamic fasting-to-feeding regulation of aortic pAkt and pFoxO1 is lost in a diet-induced model of atherosclerosis. These data suggest that nuclear FoxO1 activity is chronically active in the aorta, which likely contributes to the sustained accumulation of FoxO1 target genes such as *I11b* (Su et al., 2009), *Icam1* and *Ccl3* (Chapter 2). This hypothesis is supported by the paradigm that atherogenesis is a longitudinal process associated with chronic low-grade inflammation (Glass and Witztum, 2001, Libby et al., 2011). Importantly, we found that GW1516-intervention to the HFHC diet completely reversed the fasting-to-feeding regulation of aortic pAkt and pFoxO1 back to levels in chow-fed controls. These data suggest that part of the ability of PPAR δ activation to protect mice from lesion progression is mediated by restoration of normal aortic insulin signaling.

6.2.6 CHAPTER 4 FUTURE DIRECTIONS

A caveat to the conclusions from the findings in Chapter 4 is the leap from drug-treatment to causal relationship. In other words, the ability of GW1516 to lower plasma

lipids is unequivocally a major contributor to protection from lesion progression. However, the data also provide compelling evidence that GW1516 exerts lipid lowering, anti-inflammatory and insulin-sensitizing at the level of the aorta. The relative contribution of lipid lowering and direct vessel wall effects cannot be deciphered from the experiments performed. Furthermore the lesions after 4-weeks of induction were early lesions, which were prevented from further development. Moving forward it will be important to determine if PPAR δ activation improves the pathology of more advanced lesions, and whether extended treatment is able to achieve regression.

Given that the use of *Ppar δ ^{-/-}* mice results in the experimental confounder discussed above, alternative strategies will need to be employed to reconcile the issue of lipid lowering versus direct vessel wall effects. To address this issue, and to determine if extended treatment is able to achieve regression, one potential experiment would be to induce lesion development with HFHC feeding for 12-weeks prior to a 12-week intervention with GW1516. Additionally, the introduction of HFHC-fed mice transferred to chow with or without GW1516 would provide unique insight into the contribution of PPAR δ activation within the aorta to improved lesion pathology. The justification for this statement arises from ongoing experiments in our laboratory, in which 12-weeks of HFHC feeding prior to the introduction of chow for the remaining 12-weeks, completely normalizes all metabolic parameters back to levels observed in 24-week chow-fed mice. Thus, examining lesion pathology in GW1516-intervention during chow feeding would eliminate the variable of drastic lipid lowering contributing to inhibition of plaque progression or stimulation of plaque regression. The reversa mouse (Cre-induced deletion of hepatic *Mttp*) provides a similar platform to test the impact of a drug on atherosclerosis development independent of lipid lowering (Feig et al., 2011), but is unfortunately commercially unavailable.

Another strategy to help reconcile lipid lowering versus direct vessel wall effects is the utilization of laser-capture microdissection (LCM). Analysis of gene expression from LCM samples would allow us to determine the contribution of a particular cell-type to the changes we observed in full-length aorta. Specifically, LCM of MOMA-2 positive macrophages would provide a tool for the macrophage-specific measurement of *Adrp*, *Angptl4* and *Cpt1a* expression. Additionally, the measurement of cytokines in MOMA-2 positive macrophages isolated by LCM would provide a more definitive conclusion of lesion macrophage polarization in all diet groups. Answering these questions would provide a PPAR δ -specific mechanism in macrophages for reduced foam cell formation and inhibition of inflammatory cytokine expression, particularly in the condition of HFHC transferred to chow plus GW1516.

GW1516 increased lesion collagen deposition without altering lesion SMC content. This observation is possibly due to a direct effect of PPAR δ activation on plaque SMCs, enhancing their capacity to synthesize and deposit extracellular matrix. This hypothesis is supported by a report that PPAR δ activation in vascular smooth muscle cells (VSMCs) inhibits IL-1 β -induced matrix metalloproteinase (MMP)-2 and MMP-9 expression (Kim et al., 2010). Although reduced lipid deposition in VSMCs restores their capacity to synthesize extracellular matrix (Beyea et al., 2012, Frontini et al., 2009), the ability of PPAR δ agonists to improve VSMC function in response to a lipid load is unknown. In addition, LCM of smooth muscle cells from aortic lesions would allow us to determine whether GW1516-treatment enhanced collagen and elastin expression specifically in VSMCs, thus contributing to enhanced matrix deposition.

An interesting and novel finding in the Chapter 4 studies was the increased aortic expression of *Ptpn6* and *Trib3*, which are known negative regulators of hepatic insulin signaling (Du et al., 2003, Dubois et al., 2006). While it has recently been demonstrated that silencing *Trib3* using siRNA suppresses atherosclerosis in diabetic mice (Wang et

al., 2012), the role of *Ptpn6* in atherogenesis has not been reported. Experiments using siRNA against *Ptpn6* in a setting of HFHC diet-induced atherosclerosis would identify the contribution of induced *Ptpn6*, and its protein product SHP-1, to atherogenesis. Moreover, the ability of GW1516 to inhibit lesion progression in a setting of already improved (vascular) insulin signaling (such as *Trib3* and/or *Ptpn6* knockdown) would help determine the impact of improved aortic insulin signaling on atherosclerosis. Alternatively, examining the ability of GW1516 to inhibit plaque progression in the setting of bone marrow transplantation from *Insr*^{-/-} mice to *Ldlr*^{-/-} recipients would also provide valuable information regarding the contribution of improved vascular insulin sensitivity by PPAR δ activation to the atheroprotective effect. If in this scenario GW1516 can still inhibit atherogenesis, it will be important to determine the mechanism by which PPAR δ activation reverses insulin resistance, as discussed in Chapter 2 future directions (Section 6.2.2).

6.2.7 CHAPTER 5 CONCLUSIONS

In Chapter 5 we demonstrated that intervention to a HFHC diet with a synthetic PPAR δ agonist attenuates the progression of hepatic steatosis, as evidenced by a complete halting of liver TG accumulation from 4-week baseline levels. The addition of GW1516 to the HFHC diet did not affect hepatic expression of *Pgc1a*, *Ppara*, *Acox* or *Fabp4*, which led us to conclude that GW1516 did not activate PGC1 α , PPAR α or PPAR γ . However, GW1516-treatment enhanced the hepatic expression of *Adfp* and *Cpt1a* in the liver, which was coupled to increased FA oxidation. These data strongly suggest that GW1516 increases CPT1 α -mediated β -oxidation in the liver, and that with respect to PPARs, this effect is PPAR δ specific.

The studies in Chapter 5 also revealed that AMPK is not required for PPAR δ -mediated stimulation of liver fat oxidation, as the increase in β -oxidation observed in isolated WT primary mouse hepatocytes persisted in AMPK β 1^{-/-} hepatocytes.

Irrespective of AMPK β 1 genotype, GW1516-treatment significantly increased *Cpt1a* expression, further demonstrating that PPAR δ activates CPT1 α -mediated FA oxidation independent of AMPK.

As alluded to above, GW1516-intervention inhibited hepatic fatty acid synthesis, which is partially attributable to AMPK activation. We also found that intervention to a HFHC diet with GW1516 in mice, corrected selective hepatic insulin resistance, which reduced lipogenic gene expression and prevented any further increase in fasting FA synthesis. Our findings are supported by a number of studies reporting that PPAR δ plays a role in improving whole-body insulin sensitivity, which reduces metabolic disturbance (Lee et al., 2006b, Tanaka et al., 2003, Wang et al., 2003). However, we extended this concept in Chapter 5, as we provided evidence that improved insulin signaling specifically in the liver contributes to reduced hepatic steatosis.

A previous study demonstrated that transplanatation of bone marrow from *Ppar δ ^{-/-}* mice into WT mice polarized hepatic Kupffer cells to the proinflammatory M1 phenotype, which resulted in increased liver TG accumulation and hepatic dysfunction (Odegaard et al., 2008). Given that deletion of PPAR δ mimics the liganded state of the receptor as discussed in Section 6.2.4, the study by Odegaard and colleagues would imply that PPAR δ activation in hepatic Kupffer cells is proinflammatory. Although the studies performed in Chapter 5 cannot distinguish between the effects of PPAR δ activation in hepatocytes versus Kupffer cells, the results suggest an anti-inflammatory rather than a proinflammatory effect. This is consistent with the notion that activation of PPAR δ in hepatocytes protects from inflammatory responses induced by non-lipid stimuli such as cytokines or LPS (Serrano-Marco et al., 2011). Even so, it remains to be determined whether the inhibition of hepatic inflammation by GW1516 contributed to correction of hepatic insulin signaling, FA synthesis and hepatic steatosis, or was a secondary effect of reduced liver TG accumulation.

6.2.8 CHAPTER 5 FUTURE DIRECTIONS

Moving forward it will be important to determine the mechanism by which PPAR δ activation corrects insulin signaling. The discussion in Chapter 2 highlighted the fact that GW1516 activated Akt and FoxO1 phosphorylation in macrophages. Here, the situation is vastly different. If GW1516 activated hepatic insulin signaling, mTORC1 phosphorylation and *Srebf1c* expression would have been increased compared to HFHC-fed mice. Furthermore, fatty acid synthesis would have been increased, or perhaps unchanged due to activation of AMPK mitigating the increase in insulin-stimulated lipogenesis, but certainly not decreased. The simplest explanation for the correction of hepatic insulin signaling is improved peripheral insulin sensitivity, which would result in enhanced peripheral glucose uptake and a reduction in hyperinsulinemia. This hypothesis is supported by: (1) the known ability of PPAR δ activation to enhance glucose uptake in skeletal muscle (Kramer et al., 2005), (2) the fact that GW1516 treated mice exhibit increased insulin stimulated glucose disposal under hyperinsulinemic-euglycemic clamps (Lee et al., 2006b) and (3) that PPAR δ activation in pancreatic islet cells increases glucose stimulated insulin secretion (Iglesias et al., 2012). Taken together, these studies suggest that the PPAR δ -mediated correction of peripheral insulin resistance may contribute to reduced fasting hyperinsulinemia, and therefore the lower drive on hepatic insulin receptor signaling to stimulate the mTORC1-SREBP1c lipogenic axis. Hence, examining the contribution of corrected selective hepatic insulin resistance to reduced liver TG accumulation in GW1516-treated animals is not particularly straightforward.

Considering AMPK activation by GW1516 is required for the inhibition of lipogenesis, but is not required for the induction of FA oxidation, AMPK β 1^{-/-} mice provide an appropriate platform to test the relative contribution of these parameters in the

GW1516-mediated inhibition of liver TG accumulation. Furthermore, AMPK β 1^{-/-} mice are protected from diet-induced hepatic insulin resistance (Dzamko et al., 2010). Therefore, AMPK β 1^{-/-} mice also represent a model which can be used to decipher the relative contribution of corrected insulin signaling and AMPK activation to reduced lipogenesis by PPAR δ activation. We propose to examine the ability of GW1516 intervention to a HFHC diet to attenuate hepatic steatosis in AMPK β 1^{-/-} mice. We hypothesize that the ability of GW1516 to inhibit liver TG accumulation will be partially attenuated in AMPK β 1^{-/-} mice. Furthermore, the addition of a group of mice treated with adenoviral *Cpt1a* siRNA in the presence or absence of GW1516 would inhibit PPAR δ activation induced FA oxidation. The proposed experiments would provide unique insight into the mechanism of GW1516-mediated inhibition of hepatic steatosis.

In the fasting, acute feeding, injection and re-fasting protocol we found that GW1516 acutely stimulated carbohydrate oxidation, while not suppressing fat oxidation. Furthermore, in the intervention study, a setting of prolonged PPAR δ activation, GW1516 increased total EE yet had no further effect on average RER through a 24hr period. Taken together, these results suggest that PPAR δ activation can simultaneously stimulate carbohydrate and fat oxidation. The mechanism by which this occurs has been postulated to involve increased glucose flux through the pentose phosphate pathway coupled to increased hepatic fatty acid synthesis (Lee et al., 2006b). The consequence of these processes being upregulated in response to a PPAR δ agonist is that the former can consume up to 20% of hepatic glucose, while providing reducing power to stimulate fatty acid synthesis (Lee et al., 2006b); hence increased simultaneous carbohydrate and fat utilization. Although we did not measure activity of the pentose-phosphate pathway in livers of GW1516-treated animals, we did observe a significant reduction in the rate of hepatic fatty acid synthesis, thus challenging the theory of Lee and colleagues with respect to the liver. However, preliminary experiments in our lab have revealed that in

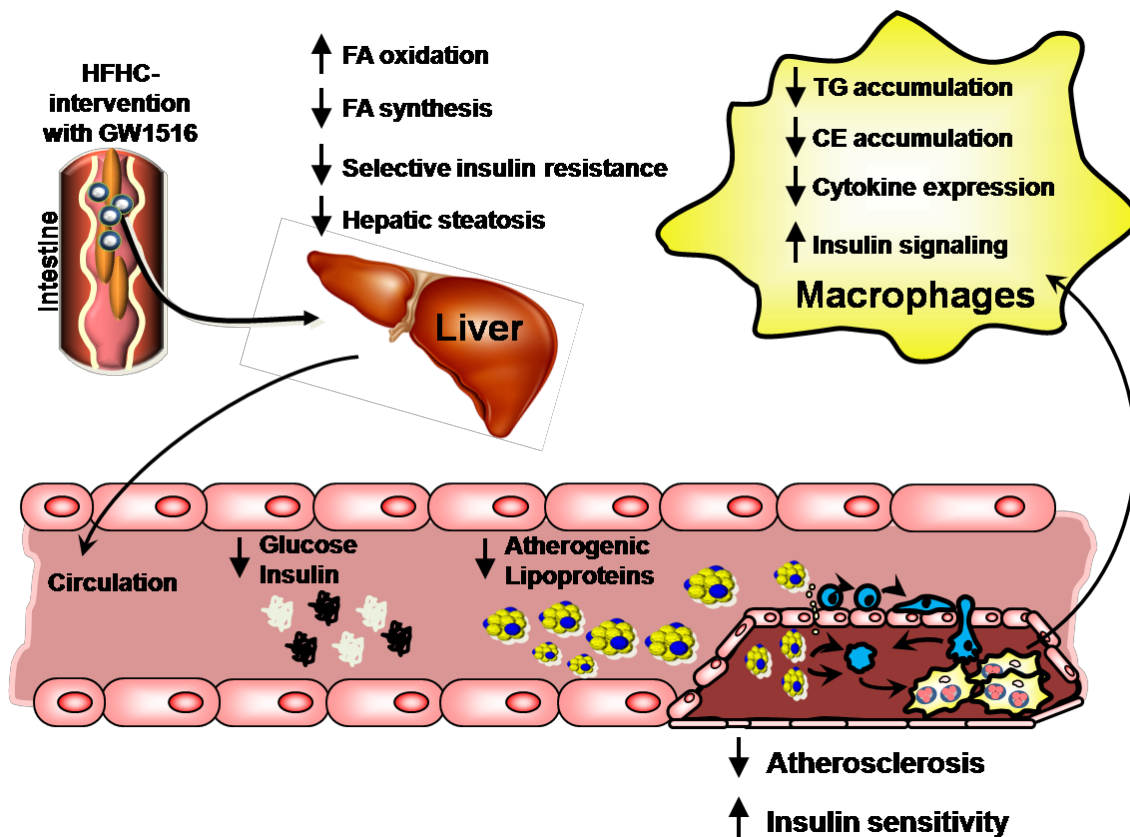
muscle, GW1516 does not inhibit HFHC feeding-induced fatty acid synthesis despite the resolution of hyperinsulinemia. Importantly GW1516-treatment significantly increases muscle FA oxidation (~2-fold). Together, these data suggest that PPAR δ activation may stimulate the pentose-phosphate shunt and fatty acid synthesis in muscle, where the oxidative machinery to utilize the newly synthesized FAs is upregulated. This would create futile cycling of FA synthesis and oxidation which: (1) increases carbohydrate consumption as a consequence of increased pentose-phosphate activity to provide reducing power for FA synthesis, and (2) simultaneously increases fat oxidation to deplete the newly synthesized FAs. However, this is highly speculative and substantial experimentation would be required to test this hypothesis. Nevertheless, identifying the mechanism by which PPAR δ activation stimulates simultaneous utilization of carbohydrate and fat is exciting and warrants further study.

6.3 OVERALL THESIS CONCLUSION

A substantial body of preclinical evidence supports the hypothesis that PPAR δ activation represents a favourable therapeutic strategy for the treatment and prevention of dyslipidemia, insulin resistant syndromes and atherosclerosis. Despite this wealth of knowledge, a significant gap between preclinical and clinical studies has stalled the development of PPAR δ agonists. The studies described in this thesis have contributed to the narrowing of this gap by elaborating on how PPAR δ activation confers protection from metabolic insult in macrophages, in the aorta and in the liver (Figure 6.2). Specifically, Chapters 2-5 of this thesis provided molecular and physiological evidence that PPAR δ activation favourably regulates lipid metabolism and inflammatory signaling, which results in the protection from atherosclerosis and hepatic steatosis in states of metabolic disturbance such as dyslipidemia, insulin resistance and type 2 diabetes.

Figure 6.2: Thesis Summary.

PPAR δ activation in macrophages attenuates TG and CE accumulation in response to lipoproteins, corrects impaired insulin signaling and inhibits the inflammatory response (Chapters 2 and 3). The ability of PPAR δ activation to inhibit foam cell formation, likely contributes to attenuation of diet-induced aortic insulin resistance and atherosclerosis *in vivo* (Chapter 4). In the liver, PPAR δ activation attenuates hepatic steatosis via increased FA oxidation and inhibition of *de novo* lipogenesis, which is associated with the correction of hyperlipidemia, hyperglycemia and hyperinsulinemia (Chapter 4 and 5).



6.4 REFERENCES

Anderson, E.K., Hill, A.A., and Hasty, A.H. (2012). Stearic Acid Accumulation in Macrophages Induces Toll-Like Receptor 4/2-Independent Inflammation Leading to Endoplasmic Reticulum Stress-Mediated Apoptosis. *Arterioscler Thromb Vasc Biol* 32, 1687-1695.

Argmann, C.A., Sawyez, C.G., McNeil, C.J., Hegele, R.A., and Huff, M.W. (2003). Activation of Peroxisome Proliferator-Activated Receptor Gamma and Retinoid X Receptor Results in Net Depletion of Cellular Cholesteryl Esters in Macrophages Exposed to Oxidized Lipoproteins. *Arterioscler Thromb Vasc Biol* 23, 475-482.

Barish, G.D., Atkins, A.R., Downes, M., Olson, P., Chong, L.W., Nelson, M., Zou, Y., Hwang, H., Kang, H., Curtiss, L., *et al.* (2008). Ppardelta Regulates Multiple Proinflammatory Pathways to Suppress Atherosclerosis. *Proc Natl Acad Sci U S A* 105, 4271-4276.

Beyea, M.M., Reaume, S., Sawyez, C.G., Edwards, J.Y., O'Neil, C., Hegele, R.A., Pickering, J.G., and Huff, M.W. (2012). The Oxysterol 24(S),25-Epoxycholesterol Attenuates Human Smooth Muscle-Derived Foam Cell Formation Via Reduced Low-Density Lipoprotein Uptake and Enhanced Cholesterol Efflux. *J Am Heart Assoc* 1, e000810.

Chawla, A., Lee, C.H., Barak, Y., He, W., Rosenfeld, J., Liao, D., Han, J., Kang, H., and Evans, R.M. (2003). Ppardelta Is a Very Low-Density Lipoprotein Sensor in Macrophages. *Proc Natl Acad Sci U S A* 100, 1268-1273.

Curtiss, L.K., Black, A.S., Bonnet, D.J., and Tobias, P.S. (2012). Atherosclerosis Induced by Endogenous and Exogenous Toll-Like Receptor (Tlr)1 or Tlr6 Agonists. *J Lipid Res* 53, 2126-2132.

Di-Poi, N., Tan, N.S., Michalik, L., Wahli, W., and Desvergne, B. (2002). Antiapoptotic Role of Pparbeta in Keratinocytes Via Transcriptional Control of the Akt1 Signaling Pathway. *Mol Cell* 10, 721-733.

Ding, G., Cheng, L., Qin, Q., Frontin, S., and Yang, Q. (2006). Ppardelta Modulates Lipopolysaccharide-Induced Tnfalpha Inflammation Signaling in Cultured Cardiomyocytes. *J Mol Cell Cardiol* 40, 821-828.

Du, K., Herzig, S., Kulkarni, R.N., and Montminy, M. (2003). Trb3: A Tribbles Homolog That Inhibits Akt/Pkb Activation by Insulin in Liver. *Science* 300, 1574-1577.

Dubois, M.J., Bergeron, S., Kim, H.J., Dombrowski, L., Perreault, M., Fournes, B., Faure, R., Olivier, M., Beauchemin, N., Shulman, G.I., *et al.* (2006). The Shp-1 Protein Tyrosine Phosphatase Negatively Modulates Glucose Homeostasis. *Nat Med* 12, 549-556.

Dzambo, N., van Denderen, B.J., Hevener, A.L., Jorgensen, S.B., Honeyman, J., Galic, S., Chen, Z.P., Watt, M.J., Campbell, D.J., Steinberg, G.R., *et al.* (2010). Ampk Beta1 Deletion Reduces Appetite, Preventing Obesity and Hepatic Insulin Resistance. *J Biol Chem* 285, 115-122.

Emanuelli, B., Peraldi, P., Filloux, C., Sawka-Verhelle, D., Hilton, D., and Van Obberghen, E. (2000). Socs-3 Is an Insulin-Induced Negative Regulator of Insulin Signaling. *J Biol Chem* 275, 15985-15991.

Erridge, C., and Samani, N.J. (2009). Saturated Fatty Acids Do Not Directly Stimulate Toll-Like Receptor Signaling. *Arterioscler Thromb Vasc Biol* 29, 1944-1949.

Evans, A.J., Sawyez, C.G., Wolfe, B.M., Connelly, P.W., Maguire, G.F., and Huff, M.W. (1993). Evidence That Cholesteryl Ester and Triglyceride Accumulation in J774 Macrophages Induced by Very Low Density Lipoprotein Subfractions Occurs by Different Mechanisms. *J Lipid Res* 34, 703-717.

Farese, R.V., Jr., Zechner, R., Newgard, C.B., and Walther, T.C. (2012). The Problem of Establishing Relationships between Hepatic Steatosis and Hepatic Insulin Resistance. *Cell Metab* 15, 570-573.

Febbraio, M., Podrez, E.A., Smith, J.D., Hajjar, D.P., Hazen, S.L., Hoff, H.F., Sharma, K., and Silverstein, R.L. (2000). Targeted Disruption of the Class B Scavenger Receptor Cd36 Protects against Atherosclerotic Lesion Development in Mice. *J Clin Invest* 105, 1049-1056.

Feig, J.E., Parathath, S., Rong, J.X., Mick, S.L., Vengrenyuk, Y., Grauer, L., Young, S.G., and Fisher, E.A. (2011). Reversal of Hyperlipidemia with a Genetic Switch Favorably Affects the Content and Inflammatory State of Macrophages in Atherosclerotic Plaques. *Circulation* 123, 989-998.

Frontini, M.J., O'Neil, C., Sawyez, C., Chan, B.M., Huff, M.W., and Pickering, J.G. (2009). Lipid Incorporation Inhibits Src-Dependent Assembly of Fibronectin and Type I Collagen by Vascular Smooth Muscle Cells. *Circ Res* 104, 832-841.

Galic, S., Fullerton, M.D., Schertzer, J.D., Sikkema, S., Marcinko, K., Walkley, C.R., Izon, D., Honeyman, J., Chen, Z.P., van Denderen, B.J., *et al.* (2011). Hematopoietic Ampk Beta1 Reduces Mouse Adipose Tissue Macrophage Inflammation and Insulin Resistance in Obesity. *J Clin Invest* 121, 4903-4915.

Ghisletti, S., Huang, W., Ogawa, S., Pascual, G., Lin, M.E., Willson, T.M., Rosenfeld, M.G., and Glass, C.K. (2007). Parallel Sumoylation-Dependent Pathways Mediate Gene- and Signal-Specific Transrepression by Lxrs and Ppargamma. *Mol Cell* 25, 57-70.

Glass, C.K., and Witztum, J.L. (2001). Atherosclerosis. The Road Ahead. *Cell* 104, 503-516.

Graham, T.L., Mookherjee, C., Suckling, K.E., Palmer, C.N., and Patel, L. (2005). The Ppardelta Agonist Gw0742x Reduces Atherosclerosis in Ldlr(-/-) Mice. *Atherosclerosis* 181, 29-37.

Gregor, M.F., and Hotamisligil, G.S. (2011). Inflammatory Mechanisms in Obesity. *Annu Rev Immunol* 29, 415-445.

Han, J.K., Lee, H.S., Yang, H.M., Hur, J., Jun, S.I., Kim, J.Y., Cho, C.H., Koh, G.Y., Peters, J.M., Park, K.W., *et al.* (2008). Peroxisome Proliferator-Activated Receptor-Delta Agonist Enhances Vasculogenesis by Regulating Endothelial Progenitor Cells through Genomic and Nongenomic Activations of the Phosphatidylinositol 3-Kinase/Akt Pathway. *Circulation* 118, 1021-1033.

Han, S., Liang, C.P., DeVries-Seimon, T., Ranalletta, M., Welch, C.L., Collins-Fletcher, K., Accili, D., Tabas, I., and Tall, A.R. (2006). Macrophage Insulin Receptor Deficiency Increases Er Stress-Induced Apoptosis and Necrotic Core Formation in Advanced Atherosclerotic Lesions. *Cell Metab* 3, 257-266.

Honda, A., Yamashita, K., Hara, T., Ikegami, T., Miyazaki, T., Shirai, M., Xu, G., Numazawa, M., and Matsuzaki, Y. (2009). Highly Sensitive Quantification of Key Regulatory Oxysterols in Biological Samples by Lc-Esi-Ms/Ms. *J Lipid Res* 50, 350-357.

Honda, A., Yamashita, K., Miyazaki, H., Shirai, M., Ikegami, T., Xu, G., Numazawa, M., Hara, T., and Matsuzaki, Y. (2008). Highly Sensitive Analysis of Sterol Profiles in Human Serum by Lc-Esi-Ms/Ms. *J Lipid Res* 49, 2063-2073.

Hummasti, S., and Hotamisligil, G.S. (2010). Endoplasmic Reticulum Stress and Inflammation in Obesity and Diabetes. *Circ Res* 107, 579-591.

Iglesias, J., Barg, S., Vallois, D., Lahiri, S., Roger, C., Yessoufou, A., Pradevand, S., McDonald, A., Bonal, C., Reimann, F., *et al.* (2012). Pparbeta/Delta Affects Pancreatic Beta Cell Mass and Insulin Secretion in Mice. *J Clin Invest* 122, 4105-4117.

Im, S.S., and Osborne, T.F. (2011). Liver X Receptors in Atherosclerosis and Inflammation. *Circ Res* 108, 996-1001.

Janabi, M., Yamashita, S., Hirano, K., Sakai, N., Hiraoka, H., Matsumoto, K., Zhang, Z., Nozaki, S., and Matsuzawa, Y. (2000). Oxidized Ldl-Induced Nf-Kappa B Activation and Subsequent Expression of Proinflammatory Genes Are Defective in Monocyte-Derived Macrophages from Cd36-Deficient Patients. *Arterioscler Thromb Vasc Biol* 20, 1953-1960.

Kannan, Y., Sundaram, K., Aluganti Narasimhulu, C., Parthasarathy, S., and Wewers, M.D. (2012). Oxidatively Modified Low Density Lipoprotein (Ldl) Inhibits Tlr2 and Tlr4 Cytokine Responses in Human Monocytes but Not in Macrophages. *J Biol Chem* 287, 23479-23488.

Kim, H.J., Kim, M.Y., Hwang, J.S., Kim, H.J., Lee, J.H., Chang, K.C., Kim, J.H., Han, C.W., Kim, J.H., and Seo, H.G. (2010). Ppardelta Inhibits Il-1beta-Stimulated Proliferation and Migration of Vascular Smooth Muscle Cells Via up-Regulation of Il-1ra. *Cell Mol Life Sci* 67, 2119-2130.

Kramer, D.K., Al-Khalili, L., Perrini, S., Skogsberg, J., Wretenberg, P., Kannisto, K., Wallberg-Henriksson, H., Ehrenborg, E., Zierath, J.R., and Krook, A. (2005). Direct Activation of Glucose Transport in Primary Human Myotubes after Activation of Peroxisome Proliferator-Activated Receptor Delta. *Diabetes* 54, 1157-1163.

Lee, C.H., Chawla, A., Urbiztondo, N., Liao, D., Boisvert, W.A., Evans, R.M., and Curtiss, L.K. (2003). Transcriptional Repression of Atherogenic Inflammation: Modulation by Ppardelta. *Science* 302, 453-457.

Lee, C.H., Kang, K., Mehl, I.R., Nofsinger, R., Alaynick, W.A., Chong, L.W., Rosenfeld, J.M., and Evans, R.M. (2006a). Peroxisome Proliferator-Activated Receptor Delta Promotes Very Low-Density Lipoprotein-Derived Fatty Acid Catabolism in the Macrophage. *Proc Natl Acad Sci U S A* 103, 2434-2439.

Lee, C.H., Olson, P., Hevener, A., Mehl, I., Chong, L.W., Olefsky, J.M., Gonzalez, F.J., Ham, J., Kang, H., Peters, J.M., *et al.* (2006b). Ppardelta Regulates Glucose Metabolism and Insulin Sensitivity. *Proc Natl Acad Sci U S A* 103, 3444-3449.

Li, Y., Schwabe, R.F., DeVries-Seimon, T., Yao, P.M., Gerbod-Giannone, M.C., Tall, A.R., Davis, R.J., Flavell, R., Brenner, D.A., and Tabas, I. (2005). Free Cholesterol-Loaded Macrophages Are an Abundant Source of Tumor Necrosis Factor-Alpha and Interleukin-6: Model of Nf-Kappab- and Map Kinase-Dependent Inflammation in Advanced Atherosclerosis. *J Biol Chem* 280, 21763-21772.

Libby, P., Ridker, P.M., and Hansson, G.K. (2011). Progress and Challenges in Translating the Biology of Atherosclerosis. *Nature* 473, 317-325.

Michelsen, K.S., Wong, M.H., Shah, P.K., Zhang, W., Yano, J., Doherty, T.M., Akira, S., Rajavashisth, T.B., and Arditì, M. (2004). Lack of Toll-Like Receptor 4 or Myeloid Differentiation Factor 88 Reduces Atherosclerosis and Alters Plaque Phenotype in Mice Deficient in Apolipoprotein E. *Proc Natl Acad Sci U S A* 101, 10679-10684.

Moore, K.J., and Freeman, M.W. (2006). Scavenger Receptors in Atherosclerosis: Beyond Lipid Uptake. *Arterioscler Thromb Vasc Biol* 26, 1702-1711.

Moore, K.J., and Tabas, I. (2011). Macrophages in the Pathogenesis of Atherosclerosis. *Cell* 145, 341-355.

Mullick, A.E., Fu, W., Graham, M.J., Lee, R.G., Witchell, D., Bell, T.A., Whipple, C.P., and Crooke, R.M. (2011). Antisense Oligonucleotide Reduction of Apob-Ameliorated Atherosclerosis in Ldl Receptor-Deficient Mice. *J Lipid Res* 52, 885-896.

Mullick, A.E., Tobias, P.S., and Curtiss, L.K. (2005). Modulation of Atherosclerosis in Mice by Toll-Like Receptor 2. *J Clin Invest* 115, 3149-3156.

Nguyen, M.T., Favelyukis, S., Nguyen, A.K., Reichart, D., Scott, P.A., Jenn, A., Liu-Bryan, R., Glass, C.K., Neels, J.G., and Olefsky, J.M. (2007). A Subpopulation of Macrophages Infiltrates Hypertrophic Adipose Tissue and Is Activated by Free Fatty Acids Via Toll-Like Receptors 2 and 4 and Jnk-Dependent Pathways. *J Biol Chem* 282, 35279-35292.

Nicholson, K.M., and Anderson, N.G. (2002). The Protein Kinase B/Akt Signalling Pathway in Human Malignancy. *Cell Signal* 14, 381-395.

Odegaard, J.I., Ricardo-Gonzalez, R.R., Red Eagle, A., Vats, D., Morel, C.R., Goforth, M.H., Subramanian, V., Mukundan, L., Ferrante, A.W., and Chawla, A. (2008). Alternative M2 Activation of Kupffer Cells by Ppardelta Ameliorates Obesity-Induced Insulin Resistance. *Cell Metab* 7, 496-507.

Ozcan, U., Cao, Q., Yilmaz, E., Lee, A.H., Iwakoshi, N.N., Ozdelen, E., Tuncman, G., Gorgun, C., Glimcher, L.H., and Hotamisligil, G.S. (2004). Endoplasmic Reticulum Stress Links Obesity, Insulin Action, and Type 2 Diabetes. *Science* 306, 457-461.

Qiu, G., Ho, A.C., Yu, W., and Hill, J.S. (2007). Suppression of Endothelial or Lipoprotein Lipase in Thp-1 Macrophages Attenuates Proinflammatory Cytokine Secretion. *J Lipid Res* 48, 385-394.

Rodriguez-Calvo, R., Serrano, L., Coll, T., Moullan, N., Sanchez, R.M., Merlos, M., Palomer, X., Laguna, J.C., Michalik, L., Wahli, W., *et al.* (2008). Activation of Peroxisome Proliferator-Activated Receptor Beta/Delta Inhibits Lipopolysaccharide-Induced Cytokine Production in Adipocytes by Lowering Nuclear Factor-Kappab Activity Via Extracellular Signal-Related Kinase 1/2. *Diabetes* 57, 2149-2157.

Rui, L., Yuan, M., Frantz, D., Shoelson, S., and White, M.F. (2002). Socs-1 and Socs-3 Block Insulin Signaling by Ubiquitin-Mediated Degradation of Irs1 and Irs2. *J Biol Chem* 277, 42394-42398.

Saraswathi, V., and Hasty, A.H. (2006). The Role of Lipolysis in Mediating the Proinflammatory Effects of Very Low Density Lipoproteins in Mouse Peritoneal Macrophages. *J Lipid Res* 47, 1406-1415.

Senokuchi, T., Liang, C.P., Seimon, T.A., Han, S., Matsumoto, M., Banks, A.S., Paik, J.H., DePinho, R.A., Accili, D., Tabas, I., *et al.* (2008). Forkhead Transcription Factors (Foxos) Promote Apoptosis of Insulin-Resistant Macrophages During Cholesterol-Induced Endoplasmic Reticulum Stress. *Diabetes* 57, 2967-2976.

Serrano-Marco, L., Barroso, E., El Kochairi, I., Palomer, X., Michalik, L., Wahli, W., and Vazquez-Carrera, M. (2011). The Peroxisome Proliferator-Activated Receptor (Ppar)

Beta/Delta Agonist Gw501516 Inhibits Il-6-Induced Signal Transducer and Activator of Transcription 3 (Stat3) Activation and Insulin Resistance in Human Liver Cells. *Diabetologia* 55, 743-751.

Shi, H., Kokoeva, M.V., Inouye, K., Tzameli, I., Yin, H., and Flier, J.S. (2006). Tlr4 Links Innate Immunity and Fatty Acid-Induced Insulin Resistance. *J Clin Invest* 116, 3015-3025.

Spann, N.J., Garmire, L.X., McDonald, J.G., Myers, D.S., Milne, S.B., Shibata, N., Reichart, D., Fox, J.N., Shaked, I., Heudobler, D., *et al.* (2012). Regulated Accumulation of Desmosterol Integrates Macrophage Lipid Metabolism and Inflammatory Responses. *Cell* 151, 138-152.

Stewart, C.R., Stuart, L.M., Wilkinson, K., van Gils, J.M., Deng, J., Halle, A., Rayner, K.J., Boyer, L., Zhong, R., Frazier, W.A., *et al.* (2010). Cd36 Ligands Promote Sterile Inflammation through Assembly of a Toll-Like Receptor 4 and 6 Heterodimer. *Nat Immunol* 11, 155-161.

Stollenwerk, M.M., Schiopu, A., Fredrikson, G.N., Dichtl, W., Nilsson, J., and Ares, M.P. (2005). Very Low Density Lipoprotein Potentiates Tumor Necrosis Factor-Alpha Expression in Macrophages. *Atherosclerosis* 179, 247-254.

Straus, D.S., and Glass, C.K. (2007). Anti-Inflammatory Actions of Ppar Ligands: New Insights on Cellular and Molecular Mechanisms. *Trends Immunol* 28, 551-558.

Su, D., Coudriet, G.M., Hyun Kim, D., Lu, Y., Perdomo, G., Qu, S., Slusher, S., Tse, H.M., Piganelli, J., Giannoukakis, N., *et al.* (2009). Foxo1 Links Insulin Resistance to Proinflammatory Cytokine Il-1beta Production in Macrophages. *Diabetes* 58, 2624-2633.

Takata, Y., Liu, J., Yin, F., Collins, A.R., Lyon, C.J., Lee, C.H., Atkins, A.R., Downes, M., Barish, G.D., Evans, R.M., *et al.* (2008). Ppardelta-Mediated Antiinflammatory Mechanisms Inhibit Angiotensin Ii-Accelerated Atherosclerosis. *Proc Natl Acad Sci U S A* 105, 4277-4282.

Tanaka, T., Yamamoto, J., Iwasaki, S., Asaba, H., Hamura, H., Ikeda, Y., Watanabe, M., Magoori, K., Ioka, R.X., Tachibana, K., *et al.* (2003). Activation of Peroxisome Proliferator-Activated Receptor Delta Induces Fatty Acid Beta-Oxidation in Skeletal Muscle and Attenuates Metabolic Syndrome. *Proc Natl Acad Sci U S A* 100, 15924-15929.

Tarling, E.J., Bojanic, D.D., Tangirala, R.K., Wang, X., Lovgren-Sandblom, A., Lusis, A.J., Bjorkhem, I., and Edwards, P.A. (2010). Impaired Development of Atherosclerosis in *Abcg1*^{-/-} *Apoe*^{-/-} Mice: Identification of Specific Oxysterols That Both Accumulate in *Abcg1*^{-/-} *Apoe*^{-/-} Tissues and Induce Apoptosis. *Arterioscler Thromb Vasc Biol* 30, 1174-1180.

Wang, Y.X., Lee, C.H., Tjep, S., Yu, R.T., Ham, J., Kang, H., and Evans, R.M. (2003). Peroxisome-Proliferator-Activated Receptor Delta Activates Fat Metabolism to Prevent Obesity. *Cell* *113*, 159-170.

Wang, Z.H., Shang, Y.Y., Zhang, S., Zhong, M., Wang, X.P., Deng, J.T., Pan, J., Zhang, Y., and Zhang, W. (2012). Silence of Trib3 Suppresses Atherosclerosis and Stabilizes Plaques in Diabetic Apoe^{-/-}/Ldl Receptor^{-/-} Mice. *Diabetes* *61*, 463-473.

Whitman, S.C., Argmann, C.A., Sawyez, C.G., Miller, D.B., Hegele, R.A., and Huff, M.W. (1999a). Uptake of Type Iv Hypertriglyceridemic Vldl by Cultured Macrophages Is Enhanced by Interferon-Gamma. *J Lipid Res* *40*, 1017-1028.

Whitman, S.C., Hazen, S.L., Miller, D.B., Hegele, R.A., Heinecke, J.W., and Huff, M.W. (1999b). Modification of Type Iii Vldl, Their Remnants, and Vldl from Apoe-Knockout Mice by P-Hydroxyphenylacetaldehyde, a Product of Myeloperoxidase Activity, Causes Marked Cholesteryl Ester Accumulation in Macrophages. *Arterioscler Thromb Vasc Biol* *19*, 1238-1249.

Yvan-Charvet, L., Ranalletta, M., Wang, N., Han, S., Terasaka, N., Li, R., Welch, C., and Tall, A.R. (2007). Combined Deficiency of Abca1 and Abcg1 Promotes Foam Cell Accumulation and Accelerates Atherosclerosis in Mice. *J Clin Invest* *117*, 3900-3908.

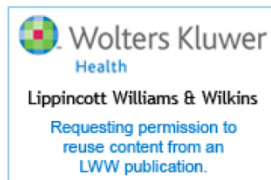
Appendix 7.1

4/12/13

Rightslink® by Copyright Clearance Center



RightsLink®

[Home](#)
[Account Info](#)
[Help](#)


Title: Peroxisome proliferator-activated receptor δ : a multifaceted metabolic player

Logged in as:
Lazar Bojic

Author: Lazar Bojic and Murray Huff

[LOGOUT](#)

Publication: Current Opinion in Lipidology

Publisher: Wolters Kluwer Health

Date: Jan 1, 2013

Copyright © 2013, (C) 2013 Lippincott Williams

Order Completed

Thank you very much for your order.

This is a License Agreement between Lazar Bojic ("You") and Wolters Kluwer Health ("Wolters Kluwer Health"). The license consists of your order details, the terms and conditions provided by Wolters Kluwer Health, and the [payment terms and conditions](#).

[Get the printable license.](#)

License Number	3126641196658
License date	Apr 12, 2013
Licensed content publisher	Wolters Kluwer Health
Licensed content publication	Current Opinion in Lipidology
Licensed content title	Peroxisome proliferator-activated receptor δ : a multifaceted metabolic player
Licensed content author	Lazar Bojic and Murray Huff
Licensed content date	Jan 1, 2013
Volume number	24
Issue Number	2
Type of Use	Dissertation/Thesis
Requestor type	Individual
Author of this Wolters Kluwer article	Yes
Title of your thesis / dissertation	Regulation of Lipid Homeostasis, Inflammatory Signalling and Atherosclerosis by the Peroxisome Proliferator-Activated Receptor Delta
Expected completion date	Jun 2013
Estimated size(pages)	300
Total	0.00 USD

[ORDER MORE...](#)
[CLOSE WINDOW](#)

Copyright © 2013 [Copyright Clearance Center, Inc.](#) All Rights Reserved. [Privacy statement](#).
Comments? We would like to hear from you. E-mail us at customercare@copyright.com

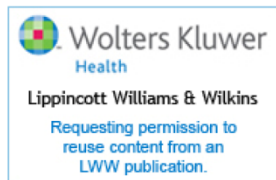
Appendix 7.2

4/12/13

Rightslink® by Copyright Clearance Center



RightsLink®

[Home](#)
[Account Info](#)
[Help](#)


Title: Activation of Peroxisome Proliferator-Activated Receptor δ Inhibits Human Macrophage Foam Cell Formation and the Inflammatory Response Induced by Very Low-Density Lipoprotein

Logged in as:
Lazar Bojic

[LOGOUT](#)

Author: Lazar A. Bojic, Cynthia G. Sawyez, Dawn E. Telford, Jane Y. Edwards, Robert A. Hegele, Murray W. Huff

Publication: ATVB

Publisher: Wolters Kluwer Health

Date: Dec 1, 2012

Copyright © 2012, Wolters Kluwer Health

Order Completed

Thank you very much for your order.

This is a License Agreement between Lazar Bojic ("You") and Wolters Kluwer Health ("Wolters Kluwer Health"). The license consists of your order details, the terms and conditions provided by Wolters Kluwer Health, and the [payment terms and conditions](#).

[Get the printable license.](#)

License Number	3126650169257
License date	Apr 12, 2013
Licensed content publisher	Wolters Kluwer Health
Licensed content publication	ATVB
Licensed content title	Activation of Peroxisome Proliferator-Activated Receptor δ Inhibits Human Macrophage Foam Cell Formation and the Inflammatory Response Induced by Very Low-Density Lipoprotein
Licensed content author	Lazar A. Bojic, Cynthia G. Sawyez, Dawn E. Telford, Jane Y. Edwards, Robert A. Hegele, Murray W. Huff
Licensed content date	Dec 1, 2012
Volume number	32
Issue Number	12
Type of Use	Dissertation/Thesis
Requestor type	Individual
Author of this Wolters Kluwer article	Yes
Title of your thesis / dissertation	Regulation of Lipid Homeostasis, Inflammatory Signalling and Atherosclerosis by the Peroxisome Proliferator-Activated Receptor Delta
Expected completion date	Jun 2013
Estimated size(pages)	300
Total	0.00 USD

[ORDER MORE...](#)
[CLOSE WINDOW](#)

Copyright © 2013 [Copyright Clearance Center, Inc.](#) All Rights Reserved. [Privacy statement](#).
Comments? We would like to hear from you. E-mail us at customercare@copyright.com

Appendix 7.3

Subject: eSirius Notification - New Animal Use Protocol is APPROVED2012-028::1



AUP Number: 2012-028

PI Name: Huff, Murray W

AUP Title: Regulation Of Lipids And Lipoproteins In Mouse Models Of Atherosclerosis.

Approval Date: 09/13/2012

Official Notice of Animal Use Subcommittee (AUS) Approval: Your new Animal Use Protocol (AUP) entitled "Regulation Of Lipids And Lipoproteins In Mouse Models Of Atherosclerosis." has been APPROVED by the Animal Use Subcommittee of the University Council on Animal Care. This approval, although valid for four years, and is subject to annual Protocol Renewal.2012-028::1

This AUP number must be indicated when ordering animals for this project.

Animals for other projects may not be ordered under this AUP number.

Purchases of animals other than through this system must be cleared through the ACVS office. Health certificates will be required.

The holder of this Animal Use Protocol is responsible to ensure that all associated safety components (biosafety, radiation safety, general laboratory safety) comply with institutional safety standards and have received all necessary approvals.

Please consult directly with your institutional safety officers.

Submitted by: Copeman, Laura
on behalf of the Animal Use Subcommittee
University Council on Animal Care

https://iwc.uwo.ca/iwc_static/layout/shell.html?lang=en&2-4.01_224943

19/09/2012

Curriculum Vitae

NAME: Lazar Alexander Bojic
PLACE OF BIRTH: Toronto, Ontario, Canada
DATE OF BIRTH: 16 June 1985

Education and Training

2007 – 2013 University of Western Ontario
 London, Ontario Canada
 Ph.D. Candidate, Department of Biochemistry
 Supervisor: Dr. Murray Huff

2003 – 2007 University of Western Ontario
 London, Ontario Canada
 Bachelor of Medical Science (Honours)
 Department of Medical Sciences

Honours and Awards

2012 Best PhD Oral Presentation
 Department of Medicine Research Day

2011-2012 Ontario Graduate Scholarship
 Ontario Graduate Scholarship Program

2011 Best PhD Poster Presentation
 Gordon Research Conference on Atherosclerosis

2011 Best PhD Oral Presentation
 Department of Medicine Research Day

2010-2011 Ontario Graduate Scholarship in Science and Technology
 Ontario Graduate Scholarship Program

2010 Best PhD Poster Presentation
 Margaret P. Moffat Research Day

2009-2011 CIHR Strategic Training Fellowship in Vascular Imaging
 Canadian Institutes of Health Research

2009 Best PhD Oral Presentation
 Canadian Lipoprotein Conference

2009 Best PhD Oral Presentation
 Department of Medicine Research Day

2009	ATVB Conference Young Investigator Award Conference on Arteriosclerosis, Thrombosis and Vascular Biology
2008	CIHR National Training Program on Lipids, Lipoproteins and Atherosclerosis Canadian Institutes of Health Research
2007	Scholarship for Medical Research Schulich School of Medicine & Dentistry
2007-2012	Graduate Research Scholarship (5 year) University of Western Ontario
2006, 2007	Dean's Honour List University of Western Ontario

Related Work Experience

2012	Supervision of Undergraduate Honours Student Department of Biochemistry University of Western Ontario
2011-2012	Supervision of Undergraduate Honours Student Department of Biochemistry University of Western Ontario
2010-2011	Supervision of Undergraduate Honours Student Department of Biochemistry University of Western Ontario
2009-2010	Supervision of Undergraduate Honours Student Department of Biochemistry University of Western Ontario
2008-2012	Teaching Assistant Medical Science 4930F – Biochemistry Module University of Western Ontario

Peer Reviewed Publications

Bojic LA, Telford DE, Fullerton MD, Ford RJ, Sutherland BG, Edwards JY, Sawyez CG, Gros R, Steinberg GR and Huff MW. PPAR δ -specific activation in liver attenuates triglyceride accumulation via enhanced fatty acid oxidation, reduced fatty acid synthesis and improved insulin sensitivity in *Ldlr*^{-/-} mice. (Submitted).

Bojic LA, Telford DE, Sutherland BG, Edwards JY, Sawyez CG, Huff MW. PPAR δ agonist GW1516 attenuates diet-induced aortic inflammation, insulin resistance and atherosclerosis in *Ldlr*^{-/-} mice. (Under revision).

Bojic LA, Huff MW. PPAR-delta: a multifaceted metabolic player. *Curr Opin Lipidol* 2013 Apr;24(2):171-7.

Bojic LA, Sawyez CG, Telford DE, Edwards JY, Hegele RA, Huff MW. Activation of Peroxisome Proliferator-Activated Receptor Delta Inhibits Human Macrophage Foam Cell Formation and the Inflammatory Response Induced by Very Low-Density Lipoprotein. *Arterioscler Thromb Vasc Biol.* 2012 Dec;32(12):2919-28.

Published Refereed Abstracts

Bojic LA, Telford DE, Sutherland BG, Edwards JY, Sawyez CG, Huff MW. PPARdelta agonist GW1516 attenuates diet-induced dyslipidemia, insulin resistance, aortic inflammation and atherosclerosis in *Ldlr^{-/-}* mice. Gordon Research Conference (Lipids and Lipoproteins), Waterville Valley, NH, June 2012.

Bojic LA, Telford DE, Sutherland BG, Edwards JY, Sawyez CG, Huff MW. PPARdelta agonist GW1516 attenuates diet-induced dyslipidemia, insulin resistance and aortic inflammation in *Ldlr^{-/-}* mice. Conference on Arteriosclerosis, Thrombosis and Vascular Biology, Chicago, IL, April 2012

Bojic LA, Sawyez CG, Telford DE, Edwards JY, Hegele RA, Huff MW. Inhibition of very low-density lipoprotein-induced macrophage inflammation by the peroxisome proliferator-activated receptor delta. Canadian Lipoprotein Conference, Halifax, NS, November 2011.

Bojic LA, Sawyez CG, Telford DE, Edwards JY, Hegele RA, Huff MW. Inhibition of VLDL-induced macrophage inflammation by activation of PPAR delta. Gordon Research Conference (Atherosclerosis), Newport, RI, June 2011.

Bojic LA, Sawyez CG, Telford DE, Edwards JY, Hegele RA, Huff MW. Inhibition of very low-density lipoprotein-induced macrophage inflammation by the peroxisome proliferator-activated receptor delta. Conference on Arteriosclerosis, Thrombosis and Vascular Biology, Chicago, IL, April 2011

Bojic LA, Telford DE, Sutherland BG, Edwards JY, Sawyez CG, Huff MW. Modulation of VLDL-induced Macrophage Inflammation by PPARdelta. Canadian Lipoprotein Conference, Niagara-on-the-Lake, ON, October 2010.

Bojic LA, Sawyez CG, Telford DE, Edwards JY, Hegele RA, Huff MW. Inhibition of Macrophage Foam Cell Formation and Expression of Inflammatory Mediators by PPAR δ . Conference on Arteriosclerosis, Thrombosis and Vascular Biology, San Francisco, CA, April 2010.

Bojic LA, Sawyez CG, Telford DE, Edwards JY, Hegele RA, Huff MW. Inhibition of Macrophage Foam Cell Formation and Expression of Inflammatory Mediators by PPARdelta. Canadian Lipoprotein Conference, Windsor, ON, October 2009.

Bojic LA, Sawyez CG, Edwards JY, Hegele RA, Huff MW. Inhibition of Macrophage Foam Cell Formation and Expression of Inflammatory Mediators by PPAR δ . Conference on Arteriosclerosis, Thrombosis and Vascular Biology, Washington DC, April 2009.

Bojic LA, Sawyez CG, Edwards JY, Hegele RA, Muff MW. Inhibition of Macrophage Foam Cell Formation and Expression of Inflammatory Mediators by PPARdelta. Canadian Lipoprotein Conference, Whistler, BC, October 2008.